# ABSTRACT

SUMANASINGHE, RUWAN DEEPAL. Functional Bone Tissue Engineering using Human Mesenchymal Stem Cells and Polymeric Scaffolds. (Under the direction of Elizabeth G. Loboa and Martin W. King).

Functional bone tissue engineering has been necessitated by the need to treat critical size defects in bones due to birth abnormalities, trauma, and pathological conditions. Appropriate conditions for *in vitro* osteogenesis need to be identified to establish protocols for engineering bone tissues. The success of *in vitro* osteogenesis lies on the type of cell source, stimuli, and scaffold material used for engineering bone constructs. Recent investigations have established the pluripotency of mesenchymal stem cells (MSCs) and their ability to differentiate down a multitude of pathways including osteogenenic. *In vivo* studies have shown that MSCs are primarily responsible for bone growth and regeneration and therefore have become a major candidate for bone tissue engineering. Osteogenic differentiation of MSCs via chemical stimuli has been extensively investigated using both monolayer and three-dimensional (3D) culture conditions. These investigations provided useful information on media conditions, cell seeding densities, and differentiation capabilities of MSCs. However, chemical stimulation alone might not be sufficient to accelerate osteogenesis and impart necessary mechanical strength to the final tissue construct. Mechanical strength of the final tissue construct is vital to maintain its structural integrity when exposed to physiological stresses *in vivo*. Stimulation of MSCs using mechanical strain might provide another method to induce MSC osteogenesis while also obtaining desired mechanical strength of the final tissue constructs. Although *in vivo* studies and experimental models have

indicated that cyclic tensile strain could induce MSC osteogenesis, its effect on MSC osteogenesis in 3D cultures *in vitro* has not been investigated. The need to maintain cell viability and be able to provide chemical or mechanical cues to cells in 3D cultures requires improvements in scaffold architecture and design. While collagen provides a natural matrix for cell adhesion and growth, its contraction during culture can greatly limit culture duration and mechanical stability of the matrix. Although fibrous scaffolds can be used as an alternative to collagen scaffolds, insufficient media diffusion to the center of these 3D scaffolds could detrimentally affect uniform cell growth throughout the scaffold; hence, scaffolds with better diffusional properties need to be developed. This study investigated the use of 3D collagen matrices as a scaffold material to determine the effects of strain and chemical stimuli on osteogenic differentiation of human MSCs (hMSCs). Major attention was given to the analyses of: cell viability, matrix contraction, nuclei morphology, expression of osteogenic markers and proinflammatory cytokines, as well as changes in mechanical properties of the final tissue construct. As an approach to develop 3D fibrous scaffolds with enhanced diffusional properties, fabrication of melt spun microporous fibers using a blend of poly (lactic acid) (PLA) and sulfopolyester that could be used in 3D nonwoven scaffolds was also investigated.

The findings of this study clearly illustrated the ability of cyclic tensile strain to induce osteogenic differentiation of hMSCs when cultured in a 3D environment. Expression of proinflammatory cytokines by strained hMSCs suggested that cyclic strain might have induced modulation of bone resorption in hMSCs. The results also illustrated the effects of strain on the mechanical properties of the final tissue construct.

Microporous fibers created from melt spun composite fibers using binary blends of poly (lactic acid) and sulfopolyester could enhance diffusional properties of 3D nonwoven scaffolds fabricated using these fibers. As this body of work demonstrates, use of cyclic tensile strain combined with chemical stimulation to induce osteogenic differentiation of hMSCs could greatly assist the engineering of functional bone tissues *in vitro*. Microporous fibers created using polymer blends could provide an effective method to improve diffusional properties of 3D polymeric scaffolds.

# FUNCTIONAL BONE TISSUE ENGINEERING USING HUMAN MESENCHYMAL STEM CELLS AND POLYMERIC SCAFFOLDS

by
**RUWAN DEEPAL SUMANASINGHE**

A dissertation submitted to the Graduate Faculty of
North Carolina State University
in partial fulfillment of the
requirements for the Degree of
Doctor of Philosophy

**FIBER AND POLYMER SCIENCE**
**&**
**BIOMEDICAL ENGINEERING**

Raleigh, North Carolina

2006

**APPROVED BY**

| | | |
|---|---|---|
| Dr. Nancy Monteiro-Riviere<br>Committee Member | Dr. Behnam Pourdeyhimi<br>Committee Member | Dr. Alan E. Tonelli<br>Committee Member |

| | |
|---|---|
| Dr. Elizabeth G. Loboa<br>Chair of Advisory Committee | Dr. Martin W. King<br>Co-chair of Advisory Committee |

# DEDICATION

To my dear mother and father for raising me through many hardships, guiding and encouraging me enough to reach higher goals in education.

# BIOGRAPHY

Ruwan Deepal Sumanasinghe was born on July 3, 1971, in Gampaha, Sri Lanka, to Keerthisinghe Dharmadasa Sumanasinghe and Meththadari Susima Sumanasinghe. Ruwan's family comprises of a younger brother, Lalith Buddhika Sumanasinghe and an elder brother, Thisun Aruna Sumanasinghe. Ruwan gained his primary and high school education at Mahanama College in Colombo, Sri Lanka. He gained entrance to the Faculty of Engineering at the University of Moratuwa, Sri Lanka in 1994 where he earned his Bachelor of Science Degree (Eng) specializing in Textiles in 1998. Ruwan graduated with First Class Honors and was awarded the Textile Institute award for the best graduate in that year. After graduation, he joined the department of textile and clothing technology at the University of Moratuwa, Sri Lanka as an assistant lecturer. He got married to his beloved wife, Shantha Ramani Sumanasinghe in 2000 and they both arrived to North Carolina State University in pursuit of higher studies. Ruwan's MS program in Textile Management and Technology at the College of Textiles included research on analyzing biomaterials used for endovascular prostheses under Dr. Martin King. He obtained his MS degree in December 2002 and continued to pursue for a PhD degree in Fiber and Polymer Science under Dr. Martin King. His interest in tissue engineering led him to add a Biomedical Engineering co-major to his PhD program in 2004. Ruwan started research on functional bone tissue engineering under Dr. Elizabeth Loboa in the joint department of biomedical engineering in summer 2004. In February 2006, Ruwan and Shantha had another major turn in their lives when their son, Chamudu Minuka Sumanasinghe was born.

# ACKNOWLEDGEMENTS

The work in this study would have been impossible without the advice, guidance, and help from the persons mentioned below. I owe immense gratitude to my parents for their guidance and commitment, my wife for all her help and encouragement and my son for enduring my long work hours.

I cannot express my appreciation enough for my advisors Drs. Elizabeth Loboa and Martin King whose knowledge, experience, and enthusiasm have made my graduate studies successful. Without their timely guidance and advice, this study would have not been successful. I am always grateful to Dr. Behnam Pourdeyhimi for his initiative in giving me an opportunity to pursue graduate studies at North Carolina State University and being always there to encourage and assist in my research. I would like to extend my special thanks to Dr. Alan Tonelli for his comments and suggestions to make this study successful. I wish to express my greatest appreciation to Dr. Nancy Monteiro-Riviere for her guidance and assistance throughout my research.

I greatly appreciate Dr. Albert Banes for his advice and for providing the Tissue Train equipment and necessary training to carry out my research. I would like to offer my greatest appreciation to Drs. Susan Bernacki and Michelle Wall for their advice and assistance throughout this study. I am much obliged to Drs. Peter Mente, Svetlana Verenich, Mehdi Afshari, as well as Birgit Andersen, Alfred Inman, Valeri Knowlton and Prasath Mageswaran for their technical assistance. My thanks also go to Carla Haslauer for her dedication in assisting my research work. I extend my appreciation to Wayne Pfeiler, Ariel Hanson,

Allison Finger, Rekha Balasubramanyam, and Ajit Moghe for their help and suggestions. My special thanks go to Dr. Frank Abrams for giving me the opportunity to pursue a Biomedical Engineering co-major and for his continued advice and encouragement to make my study a meaningful one. I would like to express my appreciation to Dr. William Oxenham for his guidance throughout my stay at the College of Textiles. Also, I wish to express my appreciation to the College of Textiles and the Joint Department of Biomedical Engineering for providing financial support for my graduate program.

Finally, my thanks go to Carolyn Krystoff, Robert Cooper, Heather Kirks, Linda Simerson and Nancy McKinney for all their time and hard work to make my graduate studies at North Carolina State University convenient.

# TABLE OF CONTENTS

# LIST OF TABLES

**Page**

# LIST OF FIGURES

**Page**

# NOMENCLATURE

| | |
|---|---|
| ALPL | Alkaline phosphatase |
| ANOVA | Analysis of variance |
| AQ | Sulfopolyester |
| AsAP | Ascorbic acid |
| ATR | Attenuated total reflectance |
| AUC | Area under the curve |
| BMP | Bone morphogenetic protein |
| BSP | Bone sialoprotein |
| Cbfa1 | Core- binding factor -1 |
| CICP | Procollagen I propeptide |
| COL1 | Type 1 collagen |
| DAPI | 4′, 6-diamidino-2-phenylindole dihydrochloride |
| Dex | Dexamethasone |
| DNA | Deoxy ribonucleic acid |
| DMEM | Dulbecco's modified Eagle medium |
| DSC | Differential scanning calorimetry |
| DTGS | Deuterated triglycine sulfate |
| EALP | Endogenous alkaline phosphatase |
| ECM | Extracellular matrix |
| EDTA | Ethylenediaminetetraacetic acid |
| ELF | Enzyme labeled fluorescence |
| EthD-1 | Ethedium homodiamer-1 |
| FBS | Fetal bovine serum |
| FDA | Food and drug administration |
| FTIR | Fourier transform infrared spectrophotometer |
| GAPDH | Glyceraldehyde-3-phosphate dehydrogenase |
| HA | Hydroxyapatite |
| HDPE | High density polyethylene |
| HEK | Human epidermal keratinocytes |
| HLH | Helix-loop-helix |
| hBMSCs | Human bone marrow stromal cells |
| hMSCs | Human mesenchymal stem cells |
| IGF | Insulin-like-growth factor |
| IL | Interleukin |
| mRNA | Mesenger ribonucleic acid |
| MSCs | Mesenchymal stem cells |
| MSCGM | Mesenchymal stem cell growth medium |
| NAP | Neutrophil attractant/activating protein |
| OCN | Osteocalcin |

# NOMENCLATURE - CONTINUED

| | |
|---|---|
| ODM | Osteogenic differentiating medium |
| OPN | Osteopontin |
| OSN | Osteonectin |
| PBS | Phosphate buffered saline |
| PCL | Poly -ε- caprolactone |
| PCR | Polymerase chain reaction |
| PE | Polyethylene |
| PET | Poly(polyethylene terephthalate) |
| PGA | Polyglycolic acid |
| PLA | Polylactic acid |
| PLGA | Copolymer of PLA and PGA |
| PLLA | Poly(L-lactic acid) |
| PP | Polypropylene |
| PU | Polyurethane |
| rMSCs | Rat mesenchymal stem cells |
| RNA | Ribonucleic acid |
| RT | Reverse transcriptase |
| RT-PCR | Real time polymerase chain reaction |
| SEM | Scanning electron microscope |
| TBSA | Triton X-100/ 0.5% bovine serum albumin |
| TEM | Transmission electron microscopy |
| TGA | Thermogravimetric analysis |
| TGF-β | Transforming growth factor-β |
| TNF-α | Tumor necrosis factor-α |
| 2D | Two-dimensional |
| 3D | Three-dimensional |
| βGP | β-glycerophosphate |

# 1 Introduction and Objectives

## 1.1 Background

Treatment of critical size bone defects requires functional bone tissues to be created *in vitro* and subsequently implanted in the defect area. Successful engineering of functional bone tissues *in vitro* requires essential elements such as; 1) appropriate cell source, 2) adequate culture conditions with stimuli for differentiation, and 3) scaffold material to which cells can adhere and proliferate uniformly.[1, 2] In addition, experimental techniques have to be established to determine the extent of differentiation of cells and chemical and mechanical properties of the tissue engineered bone constructs.

Mesenchymal stem cells (MSCs) have been widely accepted as a candidate for bone tissue engineering due to their ability to readily differentiate down an osteogenic pathway in the presence of appropriate chemical stimuli.[3-5] However, the response of mesenchymal stem cells to these differentiating culture conditions may be influenced by the type of tissue from which the cells are isolated (bone, bone marrow, adipose tissue and others), age, gender and ethnicity of the donor, and passage number of the cells.[6, 7] Therefore, thorough investigation of these factors are needed to establish standard procedures for isolation and characterization of these cells to be utilized for engineering bone constructs.

Use of optimal media conditions to achieve MSC osteogenesis is of paramount importance. Recent investigations have been able to establish media formulations to achieve osteogenesis of mesenchymal stem cells within a short period.[8-11] Media supplements such as

dexamethasone, ascorbic acid, and β-glycerophosphate provide chemical elements and cues to initiate osteogenic differentiation of MSCs.[8-11] In contrast to the stimulation of MSCs obtained through osteogenic media supplements, cyclic tensile strain when used as a stimulant not only induces MSC osteogenesis, but might also facilitate improved mechanical properties of the final tissue construct. Application of cyclic tensile strain to MSCs for inducing osteogenesis has recently been discussed[12-17], but requires more investigation to determine the optimum strain protocols to achieve osteogenesis in MSCs.

The third major factor that ensures interaction of cells and culture media and greatly affects the successfulness of functional bone tissue engineering is the use of a proper scaffold. Scaffold material plays a major role in bone tissue engineering, first by providing a stable surface for the cells to adhere and proliferate, and then by allowing gradual bioresorption for tissue ingrowth and angiogenesis. Biopolymers such as collagen are able to mimic the natural extracellular matrix providing RGD (arginine-glycine-aspartic acid) sequences for cell adhesion. However, limited control of strength, dimensional stability, and accessability of collagen has limited its use as a scaffold material. Synthetic polymeric scaffolds have been used extensively as a substrate to culture human MSCs (hMSCs) and osteoblasts [18-21]. The development of an appropriate biomaterial structure that would facilitate *in vitro* cell culture and also be a potential *in vivo* implant material poses a significant challenge.

Seeding and proliferation of cells evenly throughout a scaffold and their subsequent differentiation is greatly influenced by the composition, architecture, and 3D environment of the scaffold and biocompatibility of the biomaterial used. The biomaterial should function as

an artificial extracellular matrix (ECM) and elicit biological and mechanical functions of the native ECM. In general, an ideal scaffold for tissue engineering should meet several design criteria: (1) the surface of the scaffold should allow cell adhesion, promote cell growth, and permit the retention of differentiated cell functions; (2) the scaffold should be biocompatible and not produce any degradation by-products that provoke inflammation reactions *in vivo*; (3) the scaffold should be biodegradable ensuring eventual elimination from the body; (4) porosity should be sufficient to provide space for cell adhesion, extracellular matrix regeneration, and to minimize diffusional constraints in culture; (5) the pore structure should allow for even cell distribution throughout the entire scaffold to allow homogenous tissue formation; and, (6) the material should be mechanically stable and processable into a three-dimensional structure [22].

Advantages of synthetic polymers lie in their ability to be reproduced in large scale with controlled microstructures strengths, and degradation rates [2]. Several types of polymers have been used to fabricate three-dimensional (3D) scaffolds for MSC and osteoblast cultures. Among them are polyesters of naturally occurring α-hydroxy acids including polyglycolic acid (PGA), polylactic acid (PLA) [19] and PLGA (copolymer of PLA and PGA). While these polymers are widely accepted, the use of poly -ε- caprolactone (PCL) [21] and polyurethane (PU) [23] are still being investigated. These polyester-based polymers remain popular for a variety of reasons including the fact that these materials have properties that allow hydrolytic degradation through de-esterification. Once degraded, the monomeric components of each polymer are removed by natural pathways; glycolic acid can be converted to other metabolites or eliminated by other mechanisms and lactic acid can be removed through the

tricarboxylic acid cycle [24]. Due to these properties, PLA, PGA, and PLGA have been used in products such as biodegradable sutures for decades and both have received approval by the Food and Drug Administration (FDA).

Although several methods such as gas forming, three dimensional printing, phase separation, emulsion freeze drying, and porogen leaching[22] have been used to fabricate three-dimensional scaffolds with the required thickness and pore size, achieving uniform cell growth throughout the scaffold is still a difficulty due to limited media diffusion to the center of the scaffold. In addition, many of the scaffolds fabricated through gas forming or phase separation methods lack the elasticity required for applying mechanical strain after cell seeding. In fact, most of the studies reported to date on osteogenic differentiation of hMSCs or osteoblasts using 3-D polymeric scaffolds have been carried out in static conditions rather than in dynamic conditions. Therefore, there is a greater need to fabricate a 3-D scaffold with improved media diffusibility and elasticity in order to be able to grow cells uniformly and apply cyclic tensile strains.

## 1.2 Objectives

This body of work was designed to address multiple issues in functional bone tissue engineering. The objectives of this research include: 1) determination of potential uses and limitations of Type 1 collagen as a 3D scaffold for culture and mechanical stimulation of hMSCs; 2) determination of the effects of uniaxial cyclic tensile strain, culture media, and culture duration on osteogenic differentiation of bone marrow derived hMSCs cultured at low

and high density in 3D Type I collagen scaffolds and resulting mechanical properties of such 3D tissue constructs; 3) determination of the effects of uniaxial cyclic tensile strain, culture media and culture duration on the expression of proinflammatory cytokines by hMSCs; and, 4) analysis of the feasibility of using binary polymer blends to fabricate microporous fibers to be used in nonwoven scaffolds for tissue engineering applications.

## 1.3 Manuscript preparation

The findings of this study were presented at nine annual conferences of recognized scientific organizations and published in conference proceedings as peer reviewed abstracts. In addition, these studies resulted in nine manuscripts from which two manuscripts have been published. The remaining manuscripts are in preparation, submitted or in revision. The list of manuscripts is presented below.

**Ruwan Sumanasinghe**, Elizabeth G. Loboa. Cyclic tensile strain upregulates genes indicative of osteogenesis in human mesenchymal stem cells cultured in collagen matrices. *Ann Biomed Eng* - Submitted

**Ruwan Sumanasinghe**, Jason A. Osborne, Elizabeth G. Loboa. Mesenchymal stem cell seeded collagen matrices for bone repair: Changes in nuclear morphology and orientation *in vitro. Ann Biomed Eng* - Submitted

**Ruwan Sumanasinghe**, Jason A. Osborne, Elizabeth G. Loboa. Mesenchymal stem cell seeded collagen matrices for bone repair: Effects of uniaxial cyclic tensile strain, cell density and media conditions on matrix contraction *in vitro. J Biomed Mater Res Part A*- Under review

**Ruwan Sumanasinghe**, Elizabeth G. Loboa. Cyclic tensile strain promotes osteogenesis and increases stiffness of hMSC-seeded collagen matrices but decreases ultimate strength. *Bone* – Submitted

**Ruwan Sumanasinghe**, Elizabeth G. Loboa. Human mesenchymal stem cells cultured at high density upregulate bone markers under cyclic tensile strain. *Biotechnology and Bioengineering* - Submitted

**Ruwan Sumanasinghe**, Nancy Monteiro-Riviere, Elizabeth G. Loboa. Expression of proinflammatory cytokines by bone derived human mesenchymal stem cells under cyclic tensile strain – *J Cell Physiol*- To be submitted

**Ruwan Sumanasinghe**, Carla Haslauer, Behnam Pourdeyhimi, Elizabeth G. Loboa. Melt spun microporous fibers using poly(lactic acid) and sulfopolyester blends for tissue engineering applications – To be submitted

**Ruwan Sumanasinghe**, Susan H. Bernacki, Elizabeth G. Loboa. Osteogenic differentiation of human mesenchymal stem cells in collagen matrices: Effect of uniaxial cyclic tensile strain on bone morphogenetic protein (BMP-2) mRNA expression. *Tissue Engineering* – 2006 epub ahead of print

**Ruwan Sumanasinghe**, Martin W. King. The applications of biotextiles in tissue engineering. *Res J of Textile and Apparel*, 2005: 9(3): 80-90.

# 2 Review of Literature

## 2.1 Introduction

Bone tissue engineering has gained wide attention in the tissue engineering field due to the increased difficulty in performing bone reconstruction and replacement surgeries in older patients and patients with diseases such as osteoporosis. Mesenchymal stem cells (MSCs) have been identified as the primary cells responsible for the generation of bone during fracture repair. Some patients, due to old age and/or disease conditions, lack the ability to continuously generate mesenchymal stem cells; hence their bone regeneration capacity drastically decreases. Several studies have indicated that MSCs, when exposed to appropriate chemical and mechanical stimuli *in vitro*, can undergo osteogenic differentiation[5]. Chemical stimulation includes the use of growth factors and other biochemicals, while mechanical stimuli may include tensile strains, hydrostatic stresses and other means of mechanical stimulation [25]. Some mechanobiological models suggest that intramembranous bone formation is promoted in areas of low to moderate tensile strain and at low compressive hydrostatic stresses [13]. Based on finite element analyses and investigations carried out on animal distraction osteogenesis models, investigators have shown that intramembranous bone formation may be promoted with the application of intermittent tensile strains less than 5% [26] or as high as 10 -12.5% [15] at the fracture site.

These valuable findings on *in vivo* cyclic tensile strain levels provide opportunities to formulate a protocol to facilitate osteogenic differentiation of MSCs *in vitro*. Studies are being conducted to determine the optimum magnitude, frequency and duration of tensile

strain as well as optimal media conditions to induce osteogenesis [16, 17, 27, 28]. While some studies have been performed in 2D cultures under both static and dynamic conditions [9, 10, 17], others have focused on using 3D scaffolds fabricated with biopolymers and various synthetic polymers under static (unloaded) conditions [29, 30]. Although 2D culture conditions offer the advantage of easier analysis of results, the cells may additionally be exposed to fluid shear stresses during the application of cyclic tensile strains [31, 32]. The 3D culture conditions not only provide a way to mimic the *in vivo* environment but also minimize the effects of shear stresses on cells. A 3D culture system also facilitates the investigation of angiogenesis during *in vitro* bone formation. Mesenchymal stem cells may exhibit heterogenic behavior in terms of their proliferation and differentiation capabilities depending on the source, passage number, previous culture conditions, and type of serum used for culture.[6] Due to the large number of factors involved in mechanical and chemical induced osteogenic differentiation, these investigations have become increasingly complex.

The rest of this chapter provides a review of specific literature published to date with respect to the above described items. Although previous investigations have reported their findings on osteogenic differentiation of hMSCs in 2D culture conditions under static and dynamic loading, no work to date has been published on dynamic loading in 3D cultures. In addition, no studies to date have been published on the use of 3D polymeric scaffolds for the application of cyclic tensile strains to hMSCs. Tha body of work was performed for this dissertation and findings from those studies comprise chapters 3-10.

## 2.2 Cellular and Molecular Biology of Bone Formation and Fracture Healing

### 2.2.1 Endochondral bone formation

The bones of the body differ in their shapes, lengths and cellular origins. The cranial and facial bones and the tibia have entirely different physical shapes and are derived from cells of completely different embryonic lineages. Facial bone is derived from ecto-mesenchyme (neural crest), while tibiae are derived from lateral plate mesenchyme. The first studies of chick long bone development were carried out by H.B Fell. [33-35]. Those studies reported the cellular events and phosphatase activity that occurs during bone growth *in vivo* and *in vitro*. In addition, Fell also showed a correlation between hypertrophy of cartilage and the presence of phosphatase activity during calcification. Embryonic bone formation in the chick tibia was extensively studied and compared to mammalian long bone formation by Caplan and Pechak in 1987. They used type 1 collagen and alkaline phosphatase staining on embryonic material to identify initial events of osteogenesis, while type 2 collagen localization and toluidine blue were used to follow changes that occur in cartilage. The matrix surrounding the chondrocytes at the beginning of hypertrophy when stained with toluidine blue appeared darker than nonhypertrophic regions [33, 34, 36]. These investigations provide the primary source for understanding the cellular and molecular events which occur during embryonic bone formation, i.e., chondrogenic and osteogenic cell differentiation. From the above studies, it is clear that the sequence of bone formation: initial formation of the cartilaginous rod, formation of osteoid layer from the stacked osteoprogenitor cells,

erosion and vascular penetration at the mid-diaphysis of the cartilaginous core, and cartilaginous core replacement by marrow and vasculature, are identical during human, mouse and chick bone development. The following steps describe Caplan and Pechak's model of long bone formation in the chick embryo [4].

1) Osteoprogenitor cells arranged in stacked conformation around a pre-chondrogenic core of cells during limb bud formation.
2) Cartilage core forms a rod which can be referred to as the model of the bone.
3) Osteogenic progenitor cell layers closest to the cartilage differentiate to become osteoblasts which forms a unique matrix, the osteoid. The osteoid is formed at the mid-diaphysis as a continuous collar around and outside of the cartilage rod.
4) Osteoid acts as a physical and diffusion barrier to the cells of the cartilage core, which then shows signs of hypertrophy.
5) The osteoid collar becomes mineralized and chondrocyte hypertrophy continues. The osteoid layer is continuously fabricated in both the proximal and distal direction from the mid diaphyseal region. The osteoblasts reside on both the endosteal and periosteal surfaces, allowing thicker bone deposition in humans in contrast to that of the chick.
6) The cartilaginous core at the mid-diaphysis region becomes mineralized. This early hypertrophy and mineralization of cartilage and subsequent resorption of the calcified cartilage in mammals contrast to the sequence observed in chick embryos.
7) Capillaries invade from outside the osteoprogenitor layer, which lies as a web on top of the first layer of bone.

8) Vascular and marrow invasion of the cartilage core occurs through the partially resorbed first bony collar. The cartilage core is completely replaced by marrow and vasculature. Marrow derived mesenchymal stem cells migrate to the resorbed site where they differentiate along the osteogenic lineage to produce bone matrix.
9) Vertical osteoid struts are fabricated perpendicular to this layer and in between capillaries. These osteoids then become mineralized.
10) Deposition of the second layer of bone follows, so that the capillaries are surrounded and the trabeculae are thus formed. Marrow cells are observed to be associated with these capillaries.
11) More layers of trabecular bone are laid down in a sequence involving directional differentiation of osteoblasts from the continually expanding osteoprogenitor layer. The outer osteoprogenitor layers organize and anchor tendons which integrate with newly formed muscles. This process of bone formation is referred to as endochondral bone formation (Figure 2.1).

Since the initial and subsequent positioning of the vasculature is responsible for the formation of bone in a directed manner, it is clear that vasculature is necessary for osteogenic differentiation [3]. From the above it is clear that (MSCs) are extensively used for endochondral bone formation.

### 2.2.2 Intramembranous bone formation

During intramembranous bone formation mesenchymal cells migrate to the site of eventual bone formation. After condensation and alignment in a stacked layer, these mesenchymal stem cells secrete an organic framework of extracellular matrix, the osteoid. Irrespective of their differentiation stage, the cells continue to proliferate during this process. The mesenchymal stem cells that differentiated into osteoblasts begin depositing calcium leading to the formation of bone matrix. This can be termed as direct bone formation compared to endochondral bone formation in which the mesenchymal cells first differentiate into prechondroblasts, mature chondroblasts and subsequently calcify after undergoing cartilage hypertrophy [4, 37].

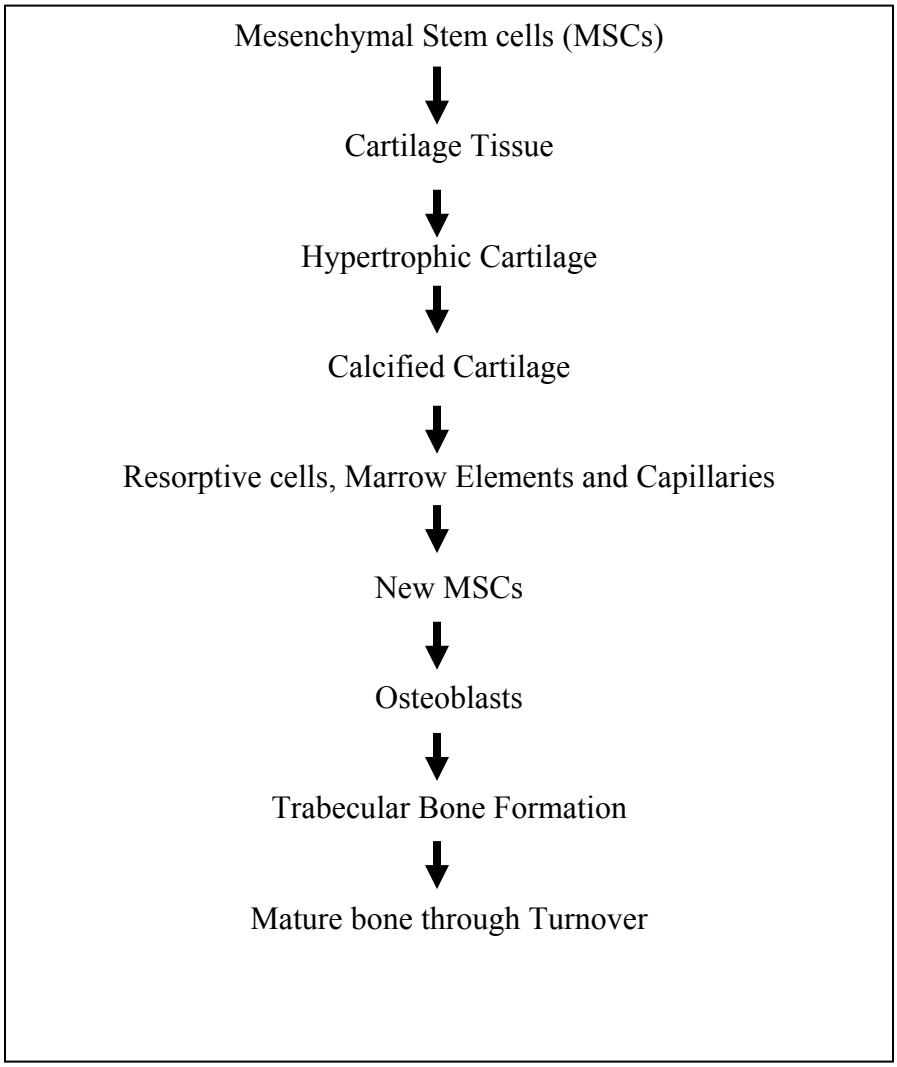


**Figure 2.1.** Endochondral bone formation (Adapted from Caplan and Pechak[1])

### 2.2.3 Mechanobiology of fracture healing

Mechanobiology can be defined as the study of the regulation of biological processes at organ, tissue, cellular and molecular levels by mechanical or physical conditions[13]. Mechanobiological processes play an important role during fracture healing. Bone fracture

is followed by a complex series of events. These events are modulated in part by the mechanics of the fracture, the presence of local and systemic growth factors and biomolecules, and the ability of the body to initialize an appropriate cellular response[3]. Carter and Beaupré [13] divided the fracture repair process into three phases: 1) rapid proliferation of pluripotential tissue; 2) endochondral ossification of the cartilage formed at the fracture site; and, 3) remodeling of the already formed intramembranous and endochondral bone. According to a mechanobiological tissue differentiation concept developed by Carter et al.[38], Blenman et al.[39], and Giori et al.[40], relating tissue differentiation to mechanical loading, direct bone formation is allowed in areas of low to moderate tensile strain and low hydrostatic stresses. Fibrous tissue is formed in areas of moderate to high tensile strain while chondrogenesis takes place in areas of hydrostatic compressive stress (pressure). A model for the mechanoregulation of tissue differentiation proposed by Lacroix and Prendergast [41] involves two biophysical stimuli: tissue strain and interstitial fluid flow. They suggested that fluid flow increases the biomechanical stress and deformation of cells in addition to the stresses and strains generated by collagenous material.

Loboa et al. [15] investigated tensile stresses and strains that exist during mandibular distraction osteogenesis in male rats. The authors proposed that tensile strains between 10 - 12.5% could promote a high rate of intramembranous bone formation. However, much lower strain levels have also been observed to generate new bone. Claes and Heigele [26] used a finite element model to calculate local strains and stresses in a fracture callus and compared them with histological data from a sheep fracture model. They predicted that intramembranous bone

formation occurs for strains smaller than ± 5% and hydrostatic stresses less than ± 0.15 MPa.

The above studies on cell and molecular biology of bone formation and fracture healing reveal that mesenchymal stem cells are extensively recruited during bone generation and fracture repair and that differentiation can be triggered by mechanical loading. The investigations on distraction osteogenesis and fracture repair suggest that intramembranous bone formation is promoted by intermittent tensile strains in ranges at or below 5% and as high as 10% to 12.5%.

## 2.3 Role of Biomolecules and Biochemical Factors on *In vitro* Osteogenic Differentiation

### 2.3.1 Osteogenic markers

In order to better understand the differentiation of MSCs down an osteogenic lineage, it is necessary to identify the roles of growth factors, molecular and biochemical factors, as well as phenotypic markers of bone progenitor cells. Osteogenic differentiation of MSCs can be divided into different stages to facilitate analysis of the function and role of each of these factors: MSCs, osteoprogenitor cells, preosteoblasts, and osteoblasts. MSCs can be defined as cells having the capacity to self-renew and the potential to clonally produce multiple lineages of cells that generate cells of bone, cartilage, muscle, adipose and tendon phenotypes [3]. Osteoprogenitor cells, in contrast, lack self renewal capacity but are able to generate cells of one or more lineages [42]. Preosteoblasts are in a transitional state between the highly proliferative osteoprogenitor stage and mature osteoblasts. They express low levels of bone

markers such as alkaline phosphatase (ALPL), osteocalcin (OCN), and osteopontin (OPN) [42]. Several markers of osteogenesis have been identified and assigned to different stages of bone development. Most of these markers are produced during the differentiation stages of stem cells into preosteoblasts or osteoblasts.

**Type 1 collagen (COL1)** is one of the major extracellular matrix proteins produced in large quantities by osteoblasts. COL1 is organized into large distinct fibrils resulting in a dense collagenous matrix [43]. This high density matrix, referred to as an osteoid, has been found to be produced by osteoblasts during the pre-mineral phase of bone formation, i.e. during 5- 6 days of chick tibia development (40 - 42 days of human tibia development) [4].

**Alkaline phosphatase (ALPL)** has been found to be one of the earliest cellular and extracellular markers of osteogenesis. Studies by Caplan and Pechak [4] showed that ALPL activity initially appears during the formation of cartilage and first osteoid (between 5 and 6 days) in chick tibia development. This is equivalent to 42-50 days of tibia development in human embryos.

**Osteocalcin (OCN),** also known as bone gla protein (BGP), is a 5700-Da molecule that consists of several gamma carboxy-glutamic acid residues. OCN is a strong calcium binding protein which normally functions to limit bone formation without blocking bone mineralization or resorption [44, 45]. Similar to the above markers, osteocalcin first appears at 5 - 6 days of chick tibia development (40 - 42 days of human tibia development) [4].

**Osteonectin (OSN),** a 32-kDa protein, has been found to bind to calcium, hydroxyapatite and collagen [46]. It is synthesized by osteoblasts and deposited within the collagenous matrix of bone. It has been found that osteonectin-collagen complexes support plasminogen binding,

which is speculated to play an important role in the degradation and remodeling of bone matrix proteins during resorption *in vivo* through local activation of plasminogen [47].

**Osteopontin (OPN),** also known as secreted phosphoprotein-1 (SPP1), is a multifunctional phosphorylated glycoprotein found in bone. The mRNA of osteopontin is found to be up-regulated in response to vitamin D3 [48]. Parathyroid hormone [49] and elevated phosphate levels [50] in bone osteopontin have been shown to affect both the differentiation and recruitment of osteoclasts [51] and to inhibit hydroxyapatite (HA) formation and growth [52].

### 2.3.2 Growth factors

MSCs and osteoblasts respond to a number of bone specific and other soluble growth factors. Among the multiple cytokines involved in osteogenesis, two cytokines: Transforming growth factor-β (TGF-β) and insulin-like-growth factor (IGF) play vital roles.

**TGF-β** is one of the most abundant mitogens found in human bone extracellular matrix. It has been found to be localized in active centers of bone differentiation, i.e., cartilage canals and osteocytes [53]. TGF-β belongs to a superfamily of polypeptide growth factors, i.e., transforming growth factors (TGFs), which also include bone morphogenetic proteins (BMPs), activins, and growth and differentiation factors (GDFs). TGF-β affects cell growth and differentiation during the developmental stages of embryos and also during tissue repair [54]. It has been reported that TGF-β can provide competency for early stages of osteoblastic differentiation, but inhibits late stage osteoblast differentiation [55]. TGF-β is believed to be activated by an acidic environment created by osteoclasts, where increased bone resorption

results in an increased release of TGF-β. This subsequently stimulates osteogenic cells [56].

**Insulin-like-growth factors (IGFs)**, are the second most abundant growth factors in bone. IGFs are synthesized by osteoblasts and have been found to stimulate osteoblast proliferation [57]. IGFs are present in bone, complexed to IGF-binding proteins (IGFBPs) which inhibit the function of IGFs in a dose dependent manner [58]. Some of the IGFBPS e.g. IGFBP5s have been shown to increase osteoblast proliferation while others inhibit it [59]. In addition, TGF-β also inhibits some of the IGFBPs resulting in stimulation of osteoblast development [54].

**Bone morphogenetic proteins (BMPs)** are low molecular weight glycoproteins that function as morphogens and belong to the TGF-β super family [60]. More than 40 of the BMP proteins have been isolated. These include BMP-2 to BMP-6, BMP-7, also known as osteogenic protein-1 (OP-1), and BMP-8 (OP-2), as well as growth and differentiation factors-5 (GDF-5) to GDF-7 [61]. Similar to the other proteins in the TGF superfamily, BMPs are synthesized within the cells as precursor forms and then subsequently proteolytically processed at the carboxy-terminal region resulting in a mature protein with approximately 130 amino acids [61]. Among the BMPs, BMP-2 and BMP-4 are closely related in their amino acid sequence while BMP-5 and BMP- 7 show the same relationship. GDF-5 and GDF-7 also have similar amino acid sequences. Studies by Wang et al. [62] have shown that application of BMP-4 and high concentration of BMP-2 to mouse mesodermal progenitor cells induced them to differentiate to osteoblasts. Human MSCs (passage 4) were reported to have increased proliferation when cultured in serum free basal growth medium with physiological concentrations of BMP-2 [63]. Oreffo et al. [64] investigated expression of different osteogenic markers in hMCSs cultured in both complete basal and osteogenic media up to 14 or 21 days.

Highest levels of BMP-2 and BMP-4 expressions were observed after 21 days in osteogenic medium. These expressions were found to correlate with the induction of an osteoblast phenotype corresponding to ALPL, COL1 and OCN expressions. In another study [65], hMSCs were cultured in both osteogenic (but without dexamethasone) and basal medium containing BMP-7 under static conditions and osteogenic differentiation was investigated after 2 and 4 weeks. BMP-7 in osteogenic medium was observed to stimulate hMSCs into mature bone cells which deposited mineral and increased ALPL activity.

### 2.3.3 Biomolecules

Apart from the markers and growth factors, several biomolecules are involved during bone cell development and bone growth. Recent studies reveal that several transcription factors function as regulators for the expression or maintenance of the osteo-phenotype. Transcription factors are nuclear proteins that regulate the activation of multiple other genes. They are typically a part of a large regulatory protein complex. With respect to bone, core-binding factor -1 (Cbfa1) plays a major role in the formation and maintenance of bone cell lineage [66]. Cbfa1 binds to the promoter regions of all osteoblast specific genes such as OCN, COL1, bone sialoprotein, OPN and ALPL and controls their expression [67]. It is regulated by vitamin D3 and BMP-7. It has been shown that low levels of mechanical deformation (stretching) of human osteoblastic cells in basal media up-regulates the expression and DNA binding activity of Cbfa1[68]. TWIST, another helix-loop-helix (HLH) transcriptional factor, appears to play a negative role in osteogenesis of progenitor cells. It has been reported [69] that

overexpression of TWIST in human osteoblast-like sarcoma cells caused cells to be maintained in a more osteoprogenitor cell-like phenotype whereas inhibition of TWIST caused an increase in ALPL and COL1 expression. This study indicates the dual role played by TWIST depending on its concentration and activity in human osteoblast cells.

### 2.3.4 Biochemicals

Presence of stimulatory chemicals in the culture media can also impart a significant effect on the extent and rate of proliferation and differentiation of MSCs and pre-osteoblasts. Osteogenic media used in most studies for osteogenic differentiation of MSCs contains osteogenic supplements such as dexamethasone (Dex), ascorbic acid (AsAP) and β-glycerophosphate (βGP).

**Dexamethasone** is a synthetic glucocorticoid which functions as an anti-inflammatory agent, and regulates T cell survival, growth, and differentiation [70]. It also inhibits the induction of nitric oxide synthase [71]. Studies by Tenenbaum and Heersche [72] have demonstrated that Dex stimulates *in vitro* osteogenesis through stimulation of progenitor cell proliferation. However, an excess of dexamethasone *in vivo* in animals has been shown to decrease bone formation and increase bone resorption [73].

**Ascorbic acid,** also known as vitamin C, plays a major role in the assembly of mature collagen fibrils. The formation of interchain hydrogen bonds between collagen fibrils affects the self assembly and stability of collagen fibrils. This is found to be facilitated by ascorbic acid which acts as a cofactor for the enzyme prolylhydroxylase that transfers hydroxyl groups to selected proline and lysine residues in the procollagen chain [74] .

**β-glycerophosphate** has been found to be a source of phosphate for matrix mineralization [75]. Investigations have shown that ALPL is required for βGP mediated mineralization indicating that release of phosphate from βGP is mediated by ALPL [76].

Jaiswal et al. [9] investigated the osteogenic differentiation of hMSCs (passage 2-3) under static conditions at different concentrations of Dex, AsAP and βGP in basal media containing 10% fetal bovine serum (FBS). The optimal osteogenic conditions in terms of the presence of osteoblastic morphology, ALPL activity, osteocalcin mRNA expression and matrix mineralization were shown with basal medium supplemented with 100 nM Dex, 0.05 mM AsAP and 10 mM βGP. Studies carried out by Halvorsen et al. [10] showed that hMSCs in the presence of 10 nM Dex, 50 μg/ml AsAP and 10 mM βGP with complete basal medium had higher matrix mineralization accompanied with higher expression levels of ALPL, OCN and OPN compared to control cells in basal medium.

## 2.4 Effects of Cyclic Tensile Strain on *In vitro* Osteogenic Differentiation

### 2.4.1 Application of tensile strain in 2D culture conditions

Most studies on the mechanical stimulation of either osteoblasts or mesenchymal stem cells have been carried out in 2D culture conditions. Although the behavior of the cells in 2D culture conditions could be entirely different from that in 3D, these studies provide the basis for understanding the expression of osteogenic markers and the extent of osteogenic differentiation upon application of cyclic tensile strains.

One study performed on mesenchymal stem cells (MSCs) cultured in osteogenic media (serum containing complete growth medium supplemented with 50 μg/mL ascorbic acid, 10 mM β-glycerophosphate, and 0.1 μM dexamethasone) investigated the application of 3% cyclic tensile strains applied equibiaxially at 0.25 Hz for up to 16 days on type 1 collagen (COL1) coated six well plates [17]. The MSCs used in that study were isolated from adult human bone marrow and passaged through 4 to 7 prior to experimentation. They found that strain slowed proliferation of hMSCs over a 10 day period. Alkaline phosphatase (ALPL) expression was not affected by strain and there was a one fold increase in matrix mineral deposition in strained cells after 16 days.

Other investigations looked at human bone marrow stromal cells (hBMSCs) from seven donors (passage 2) to investigate osteogenic differentiation under 2 and 8% cyclic tensile strains at 1 Hz [16]. The cells were strained for three 2 hour durations with 1 hour rest period in between. Those cells were cultured in Dulbecco's modified Eagle (DMEM)

medium containing 5 μg/mL ascorbic acid with and without 2.55 μM dexamethasone to determine the effect of both dexamethasone and mechanical strain on hBMSCs. The protein content measurements carried out after 3 days showed that hBMSCs cultured with dexamethasone and cyclically strained at 8% expressed significantly greater ALPL than the stretched controls or 2% strained cells after 4 and 7 days. The hBMSCs cultured without dexamethasone also showed a significant increase in ALPL after 7 days. Cells cultured without dexamethasone and strained at 8% showed the highest increase in osteocalcin (OCN) after 4 days compared to 2% and unstrained controls. The effects of cyclic strain on the increase of both ALPL and OCN expressions were greater than that resulting from the addition of dexamethasone alone. Compared to unstrained and 2% strained cells, hBMSCs cultured with dexamethasone and strained at 8% exhibited the highest collagen 1 mRNA expression after 4 and 7 days. Similar to ALPL and OCN, mechanical straining of hBMSCs had significantly more influence than dexamethasone on increasing COL1 expression.

Comparable results have been reported with stromal cell lines isolated from mouse bone marrow and cultured in osteogenic medium, with reduced fetal bovine serum, under equibiaxial cyclic tensile strain [28]. Those cells were cultured in osteogenic medium for 7 days prior to the application of cyclic tensile strain at 0.8, 5, 10 and 15% elongation, at 1 Hz for 2 days. After 2 days, a significant increase in cell proliferation was observed at 10 and 15% elongation compared to unstrained controls. ALPL activity of 0.8 and 5% elongated cells was significantly increased after 24 hrs, with 0.8% still showing a significant increase at 48 hrs. Expression levels of COL1 mRNA significantly increased in cells strained at 10% and 15% for 48 hrs, while OCN expression was significantly decreased by mechanical strain at all

strain levels and time points. From that study, it appears that high magnitudes of strain applied to stromal cells result in significant increases in cell proliferation and COL1 mRNA levels, and significant decreases in ALPL activity and osteocalcin mRNA levels. In contrast, low magnitude strains increased the ALPL activity.

Findings from these three studies indicate that the expression of osteogenic markers differs depending on the cyclic tensile strain level, frequency, strain period, culture duration, and growth factors used in culture. Not only these factors but also the methods to isolate and subcultivate hMSCs, pre-culture conditions, and the lot of fetal bovine serum used might also play vital roles in osteogenic differentiation of hMSCs.[77]

It has also been shown that MSC cultures fed daily with complete basal growth media instead of twice weekly grew at a faster rate.[6] With higher passage numbers, hMSC growth rate decreasedd resulting in a reduced number of cells at the end of 9 days in culture. It was also observed that the self renewal capacity, i.e. the number of population doublings, declined after the $10^{th}$ passage.

The ability of cells cultured *in vitro* to respond to a mechanical signal depends on the sensitivity of the cells and how the mechanical stimulation is transferred from the surrounding environment to the cell nucleus. A window of mechanical usage for bone has been defined by an upper boundary of 1500 μstrain (0.15% strain), also termed the minimum effective strain, above which bone undergoes modeling and structural changes in order to reduce the local strains.[78] Below a lower threshold of 50 μstrain (0.005% strain), bone is resorbed until the local strains are increased [78]. The extent of mechanical stimulation applied to the cells by means of cyclic tensile strain may depend on the strain level, or amplitude,

frequency, number of cycles, strain duration, or combination of all these factors. It is important to determine which of the above factors, when used alone or in combination, would create an optimal environment for bone generation from MSCs. The responsiveness of bone derived cells to strain amplitudes, frequency, cycle number, and strain duration *in vitro* has been well documented [27, 79-81]. A recent study was conducted on proliferation of osteoblasts using a number of different donor derived osteoblast-like cells grown on silicon dishes under cyclic homogenous stretching (achieved by 4-point bending in basal growth medium without penicillin and reduced amount (2%) of fetal calf serum). That study showed that maximum cell number was achieved with 1800 bending cycles/day at 1 Hz and 1000 μstrain for 2 days compared to 40, 60, 3600 cycles and unstimulated cultures [82]. The number of cells was reduced when the number of cycles was increased to 3600. This could be due to either a decrease or increase in DNA synthesis or activation of apoptosis pathways. At a constant strain magnitude and number of strain cycles, cell proliferation did not show a significant dependency on the frequency of cyclic strain, although at all frequencies cell proliferation significantly increased compared to unstimulated controls. When strain magnitude and stimulation time were made constant with varying frequency and number of cycles, highest proliferation was observed with 1 Hz and 300 cycles compared to other frequencies. This suggests that an appropriate frequency together with a sufficient number of cycles will be needed for effective mechanical stimulation of osteoblasts. It is clear that the effects of frequency should not be considered separately from the cycle number. In that study, the number of cells was counted 48 hrs after the final stimulation. Since this time period is enough for cells to divide multiple times, the values likely do not correctly reflect

actual cell proliferation due to the effect of mechanical strain at the end of two days.

A similar study was carried out by the same group [83] on five different osteoblast populations subjected to cyclic homogenous stretching by 4-point bending at 1800 cycles/day, 1 Hz and 1000 μstrain (0.1%) for 2 days. In addition to an increase in cell proliferation, procollagen I propeptide (CICP) concentration was increased in cyclically strained cells compared to unstrained controls. In contrast, ALPL activity and OCN concentration were both reduced in mechanically strained cells. This showed that cyclic tensile strains at physiological levels caused an increase of osteoblast proliferation with an increase in matrix production. These are characteristic activities of early osteoblasts. The decrease of ALPL and OCN activity suggests that differentiated osteoblasts activities including matrix mineralization were reduced due to the mechanical strain.

It is important to determine whether there is a difference in the response of mesenchymal stem cells and osteoblasts when the applied cyclic tensile strain is continuous versus intermittent. A study carried out to determine the response of primary rat osteoblast like cells to continuous (1 hour) or intermittent (four 15 min cyclic strain durations with 15 min relaxation in between) uniaxial cyclic tensile strains at 1000 μstrain and 1 Hz in osteogenic differentiation medium revealed that intermittent strains resulted in increased cell proliferation (up to 8 days) and calcium deposition (up to 24 days) compared to unstrained and continuously strained cells [84]. However, ALPL activity in intermittently strained cells was lower than that of unstrained controls but higher than continuously strained cells after both 4 and 8 days. This study showed that osteoblasts can be more effectively stimulated by intermittent uniaxial cyclic strain than continuous strain. Similar to the previously mentioned

investigations, this also shows that cyclic strain regimens lead to an increase in cell proliferation and matrix production.

Another factor that influences the response of osteoblasts to mechanical strain is the differentiation stage of the osteoblasts at the time of the application of strain. A recent study by Weyts F.A. [85] on human fetal osteoblast cells cultured in osteogenic differentiation media (2% fetal calf serum, 1 μM dexamethasone and 10 mM β-glycerophosphate) for 4, 11, and 18 days prior to the application of equibiaxial cyclic tensile strains of 0.4, 0.9 and 2.5%, applied at a frequency of 0.5 Hz for 72 hrs showed that a proliferative response, i.e. increase of cell number and decrease of apoptosis, was observed in osteoblasts in the matrix maturation stage (14 days) at which ALPL activity in the cells was high. This response was independent of the strain levels applied. That study also revealed that combined mechanical strain and differentiation induced proliferation in 7 day old differentiating osteoblasts irrespective of the strain levels used.

In addition to the use of silicone membranes as a culture material, other types of materials have also been used to culture and mechanically strain osteoblasts.[86] Di palma et al.[86] isolated osteoblasts from trabecular bone and cultured them on an alumina coated ceramic substrate (Ti-6Al-4V titanium alloy) in media supplemented with 0.05 μM vitamin D3 and 50 μg/mL ascorbic acid. The cells were cyclically strained at 600 μstrain and 0.25 Hz for 15 mins three times a day for either 5 or 15 days. They found that mechanical stimulation Significantly increased cell proliferation after 5 days while no effect was observed on ALPL activity compared to unstrained cultures grown on polystyrene discs. However, when the application of strain was continued for 15 days, cell number decreased and ALPL activity

was significantly increased. This result could be due to the fact that osteoblasts reach confluence between 5 -15 days and start differentiation afterwards.

### 2.4.2 Application of tensile strain using three-dimensional biopolymeric scaffolds

#### 2.4.2.1 Advantages of using 3D biopolymeric scaffolds for culture

Far fewer studies have investigated the effects of mechanical strain on mesenchymal stem cells or osteoblasts in a 3D environment. Although a vast number of studies have been reported on various types of 3D scaffolds in static culture conditions [18, 30, 87], very few of these scaffolds have the ability to be mechanically deformed or exposed to cyclic tensile strain without harming the structural integrity of the scaffold [29, 88].

Several advantages exist in the use of 3D scaffolds for bone tissue engineering. The 3D *in vitro* environment more closely resembles the *in vivo* environment where the intercellular signaling and interactions between cells and extracellular matrix take place. With respect to mechanical stimulation of cells, if one needs to investigate the specific effects of uniaxial cyclic tensile strain on osteogenesis, the effects from fluid shear stress during application of strain need to be minimized. This is due to the fact that several studies have shown that bone marrow stromal cells can also undergo osteogenic differentiation upon application of fluid shear stresses [31, 32, 89]. When 2D culture conditions, i.e. the use of silicone membranes or other types of flexible substrates are used to apply mechanical strains, it is possible that the cells would also experience shear stresses by the volume of media resting on

top of the cell layer. Therefore, one way to minimize this fluid shear stress is to use a 3D scaffold in which the cells are entrapped inside the scaffold minimizing exposure to moving volumes of media.

Biopolymers such as collagen and fibrin have sufficient tensile strength to withstand cyclic mechanical strains [90]. Therefore, these polymers have been used frequently as 3D matrices to grow and mechanically stimulate MSCs and osteoblasts. In addition to the inherent characteristics of non-toxicity, biodegradability and easy accessibility [90], both collagen and fibrin offer the added advantage of possessing integrin binding sequences such as RGD (arginine-glycine-aspartic acid) [2] sequences, which cells can attach; leading to an increase in growth and proliferation as compared to seeding on a synthetic scaffold. Since collagen and fibrin are the most common fibrous proteins found in the extracellular matrix, use of these provides an *in vitro* means of mimicking the natural extracellular matrix *in vivo*.

#### 2.4.2.2 Effect of cyclic tensile strain on the osteogenic differentiation of osteoblasts in 3D biopolymeric scaffolds

Osteoblasts have been used as the main source of cells in the few studies reported so far to investigate increased osteogenesis under mechanical stimuli in 3D cultures [29, 88, 91]. Ignatius et al [29] used human osteoblastic precursor cells in complete growth medium to investigate the effects of uniaxial cyclic tensile strain at 10,000 μstrain (1%), 1 Hz and 1800 cycles (30 mins) everyday for 3 weeks. An initial cell seeding density of $1.5 \times 10^5$ cells/ml was used for their study. Cells harvested on days 3, 7, 10, 14, 17 and 21 showed a significant increase (12-25%) in cell proliferation at all time points compared to the unstrained controls.

With respect to mRNA expression of differentiation markers, compared to controls, a significant increase of ALPL was observed only at days 7 and 17 while the expression of OCN significantly increased at both 3 and 21 days. In contrast, the expression of COL1 was nearly constant from day 7 to 21, but showed a significant increase compared to the control only at days 3 and 7. A significant increase in osteopontin (OPN) was observed at days 3 and 14. The observed contraction of the collagen matrix was dependent on the seeding density, such that at a lower cell density contraction was reduced.

It is evident from that study that COL1, OCN and OPN mRNA expressions were up-regulated early in the culture period and then subsequently down-regulated until the latter part of the culture duration. Although the first upregulation of ALPL mRNA expression was delayed when compared to the other markers, the second upregulation occurred at approximately the same time as the others. The fact that osteogenic differentiation observed in that study resulted solely from mechanical stimulation, .i.e. without the addition of osteogenic growth factors to the medium, shows that osteoblast precursors can be positively mechanically stimulated towards osteogenic differentiation.

The effect of uniaxial mechanical strain on MC3T3-E1 mouse cells seeded at $4.0 \times 10^5$ cells/ml in type 1 collagen matrices was reported by Tanaka et al [91]. Their study analyzed the application of strains with large amplitude and low frequency (3000 μstrain and 3 Hz), or low amplitude and broad frequency (300 μstrain up to 50 Hz) or the combination of the two for 3 mins per day up to 3 or 7 days. Although cell proliferation was decreased in all strained cells compared to unstrained controls, the decrease was significant when two types of strains were combined. However, OCN expression in those cells exposed to combined strain profiles

was up regulated after 7 days. No difference due to mechanical stimulation was observed in ALPL activity or mRNA expression levels of COL1 and OPN.

Akhouayri et al [88] investigated the effect of static and dynamic stresses or strains on the osteogenic differentiation of rat osteosarcoma cells cultured in 3D collagen matrices. Dynamic forces in that study were created by shaking freely floating collagen constructs on a shaking platform at 25 and 50 rpm up to 18 days. The authors found a lower cell growth in dynamically stressed cells than in unloaded controls or statically stressed (stress was constant throughout culture period) cells. On average, ALPL activity was also lower in dynamically stressed cells than in both control and statically stressed cells. In contrast, the OCN activity was higher from 8 to 14 days in dynamically stressed cells compared to the others. Increased mineralization in static and dynamic conditions was observed starting from 15 days through the end of the culture period (18 days) at which point the dynamically stressed cells exhibited the highest mineralization. The transmission electron microscopic (TEM) analysis revealed 3 types of mineralization: mineral crystals along the collagen fibers, mineral nucleations in matrix vesicules, and those created by cell debris mineralizations. One limitation of that study was the unknown magnitude of the applied mechanical stimulus. The authors also failed to categorize or define the type of stress imparted on the rat osteosarcoma cells which limited the data to be used for comparison purposes.

Studies have also been reported on the use of other types of scaffolds such as mineralized collagen sponges (cross linked type 1 collagen fibers coated with non-crystalline hydroxyl apatite) having pore sizes ranging from 4-200 μm and a porosity greater than 95% [92]. Human MSC cultures on these scaffolds revealed an increase in cell proliferation up to 8

days and consistent increase in the expression of ALPL, OCN, BSP and BMP-2 throughout the entire culture period.

It is clear from the results of the first two studies described in this section that the extent of proliferation and differentiation of osteoblasts upon application of strain greatly depends on the strain profiles, i.e. the combination of strain magnitude, frequency and cycle time (duration). The proliferation of osteoblast precursors appears to increase upon application of strains at physiological frequencies but above physiological magnitudes. At these conditions all osteogenic markers such as COL1, OCN, OPN and ALPL mRNA seemed to up regulate between 14 -21 days. However, when strain amplitudes are decreased below physiological levels keeping frequencies much above normal levels (mild to strenuous exercise frequency), the proliferation appears to decrease. Other than OCN mRNA which showed an up regulation only after 7 days, all other markers were not affected.

## 2.5 Use of Synthetic Polymeric Scaffolds for 3D Culture

### 2.5.1 Types of polymeric scaffolds

In addition to those studies that involve application of strain [29, 88, 91], many studies have been performed investigating the osteogenic differentiation of MSCs and osteoblasts using static culture conditions within a variety of 3D scaffolds. Among various materials used to fabricate these scaffolds, poly(glycolic acid) (PGA), poly(L-lactic acid) (PLLA), poly(D, L-lactic acid-co-glycolic acid) (PLGA), poly(polyethylene terephthalate) (PET),

polyurethane (PU), poly(ε-caprolactone) (PCL) and silk are widely used [21, 30, 93, 94]. Studies are also being carried out to investigate the possibility of combining biopolymers such as collagen and fibrin with polymeric scaffolds by means of coating or spraying to enhance cell adhesion and proliferation.

A number of methods have been used to prepare porous three-dimensional biodegradable scaffolds using PGA, PLLA and PLGA. These include: (1) gas forming, (2) fiber extrusion and bonding, (3) three dimensional printing, (4) phase separation, (5) emulsion freeze drying, and (6) porogen leaching [22].

Macroporous sponges of PLLA, PLGA and PGA polymers are formed by a gas forming technique that uses high pressure $CO_2$ gas. These macroporous sponges are fabricated by equilibrating polymer discs with high pressure $CO_2$ gas and then generating thermodynamic instability to create macropores. The porosity and pore structure can be controlled by controlling the volume of gas dissolved, the rate and type of gas nucleation, and the diffusion rate of gas molecules through the polymer [22]. Gas forming and particulate leaching techniques have been combined to prevent the formation of closed cellular structure within the scaffold. This is achieved by a process in which a mixture of polymer discs and salt particulates are compression molded and allowed to equilibrate with high pressure $CO_2$ gas. To obtain macro pores within the polymer scaffold the salt particulate are leached out after expansion.

Fiber meshes in the form of woven or knitted and non-woven structures have also been widely used for scaffolds. Scaffolds fabricated with PGA, PLGA and PLLA fibers have been investigated for various tissue engineering applications. The large surface area due to

the fibrous form of the structure, and open pore configuration, owing to the inherent porosity of these structures, improve cell attachment and rapid diffusion of nutrients assisting cell survival and growth. Nonwoven scaffold materials have been prepared by spraying atomized solutions of PLLA or PLGA on to a non-bonded PGA fiber mesh [95]. The thickness of the polymer coating can be controlled by changing the spraying time. Such a composite material exhibits mechanical properties of the PGA core and surface properties of the PLLA and PLGA coating, thus enhancing cell attachment, growth and function. 3D scaffolds have also been fabricated by thermal compression of nonwoven polyethylene terephthalate (PET) fabrics and used to culture human tropoblast cells ($ED_{27}$ cells) and NIH 3T3 fibroblast cells [87]. It was found that the spatial organization and proliferation rates of the above cells were affected by the pore size of the matrix. Compared to larger pores, the small pores in the matrix allowed cells to spread better and proliferate faster.

Three dimensional printing, a solid free-form fabrication process, uses an ink jet printer to print a binder into sequential powder layers to fabricate a 3D matrix. A porous three-dimensional scaffold is created by sequential deposition and delivery of powder and binder, respectively onto an initial powder bed to form layers [96]. Although the 3D printing technique appears to be useful for preparing predetermined porous structures, its application in bone tissue engineering is still in its infancy.

Scaffolds fabricated using the phase separation technique can be classified as foams. The phase separation technique is based on thermodynamic demixing of a homogenous polymer solvent solution into a polymer-rich phase and a polymer poor phase [97]. Foam results when the solvent in the polymer mix is removed by freeze-drying. Such an emulsion

freeze-drying method has been used to fabricate aliphatic polyester based scaffolds [98]. The porosity and the pore size of the resultant structure can be controlled by varying the volume fraction of the dispersed phase, polymer concentration and molecular weight. Natural biopolymers such as collagen in aqueous solutions can also be used with the freeze drying technique to produce porous matrices [22]. Since manipulations during both phase separation and emulsion freeze-drying techniques are conducted at low temperature, these two techniques can be combined to incorporate proteins into the scaffold [99]. However, drawbacks such as difficulty in controlling pore size and obtaining large open pores exist. In porogen leaching, pores are created by casting a mixture of a polymer solution and porogen in a mould, drying the mixture, and leaching out the porogen with water. Normally water-soluble particulates such as salts and carbohydrates are used as porogen materials. The pore size can be controlled by varying the property and fraction of porogen [93, 100].

Polymeric scaffolds are usually treated with cell culture medium containing serum prior to cell seeding to allow deposition of protein layers on the scaffold material so as to enhance cell adhesion and growth. However, scaffolds derived from biodegradable materials lack cell recognition and adhesion sites. In order to provide cell recognition and adhesion sites to synthetic scaffolds, they can be hybridized with naturally derived collagen which possesses these sites but lacks sufficient strength for bone tissue engineering if used alone to form a scaffold. In studies carried out by Chen et al [101], synthetic porous matrices were immersed in a collagen solution under vacuum to fill the pores and then frozen and freeze-dried to allow the formation of collagen microsponges within the polymer pores. Subsequently, the collagen microsponges were crosslinked by treatment with glutaraldehyde.

Mouse fibroblasts seeded onto these hybrids sponges adhered well and proliferated to secrete their respective extracellular matrices during the culture period [102].

Finally, any three dimensional scaffolds prepared for bone tissue engineering should be osteoconductive to allow osteoblasts and osteoconductive cells to adhere, migrate, differentiate and synthesize new bone matrix.

### 2.5.2 Osteogenic differentiation of MSCs in 3D polymeric scaffolds under static condition

Yoneno et al.[11] recently investigated the multidifferentiation potential of bone marrow derived hMSCs cultured in 3D collagen matrices. Human MSCs were cultured in osteogenic differentiation medium containing 100 nM dexamethasone, 10 mM β-glycerophosphate and 0.05 mM ascorbic acid for 14 days. Expression levels of COLI, bone sialoprotein and ALPL mRNAs increased significantly after 5 days of culture in osteogenic medium. In addition, they observed significant positive staining for ALPL activity and alizarin red in osteogenic medium compared to those cultured in growth medium.

Takahashi and Tabata [30] investigated the proliferation and osteogenic differentiation of rat mesenchymal stem cells (rMSCs) (passage 2) cultured on different melt blown PET nonwoven scaffolds with fiber diameters ranging from 2.0 - 42.0 μm and porosities ranging from low (93%) to high (97%) for 3 days in both complete basal and osteogenic medium. These cultures were maintained in static conditions at all times. The morphology of the cells became flatter with increasing fiber diameter while there appeared to be no effect due to porosity of the structure. The number of cells attached during seeding was greater with larger

diameter fibers (again, no effect from porosity). Cell proliferation showed a significant increase when the fiber diameters were larger than 12μm while high porosity structures showed a significantly greater proliferation. ALPL activity of the cells was highest in structures with 9 μm fibers irrespective of porosity. Similarly, OCN activity was highest in cells cultured in structures with 9 μm and 12 μm fibers irrespective of the porosity. In addition, lower porosity structures showed a significantly higher ALPL and OCN activity than higher porosity scaffolds. All these effects were only observed in cells cultured in osteogenic medium [30].

Grayson et al. [18] reported that proliferation of hMSCs grown on PET non-woven scaffolds with porosities greater than 85% and in basal medium under static conditions was lower than that of 2D cultures after 1 month. However, the expression of extracellular protein such as COL1, COL1V, and laminin were significantly greater in the cells grown on the PET non-woven scaffolds. COL1 and laminin were observed as distinct fibrils in the extracellular matrix. The ALPL activity of the cells grown in osteogenic medium and on PET scaffolds peaked after 12 days of culture and subsequently reduced through 25 days. However, the ALPL activity was higher than that of the 2D controls throughout the entire culture period. Rat MSCs (passage 2 or 3) grown in osteogenic medium on type 1 collagen coated electrospun non-woven PCL scaffolds under dynamic conditions (rotating bioreactor at 4 rpm) for 4 weeks were also observed to migrate and produce extracellular matrix proteins [94]. These non-woven scaffolds had a mean fiber diameter of 400 nm (± 200 nm). An abundance of calcified matrix and COL1 was observed in the extracellular matrix after 4 weeks.

Similar results were observed with hMSCs cultured in osteogenic medium on

electrospun non-woven PCL scaffolds under static conditions up to 21 days [21]. The scaffolds used in that study had an average fiber diameter of 700 nm. Porosity values of the scaffolds were not reported. After 21 days in osteogenic medium, the cells appeared to be polygonal osteoblast/osteocyte like cells with significant matrix mineralization and ALPL activity. Further, the matrices in osteogenic media conditions stained positively for COL1 and bone sialoprotein (BSP). Addition of osteogenic medium dramatically increased gene expression levels of ALPL, BSP and OC with negligible effect on COL1 compared to the control cultures maintained in complete basal growth medium.

In another study reported by the same authors [103], PLGA was used to fabricate electrospun non-woven scaffolds. Fiber diameters of these scaffolds ranged from 500 - 800 nm with a mean porosity of 91.63% and pore diameters from 2.0 – 465.0 μm. The authors reported that the proliferation of hMSCs (passage 2) when cultured in complete basal growth medium under static conditions increased throughout the entire culture period of 10 days.

In most of the above studies, MSCs were cultured at static conditions without any dynamic strains and, in some cases, in the absence of chemical stimulation. These studies show that MSCs can be successfully grown on fibrous 3D scaffolds with considerably high rates of proliferation, in most cases leading to osteogenic differentiation. According to the above studies it is clear that a scaffold for hMSC proliferation and differentiation under static conditions should have porosity above 90%. The differentiation and mineralization of hMSC was observed in structures with fiber diameters ranging from the nanoscale to microscale. It is difficult to determine a common time frame for the activation of osteogenic differentiation due to the existence of experimental variations between different studies.

Apart from using fibrous non-woven scaffolds to culture MSCs, use of other types of scaffolds have also been investigated. A study conducted by Ren et al. [93] used PLGA porous scaffolds formed by a solution casting /salt leaching method to culture rabbit MSCs in osteogenic medium up to 3 weeks. The pore sizes of the scaffold ranged from 100 - 250 μm with porosity over 85%. Cell proliferation was observed to increase throughout the culture period while calcification started after 2 weeks and continued through the end of the culture period.

Meinel et al. [20] compared osteogenic differentiation of hMSCs (passage 2) under static conditions in scaffolds fabricated by a porogen leaching technique using collagen, silk and silk with covalently bound RGD sequences. These scaffolds had a porosity of 98%. Throughout 4 days of culture, calcium content consistently increased in cell layers cultured with osteogenic medium and in both silk and silk-RGD scaffolds compared to collagen. Silk-RGD scaffolds showed the highest calcium deposition. A similar trend was exhibited in ALPL activity. Compared to collagen expression, both BSP and BMP-2 was greater in cells cultured on silk and silk-RGD scaffolds in the presence of osteogenic media at all time points. Expression of BSP and BMP-2 decreased after 2 weeks in all scaffolds. Cells cultured in silk and silk-RGD scaffolds showed a similar expression of OPN after 4 weeks in osteogenic medium. With respect to mineralization, after 4 weeks, silk-RGD was more extensively mineralized than others.

# 3 Mesenchymal Stem Cell Seeded Collagen Matrices for Bone Repair: Effects of Uniaxial cyclic Tensile Strain, Cell Density and Media Conditions of Matrix Contraction *In vitro*

Bone mechanobiology and main factors influencing functional bone tissue engineering was reviewed in the previous chapter. The contraction of collagen matrices over time upon seeding of MSCs could detrimentally affect the dimensional stability of the matrix and shorten the duration that hMSCs can be cultured in collagen matrices. These limitations pose a challenge to engineering large three-dimensional bone tissue constructs *in vitro* using collagen as a scaffold. In order to create large bone tissue constructs successfully and be able to predict the final dimensions of the tissue constructs, the amount of matrix contraction by hMSCs under different osteogenic culture conditions needs to be determined. This chapter describes the effects of initial cell density, culture medium, cyclic strain level, and culture duration on matrix contraction by hMSCs.

## 3.1 Introduction

Creation of bone tissue constructs *in vitro* requires a suitable cell source, scaffold, and appropriate culture conditions. In recent studies, mesenchymal stem cells (MSCs) have shown a great potential for bone tissue engineering due to their ability to differentiate down an osteogenic pathway in both two dimensional (2D)[3, 5, 9, 10] and three dimensional (3D)[18, 20, 21, 30, 93, 94] culture conditions *in vitro*. Among many potential scaffolds for bone tissue engineering, collagen has proven to be one of the optimal scaffold materials due to its inherent ability to mimic the natural extracellular matrix.[90] However, high contraction of collagen scaffolds observed during culture might greatly limit the size of the final tissue construct.[104] Characterization of the degree of collagen contraction during MSC culture conditions appropriate for bone tissue engineering would provide valuable information to predict the final dimensions of MSC-seeded collagen scaffolds. Intramembranous and endochondral bone formation is initiated from MSCs and therefore MSCs are regarded as a better source of cells for bone tissue engineering.[4] Studies have shown that, in 3D cultures under static conditions, and in the presence of appropriate chemical stimuli, MSCs can differentiate down an osteogenic pathway.[20, 21, 30, 92, 93] It is also of paramount importance to create a bone tissue construct structurally robust enough to withstand physiological stresses and strains in a dynamic mechanical environment *in vivo*.[1, 105] *In vitro*, mechanical stimulation of MSCs during culture would facilitate an increase in ultimate strength of the final tissue construct; as well as accelerate osteogenic differentiation. Previous investigations by one of the authors indicated that 10-12% tensile strain accelerated intramembranous bone formation during distraction osteogenesis in a rat model.[14, 15] In addition, two of the authors

have recently shown that human MSCs (hMSCs) cultured in 3D collagen matrices and exposed to 10 and 12% uniaxial cyclic tensile strain upregulated genes indicative of osteogenic differentiation.[106] However, there are no studies that have investigated the contraction of MSC seeded collagen matrices *in vitro* under combined conditions of: 1) cyclic tensile strain; 2) varying initial seeding densities; and, 3) varying media conditions – all of which are vital components for bone tissue engineering using MSC seeded collagen constructs.

We hypothesized that collagen matrix contraction by hMSCs would increase with higher hMSC seeding densities but decrease both with application of uniaxial cyclic tensile strains of 10 or 12%, and with use of osteogenic differentiating medium. To test our hypotheses, hMSC seeded type I collagen matrices were subjected to cyclic tensile strains for up to 14 days in both osteogenic differentiating and complete growth medium and analyzed for cell viability and matrix contraction.

## 3.2 Materials and Methods

### 3.2.1 Fabrication of hMSC-seeded 3D collagen matrices

Prior to fabricating the hMSC-seeded collagen matrices, bone marrow derived-hMSCs from a 26 year old male donor (Cambrex Bio Science, Walkersville, MD) were expanded to passage 3 or 4 and maintained in complete non-differentiating growth medium (MSCGM, Cambrex) supplemented with 10% fetal bovine serum (FBS), 4 mM L-glutamine, 0.05 units/ml penicillin, and 0.05 µg/ml streptomycin (Cambrex). The Tissue Train$^{TM}$ culture system (Flexcell International, Hillsborough, NC)[107] was used to create cell-seeded linear 3D collagen matrices.

Human MSCs were cultured until 80-85% confluent, detached with 0.05% trypsin/0.53 mM EDTA, and suspended at 30,000 and 60,000 cells per 200 µl collagen solution. The collagen solution consisted of 70% v/v Vitrogen (3mg/mL type I collagen; Angiotech BioMaterials Corp, Palo Alto, CA; neutralized to pH 7.0 with 1 N sodium hydroxide), 20% v/v 5x minimum essential medium (Sigma, St. Louis, MO), and 10% v/v FBS (Cambrex). The hMSC-seeded collagen solution was dispensed into linear troughs after applying vacuum to the Tissue Train$^{TM}$ plate assembly as described above. The assembly was then incubated at 5% $CO_2$ and 37 $^0$C for 2 hours to allow the collagen to polymerize and attach to the nonwoven anchors (Fig. 3.1). The vacuum was released after 2 hours and 3 mL of complete growth medium (MSCGM) was added to each well. This was followed by another 24 hour incubation period after which the medium was changed. One group of hMSC seeded collagen matrices was maintained in MSCGM while the other was maintained in

osteogenic differentiating medium (ODM) consisting of MSCGM combined with 0.5% dexamethasone, 1% β-glycerophosphate and 0.5% ascorbic acid (Cambrex).

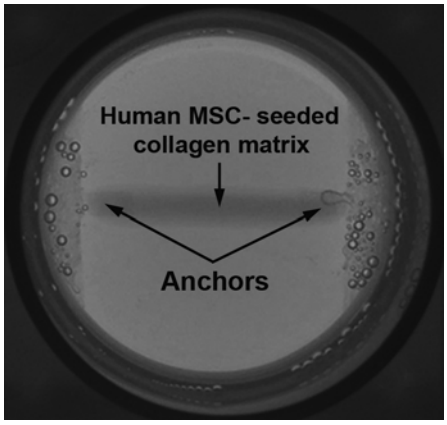


**Figure 3.1.** Top view of an hMSC-seeded collagen matrix loaded into a well of a Tissue TrainTM culture plate 2 hours after loading. Approximate length with anchors= 34mm, width= 3mm

### 3.2.2 Application of cyclic tensile strain

The hMSC-seeded collagen matrices in both MSCGM and ODM were subjected to either 10 or 12% uniaxial cyclic tensile strains at a loading rate of 1 Hz for 4 hours/day, for 7 or 14 days. The Flexercell FX-4000 strain unit (Flexcell International) was used to apply and control uniaxial cyclic tensile strain. Human MSCs seeded into collagen matrices as

described above but maintained in static culture (strain = 0%) served as the unloaded controls. For each combination of strain, initial cell seeding density, medium, and time point, three separate hMSC seeded collagen matrices were analyzed.

### 3.2.3 Cell viability

Viability of hMSCs in collagen matrices after 24 hours, 7 days, and 14 days was determined using a live/dead viability/cytotoxicity kit (Molecular Probes, Eugene, OR). The matrices were washed twice in phosphate buffered saline (PBS) and incubated in a staining solution containing 4 μM calcein AM and 4 μM EthD-1 for 45 minutes in the dark. Live cells were stained green by Calcein AM, and dead cells were stained red by ethidium homodimer-1 (EthD-1). Matrices were then mounted on glass slides and the center and two ends of the matrices were imaged using a fluorescence microscope (Leica Microsystems Inc., Bannockburn, IL) (10 × objective) and SimplePCI image analysis software (Compix Inc. Imaging systems, Cranberry Township, PA). At least 2 different images were obtained at each location. The area occupied by live and dead cells in each image was measured using Adobe Photoshop (Adobe Systems Inc., San Jose, CA) and the percentage area of live and dead cells in each image was calculated.

### 3.2.4 Measurement of contraction

Contraction of area and diameter of the cell-seeded collagen matrices was analyzed using plane views of the matrices. Each plate of cell-seeded collagen matrices was imaged every 24 hours prior to cyclic straining using a Plustek Opticpro U24 scanner at 150 dpi resolution and Scanflex software (Flexcell, Hillsborough, NC). The images were analyzed with Kodak ID image analysis software v3.6 (Eastman Kodak Co., NY). The areas and the diameters at the center and half way between the center and each end of the matrix were measured (n = 3) and the contraction calculated as a percent of initial area or diameter. These percentage contractions of each matrix were plotted against time. For each matrix, the area under the percent of initial diameter – time and the percent of initial area – time plots were calculated using Excel (Microsoft Corporation, Redmond, WA). These area under the curve (AUC) values were defined as representative values of diameter and area contraction of each matrix and used for comparison of contraction between matrices. The profiles with more rapid declines in contraction over time would have lower AUC values.

### 3.2.5 Statistical analysis

Factorial effects of strain, density and medium on diameter and area contraction were investigated using F-tests from an analysis of variance appropriate to the complete, crossed, 2 × 2 × 3 experimental design, taking area under the curve (AUC) as the response variable indicative of cumulative contraction over time. For both diameter and area, responses were contrasted with reference to those of same day unstrained matrices having similar experimental conditions.

## 3.3 Results

### 3.3.1 Cell viability

Assessment of the center and both ends of the stained matrices revealed that there was no clear difference of cell viability at different locations within the matrix. This indicates that varying local strain levels within the matrix did not play a role in cell death. The strain levels and media conditions did not affect the viability of cells. On average, irrespective of strain level, medium and culture duration, the area occupied by dead cells in all images was less than 1% (Fig. 3.2). This indicates that cell viability was maintained significantly throughout the culture period.

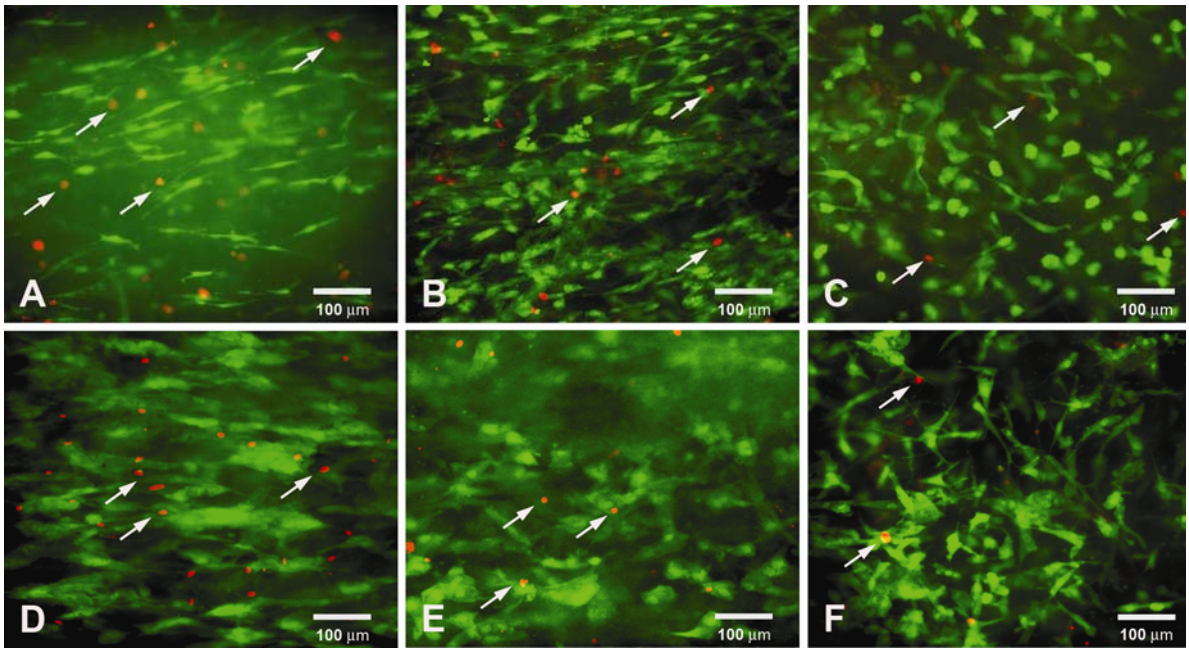


**Figure 3.2.** Live (green) and dead (red) cells in strained and unstrained hMSC-seeded type 1 collagen matrices stained with calcein AM and EthD-1 respectively. Arrows indicate dead cells. A, B and C) Matrices seeded with 30,000 cells and strained at 0% (A), 10% (B) and 12% (C) in complete growth medium (MSCGM) for two weeks. D, E and F) Matrices seeded with 60,000 cells and strained at 0% (D), 10% (E) and 12% (F), in MSCGM for two weeks.

### 3.3.2 Contraction of matrix diameter

All matrices contracted more at the center than at the ends (Fig. 3.3). The diameter of most matrices contracted rapidly up to the third day and continued contracting at a slower rate through day 14 (Fig. 3.4).

The three-way interaction of strain, initial cell seeding density and medium on contraction of diameter was not significant. However, there was a significant strain-by-medium ($p < 0.0001$) and strain-by-density ($p = 0.0107$) interaction (Fig. 3.5A). In order to further investigate the strain-by-medium interaction, the area-under-curve (AUC) values of two media were compared by averaging over density (Fig. 3.5A and 3.5B). A lower AUC value indicates a higher contraction of the matrix diameter. Matrices cultured in MSCGM and strained at 10% had a significantly higher contraction (lower AUC) ($p = 0.0009$) than unstrained (0%) and 12% strained matrices (Fig. 3.4A, B & 3.5A, B). The matrices strained at 12% had a significantly lower contraction (higher AUC) ($p < 0.0001$) than all others (Fig. 3.4B & 3.5B). In contrast to MSCGM culture, in ODM, 10% strained matrices had a significantly lower contraction compared to both unstrained ($p = 0.0112$) and 12% strained matrices ($p < 0.0001$) (Fig. 3.4C, D & 3.5B). In general, matrices seeded with 60,000 cells (Fig. 3.4B, D & 3.5A) exhibited higher final contractions than those seeded with 30,000 cells (Fig. 3.3A, C & 3.5A). The effect of initial cell seeding density on the contraction of diameter was similar for both unstrained and 10% strained matrices (Fig. 3.5A). Irrespective of the type of medium used, the unstrained ($p = 0.0135$) and 10% ($p = 0.0007$) strained matrices seeded with 60,000 cells showed a significantly higher contraction than those

seeded with 30,000 cells (Fig. 3.5A). Interestingly, the initial hMSC-seeding density did not significantly affect the contraction of 12% strained matrices (Fig. 3.5A).

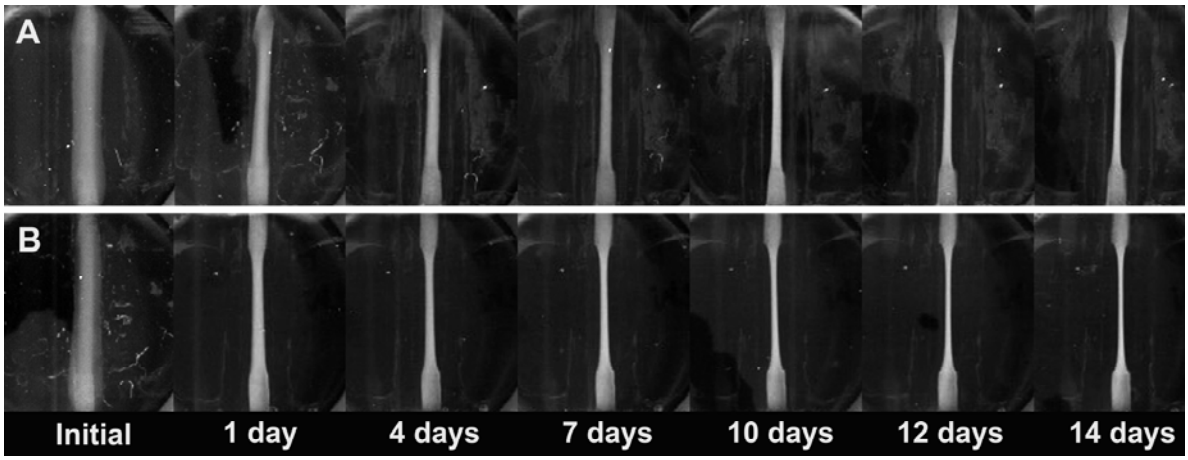


**Figure 3.3.** Change in matrix diameter of unstrained matrices cultured in MSCGM with an initial hMSC-seeding density of A) 30,000 cells/ 200µL, B) 60,000 cells/ 200µL.

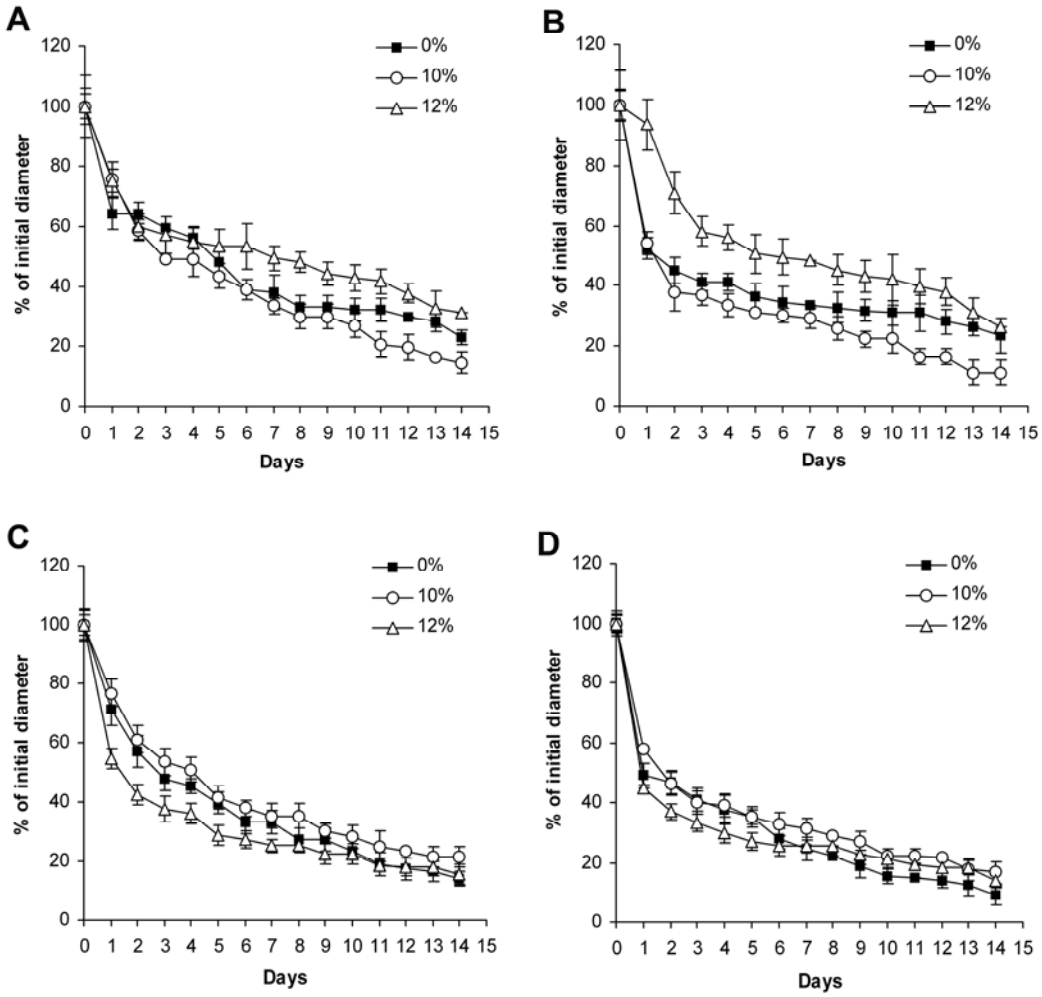


**Figure 3.4.** Effects of strain, hMSC-seeding density and culture medium on contraction of matrix diameter. A) Seeding density 30,000 cells/ 200µL, cultured in MSCGM, B) Seeding density 60,000 cells/ 200µL, cultured in MSCGM, C) Seeding density 30,000 cells/200µL, cultured in ODM, D) Seeding density 60,000 cells/ 200µL, cultured in ODM.

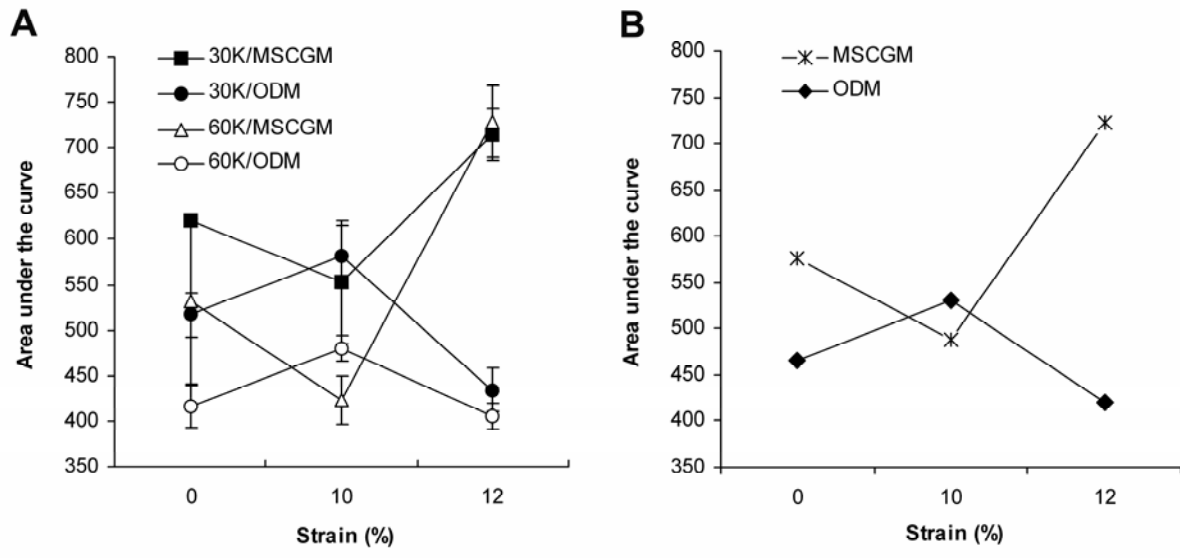


**Figure 3.5.** Change in area under diameter contraction plots (AUC) by different combinations of strain, cell seeding density and culture medium. A) Strain-by-medium and strain-by-density interactions, B) Strain-by-medium interaction averaged over hMSC-seeding densities to compare effect of medium. A low AUC value indicates a high contraction. 30K = 30,000 cells/200 µL collagen gel, 60K = 60,000 cells/200 µL collagen gel. MSCGM = complete growth medium; ODM = osteogenic differentiating medium.

### 3.3.3 Contraction of matrix area

As expected, similar to diameter contractions, the area of most matrices contracted rapidly up to the third day then continued contracting at a slower rate through day 14 (Fig. 3.6). A higher rate of contraction was observed in matrices seeded with 60,000 cells (Fig. 3.6B, D) than those seeded with 30,000 cells (Fig. 3.6A, C). While the three-way interaction between strain, initial cell seeding density and medium on contraction of area was not significant, there was evidence of strain-by-medium ($p$ = 0.0002) and medium-by-density ($p$ = 0.0304) interactions on the area contraction (Fig. 3.7). All matrices cultured in ODM

had a significantly higher contraction ($p < 0.0001$) than those cultured in MSCGM (Fig. 3.7A). This was not affected by the initial hMSC-seeding density (Fig. 3.7B). The contractions observed in 12% strained matrices cultured in MSCGM were significantly lower than the unstrained ($p = 0.0010$) and 10% ($p < 0.0001$) strained matrices (Fig. 3.7A). Increased initial cell seeding density caused a higher area contraction only in matrices cultured in ODM (Fig. 3.7B).

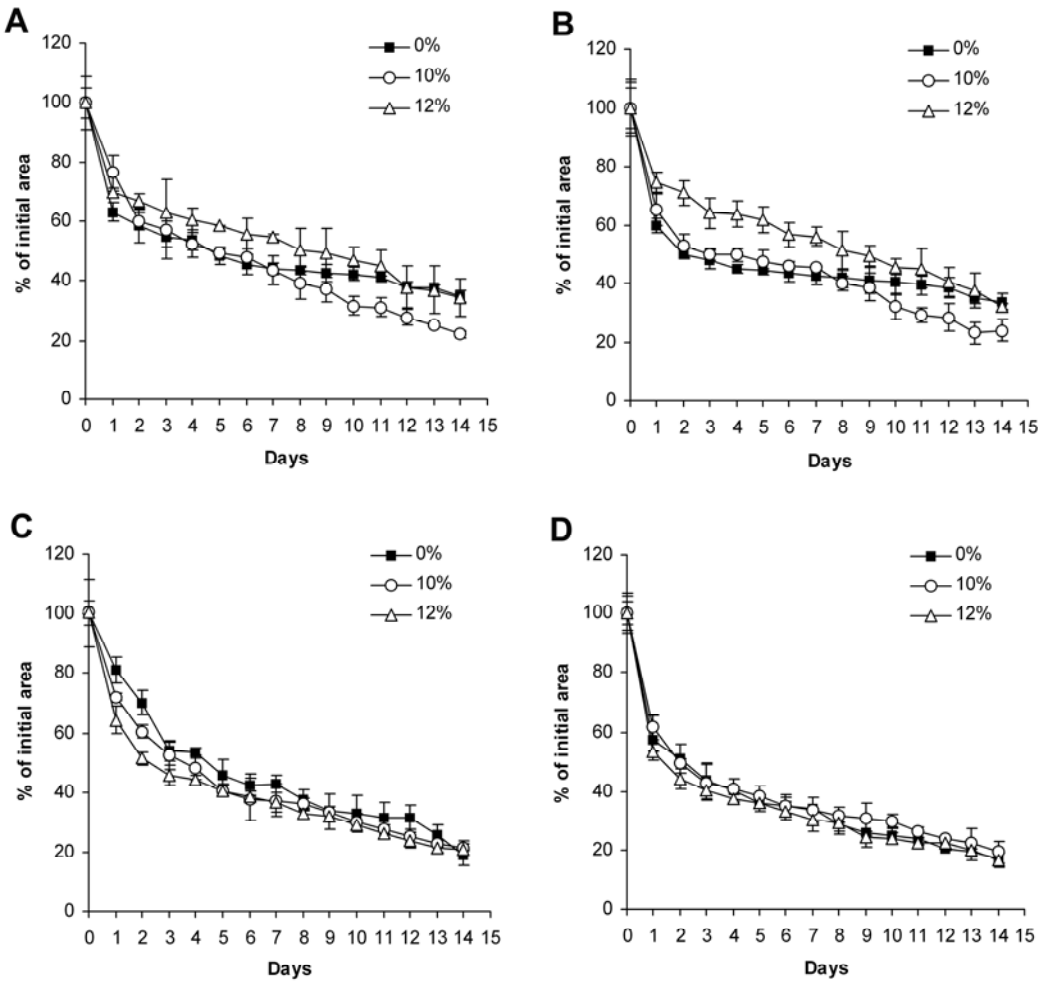


**Figure 3.6.** Effects of strain, hMSC-seeding density and culture medium on contraction of matrix area. A) Seeding density 30,000 cells/ 200µL, cultured in MSCGM, B) Seeding density 60,000 cells/ 200µL, cultured in MSCGM, C) Seeding density 30,000 cells/200µL, cultured in ODM, D) Seeding density 60,000 cells/ 200µL, cultured in ODM.

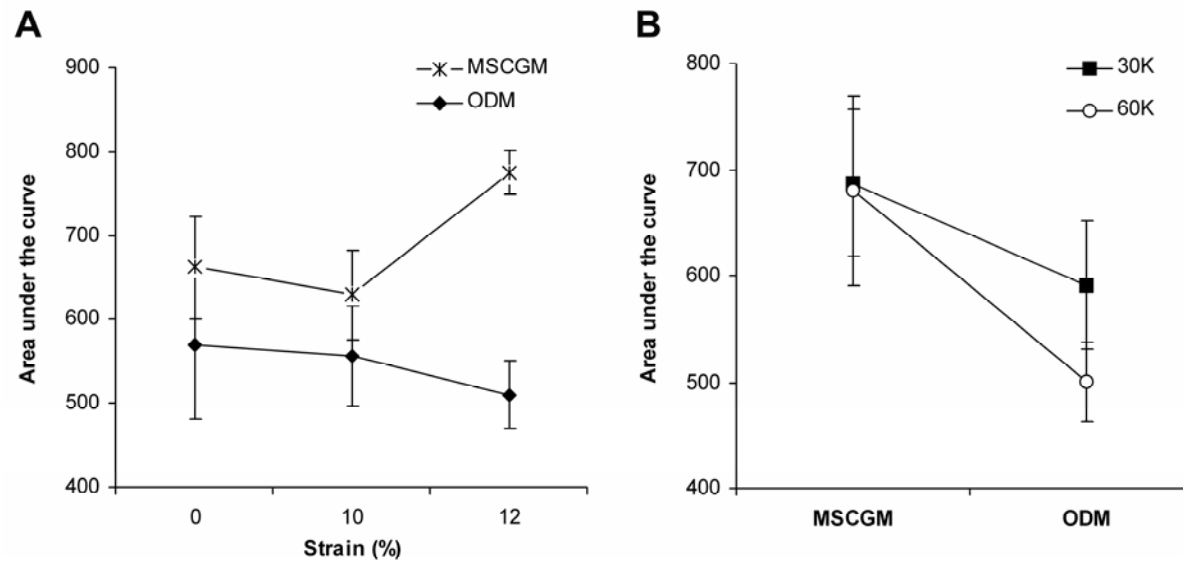


**Figure 3.7.** Change in area under area contraction plots (AUC) by different combinations of strain, cell seeding density and culture medium. A) Strain-by-medium interaction averaged over initial cell seeding density, B) Medium-by-initial cell seeding density interaction averaged over strain. A lower AUC value indicates higher contraction. 30K = 30,000 cells/200 μL, 60K = 60,000 cells/200 μL. MSCGM = complete growth medium; ODM = osteogenic differentiating medium.

## 3.4 Discussion

Type I collagen is the most abundant extracellular matrix protein found in bone and contains cell adhesion RGD (arginine-glycine-aspartic acid) sequences; it has been reported to be the best scaffold material to mimic the *in vivo* environment.[2] The growth and proliferation capacity of hMSCs in collagen matrices under static (i.e., no mechanical load) conditions has already been demonstrated.[11, 104]

While application of mechanical load to hMSC-seeded collagen matrices might facilitate an increase in their mechanical strength and/or initiate desired differentiation pathways, the effects of mechanical load on the contraction of hMSC-seeded collagen matrices has not been investigated. Excessive contraction of hMSC-seeded collagen matrices could affect cell viability and limit the size of a bone tissue construct developed *in vitro*. Therefore, the goals of this study were to investigate the effects of uniaxial cyclic tensile strain, hMSC-seeding density and media conditions on hMSC viability and contraction of hMSC seeded type I collagen matrices.

### 3.4.1 Viability

The current study has shown that hMSCs can be cultured in Type I collagen matrices under uniaxial cyclic tensile strains of 10 and 12% for up to 2 weeks. The strain levels and media (MSCGM and ODM) used in this study did not affect the cell viability throughout the entire culture period. The few dead cells that were observed after two weeks in all matrices could be due to lack of extracellular space caused by increased matrix contraction. The

current results indicate that type I collagen can be successfully used as a scaffold material for 3D culture of hMSCs and for subjecting hMSCs to mechanical strains without inducing significant cell death.

### 3.4.2 Matrix contraction

Contraction of collagen matrices in an unloaded/static environment has been observed with many cells such as fibroblasts, [108-114] endothelial cells,[115] chondrocytes,[116] osteoblasts[117] and rabbit MSCs.[104] Translocation and compaction of collagen fibrils by tractional forces imposed by the cells have been found to be the main causes for collagen matrix contraction.[118] In the present study, contraction of matrix diameter was predominantly affected by uniaxial cyclic tensile strain and hMSC-seeding density. The matrices contracted rapidly up to the third day and then continued contraction at a slower rate. Nishiyama et al.[111] observed three distinct phases of contraction by human fibroblasts in collagen matrices, an initial lag phase, a rapid contraction phase and a slower contraction phase. In contrast, hMSC-seeded collagen matrices in our study did not exhibit an initial lag phase. The contraction profile of human MSCs in the present study matches that of rabbit MSCs,[104] which also exhibited a rapid then slower contraction phase. This confirms that matrix contraction by MSCs follows a different profile than fibroblasts. Similar to the observation made with fibroblasts,[108, 111] endothelial cells,[115] chondrocytes[116] and rabbit MSCs,[104] the rate of matrix contraction by human MSCs was dependent on the initial cell seeding density. The rate of matrix contraction was higher with higher initial cell seeding density.

The effect of cyclic tensile strain on diameter contraction of hMSC-seeded collagen matrices was dependent on medium. Matrices treated with MSCGM contracted in the order of 10%> 0%> 12% strain levels. In contrast, matrices treated with ODM had maximum contraction in the order of 12%> 0%> 10% strain levels. In addition, increase of initial seeding density to 60,000 cells/ 200 μL from 30,000 cells/ 200 μL only affected the unstrained and 10% strained matrices, such that contraction was higher in these matrices compared to those with low initial cell seeding density of 30,000 cells/ 200 μL. From these data, it is clear that the type of medium combined with strain level plays a major role in the contraction of hMSC-seeded collagen matrices.

It is possible that several factors operate in conjunction to bring about this contraction behavior. Cell proliferation has been found to be maximal in growth medium that does not support any differentiation of cells. Therefore, we can expect the matrices treated with MSCGM to have a higher cell proliferation leading to higher matrix contraction. Considering the order of contraction by strain level, it is possible that cells proliferate to a greater extent under 10% cyclic tensile strain than 12% strain. The difference of the order of contraction in matrices treated with ODM versus MSCGM could be due to the differentiation capacity of hMSCs in ODM. It can be expected that hMSCs cultured in ODM will produce more collagen I, thus making the matrices more stable. As seen from the order of contraction, since the 10% strain level had minimum contraction in ODM, this strain level may be causing hMSCs to produce higher levels of collagen.

On the other hand, studies by Bowman et al.[117] have shown that cellular coupling via gap junctions is required to express osteogenic markers by fully differentiated osteoblastic

cells. Since an increase in gap junctional coupling could elevate matrix contraction, they suggested that differentiated osteoblasts would increase collagen matrix contraction. Therefore, it may also be possible that the highest contraction observed in matrices strained at 10% in MSCGM and 12% in ODM could be due to an increased production of gap junctions, thus indicating more differentiated hMSCs in these matrices. This is partly confirmed by recent studies from our laboratory which showed that when hMSCs seeded in collagen matrices are treated with MSCGM and subjected to 10% uniaxial cyclic strain, they continue to express bone morphogenetic protein-2 mRNA for up to two weeks.[106] It is possible that the applied cyclic tensile strain acts as a temporary shield to the traction forces exerted by the hMSCs on the collagen fibrils. Collagen fibrils temporarily become rigid due to the application of strain causing an increase in the work that the cells have to invest to move the fibers closer. Even though the strain applied was cyclic, its continuous periodic application could have considerable effect on opposing cellular tractional forces. This phenomenon can lead to a reduction in lateral contraction of the collagen matrix.

As expected, the contraction profiles and the effect of initial cell seeding density on rate of matrix area contraction were similar to those of matrix diameter contraction. The effect of strain on area contraction of collagen matrices was also dependent on medium. Apart from a few minor differences determined by cell seeding density, the effect of strain on area contraction in matrices treated with MSCGM and ODM followed a similar order as in the case of diameter contraction. In general, matrices treated in ODM had a higher contraction than those treated with MSCGM. This was more prominent in matrices, which had a higher seeding density. The aim of analyzing the contraction of area in this study was

to consider the contraction of unaccounted regions of the collagen matrix during diameter measurements. The observations from the two analyses showed that they are comparable.

In summary, we have analyzed both the separate and combined effects of uniaxial cyclic tensile strain, initial cell seeding density, and medium on cell viability and collagen matrix contraction by hMSCs seeded in Type I collagen matrices. The effects of cyclic tensile strain, medium, and hMSC-seeding density on matrix contraction appear to be highly interactive. While an increase in hMSC-seeding density alone can produce increased rate of contractions, strain and medium produced combined affects on contraction. Due to the high interaction between strain and medium, it is difficult to characterize their individual effects on contraction. The potential influence of osteogenic differentiation and cell proliferation on matrix contraction in the presence of combined strain-medium effects should be further investigated. The difference in cell behavior between 10% and 12% strain suggests an existence of a threshold level of strain, which determines cellular response to combined effects of strain and medium. Studies are presently being conducted by the authors to further analyze osteogenic differentiation of hMSCs under the conditions investigated in this study.

## 3.5 Summary

Mesenchymal stem cells (MSCs) seeded in three dimensional (3D) collagen matrices can be stimulated by tensile strain and/or appropriate media conditions to differentiate down an osteogenic pathway. However, high contraction observed in these matrices poses a challenge to creating large tissue engineered bone constructs. The effects of cyclic tensile strain, medium and human MSC (hMSC) seeding density on contraction of collagen matrices have not been investigated. This study was conducted to analyze the effects of cyclic tensile strain, medium and initial cell seeding density on matrix contraction by hMSCs cultured in collagen matrices. Human MSCs were seeded in 3D collagen matrices and subjected to cyclic tensile strain of 10 or 12% for 4 hours/day at a frequency of 1 Hz in osteogenic differentiation (ODM) or complete MSC growth media (MSCGM) for 14 days. Viability of hMSCs was not affected by strain or media conditions. While initial seeding density affected rate of matrix contraction alone, there was high interdependence of strain and medium in influencing matrix contraction. These findings suggest existence of a correlation between hMSC proliferation and osteogenic differentiation on collagen matrix contraction under the conditions investigated in this study. It is vital to control contraction of the collagen matrix in order to successfully create large tissue engineered bone constructs *in vitro*.

# 4 Mesenchymal Stem Cell Seeded Collagen Matrices for Bone Repair: Effects of Uniaxial Cyclic Tensile Strain, Cell Density, and Media Conditions on Nuclear Morphology and Orientation

In the previous chapter, effects on cell seeding density, culture medium, cyclic strain, and culture duration on contraction of 3D collagen matrix by hMSCs was described. In addition to chemical stimulation, hMSCs cultured in three-dimensional collagen matrices can also be mechanically induced to differentiate down osteogenic pathways. The extent of stimulation depends on the amount of tensile strain (deformation) experienced by hMSCs in the collagen matrix. This defomation of hMSCs is essentially dependent on their orientation in the collagen matrix. In order to understand the extent of hMSC stimulation during mechanical strain, we need to determine their morphology and orientation in collagen matrices under various osteogenic differentiation conditions. This chapter describes the effects of cyclic tensile strain, cell density, culture medium, and culture duration on nuclear morphology and orientation of hMSCs cultured in 3D collagen matrices.

## 4.1 Introduction

Mesenchymal stem cells (MSCs) cultured in two dimensional[3, 5, 9, 10] and three dimensional[18, 20, 21, 30, 93, 94] culture conditions possess the ability to differentiate down an osteogenic pathway. Stimulation of MSCs using chemical cues have already been shown to induce osteogenic differentiation.[9] Mechanical loading of MSCs cultured in three dimensional (3D) culture conditions would not only induce osteogenic differentiation[106] but could also enable the engineered bone construct to sustain its structural stability under physiological stresses and strains *in vivo*. [1, 105] Collagen is an excellent scaffold material for 3D culture of MSCs due to its inherent cell binding characteristics.[90] Collagen possesses sufficient elastic properties to withstand mechanical strains and therefore three dimensional collagen matrices can be successfully used to culture and mechanically strain MSCs.[106] The amount of tensile strain experienced by cells cultured in a collagen matrix would be determined by strain induced deformation of cells. This deformation is essentially governed by the orientation of the cells within the matrix.[119-121] Change in orientation of MSCs in a collagen matrix could affect cell proliferation, cellular mRNA levels, and protein synthesis, hindering strain induced osteogenic differentiation.[29, 88, 91] Therefore, it is important to investigate changes in orientation and morphology of MSCs cultured in 3D collagen matrices. However, due to high contraction observed in human MSC (hMSC) seeded 3D collagen matrices over time as well as inherent filipodial nature of hMSC morphology,[122, 123] it is difficult to track the changes in overall hMSC morphology and orientation. An investigation of changes in hMSC nuclear morphology and orientation due to external strains would facilitate an understanding of the intracellular response of cells to external mechanical

strain. Furthermore, it would be useful to compare this hMSC nuclear response to strain with morphological responses of other cells to strain in order to understand any correlation between the two.

It has been shown that intramembranous and endochondral bone formation are initiated from MSCs.[4] Tensile strains of 10-12% have been shown to accelerate intramembranous bone formation during distraction osteogenesis in a rat model.[14, 15] A recent study by two of the authors has also shown an upregulation of genes indicative of osteogenic differentiation in hMSCs cultured in 3D collagen matrices and exposed to 10% and 12% uniaxial cyclic tensile strain.[106] Reorientation of cells when exposed to external strain was first observed by Buck et al. in a study of fibroblasts.[121] Since then, numerous studies have shown similar behavior with human osteoblasts,[124] human endothelial cells,[120] human melanocytes,[119] rabbit smooth muscle cells,[125] and pig endothelial cells.[125] However, there are no studies that have investigated the nuclear orientation and morphology of hMSCs seeded in collagen matrices under conditions desirable for osteogenic differentiation of hMSCs *in vitro*. Therefore, the purpose of this study was to investigate the effects of cyclic tensile strain, culture medium and initial hMSC seeding density on nuclear morphology and orientation of hMSCs cultured in 3D collagen matrices. We hypothesized that both morphology and orientation of hMSC nuclei would change with application of strain at 10 and 12% but would remain unchanged with varying hMSC initial cell seeding density and culture medium. To test our hypotheses, hMSC seeded type I collagen matrices were subjected to cyclic tensile strains of 10 and 12% at a frequency of 1 Hz for up to 14 days in

both osteogenic differentiating and complete growth medium and analyzed for changes in nuclear morphology and orientation.

## 4.2 Materials and Methods

### 4.2.1 Fabrication of hMSC-seeded 3D collagen matrices

Human MSCs were derived from bone marrow of a 26 year old male donor (Cambrex Bio Science, Walkersville, MD) and culture expanded to passage 3 or 4 in complete non-differentiating growth medium (MSCGM, Cambrex) consisting of 10% fetal bovine serum (FBS), 4 mM L-glutamine, 0.05 units/ml penicillin, and 0.05 μg/ml streptomycin (Cambrex).

Human MSC seeded linear 3D collagen matrices were created using the Tissue Train™ culture system (Flexcell International, Hillsborough, NC) using a previously published protocol.[107] Briefly, hMSCs were cultured in MSCGM until 80-85% confluent and then detached with 0.05% trypsin/0.53 mM EDTA to seed hMSCs at either 30,000 or 60,000 cells per 200 μl collagen solution. Type I collagen solution was prepared by mixing 70% v/v 3mg/mL type I collagen (Vitrogen; Angiotech BioMaterials Corp, Palo Alto, CA; neutralized to pH 7.0 with 1 N sodium hydroxide) with 20% v/v 5x minimum essential medium (Sigma, St. Louis, MO), and 10% v/v FBS (Cambrex). The hMSC-seeded 3D collagen matrices were created by dispensing the hMSC seeded collagen solution into linear troughs of a Tissue Train™ culture plate after applying vacuum to the plate assembly. The hMSC seeded collagen solution was then polymerized by incubating the plate assembly at 5% $CO_2$ and 37 $^0$C for 2 hours. After 2 hours, the vacuum was released and complete growth medium (MSCGM) was added to each well. The hMSC seeded collagen matrices were incubated for another 24 hours after which the medium was changed to either MSCGM or osteogenic

differentiating medium (ODM) consisting of MSCGM supplemented with 0.5% dexamethasone, 1% β-glycerophosphate and 0.5% ascorbic acid (Cambrex).

### 4.2.2 Application of cyclic tensile strain

The Flexercell FX-4000 strain unit (Flexcell International) was used to apply and control uniaxial cyclic tensile strain to hMSC-seeded collagen matrices cultured in both MSCGM and ODM (Fig. 4.1). The matrices were subjected to either 10% or 12% uniaxial cyclic tensile strains at a loading rate of 1 Hz for 4 hours/day up to 14 days. Human MSC-seeded collagen matrices were also maintained in static culture (strain = 0%) for use as unloaded controls.

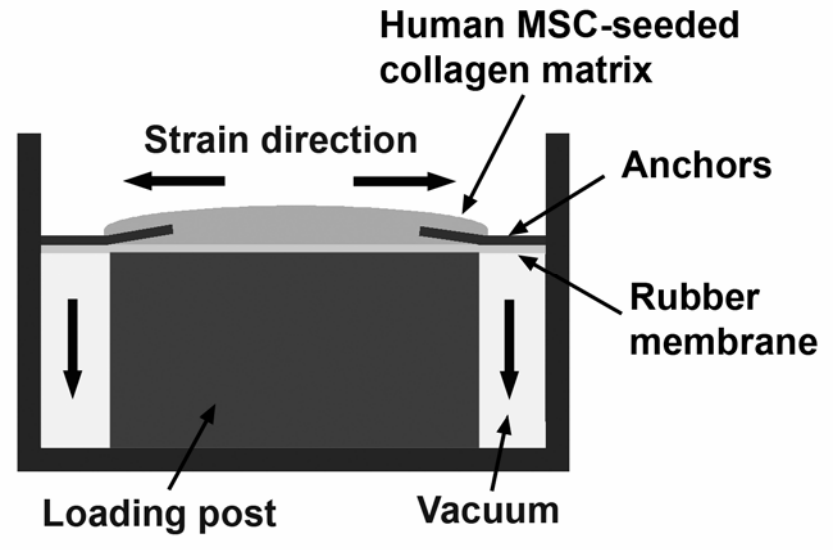


**Figure 4.1.** Human MSC-seeded collagen matrix loaded into a well of a Tissue TrainTM culture plate and showing strain direction.

### 4.2.3 Nuclear morphology and orientation

After 7 and 14 days, the actin filaments, nuclear orientation and morphology of the hMSCs in collagen matrices were determined by staining the cell nuclei and actin cytoskeleton with 4′, 6-diamidino-2-phenylindole dihydrochloride (DAPI) and Alexa 594 phalloidin, respectively.

The matrices were rinsed twice in phosphate buffered saline (PBS) and fixed by incubating in 10% formalin for 30 minutes. The cell matrices were rinsed again with PBS before permeabilizing the cell membrane by incubating in 0.2% Triton X-100/ 0.5% bovine serum albumin (TBSA) in PBS for 30 minutes. The cells were then stained by adding TBSA consisting of 1 μg/mL DAPI and 1 unit/mL phalloidin and incubating in the dark for 20 minutes. The stained cell-seeded matrices were rinsed with PBS and mounted onto glass slides and imaged (10× objective) at the center and both ends using a fluorescence microscope (Leica Microsystems Inc., Bannockburn, IL). At least three different images were obtained from each matrix location.

The images were then analyzed using SimplePCI image analysis software (Compix Inc. Imaging systems, Cranberry Township, PA) to determine orientation and aspect ratio of the nuclei. Briefly, each image was converted to grey scale and nuclei in the images were marked by adjusting the intensity threshold level. In order to select and isolate individual nuclei, artifacts and overlapped nuclei in the images were eliminated by further adjusting the maximum and minimum intensities. The nuclear orientation and aspect ratio of the nuclei were then measured using SimplePCI software. The measured orientation angles were

subtracted by $90^0$ and their absolute values were computed to determine the nuclear orientation angle with reference to the direction of applied strain. Frequency distribution of nuclear orientation angles from $0^0$ to $90^0$ in each image was then constructed based on a bin size of $5^0$, with $0^0$ indicating a nucleus parallel to the direction of applied strain and $90^0$ indicating a nucleus perpendicular to the direction of applied strain. The reciprocal of the measured aspect ratio was computed to determine maximum breadth to maximum length ratio of each nucleus and defined as the nuclear aspect ratio. Frequency distribution of nuclear aspect ratios from 0 to 1 for each image was then constructed based on a bin size of 0.1. The nuclei oriented at angles less than $15^0$ were considered as oriented parallel to the direction of strain while nuclei oriented at angles greater than $15^0$ were considered as oriented away from the direction of strain. Nuclei with aspect ratios less than 0.5 were considered having an elongated shape while those with aspect ratios greater than 0.5 were considered having a spherical shape. Percentage nuclei oriented at angles less than $15^0$ and percentage nuclei with aspect ratios less than 0.5 were calculated and used as scales to determine the effects of initial hMSC seeding density, culture duration, medium and tensile strain on hMSC orientation and morphology in 3D collagen matrices respectively. Since a considerably higher percentage of nuclei were oriented at $35^0$ and $60^0$ to the direction of strain, percentage of nuclei oriented at these angles was also calculated.

### 4.2.4 Statistical analysis

For nuclear orientation analyses, responses were defined as the percentage of nuclei that were oriented at angles less than $15^0$ to the direction of strain and those oriented at $35^0$

and $60^0$ to the direction of strain at each location of the matrices (center and each end). For nuclear morphology analysis, responses were defined as the percentage of nuclei that had aspect ratios less than 0.5 at each location of the matrices. Factorial effects of medium, density, time and strain on the above responses were investigated using F-tests from an analysis of variance appropriate to the complete, crossed, 2×2×2×3 experimental design. Because sample proportions were used as the response variable, residual diagnostics were carried out to check the assumption of homogeneity of variance underlying the ANOVA but did not reveal any, so that no transformations of the responses were necessary. For both nuclear morphology and orientation, responses were compared with reference to those of same day unstrained matrices maintained in similar experimental conditions.

## 4.3 Results

### 4.3.1 Nuclear orientation

In all unstrained and strained matrices, the actin filaments were clearly visible and most of them were oriented parallel to the longitudinal axis of the matrix (Fig. 4.2A – 4.2C). They were observed to be more compacted with an increase in culture duration. The orientation of hMSC nuclei in the collagen matrices was easily detectable after two weeks, regardless of the high contraction of collagen matrix (Fig. 4.2D – 4.2F).

Frequency distributions of hMSC nuclear orientation angle in matrices cultured in both MSCGM (Fig. 4.3) and ODM (Fig.4.4) were skewed to the right. On average, 43 - 63% of nuclei in unstrained matrices, 32 -52% of nuclei in 10% strained matrices and 28 - 55% of nuclei in 12% strained matrices were oriented at less than $15^0$ to the direction of strain. There was a significant three-way interaction between time, strain, and initial cell seeding density ($p = 0.0140$) on the percentage nuclei oriented at or below $15^0$ to the direction of strain. Since there was no significant interaction with medium, the responses were averaged over medium to study the simple effects of hMSC-seeding density and strain (Fig. 4.5). The density by strain interaction was dependent on time (Fig. 4.5)**.** Matrices having an initial cell seeding density of 30,000 cells/200 μL and strained at 10% and 12% had a significantly lower percentage of nuclei oriented at or below $15^0$ to the direction of strain when compared to the unstrained (0%) matrices at both one week ($p < 0.0001$ for 10% and $p = 0.0001$ for 12%) and two week ($p = 0.0068$ for 10% and $p < 0.0001$ for 12%) time points (Fig. 4.5). Matrices with an initial cell seeding density of 60,000 cells/200 μL and strained at 12% for one week

($p$ = 0.0106) as well as those strained at 10% for two weeks ($p$ = 0.0118) showed a significantly lower percentage of nuclei oriented at angles less than $15^0$ to the direction of strain compared to unstrained (0%) matrices (Fig. 4.5). In general, a higher percentage of nuclei were oriented at angles less than $15^0$ in strained matrices when seeded at the higher initial cell seeding density (Fig. 4.5).

Significant changes in the nuclear orientation angle were observed when the initial seeding density was changed from 30,000 cells/200 μL to 60,000 cells/200 μL. With the lower initial seeding density of 60,000 cells/ 200 μL, matrices strained at 10% and cultured for one week showed a significantly ($p$ = 0.0181) higher percentage of nuclei oriented at angles less than $15^0$ (Fig. 4.5). Similar results were observed with matrices strained at 12% and cultured for two weeks ($p$ = 0.0001) (Fig. 4.5).

Both 10% and 12% strained matrices had a considerable percentage of nuclei oriented at either $35^0$ or $60^0$ to the direction of strain in both MSCGM (Fig. 4.3) and ODM (Fig. 4.4) media. There was no significant two-way or three-way interaction between time, strain, and initial cell seeding density on the percentage of nuclei oriented at $35^0$ or $60^0$ to the direction of strain. However, strain and medium (main effects) significantly affected the percentage nuclei oriented at $35^0$ ($p < 0.0001$ for both strain and medium effects) (Fig. 4.6A and B) and $60^0$ ($p$ = 0.0008 for strain effects and $p$ = 0.0009 for medium effects) (Fig. 4.6C and D) to the direction of strain. Compared to unstrained matrices, those strained at 10 and 12% showed a significantly higher percentage of nuclei oriented at $35^0$ ($p < 0.0001$) (Fig. 4.6A and B) and $60^0$ ($p$ = 0.0074 for 10% and $p$ = 0.0002 for 12%) (Fig. 4.6C and D) to the direction of strain. The percentage nuclei oriented at $35^0$ and $60^0$ did not differ significantly between 10% and

12% strained matrices. Compared to matrices cultured in MSCGM, those cultured in ODM had a significantly higher percentage of nuclei oriented at $35^0$ ($p < 0.0001$) and $60^0$ ($p = 0.0009$) to the direction of strain (Fig 4.6).

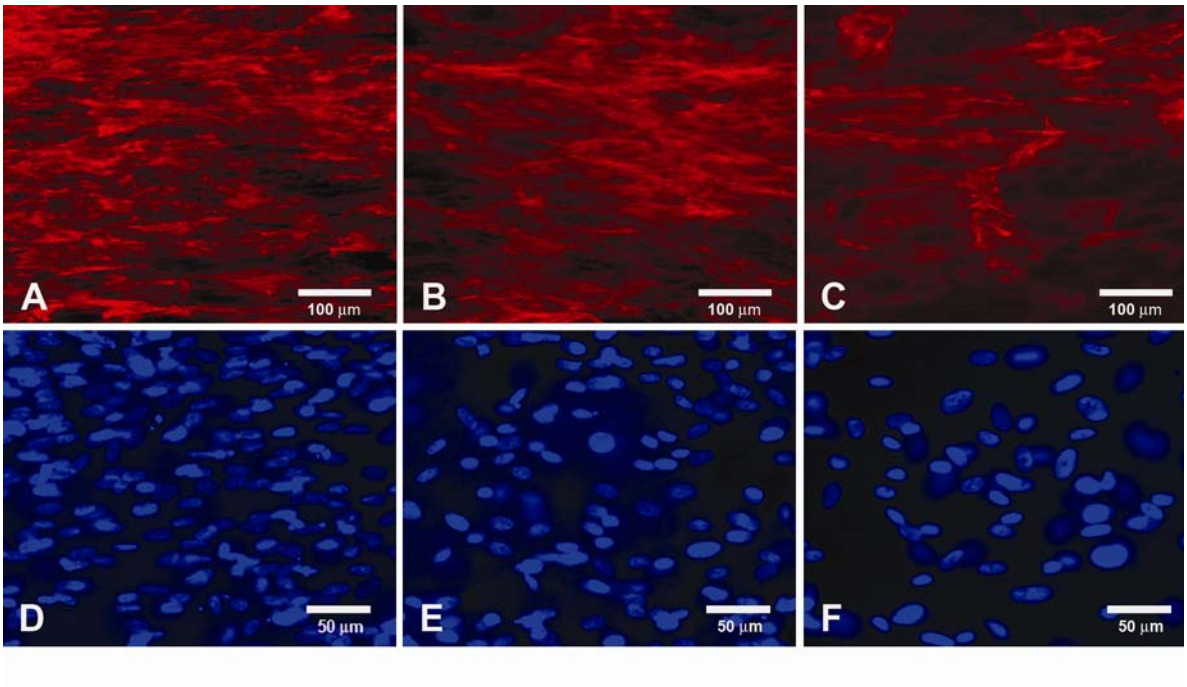


**Figure 4.2.** Orientation of actin filaments (A, B, C) and nuclei (D, E, F) of hMSCs in type 1 collagen matrices seeded with 30,000 cells and strained at 0% (A, D), 10% (B, E) and 12% (C, F) in complete growth medium (MSCGM) for two weeks. A, B and C) Matrices stained with Alexa 594 phalloidin showing orientation of actin filaments. D, E and F) Matrices stained with 4′, 6-diamidino-2-phenylindole dihydrochloride (DAPI) showing orientation of nuclei. Longitudinal axis of matrix is horizontal and also indicates the direction of tensile strain.

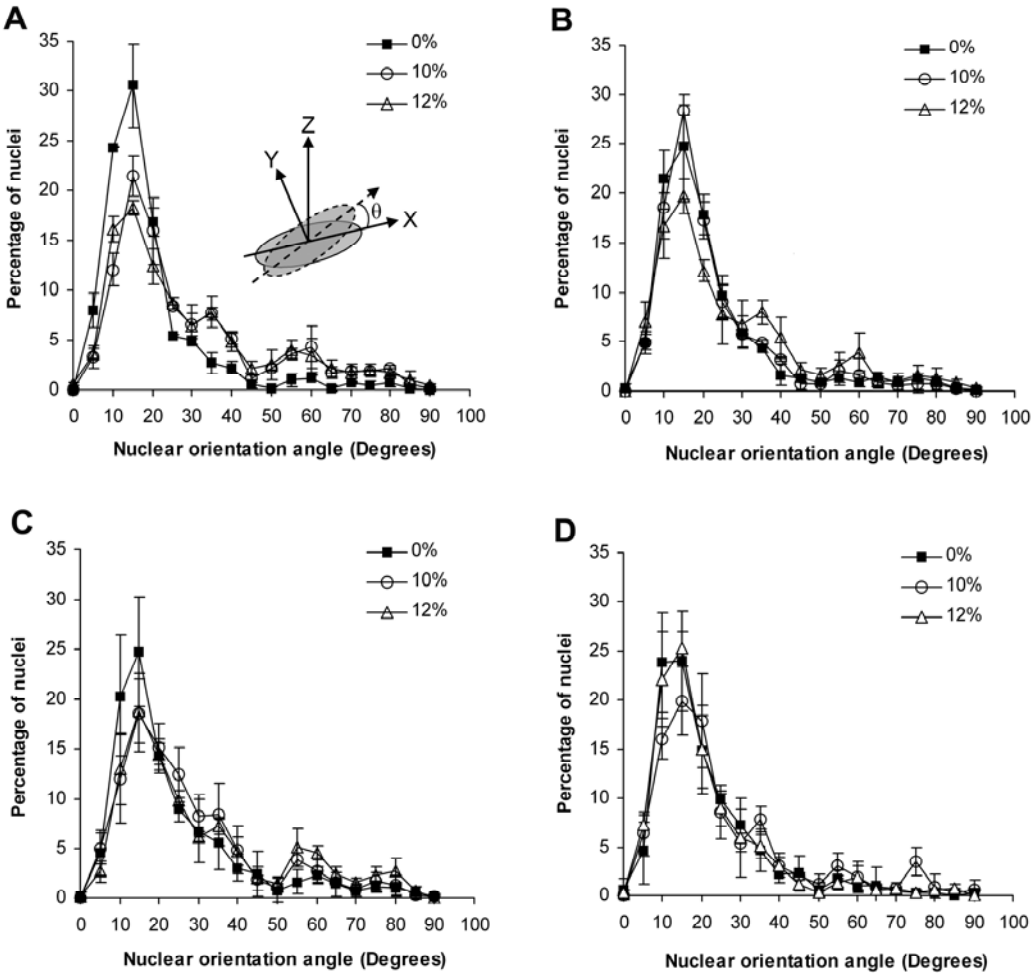


**Figure 4.3.** Effects of strain, hMSC-seeding density and culture duration on frequency distributions of hMSC nuclear orientation angles in type 1 collagen matrices cultured in complete growth medium (MSCGM). A) Seeding density 30,000 cells/ 200µL, cultured for one week, B) Seeding density 60,000 cells/ 200µL, cultured for one week, C) Seeding density 30,000 cells/200µL, cultured for two weeks, D) Seeding density 60,000 cells/ 200µL, cultured for two weeks. For nuclear orientation angle, 0° = longitudinal axis, parallel to strain; 90° = transverse axis, perpendicular to strain.

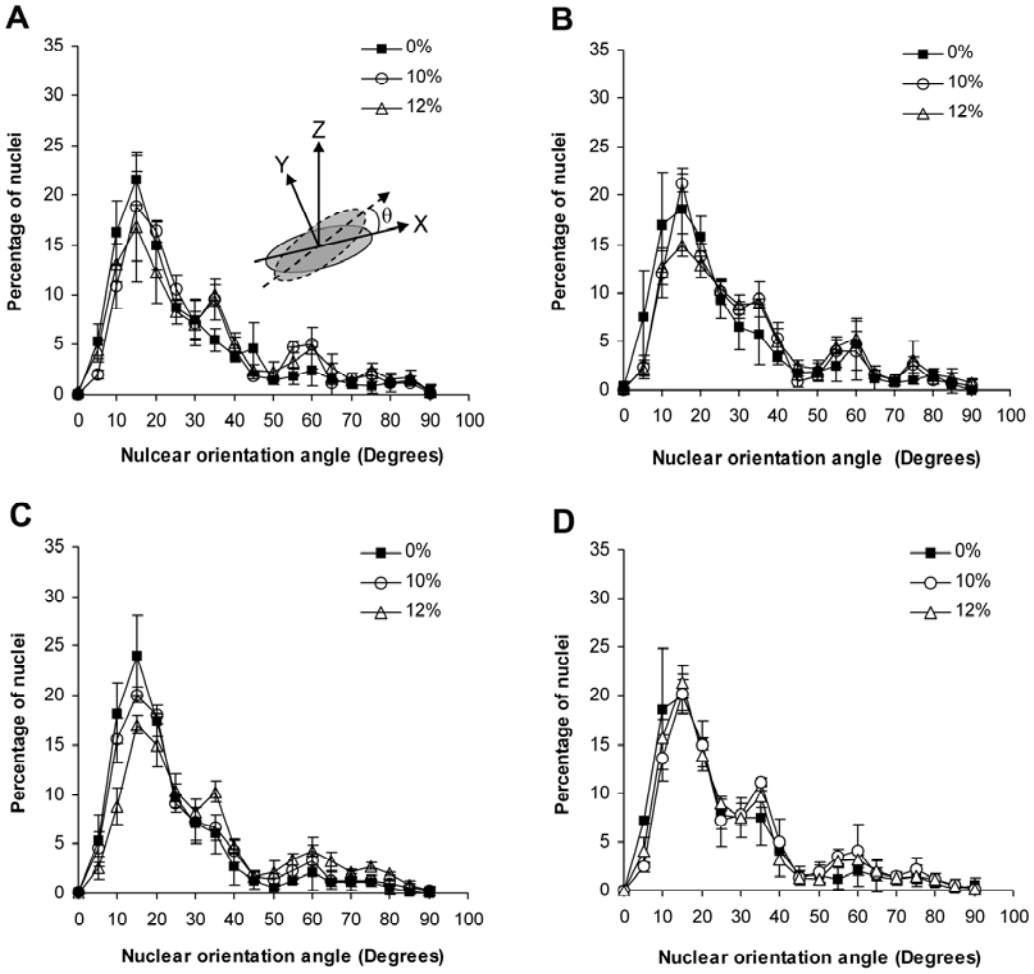


**Figure 4.4.** Effects of strain, cell seeding density and culture duration on frequency distributions of hMSC nuclear orientation angles in type 1 collagen matrices cultured in osteogenic-differentiating medium (ODM). A) Seeding density 30,000 cells/ 200µL, cultured for one week, B) Seeding density 60,000 cells/ 200µL, cultured for one week, C) Seeding density 30,000 cells/200µL, cultured for two weeks, D) Seeding density 60,000 cells/ 200µL, cultured for two weeks. For nuclear orientation angle, 0° = longitudinal axis, parallel to strain; 90° = transverse axis, perpendicular to strain.

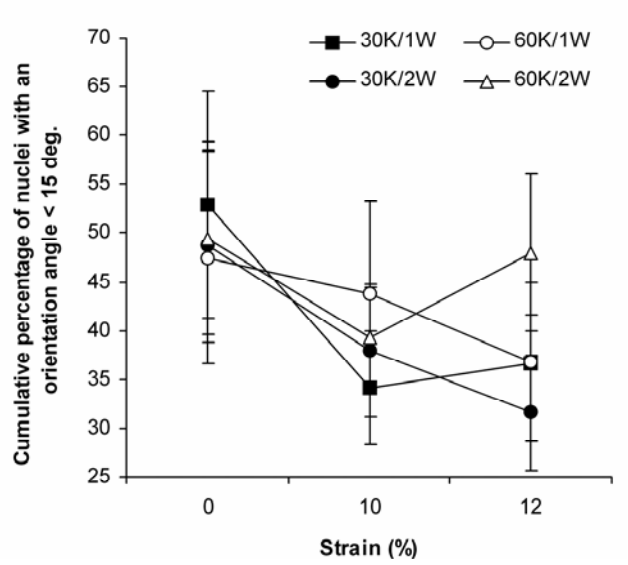


**Figure 4.5.** Interaction between strain, hMSC-seeding density and culture duration on cumulative percentage of nuclei oriented less than $15^0$ to longitudinal axis of matrix. Nuclei oriented less than $15^0$ to the longitudinal axis were considered oriented in the direction of strain. Strain, seeding density and culture duration interactions were averaged over medium. 30K = 30,000 cells/ 200µL, 60K = 60,000 cells/ 200µL, 1W = 1 week, 2W = 2 weeks.

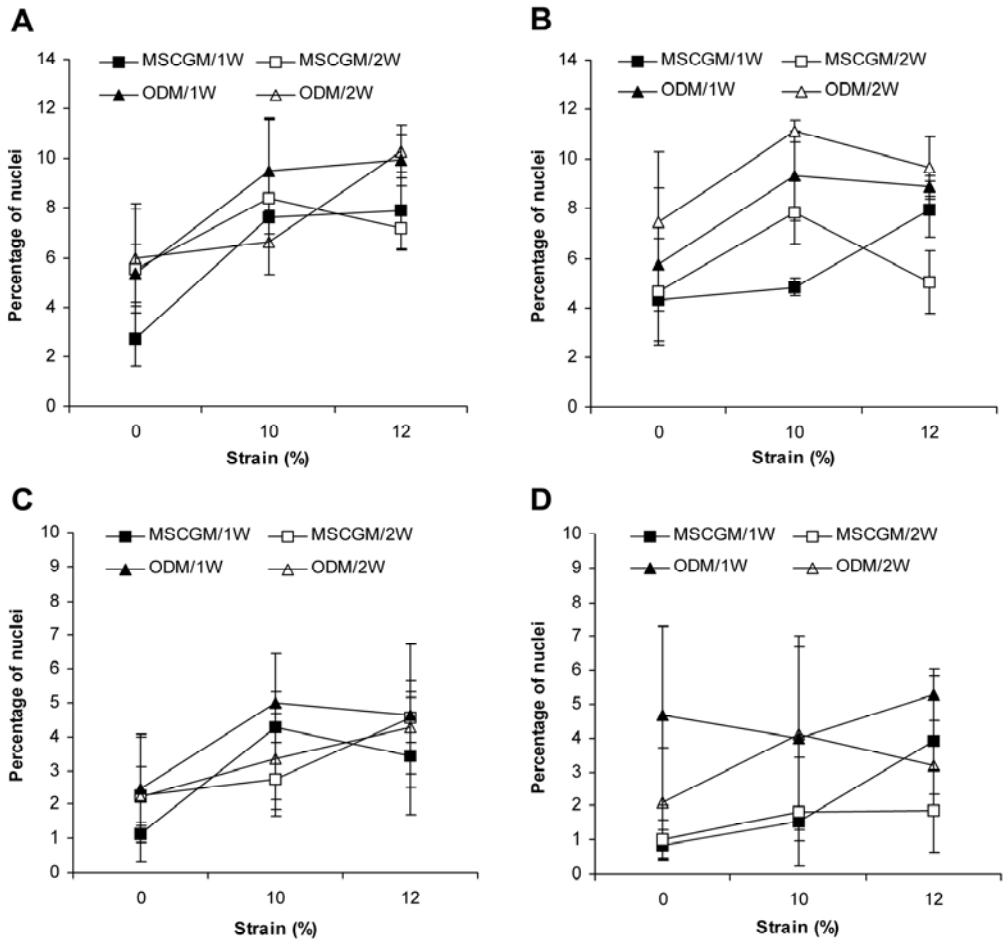


**Figure 4.6.** Percentage of hMSC nuclei oriented at $35^0$ and $60^0$ to longitudinal axis of the 3D collagen matrix. A) Orientation angle $35^0$, seeding density 30,000 cells/ 200µL, B) Orientation angle $35^0$, seeding density 60,000 cells/ 200µL, C) Orientation angle $60^0$, seeding density 30,000 cells/ 200µL, D) Orientation angle $60^0$, seeding density 60,000 cells/ 200µL. MSCGM = complete growth medium; ODM = osteogenic differentiating medium; 1W= one week; 2W= two weeks.

### 4.3.2 Nuclear morphology

The frequency distributions of nuclear aspect ratios of hMSCs cultured in both MSCGM (Fig. 4.7) and ODM (Fig. 4.8) were essentially symmetrical. The cumulative percentage of hMSC nuclei with an aspect ratio less than 0.5 (more elongated shape) was significantly affected by the two-way interactions between medium and density ($p = 0.0155$), medium and time ($p = 0.0264$), and density and strain ($p < 0.0001$). In order to analyze the simple effect of these interactions, they were averaged over other fixed effects (Fig. 4.9). The strain significantly affected the cumulative percentage of nuclei with an aspect ratio less than 0.5 irrespective of the initial seeding density. Compared to same day unstrained matrices, those strained at 10 and 12% had a significantly ($p < 0.003$) lower percentage of nuclei with aspect ratios less than 0.5 (Fig. 4.9A). Initial seeding density only significantly affected the strained matrices. Strained matrices which were seeded at a higher density had a significantly ($p = 0.0005$ for 10% and $p < 0.0001$ for 12%) higher percentage of nuclei with aspect ratios less than 0.5 compared to those seeded with a lower seeding density (Fig. 4.9A). The effect of initial seeding density was more significant in MSCGM than in ODM (Fig. 4.9C). Independent of the culture duration (Fig. 4.9B) and initial seeding density (Fig. 4.9C), matrices cultured in MSCGM had a significantly ($p = 0.0018$ for one week and $p < 0.0001$ for two weeks) higher percentage of nuclei with aspect ratios less than 0.5 compared to those treated with ODM. The effect of time was also more significant in MSCGM than in ODM (Fig. 4.9B). Matrices cultured in MSCGM for one week had a significantly ($p = 0.0040$) higher percentage of nuclei with aspect ratios less than 0.5 than those cultured for two weeks (Fig. 4.9B).

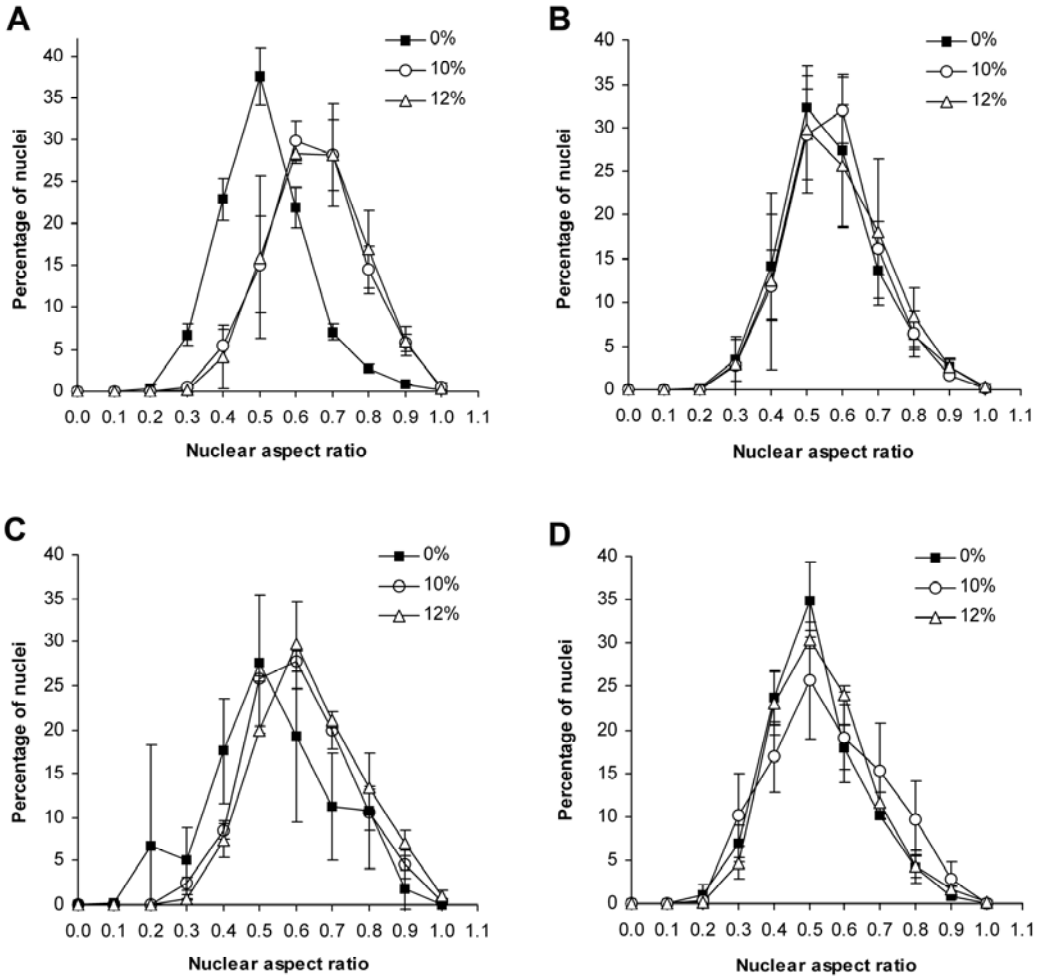


**Figure 4.7.** Effects of strain, hMSC-seeding density and culture duration on frequency distributions of hMSC nuclear aspect ratios in type 1 collagen matrices cultured in complete growth medium (MSCGM). A) Seeding density 30,000 cells/ 200µL, cultured for one week, B) Seeding density 60,000 cells/ 200µL, cultured for one week, C) Seeding density 30,000 cells/200µL, cultured for two weeks, D) Seeding density 60,000 cells/ 200µL, cultured for two weeks.

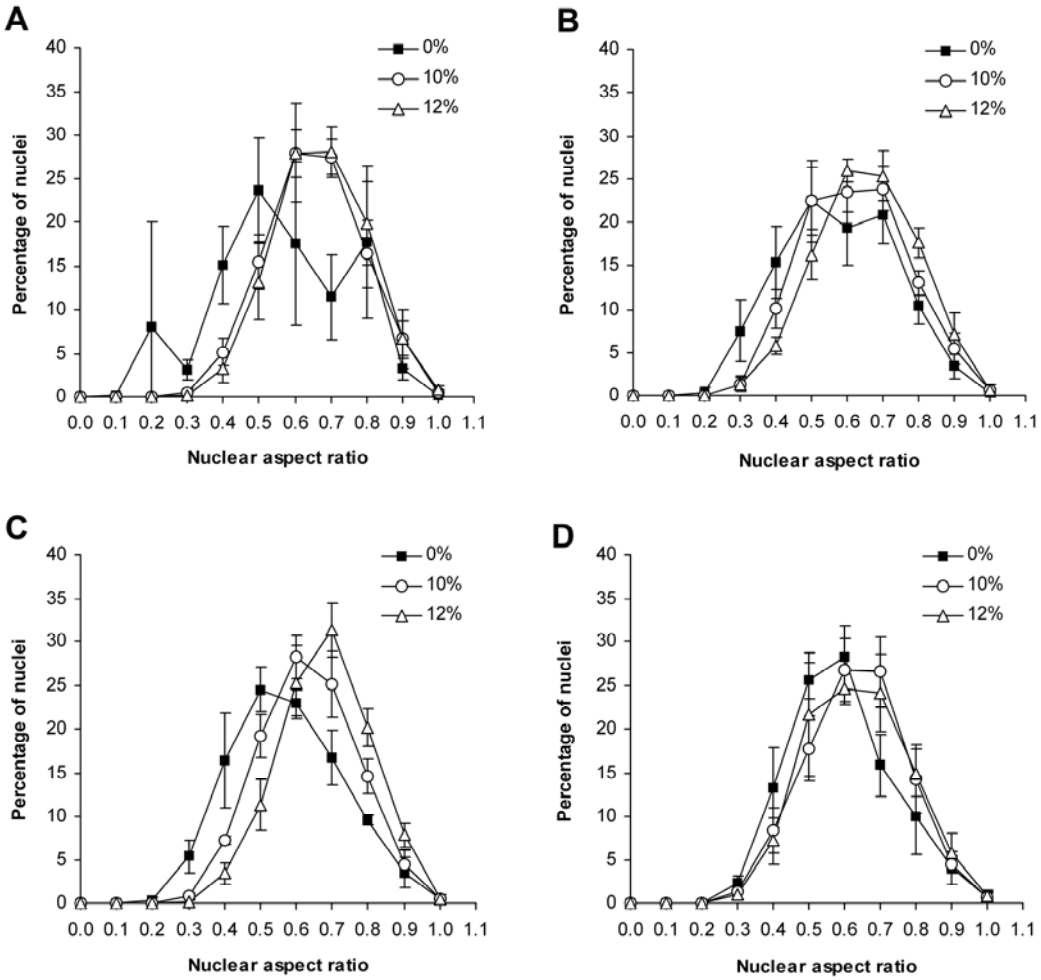


**Figure 4.8.** Effects of strain, hMSC-seeding density and culture duration on frequency distributions of hMSC nuclear aspect ratios in type 1 collagen matrices cultured in osteogenic differentiating medium (ODM). A) Seeding density 30,000 cells/ 200µL, cultured for one week, B) Seeding density 60,000 cells/ 200µL, cultured for one week, C) Seeding density 30,000 cells/200µL, cultured for two weeks, D) Seeding density 60,000 cells/ 200µL, cultured for two weeks.

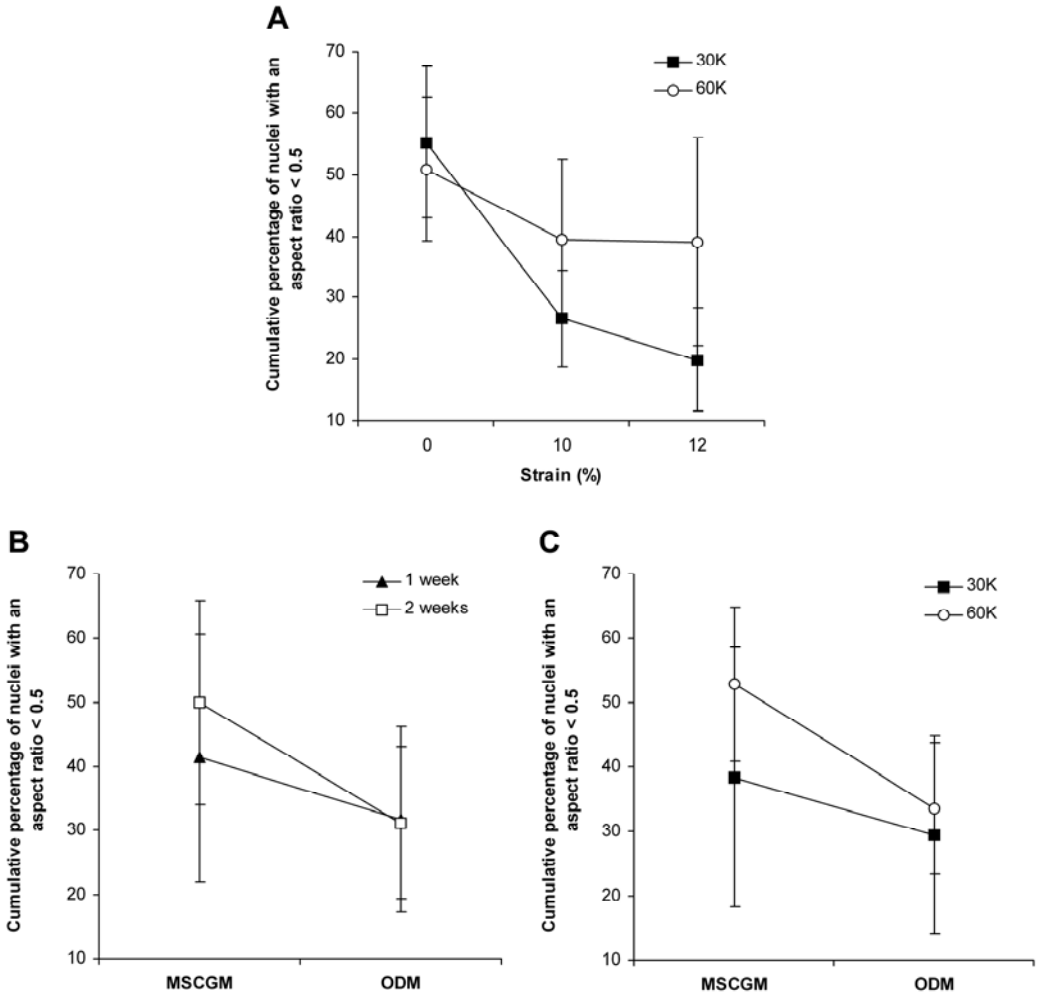


**Figure 4.9.** Influence of strain, medium and initial hMSC-seeding density on cumulative percentage of nuclei with an aspect ratio less than 0.5. An aspect ratio of 0.5 was selected to distinguish between more spherical (aspect ratio > 0.5) and more elongated (aspec aspect ratio < 0.5) nuclei in matrices. A) Strain-by-initial hMSC-seeding density interaction averaged over medium and culture duration, B) Medium-by-time interaction averaged over initial seeding density and strain, C) Medium-by-initial hMSC-seeding density interaction averaged over strain and culture duration. 30K = 30,000 cells/ 200µL, 60K = 60,000 cells/ 200µL; MSCGM = complete growth medium; ODM = osteogenic differentiating medium; Nuclear aspect ratio = 1 = perfectly spherical; Nuclear aspect ratio < 1 = elongated.

## 4.4 Discussion

Human MSCs have been found to be a useful source of cells to create tissue engineered bone constructs *in vitro* as they can readily differentiate down an osteogenic pathway under osteogenic culture conditions.[9, 10] We have recently shown that hMSCs seeded in 3D collagen matrices exhibit a potential for osteogenic differentiation when stimulated by cyclic tensile strain. The response of hMSCs to tensile strain is dependent on the deformation of the hMSCs in their collagen matrix. Reorientation of hMSCs in the collagen matrix could affect the degree of deformation they experience while straining and potentially disrupt a desirable differentiation pathway. However, difficulty in detecting hMSC morphology due to collagen matrix contraction poses a challenge to determining the changes in hMSC morphology and orientation in response to strain. As a solution, investigation of the morphological and orientation changes of hMSC nuclei in response to strain would facilitate an understanding of the intracellular response of hMSCs to strain. The response of hMSC nuclei to strain could then be used as a scale to measure strain experienced by hMSCs. It is also of importance to compare nuclear responses to strain with cell responses to strain in order to determine any correlation between the two responses. Therefore, the purpose of this study was to investigate the effects of uniaxial cyclic tensile strain, hMSC-seeding density and media conditions on nuclear morphology and orientation of hMSCs seeded in type I collagen matrices.

### 4.4.1 Nuclear orientation

Changes in nuclear morphology of hMSCs due to cyclic tensile strain and cell-seeding density were clearly evident. Similar to rabbit MSCs[12] and fibroblasts[126], in unstrained collagen matrices, hMSC nuclei were oriented parallel to the major (longitudinal) axis of the collagen matrices. However, relative to the unstrained (0%) matrices, hMSC nuclei in cyclically strained (10 and 12%) matrices were oriented away from the direction of applied strain. This phenomenon was more pronounced in matrices with lower cell densities (30,000 cells/ 200 μL vs. 60,000 cells/ 200 μL). This response is different from fibroblasts[108, 127] cultured on a monolayer which orient in the direction of principal strain when an external tensile strain is present, but similar to myofibroblasts,[128] human osteoblasts,[124] human endothelial cells,[120] human melanocytes,[119] rabbit smooth muscle cells,[125] and pig endothelial cells[125] which orient perpendicular to the direction of principle strain in two dimensional (2D) culture conditions.

The organization and orientation of cells under strain in a soft matrix such as collagen has been modeled by previous investigators. Girton et al.[129] introduced an anisotropic biphasic theory valid within the linear viscoelastic limit of cell seeded collagen matrices (15% strain) that adopts a strain-based approach to describe the orientation of cells. A recent study on the assumptions of that theory has proven that anisotropic network strain causes alignment of fibrils in a collagen matrix and that the cells in the matrix align with previously aligned fibrils.

Bischofs et al.[130] proposed a model based on linear elasticity theory, suggesting that a cell organizes and orients itself in a manner so that it experiences maximal effective stiffness

in its environment. In their model, the decisive factor on cell orientation is the local elasticity of the environment such that when rigidity of the matrix increases causing a decrease in displacement, the work that the cells have to invest on the matrix also decreases. Therefore, the cells orient in the direction of maximal rigidity.

In the current study, hMSC nuclei in unstrained matrices were oriented parallel to the longitudinal axis of the collagen matrix. This orientation of cell nuclei corresponds with Girton's model for cell orientation.[129] However, in cyclically strained matrices, the nuclei deviated from the direction of strain. Previous studies have shown that in 2D culture conditions, fibroblasts,[121] human endothelial cells,[120] endothelial cells from pig aorta,[125] rabbit arterial smooth muscle cells,[125] rabbit myofibroblasts[128] and human melanocytes[119] orient away from the direction of cyclic strain. The cues for reorientation of nuclei in strained matrices may have generated from hMSCs behaving similar to those cells. This hMSC behavior could then be explained using Bischofs' cell model based on local elasticity of a matrix.[130] In addition to the externally applied strain in the longitudinal direction of the matrix, there is also a strain normal to the longitudinal axis of the matrix due to matrix contraction by the hMSCs. As a result of these strains, there may be local differences in the rigidity of the collagen matrix that may have caused the hMSCs to have an intermediate orientation between the applied strain direction and the direction of matrix contraction. This reorientation of hMSCs could generate intracellular signals that in turn lead to a change in the orientation of nuclei.

Numerous studies have shown reorientation of cells cultured in 2D culture conditions in response to strain.[81, 119, 121, 124] Buck et al. suggested that orientation of cells away from the

strain direction was a stretch avoidance response.[121] Buckley et al. also hypothesized that the cells orient to minimize the strain acting on them.[81] Wang et al.[119] introduced a model based on the hypothesis that cells possess a peak-to-peak axial strain threshold and they reorient when this peak-to-peak axial strain threshold is reached. Based on the results of this study, it is clear that the reorientation of hMSC nuclei in strained collagen matrices resembles the reorientation of other cells such as fibroblasts, human endothelial cells, and human melanocytes in the presence of strain. Therefore, it appears that orientation of hMSC nuclei might be directly influenced by the cyclic tensile strain experienced by the hMSCs. The response of cells to cyclic tensile strain could occur via changes in integrins and focal adhesions, changes in synthesis of matrix proteins and reorientation of cells in the matrix.[25] It has been hypothesized that the cytoskeletal system transmits mechanical strain to the cell nucleus, which in turn causes changes in gene expression and cell shape.[131, 132] Ingber suggested that change in tension of the cytoskeletal system regulates cell and nuclear shapes.[132] In the current study, it is possible that reorientation of the hMSC nuclei is caused by the strain experienced by hMSC cytoskeleton and reorientation of the hMSCs in the collagen matrix. In addition, the type of cell response to mechanical strain depends on the time lapse from the initial sensing of tensile strain by cells to its actual response time to tensile strain.[25] Since matrices were analyzed after 7 and 14 days in this study, it is not possible to discuss the short term (minutes to hours) changes of nuclei orientation. However, our results at 1 and 2 weeks showed that the change in nuclei orientation of hMSCs was not dependent on culture duration. This shows that the hMSC nuclear orientation in collagen matrices was maintained throughout the culture period even though the applied strain was

periodic (4hrs/day). The nuclei did not appear to reorient during the rest period of 20 hours/day.

In the present study, on average, 43 - 63% of nuclei in unstrained matrices, 32 -52% of nuclei in 10% strained matrices and 28 - 55% of nuclei in 12% strained matrices were oriented at less than $15^0$ to the direction of strain. Although the majority of nuclei in both unstrained and strained matrices were oriented at less than $15^0$ from the direction of strain, hMSC nuclei in strained collagen matrices were also observed to orient at $35^0$ and $60^0$ from the direction of strain. The percentage of nuclei oriented at $35^0$ and $60^0$ to the strain direction was significantly different in strained matrices compared to the unstrained matrices; and matrices cultured in ODM compared to those cultured in MSCGM. Studies by Wang et al. showed that human melanocytes in two dimensional (2D) culture oriented near $60^0$ from the stretch direction when a 12% cyclic strain was applied.[119] Neidlinger-Wilke et al. reported that the percentage of cells oriented near $60^0$ does not depend on applied axial strain and the axial strain is zero near $60^0$.[124] Therefore, hMSC nuclei orientation at $60^0$ from the strain direction resembles the reorientation of human melanocytes, osteoblasts and fibroblast in the presence of strain. It is possible that hMSC nuclei orientation at $60^0$ could have resulted from reorientation of the hMSCs in collagen matrix as with other cells discussed above. The reorientation of nuclei at $35^0$ might be due to osteogenic differentiation of the hMSCs. Neidlinger-Wilke et al. showed that the axial strain threshold for human osteoblasts was 6.4 ± 0.6% and 4.2 ± 0.4% for human fibroblasts in 2D culture.[124] However, these axial strain values were not correlated to specific orientation angles in their study. Calculation of the cell orientation angle corresponding to approximately 6% axial strain in our collagen matrices

using Wang et al.'s[119] model revealed that cells reorient at $35^0$ from the direction of strain in the presence of 6% axial strain. Therefore, it is possible that hMSC nuclei oriented at $35^0$ to the strain direction represent the reorientation of hMSCs at $35^0$ that had undergone osteogenic differentiation and showed characteristics of osteoblastic phenotype.

Seeding density also affected the nuclear orientation angle. In general, more nuclei were oriented in the direction of strain at the higher seeding density. High density may have provided less freedom for the cells to orient themselves, causing most cells to align in the direction of strain.

### 4.4.2 Nuclear aspect ratio

Nuclear aspect ratio was significantly affected by strain. Interestingly, the nuclei were more elongated in unstrained matrices. This finding agrees with those of previous investigators made on rabbit MSCs[104] and rat osteoblasts[117] which had elongated shapes in the absence of tensile strain. In contrast, nuclei in strained matrices were more spherical compared to those in unstrained matrices. Bowman et al.[117] hypothesized that formation of gap junctions between cells would help to maintain cells in an elongated state. Elimination of these gap junctions would cause cells to revert back to a spherical shape and may also reduce matrix contraction by cells.[117] The cell seeding densities used in this study were higher than those by Bowman et al. (30,000 and 60,000 cells/ 200 μL vs 10,000 cells/ 200 μL) and a higher matrix contraction was observed throughout the culture period. This indicates existence and maintenance of gap junctions between hMSCs in the collagen matrix throughout the culture period. Therefore, it is highly unlikely that elimination of gap

junctions caused the hMSC nuclei to have a spherical shape in the strained matrices. Instead, it is possible that the local strain differences may have caused this morphological change in the nuclei. The effect of hMSC-seeding density on nuclei shape was similar to that observed with nuclei of rabbit MSCs.[104] At a higher cell seeding density, the nuclei in strained matrices and in matrices cultured with MSCGM had an elongated shape as compared to those in matrices seeded with a low seeding density.

The effect of medium was opposite to that of density. Compared to matrices treated with MSCGM, those in ODM had more spherically shaped nuclei. It is possible that hMSCs in ODM could produce increased amounts of collagen, thus decreasing the degree of freedom for the cells to spread and elongate. In addition, hMSCs could be undergoing osteogenic differentiation that could lead to a change in hMSC morphology more similar to the cuboidal shape of osteoblasts. These cellular functions might cause hMSCs in ODM to have more spherically shaped nuclei. Thomas et al.[133] reported that change in nuclear shape by constraining primary rat osteoblasts caused early expression of osteocalcin and increased Type I collagen synthesis. Based on their results and the findings in this study, it is possible that osteogenic differentiation of hMSCs is associated with change in nuclei shape. A possible correlation between change in nuclear shape and osteogenic differentiation of hMSCs was not investigated in this study and should be further investigated.

In summary, we have analyzed both the separate and combined effects of uniaxial cyclic tensile strain, initial cell seeding density, and medium on nuclear morphology and orientation of hMSCs seeded in Type I collagen matrices. The change of nuclear orientation angle and nuclear aspect ratio of hMSCs, especially in the presence of uniaxial cyclic tensile

strain, indicates an existence of an extracellular to intracellular signaling mechanism. The changes in tensile properties of the extracellular matrix may have triggered this mechanosensing signaling mechanism such that it alters the shape of the cytoskeleton and subsequently the shape and orientation of the nucleus. The results indicate that the change in morphology and orientation of hMSC nuclei in response to strain correspond well with changes in morphology and orientation of other cells in response to strain. This suggests a possible correlation between morphological and orientation changes of hMSC nuclei and those changes of hMSCs in response to strain. Therefore, change in nuclear morphology and orientation of hMSCs could be a good indicator of change in hMSC morphology and orientation in response to cyclic tensile strain.

## 4.5 Summary

Tensile strain can be used to induce osteogenic differentiation of mesenchymal stem cells (MSCs) seeded in three dimensional (3D) collagen matrices. However, strain induced reorientation of MSCs in collagen matrices might alter MSC deformation, potentially hindering osteogenic differentiation. At higher initial seeding densities, changes in MSC morphology and orientation in response to strain cannot be determined due to high contraction of the MSC-seeded collagen matrices and the inherent filipodial nature of MSC morphology. However, changes in morphology and orientation of MSC nuclei are easily visualized and therefore could be a better indicator of MSC response to strain. This study was performed to analyze the effects of cyclic tensile strain, medium and initial cell seeding

density on nuclear morphology and orientation of human MSCs (hMSCs) cultured in collagen matrices. Human MSC seeded 3D collagen matrices were subjected to cyclic tensile strain at 10 or 12% for 4 hours/day at 1 Hz in osteogenic differentiation (ODM) or complete growth media (MSCGM) for 14 days. In general, nuclei in strained matrices were more spherical and oriented away from the direction of strain. However, a high initial seeding density in strained matrices caused nuclei to remain spherical but orient in the direction of strain. Nuclei were more spherical in ODM than in MSCGM. Changes in morphology and orientation of hMSC nuclei appear to be caused by morphological and orientation changes of hMSCs in response to strain. Nuclear morphology and orientation of hMSCs can be successfully used to study hMSC response to strain.

# 5 Osteogenic Differentiation of Human Mesenchymal Stem Cells in Collagen Matrices: Effects of Uniaxial Cyclic Tensile Strain on Bone Morphogenetic Protein (BMP-2) mRNA Expression

In the previous chapters, the investigations on the effects of cyclic tensile strain, intial cell density, culture duration, and culture medium on collagen matrix contraction by hMSCs as well as their morphology and orientation were described. From the conclusions made in the previous two studies, it is clear that hMSCs can be cultured in three-dimensional collagen constructs for two weeks without losing their dimensional stability. The majority of the hMSCs appear to experience the tensile strains applied during mechanical stimulation. With these findings, it is necessary to determine initially how cyclic tensile strain alone can affect expression of bone markers by hMSCs. This chapter describes the effect of cyclic tensile strain on the expression of bone morphogenetic protein-2 by hMSCs.

## 5.1 Introduction

In recent years, mesenchymal stem cells (MSCs) have been utilized in studies investigating bone tissue engineering since these cells readily differentiate down an osteogenic pathway with appropriate chemical cues.[3, 5] MSCs are the primary cell source for endochondral and intramembranous bone formation *in vivo,*[4] therefore they may be ideal for cell-seeded constructs that can be utilized for bone tissue repair. However, most biological constructs lack the mechanical strength to withstand forces within the *in vivo* environment. To facilitate *in vitro* development of a tissue engineered bone construct with near physiological mechanical properties, the optimal mechanical and chemical stimuli to which MSCs should be exposed *in vitro* needs to be determined.

Mechanobiological models of osteogenic differentiation have shown that intramembranous bone formation is promoted by low to moderate tensile strains and low hydrostatic stresses.[13, 26, 41] Previous investigations of distraction osteogenesis by one of the authors indicated that 10-12% tensile strain promoted intramembranous bone formation in a rat model.[14, 15] Studies utilizing MSCs have demonstrated that MSCs in monolayer culture will differentiate down osteogenic pathways under either chemical stimulation alone or combined chemical and mechanical stimulation.[6, 8-10, 16, 17, 28] Type I collagen can be used as a scaffold material to better mimic the *in vivo* environment since type I collagen is the most abundant extracellular matrix protein found in bone. Type I collagen also contains cell adhesion RGD (arginine-glycine-aspartic acid) sequences[2] that promote cell growth and proliferation. In addition, MSCs have also been cultured on various scaffolds and examined for their proliferative and osteogenic differentiation potential under *in vitro* static

(i.e., ithout mechanical load) conditions.[18, 20, 21, 30, 93, 94, 103, 134] Irrespective of the architecture and composition of these scaffolds, MSCs proliferated and underwent osteogenesis when cultured on these static three-dimensional (3D) scaffolds.

Upregulation of bone markers such as bone morphogenic protein-2 (BMP-2), type I collagen (COL I), alkaline phosphatase (ALPL), osteocalcin (OCN) and osteopontin (OPN) have been analyzed in MSCs to determine their osteogenic differentiation potential.[9, 10] Bone morphogenic protein-2 is a low molecular weight glycoprotein that functions as a morphogen and belongs to the transforming growth factor-β (TGF-β) superfamily.[60] BMP-2 has been shown to be upregulated in human MSCs (hMSCs) during osteogenic differentiation in response to chemical stimulation.[64, 135] However, there are no studies that have investigated the effects of mechanical strain on BMP-2 expression in human MSCs in 3D culture conditions.

The aim of the present study was to investigate the effects of uniaxial cyclic tensile strain on the osteogenic differentiation potential of hMSCs cultured in 3D type I collagen matrices. We hypothesized that application of uniaxial cyclic tensile strain to hMSCs cultured in a 3D linear collagen construct would increase BMP-2 expression in both the presence and absence of chemical stimulation (osteogenic differentiating supplements). To test our hypothesis, hMSC-seeded type I collagen matrices were subjected to tensile strains for up to 14 days at a physiological frequency and analyzed for cell viability and BMP-2 mRNA expression levels.

## 5.2 Material and Methods

### 5.2.1 Cell culture

Bone marrow derived-hMSCs from a 26 year old male donor (Cambrex Bio Science, Walkersville, MD) were expanded to passage 3 or 4 and maintained in complete non-differentiating growth medium supplemented with fetal bovine serum (FBS), 4 mM L-glutamine, 0.05 units/ml penicillin, and 0.05 μg/ml streptomycin (Cambrex).

### 5.2.2 Osteogenic differentiation in static monolayer culture

To confirm the expected effects of both non-differentiating medium and medium supplemented with osteogenic factors on hMSCs in static monolayer culture, cells were cultured at 100,000 cells/10 $cm^2$ in 6-well culture plates with non-differentiating growth medium until 100% confluent. Cells were then cultured in either non-differentiating growth medium or osteogenic medium, for an additional 14 days. Osteogenic medium consisted of the complete growth medium plus osteogenic growth supplements including 0.5% ascorbic acid, 0.5% dexamethasone, and 1% β-glycerophosphate. Osteogenic differentiation was determined by the deposition of mineralized matrix as visualized by staining with Alizarin red. After 14 days of culture post confluence, cell monolayers were rinsed with PBS, fixed with 10% formalin for 30 minutes, rinsed twice in PBS and stained with 2% Alizarin red S. Hematoxylin was used as a nuclear counterstain.

### 5.2.3 Fabrication of cell seeded 3D collagen matrices

Cell-seeded linear 3D collagen matrices were created using the Tissue Train™ culture system (Flexcell International, Hillsborough, NC)[107]. Briefly, 6-well Tissue Train™ culture plates, which have flexible well bottoms and non-woven anchors on two opposing sides, were fitted atop cylindrical posts that have a linear groove across their central axes such that the groove aligned with the anchors. A vacuum was applied to the assembly, and the membranes were deformed downward into the grooves creating linear troughs into which the cell seeded collagen solution was dispensed. Human MSCs were cultured until 80-85% confluent, detached with 0.05% trypsin/0.53 mM EDTA, and suspended in a collagen solution at 30,000 cells per 200 µl. The collagen solution consisted of 70% v/v Vitrogen (type I collagen; Angiotech BioMaterials Corp, Palo Alto, CA; neutralized to pH 7.0 with 1 N sodium hydroxide), 20% v/v 5x minimum essential medium (Sigma), and 10% v/v FBS (Cambrex). The cell seeded collagen solution was dispensed into the linear troughs created by the application of vacuum to the Tissue Train™ plate assembly as described above. The assembly was then incubated at 5% $CO_2$ and 37 $^0$C for 2 hours to allow the collagen to polymerize and attach to the nonwoven anchors (Fig. 5.1). After 2 hrs, the vacuum was released and complete growth medium was added to each well. The seeded collagen gels were incubated for another 24 hrs, at which time the growth medium was changed.

### 5.2.4 Application of cyclic tensile strain

The cell-seeded collagen matrices were subjected to 10% or 12% uniaxial cyclic tensile strains at 1 Hz for 4 hours/day, for 7 or 14 days. Uniaxial cyclic strain was applied

and controlled with the Flexercell FX-4000 strain unit (Flexcell International). Cells seeded into collagen gels as described above but maintained in static culture served as the unloaded controls. For each strain and time point, three separate constructs were analyzed. Two constructs for each condition were seeded and then strained simultaneously, and a third was seeded and strained in a separate experiment to demonstrate reproducibility.

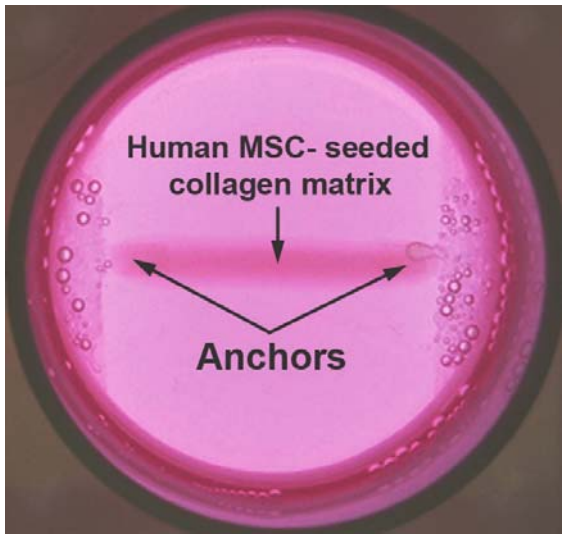


**Figure 5.1.** Cell-seeded collagen matrix loaded into a well of a Tissue Train™ culture plate. Approximate length with anchors= 34mm, width= 3mm.

### 5.2.5 Cell viability

Viability of hMSCs in cell-seeded collagen matrices after 7 and 14 days was determined using calcein AM, which stains live cells green, and ethidium homodimer-1 (EthD-1; Molecular Probes, Eugene, OR), which stains dead cells red. The constructs were washed twice in phosphate buffered saline (PBS) and incubated in a staining solution containing 4 μM calcein AM and 4 μM EthD-1 for 45 minutes in the dark. Constructs were then mounted on glass slides and the center and two ends of the constructs were imaged using a fluorescence microscope (Leica Microsystems Inc., Bannockburn, IL) with a 10 × objective. At least 2 different images were obtained from each location. The images were acquired using SimplePCI image analysis software (Compix Inc. Imaging systems, Cranberry Township, PA). The area occupied by live and dead cells in each image was measured using Adobe Photoshop (Adobe Systems Inc., San Jose, CA) and the percentage area of live and dead cells in each image was calculated.

### 5.2.6 Real-time polymerase chain reaction

After 7 and 14 days of strain, the cell-seeded constructs were removed from the culture plates and immediately frozen at -80 $^{0}$C. Total RNA was isolated using a Perfect RNA Eukaryotic Mini kit (Eppendorf, Westbury, NY). RNA concentrations were determined using a Ribogreen RNA quantitation kit (Molecular Probes Inc., OR). First strand cDNA was synthesized from 60-180 ng of total RNA for a 25 μl reverse transcriptase (RT) reaction using Superscript III RT with oligo(dT) primers (Invitrogen, Carlsbad, CA). Complimentary

DNA was amplified in the presence of primer probe oligonucleotide sets (Assays-on-Demand, Applied Biosystems, CA) for BMP-2 (Assay HS00154192_M1) and glyceraldehyde-3-phosphate dehydrogenase (GAPDH) (Assay HS99999905_M1) in an ABI Prism 7000 system (Applied Biosystems). Expression levels of BMP-2 mRNA were normalized to GAPDH expression. The fold change in expression was calculated according to the relative quantification method[136] in relation to the same day unstrained control cells. All PCR reactions were performed in triplicate. Data were analyzed using the unpaired Student t-test. Statistically significant values were defined as $p < 0.05$ and $p < 0.09$. Data are presented as mean ± standard deviation.

## 5.3 Results

### 5.3.1 Osteogenic differentiation of hMSCs in static monolayer cultures

Microscopic analysis of cell monolayers stained with Alizarin Red S indicated that hMSCs cultured in non-differentiating growth medium did not deposit calcium (Fig. 5.2A). However, for hMSCs cultured in osteogenic medium for 14 days, 50% - 60% of the culture surface was covered with calcium deposits, indicating that the hMSCs were able to undergo osteogenesis under appropriate chemical conditions (Fig. 5.2B).

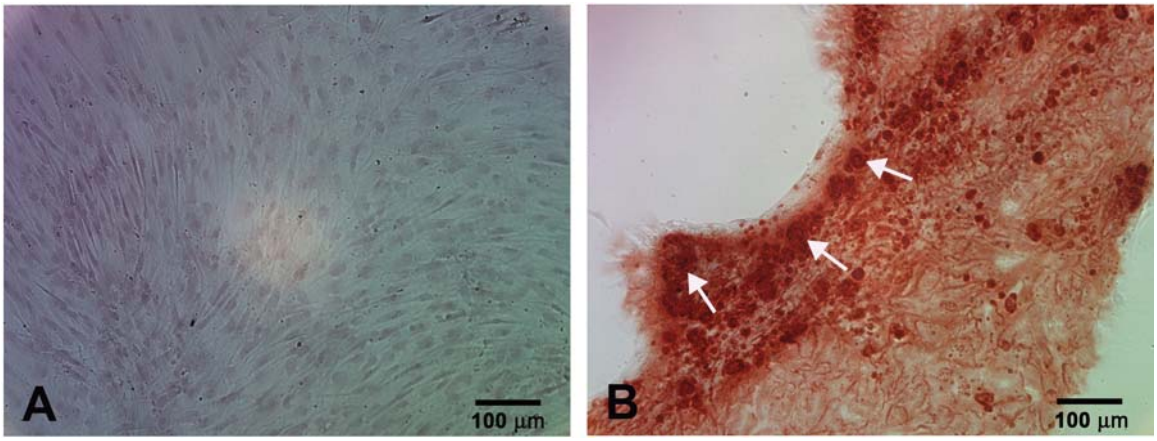


**Figure 5.2.** Alizarin red S stained calcium deposits and hematoxylin stained nuclei of hMSC in monolayer culture maintained in A) complete growth and B) osteogenic media for 14 days. Arrows indicate calcium deposits.

### 5.3.2 Cell viability

An assessment of the microscopic images from the center and both ends of the stained matrices revealed that less than 1% of the area was occupied by dead cells in all matrices after 7 days. However, on average, the area occupied by dead cells increased to 2 ± 2 % after 14 days irrespective of the strain levels (Fig. 5.3). The dead cells in the matrices were not limited to any particular area of the construct.

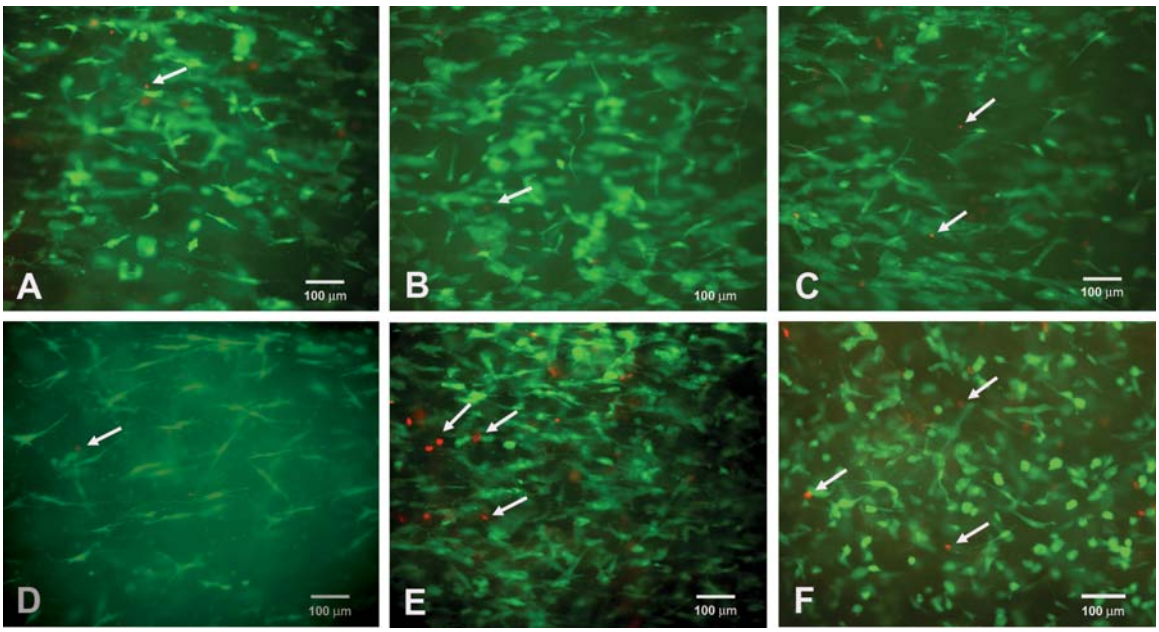


**Figure 5.3.** Representative images of strained and unstrained hMSC-seeded type 1 collagen matrices stained with calcein AM and EthD-1 showing live (green) and dead (red) cells, respectively. Arrows indicate dead cells. A) Unstrained control after 1 week, B) 10% strained after 1 week, C) 12% strained after 1 week, D) Unstrained control after 2 weeks, E) 10% strained after 2 weeks, and F) 12% strained after 2 weeks.

### 5.3.3 Effect of cyclic tensile strain on BMP-2 mRNA expression

Expression levels of BMP-2 mRNA increased in all strained hMSCs compared to their same day unstrained controls after both one and two weeks (Fig. 5.4). In constructs seeded with 30,000 cells, a significant 4-fold increase in BMP-2 expression was observed in 10% strained cells after 1 week (Fig. 5.4). Although the 12% strained cells showed an increase in BMP-2 expression after one week, it was not significant due to the high variability of the expression levels between replicates (note: for this data point only, results are derived from two rather than three constructs due to failure of one construct during straining). After two weeks, both 10 and 12% strained cells significantly increased BMP-2 expression levels compared to their same day unstrained controls (Fig. 5.4). In both 10 and 12% strained cells, the fold increase in BMP-2 expression observed after two weeks was lower than that observed after one week.

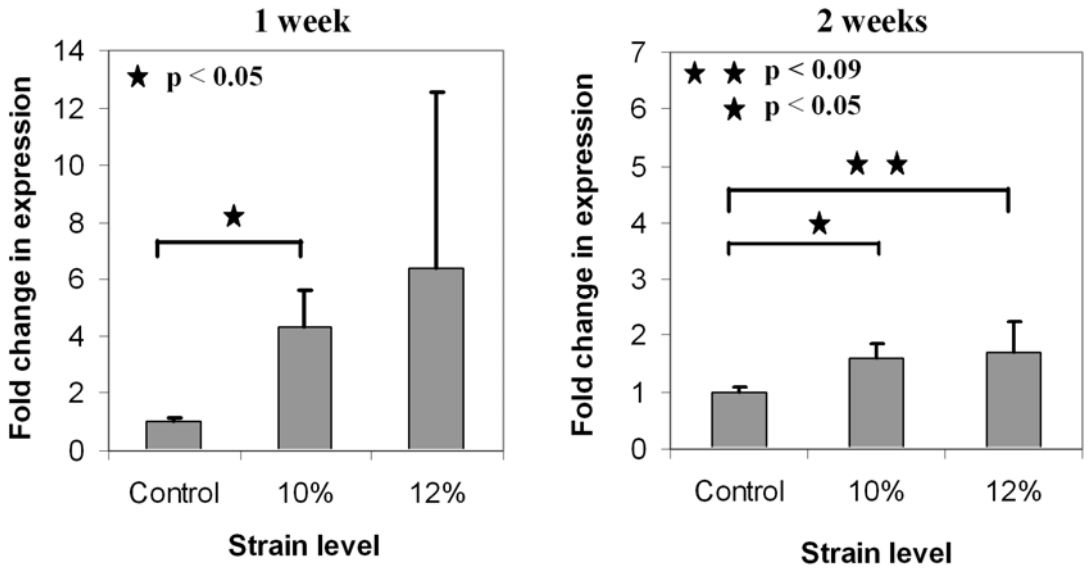


**Figure 5.4.** Fold change in expression levels of BMP-2 mRNA in hMSCs cultured in 3D collagen matrices and subjected to 10% and 12% cyclic tensile strains for 1 and 2 weeks. Control denotes the same day unstrained hMSCs maintained in identical media conditions.

## 5.4 Discussion

The ability of the MSCs to differentiate down an osteogenic pathway under chemical or mechanical stimulation can be utilized to develop cell-seeded tissue engineered bone constructs *in vitro*. However, the optimum conditions for chemical and mechanical stimulations of MSCs to achieve osteogenic differentiation *in vitro* have to be identified. The present study is the first demonstration that hMSCs can be successfully cultured in a 3D matrix under strain and that strain alone can induce osteogenic differentiation, in the absence of external chemical cues.

We investigated the effects of uniaxial cyclic tensile strain on osteogenic differentiation of bone marrow-derived hMSCs cultured in 3D type I collagen matrices. Initially, hMSCs were cultured under static (i.e. no mechanical load applied) monolayer conditions. Cells in undifferentiating growth medium had not produced a mineralized matrix at 14 days post confluence. However, prominent deposits of mineral were evident in cultures when osteogenic supplements were added to the medium.

In 3D cultures, viability of cells must be confirmed to demonstrate adequate gas exchange and nutrient availability, and general suitability of matrix and experimental conditions to sustain healthy cultures. Using fluorescent markers for live and dead cells, we have shown that hMSCs, when cultured in 3D type I collagen matrices and cyclically strained at 10 and 12%, remained viable throughout the entire construct for up to 14 days. Further, cyclic tensile strain increased expression of BMP-2 mRNA compared to unstrained controls after both one and two weeks, indicating tensile strain alone promotes osteogenic differentiation of hMSCs without osteogenic supplements.

Several studies have demonstrated the growth and proliferation capacity of MSCs in collagen matrices and found that MSCs can be successfully cultured in collagen matrices under static conditions.[104, 137, 138] In addition to confirming these findings, the current study has also shown that hMSCs can be cultured in collagen matrices under mechanical load. Human MSCs maintained their viability in type I collagen matrices for the entire culture period irrespective of the application of cyclic tensile strain. These results indicate that type I collagen can be successfully used as a scaffold material for culture of hMSCs in 3D and for subjecting hMSCs to mechanical strains without inducing significant cell death.

In addition to maintaining viability, hMSCs also increased BMP-2 mRNA expression when cultured in 3D collagen matrices and subjected to mechanical load. BMPs are directly or indirectly involved in the expression of cytokines and growth factors which affect osteogenic differentiation of MSCs[139] and therefore can serve as a marker of osteogenic differentiation. Previous studies have shown that under static monolayer culture conditions and in the presence of osteogenic growth supplements, BMP-2 expression is maximal at 21 days.[64] This maximal expression correlated with increased expressions of ALPL and OCN. Similar results were observed by Frank et al.[135] where an increased expression of BMP-2 was reported after 20 days in bone marrow derived hMSCs cultured in osteogenic medium. Several studies have shown that BMP-2 can also function as a growth factor for osteogenic differentiation. Wang et al.[62] reported that a high concentration of BMP-2 induced mouse mesodermal progenitor cells to differentiate into osteoblasts. The proliferation of hMSCs increased when cultured in serum free growth media containing physiological concentrations of BMP-2.[63] Based on these studies, it is clear that BMP-2 can function in an autocrine

pathway to increase MSC proliferation and osteogenic differentiation. Therefore, an increase in BMP-2 expression in hMSCs is expected to promote both cell proliferation and osteogenic differentiation.

The expression pattern of BMP-2 in our study resembled the expression pattern observed during fracture healing in rats[140]. Increased expression of BMP-2 was observed after 7 days which subsequently decreased by 14 days of mechanical strain. A study by Onishi et al.[140] showed that during fracture healing in rats, BMP-2 was involved in all stages of bone repair including intramembranous and endochondral ossification.[140] During intramembranous ossification BMP-2 expression was increased on day 3 and then continually decreased through day 14.[140] However, it is noted that fracture healing time in rats is shorter than in humans. [141, 142] Since expression levels in our study are similar to the expression levels observed in the study by Onishi et al.,[140] it would appear that BMP-2 expression was accelerated in hMSCs under the conditions tested in our study.

In the current study, the increased expression levels of BMP-2 in cyclically strained cells were achieved without addition of osteogenic growth supplements. Most monolayer studies reported an increase in BMP-2 expression levels after 20–21 days in the presence of osteogenic growth supplements under static conditions.[64, 135] Therefore, the results of this study indicate that culturing hMSCs in 3D type I collagen matrices and subjecting them to cyclic tensile strain not only provides a way of mimicking the *in vivo* conditions but also accelerates the expression levels of BMP-2 and perhaps promotes osteogenic differentiation of hMSCs earlier.

One limitation of this study is the contraction of the collagen matrices by the hMSCs

during culture, which causes matrix rupture. This shortens the culture time significantly and prohibited the study from being carried out for longer time periods than 2 weeks. Studies are being conducted by the authors to quantify the contraction and potentially find alternative means to maintain hMSC-seeded collagen cultures for a longer time.

In conclusion, we have shown that bone marrow derived hMSCs thrive for up to 14 days in 3D collagen matrices under uniaxial cyclic tensile strain and strain alone is sufficient to increase expression of BMP-2, in the absence of chemical factors. This demonstrates the critical nature of mechanical factors in the osteogenic differentiation process.

## 5.5 Summary

Human mesenchymal stem cells (hMSCs) will differentiate down an osteogenic pathway with appropriate mechanical and/or chemical stimuli. This study describes the successful culture of hMSCs in three dimensional (3D) collagen matrices under mechanical strain. Bone marrow-derived hMSCs were seeded in linear 3D type I collagen matrices and subjected to 0, 10 and 12% uniaxial cyclic tensile strain at 1 Hz for 4 hours/ day for 7 and 14 days. Cell viability studies indicated that hMSCs remained viable throughout the culture period irrespective of the applied strain level. Real time RT-PCR studies indicated a significant increase in BMP-2 mRNA expression levels in hMSCs strained at 10% compared to the same day unstrained controls after both 7 and 14 days. An increase in BMP-2 was also observed in hMSCs subjected to 12% strain, but the increase was significant only in the 14 day sample. This is the first report of the culture of bone marrow-derived hMSCs in 3D collagen matrices under cyclic strain, and the first demonstration that strain alone can induce osteogenic differentiation without the addition of osteogenic supplements. Induction of bone differentiation in 3D culture is a critical step in the creation of bioengineered bone constructs.

# 6 Cyclic Tensile Strain Upregulates Genes Indicative of Osteogenesis in Human Mesenchymal Stem Cells Cultured in Collagen Matrices

The previous chapter revealed that uniaxial cyclic tensile strain induces expression of bone morphogenetic protein-2 in hMSCs cultured in three-dimensional collagen matrices. In that study, hMSCs were cultured without the presence of osteogenic supplements such as dexamethasone, β-glycerophosphate, and ascorbic acid in the culture medium and stimulated using tensile strain alone. The next study was carried out to determine whether the presence of osteogenic supplements in culture medium accelerated the expression of osteogenic markers when combined with strain. The initial hMSC seeding density was maintained constant to investigate the effects of strain, culture medium, and culture duration on expression of osteogenic markers.

## 6.1 Introduction

Intramembranous bone formation *in vivo* has been found to be initiated by mesenchymal stem cells (MSCs).[4] Investigation of MSC viability and potential osteogenesis in three dimensional (3D) culture conditions *in vitro* would facilitate an understanding of MSC behavior in 3D culture conditions and aid in the creation of bone constructs *in vitro*.

Mechanobiological models have shown that low to moderate tensile strains and low hydrostatic stresses induce intramembranous bone formation *in vivo*. [13, 26, 41] Loboa *et al.* have shown by finite element analyses and experimental studies of distraction osteogenesis using a rat model that tensile strains of 10-12% promote intramembranous bone formation.[14, 15] *In vitro,* osteogenic differentiation of MSCs in monolayer cultures, in the presence of osteogenic differentiation supplements such as dexamethasone, ascorbic acid, and β-glycerophosphate have also been reported.[6, 9, 10] In the presence of these osteogenic supplements, human MSCs (hMSCs) cultured on monolayers have shown an increase in mRNA expression levels of Type I collagen (COLI),[64, 135] alkaline phosphatase (ALPL),[9, 10, 64] bone morphogenetic protein-2 (BMP-2)[64, 135] and osteocalcin (OCN)[9, 10, 64] and also exhibited osteoblastic morphology.[9] Recent investigations have shown that application of cyclic tensile strain to MSCs cultured in monolayer cultures induce osteogenic differentiation in the presence of osteogenic supplements.[16, 17, 28] Jagodzinski *et al*.[16] investigated the osteogenic differentiation of human bone marrow stromal cells in monolayer cultures under 2% and 8% cyclic tensile strain. They reported that the expression of COLI, ALPL and OCN by human bone marrow stromal cells increased with application of cyclic tensile strain at 8%

in the presence of dexamethasone and ascorbic acid.[16] These expressions were greater than those at 2%.[16]

In addition, recent studies by the authors have shown that adult bone marrow derived hMSCs cultured in 3D collagen matrices under uniaxial cyclic tensile strain at 10% and 12% without osteogenic supplements maintain their viability and increase BMP-2 mRNA expression levels. However, the osteogenic differentiation potential of human MSCs cultured in 3D culture conditions under cyclic tensile strain and in the presence of osteogenic supplements has not been investigated.

The purpose of this study was to investigate the effects of cyclic tensile strain, culture medium and culture duration on the expression of osteogenic markers by hMSCs cultured in 3D collagen matrices. We hypothesized that application of tensile strain in the presence of osteogenic supplements would increase mRNA expression levels of COLI, OCN, and BMP-2. To test our hypothesis, hMSCs were cultured in 3D collagen matrices and subjected to cyclic tensile strain at 10 or 12% in either complete growth medium or osteogenic differentiating medium for up to 14 days.

## 6.2 Materials and Methods

### 6.2.1 Cell culture

Human MSCs were derived from bone marrow of a 26 year old African American male donor (Cambrex Bio Science, Walkersville, MD) and expanded to passage 3 or 4 in complete growth medium (MSCGM) consisting of fetal bovine serum (FBS), 4 mM L-glutamine, 0.05 units/ml penicillin, and 0.05 µg/ml streptomycin (Cambrex).

### 6.2.2 Fabrication of hMSC- seeded 3D collagen matrices

Human MSC-seeded linear 3D collagen matrices were created using the TissueTrain$^{TM}$ culture system (Flexcell International, Hillsborough, NC) as previously reported. Briefly, hMSCs cultured to 80-85% confluence were detached using 0.05% trypsin/0.53 mM EDTA (Cambrex) and suspended in a premixed collagen solution at 30,000 cells per 200 µl. The collagen solution consisted of 70% v/v Type I collagen (Vitrogen; Angiotech BioMaterials Corp, Palo Alto, CA; neutralized to pH 7.0 with 1 N sodium hydroxide), 20% v/v 5x minimum essential medium (Sigma), and 10% v/v FBS (Cambrex). Six-well TissueTrain$^{TM}$ culture plates, comprised of flexible well bottoms (membrane) and non-woven anchors on two opposing sides, were fitted with cylindrical posts that have a linear groove across their central axes. The membranes were deformed downward into the grooves of the cylindrical posts creating linear troughs by applying a vacuum to the plate assembly. The hMSC seeded Type I collagen solution was then dispensed into the troughs

and the assembly was incubated at 5% $CO_2$ and 37 $^0$C for 2 hours to allow the collagen to polymerize and attach to the nonwoven anchors. After 2 hours, the vacuum was released and MSCGM was added to each well. The hMSC seeded collagen matrices were further incubated 24 hours, after which the medium was changed. One group of hMSC seeded collagen matrices were maintained in MSCGM, while another group was maintained in osteogenic differentiating medium (ODM) consisting of MSCGM supplemented with 0.5% dexamethasone, 1% β-glycerophosphate and 0.5% ascorbic acid (Cambrex), throughout the culture period. The medium was changed every 3 days through 7 and 14 days of culture.

### 6.2.3 Application of uniaxial cyclic tensile strain

Uniaxial cyclic strain was applied to the hMSC seeded collagen matrices using the Flexercell FX-4000 strain unit (Flexcell International). The hMSC seeded collagen matrices were subjected to 10 or 12% uniaxial cyclic tensile strains at 1 Hz for 4 hours/day, for up to 14 days. Human MSCs seeded into collagen gels as described above and maintained in static (strain = 0%) culture served as unloaded controls. For each combination of strain, culture medium and time point, three separate constructs were analyzed.

### 6.2.4 Cell viability

Viability of hMSCs in unstrained and strained hMSC-seeded collagen matrices after 7 and 14 days was determined using a live/dead viability/cytotoxicity kit (Molecular Probes,

Eugene, OR). The collagen matrices were washed twice in phosphate buffered saline (PBS) and incubated in a staining solution containing 4 μM calcein AM and 4 μM EthD-1 for 45 minutes in the dark. Calcein AM stained live cells green and ethidium homodimer-1 stained dead cells red. Stained matrices were then mounted on glass slides for microscopic observations. The center and two ends of the constructs were imaged using a fluorescence microscope (Leica Microsystems Inc., Bannockburn, IL) with a 10 × objective to obtain at least 2 different images each from the center and both ends of each construct. SimplePCI image analysis software (Compix Inc. Imaging systems, Cranberry Township, PA) was used to capture the images. Live and dead cells at each location of the collagen matrix were quantified by separately measuring the area they occupied using Adobe Photoshop (Adobe Systems Inc., San Jose, CA). The percentage area of live and dead cells in each image was calculated.

### 6.2.5 Real-time polymerase chain reaction

The unstrained and strained hMSC-seeded collagen matrices were removed from the culture plates after 7 and 14 days and immediately frozen at -80 $^{0}$C. Perfect RNA Eukaryotic Mini kit (Eppendorf, Westbury, NY) was used to isolate Total RNA from the hMSCs. The Total RNA concentration of each isolation was determined using a Ribogreen RNA quantitation kit (Molecular Probes Inc., OR). The Superscript III RT with oligo(dT) primers (Invitrogen, Carlsbad, CA) were used in a 25 μl reverse transcriptase (RT) reaction to synthesize first strand cDNA from 60-180 ng of total RNA isolated. Complimentary DNA

was amplified using an ABI Prism 7000 system (Applied Biosystems) in the presence of primer probe oligonucleotide sets (Assays-on-Demand, Applied Biosystems, CA) for glyceraldehyde-3-phosphate dehydrogenase (GAPDH) (Assay HS99999905_M1), collagen Type 1 alpha 2 (COL1A2, Assay HS00164099_M1), BMP-2 (Assay HS00154192_M1) and osteocalcin (OCN, Assay HS01587813_g1). Expression levels of mRNA were normalized to GAPDH expression and the fold change in expression was calculated according to the relative quantification method[136] in relation to the same day unstrained control cells. All PCR reactions were performed in triplicate. Data were analyzed using the unpaired Student's t-test. Statistically significant values were defined as $p < 0.05$, and p values of $p < 0.06$ and $p < 0.09$ are also indicated. Data are presented as mean ± standard deviation.

## 6.3 Results

### 6.3.1 Cell viability

The hMSC seeded collagen matrices cultured in both MSCGM and ODM showed greater than 99% area occupied by live cells after 7 days, irrespective of the strain level applied. On average, the area occupied by live cells in matrices cultured in both ODM (Fig. 6.1) and MSCGM (data not shown) decreased to 98 ± 2 % after 14 days.

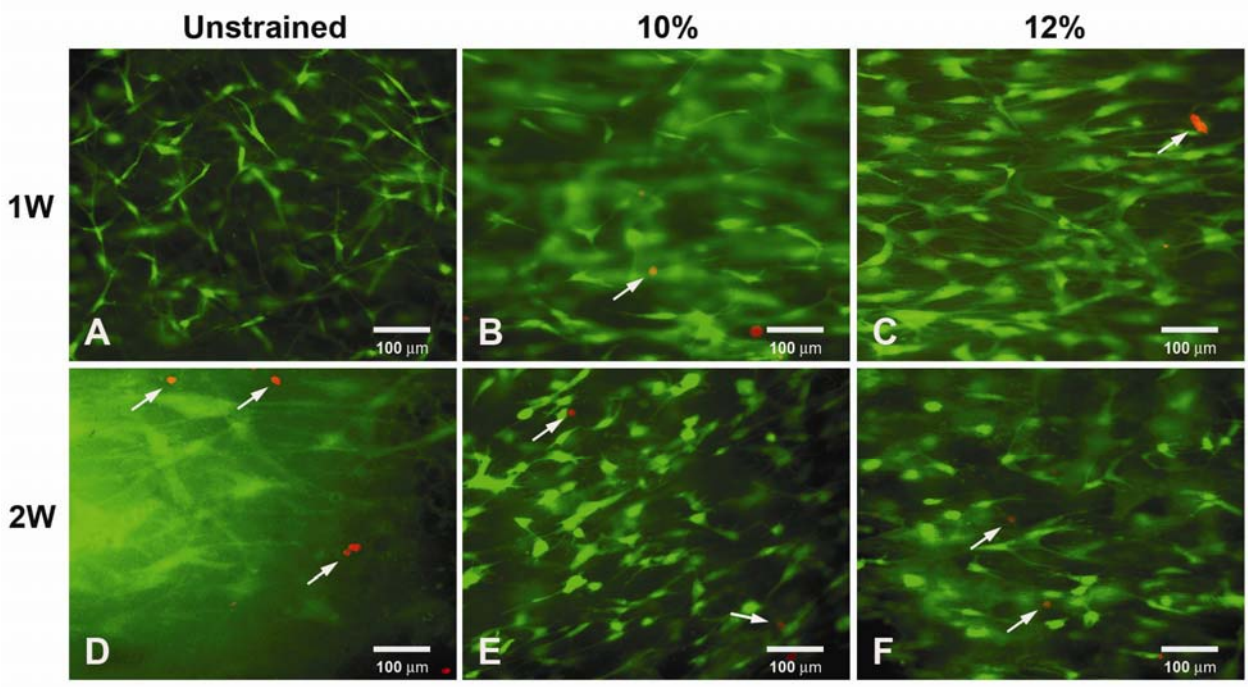


**Figure 6.1.** Strained and unstrained hMSC-seeded type 1 collagen matrices cultured in osteogenic differentiating medium (ODM) and stained with calcein AM and EthD-1 for live (green) and dead (red) cells, respectively. Arrows indicate dead cells. A, D) Unstrained for A) 1 week and D) 2 weeks, B, E) Strained at 10% for B) 1 week and E) 2 weeks, C, F) Strained at 12% for C) 1 week and F) 2 weeks. 1W = 1 week and 2W = 2 weeks.

### 6.3.2 COLI mRNA expression

Human MSCs cultured in MSCGM and cyclically strained at both 10 and 12% for one week had significantly higher COLI mRNA expression levels compared to their unstrained controls (Fig. 6.2A). Although not significant, the COLI mRNA expression levels were higher in hMSCs strained and cultured in ODM for one week compared to their same day unstrained controls. By two weeks, there was no significant change in COLI mRNA expression levels in strained hMSCs compared to their controls although the trend indicated that strained hMSCs cultured in ODM exhibited a down regulation of COLI mRNA expression (Fig. 6.2B).

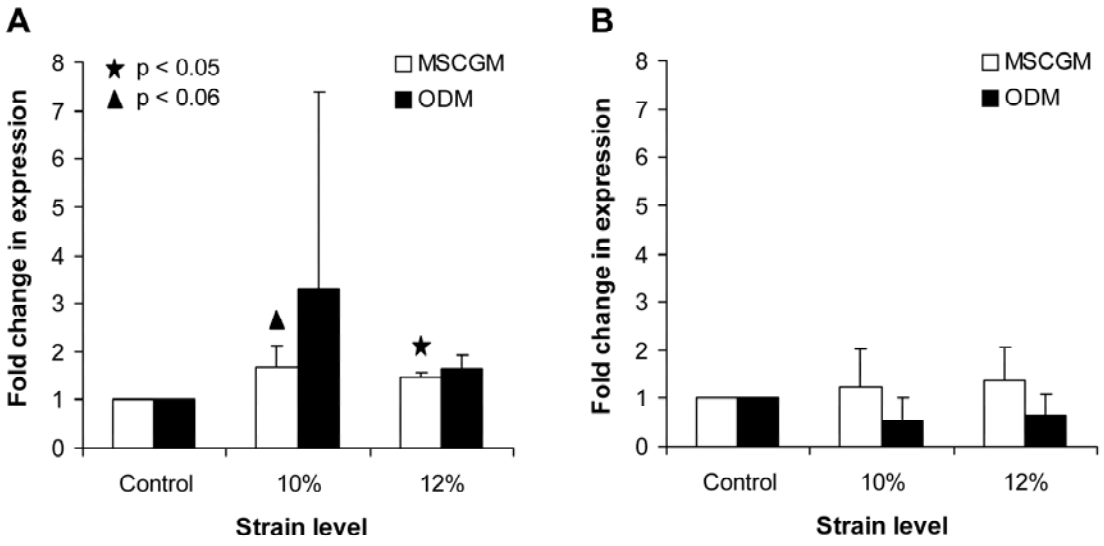


**Figure 6.2.** Fold change in expression levels of COLI mRNA in hMSCs cultured in 3D collagen matrices and subjected to 0% (control), 10%, and 12% cyclic tensile strains. A) Cultured for 1 week, B) Cultured for 2 weeks. Control denotes same day unstrained hMSCs maintained in identical media conditions. Statistical significance symbols represent significance with reference to control. MSCGM = complete growth medium; ODM = osteogenic differentiating medium.

### 6.3.3 BMP-2 mRNA expression

On average, cyclic tensile strain increased the expression levels of BMP-2 mRNA in hMSCs compared to their same day unstrained controls after both one and two weeks irrespective of the culture medium (Fig. 6.3). The expression level of BMP-2 mRNA significantly increased in hMSCs strained at 10% in MSCGM and those strained at 12% in ODM after 1 week compared to their same day unstrained controls (Fig. 6.3A). After two weeks, BMP-2 mRNA expression in all strained hMSCs cultured in both MSCGM and ODM increased compared to their unstrained controls (Fig. 6.3B). No significant difference in BMP-2 mRNA expression levels was observed between hMSCs strained at 10% and 12% either at 1 week or 2 weeks. Effect of culture medium on BMP-2 mRNA expression level was significant in strained hMSCs cultured for two weeks (Fig. 6.3B). Strained hMSCs cultured in ODM for two weeks had a higher BMP-2 mRNA expression than those cultured in MSCGM (Fig. 6.3B). Culture time significantly affected 10% strained hMSCs in MSCGM. Compared to hMSCs strained at 10% and cultured for one week, those cultured for 2 weeks in MSCGM had a significantly lower BMP-2 mRNA expression level (Fig. 6.3B) compared to same day unstrained controls. However, in ODM the BMP-2 mRNA expression level significantly increased after two weeks relative to it's expression level after one week (Fig. 6.3B).

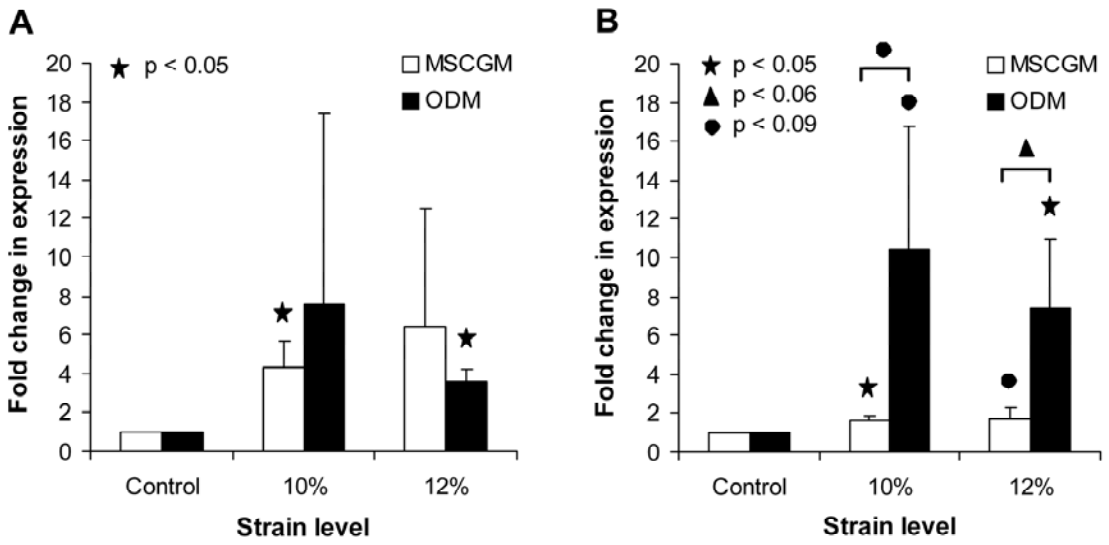


**Figure 6.3.** Fold change in expression levels of BMP-2 mRNA in hMSCs cultured in 3D collagen matrices and subjected to 0% (control), 10%, and 12% cyclic tensile strains. A) Cultured for 1 week, B) Cultured for 2 weeks. Control denotes same day unstrained hMSCs maintained in identical media conditions. Unless indicated otherwise with a horizontal bracket, statistical significance symbols represent significance with reference to same day unstrained control. MSCGM = complete growth medium; ODM = osteogenic differentiating medium.

### 6.3.4 OCN mRNA expression

Expression levels of OCN mRNA in all strained and unstrained hMSCs were at detectable levels. After one week, on average, OCN mRNA expression was higher in hMSCs strained at 10% compared to their same day unstrained controls (Fig. 6.4A). With respect to 12% strained hMSCs, the trend indicated that only those cultured in MSCGM showed an increase in OCN mRNA expression compared to the same day unstrained control (Fig. 6.4A). The cyclic tensile strain did not significantly affect OCN mRNA expression levels in strained hMSCs after two weeks as compared to their unstrained controls (Fig. 6.4B). However, after

two weeks, hMSCs strained at 10% and cultured in ODM showed a higher ($p < 0.09$) OCN mRNA expression level than those strained at 12% (Fig. 6.4B).

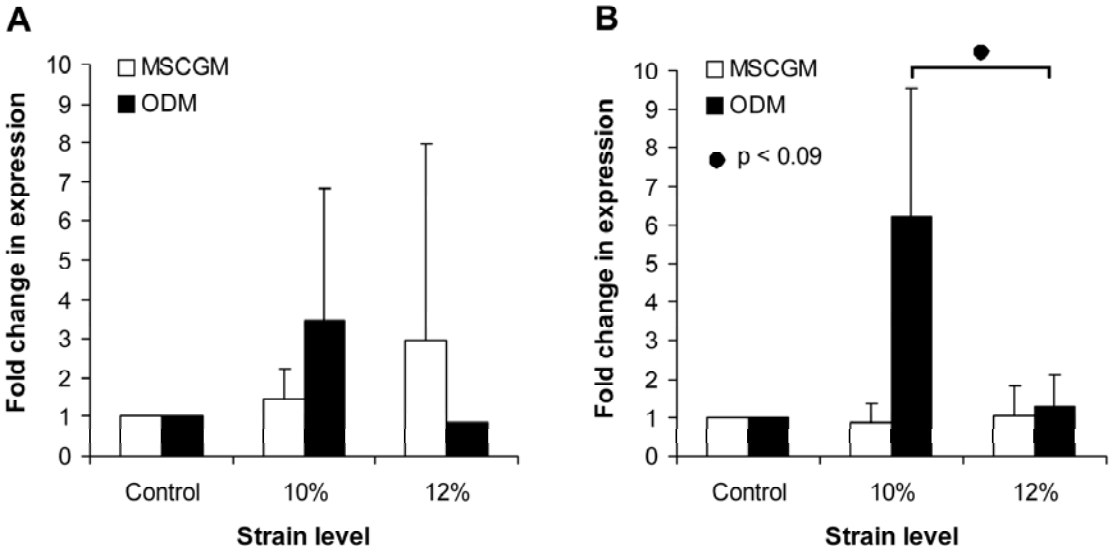


**Figure 6.4.** Fold change in expression levels of OCN mRNA in hMSCs cultured in 3D collagen matrices and subjected to 0% (control), 10%, and 12% cyclic tensile strains. A) Cultured for 1 week, B) Cultured for 2 weeks. Control denotes same day unstrained hMSCs maintained in identical media conditions. MSCGM = complete growth medium; ODM = osteogenic differentiating medium.

## 6.4 Discussion

This is the first study to demonstrate that osteogenic differentiation of hMSCs cultured in 3D collagen matrices can be induced (as measured by increased mRNA expression of BMP-2, COLI, and OCN) by the combined effects of uniaxial cyclic tensile strain and osteogenic differentiation supplements.

The effects of uniaxial cyclic tensile strain, culture medium and culture duration on osteogenic differentiation of human bone marrow derived MSCs cultured in 3D collagen matrices were investigated. Viability of hMSCs was maintained in both MSCGM and ODM through 14 days in culture. On average, after one week, expression levels of COLI mRNA increased in all strained hMSCs, whether cultured in MSCGM or ODM, as compared to their unstrained controls. However, after two weeks, neither strain nor culture medium significantly affected COLI mRNA expression levels in strained hMSCs. In contrast, strain significantly increased the expression of BMP-2 mRNA in hMSCs, especially after two weeks. While culture duration significantly affected BMP-2 mRNA expression levels only in 10% strained hMSCs, osteogenic differentiating medium significantly increased the expression levels of BMP-2 mRNA in all strained hMSCs cultured for two weeks. Expression of OCN mRNA was not significantly affected by cyclic strain, culture medium or culture duration but the trend indicated that 10% cyclic tensile strain and ODM conditions promote OCN expression in hMSCs.

Our previous studies showed that hMSCs cultured in 3D collagen matrices, when subjected to cyclic tensile strain in complete growth medium, remain viable for two weeks. The present study, confirmed these previous findings and also showed that hMSCs remain

viable while exposed to cyclic tensile strains of 10% and 12% in the presence of osteogenic differentiating medium. These results show that hMSCs can be successfully cultured in 3D collagen matrices in the presence of the combined effects of cyclic tensile strain and osteogenic differentiating medium, a promising finding in the quest to functionally engineer bone tissue constructs *in vitro*.

Type I collagen is one of the major extracellular matrix proteins produced by osteoblasts during the pre-mineral phase of bone formation. It has been shown that Type I collagen is expressed between 42 – 50 days of human tibia development.[4] Yoneno *et al.*[138] reported that the expression levels of COLI mRNA in hMSCs cultured in collagen gels with ODM under static conditions was higher than in hMSCs cultured in MSCGM. Jagodzinski *et al.*[16] showed that cyclic mechanical stimulation of bone marrow stromal cells cultured on monolayers in the presence of dexamethasone significantly affected expression of COLI mRNA. His studies showed that expression of COLI mRNA in bone marrow stromal cells subjected to 8% cyclic strain in the presence of dexamethasone was significantly higher than when dexamethasone was not present in culture medium.[16] However, when dexamethasone was used in static, unloaded conditions, COLI mRNA expression was down regulated in bone marrow stromal cells.[16] The results of our study differ from the above two studies. In our study, on average, COLI mRNA expression was higher in strained hMSCs cultured in both MSCGM and ODM after 7 days compared to their unstrained controls. However, this increase of COLI mRNA expression was significant only in hMSCs cultured in MSCGM. There was no significant difference in COLI mRNA expression between 10% strained and 12% strained hMSCs. This indicates that the increase in COLI mRNA expression in strained

hMSCs was not dependent either on osteogenic medium conditions or strain level. The discrepancies between our results and those of Yoneno *et al*. and Jagodzinski *et al*. are likely due to the difference in culture conditions (static vs. dynamic; and, 2D vs. 3D culture conditions). In addition, differences in strain regimens between the two studies might also have caused discrepancies in cell response. Therefore, it is clear that hMSCs behave differently in 3D culture conditions and when subjected to varying levels of cyclic tensile strain. Interestingly, in the current study, there was no difference in COLI expression between strained and unstrained hMSCs after two weeks. Synthesis of matrix proteins by cells depends on their extracellular matrix composition or on an external cue, such as tensile strain, to which the cells are exposed.[81, 143, 144] It is possible that hMSCs increase synthesis of COLI during the first week to strengthen the extracellular matrix to withstand tensile strains and, once sufficient amounts of COLI are synthesized, the levels of COLI synthesis are reduced.

Expression of BMP-2 has been reported in osteoblasts with the concomitant expression of ALPL, OCN and osteopontin prior to forming mineralized bone nodules.[145] A previous study by the authors has shown that hMSCs subjected to tensile strain at 10% and 12% without any osteogenic differentiating supplements had higher expression levels of BMP-2 mRNA compared to their unstrained controls.[106] In the current study, expression of BMP-2 significantly increased after 14 days when hMSCs were cyclically strained in the presence of dexamethasone, ascorbic acid and β-glycerophosphate. This increase was significant with respect to both unstrained controls and strained hMSCs cultured in MSCGM. In contrast, previous studies have shown that bone marrow derived hMSCs cultured on

monolayers in the presence of dexamethasone express maximum levels of BMP-2 after 20 days.[135] Similar results were observed by Oreffo *et al*.[64] where the highest level of BMP-2 was observed with human bone marrow progenitor cells cultured on monolayers after 21 days in the presence of dexamethasone. The fold increase in BMP-2 mRNA expression levels cannot be compared between these studies due to differences in data presentation methods. However, it is clear from the present study that hMSCs start expressing BMP-2 mRNA earlier during culture when they are subjected to a combination of cyclic tensile strain and osteogenic differentiation supplements in the culture medium. This indicates that hMSCs can be induced to differentiate down an osteogenic pathway using cyclic tensile strain and osteogenic differentiation medium.

Previous studies have reported that OCN is expressed at the initial mineralization stages of bone formation by pre-osteoblasts undergoing osteogenic differentiation.[66, 146, 147] It has also been reported that OCN is responsible for the maturation of mineral crystals[148] in addition to its inhibitory effects of bone formation through osteoclast recruitment and activity.[149, 150] In the present study, there was no significant effect by strain, medium and culture duration on OCN mRNA expression by hMSCs. Although all strained hMSCs showed detectable levels of OCN mRNA expression, they were not significantly different from unstrained hMSCs. However, the trends indicated that 10% cyclic tensile strain and ODM conditions accelerated OCN expression in hMSCs. These results suggest that hMSCs in our study had not reached the last stages of the osteoblastic phenotype development at which matrix mineralization takes place, but that strain might accelerate the rate of phenotypic development. Our results also agree with the studies by Jagodzinski *et al*.[16] where

they showed that the expression of OCN mRNA in human bone marrow stromal cells cultured on monolayers is not significantly affected by either strain or dexamethasone after 7 days. Although they used monolayer cultures, their results and our present results suggest that expression of OCN in hMSCs is independent of strain, media conditions and culture duration after 7 days. In order to achieve mineralization stages of differentiated hMSCs, the present culture duration may have to be extended to 21 or 28 days. A limitation to extending the culture duration with our system is the high contraction observed in hMSC-seeded collagen matrices which often causes matrix failure after 14 days. Studies are being conducted by the authors to overcome this limitation and extend the culture duration.

In summary, we have investigated the effects of cyclic tensile strain, medium, and culture duration on the expression of COLI, BMP-2 and OCN by hMSCs seeded in 3D Type I collagen matrices. While cyclic tensile strain alone increased COLI mRNA expression in hMSCs after 7 days, expression of BMP-2 mRNA was dependent on both strain and osteogenic medium after 14 days. The lower expression levels of OCN mRNA indicate that hMSCs needed to be cultured longer than 14 days in 3D culture conditions to achieve terminal differentiation into osteoblasts, but that strain might be accelerating this process. Results of this study suggest that cyclic tensile strain accelerates osteogenic differentiation of hMSCs cultured in 3D collagen matrices both in the absence and presence of osteogenic supplements.

## 6.5 Summary

We have shown that cyclic tensile strain in the presence of complete growth medium upregulates bone morphogenetic protein-2 mRNA (BMP-2) expression in bone marrow-derived human mesenchymal stem cells (hMSCs). However, expression of BMP-2 and other bone markers by cyclic tensile strain in hMSCs maintained in either complete growth or osteogenic media conditions had not been investigated. Human MSCs were seeded in three-dimensional Type I collagen matrices and subjected to 0, 10 and 12% uniaxial cyclic tensile strains at 1 Hz for 4 hours/day for 7 and 14 days in complete growth or osteogenic medium. Viability of hMSCs was maintained irrespective of strain level and medium conditions. Increased expression of Type I collagen (COLI) mRNA after 7 days was dependent on cyclic tensile strain. Combined effects of strain and osteogenic medium caused significantly higher expression of BMP-2 mRNA in hMSCs after 14 days. Expression of osteocalcin (OCN) mRNA was highest in 10% strained hMSCs cultured in osteogenic medium. Expression of COLI, BMP-2 and OCN mRNA indicated initial differentiation of hMSCs into the osteoblastic phenotype. This is the first demonstration that cyclic tensile strain combined with osteogenic medium conditions promotes expression of bone markers in hMSCs cultured in three-dimensional collagen matrices.

# 7 Effects of Cyclic Tensile Strain on Osteogenesis and Tensile Properties of Human Mesenchymal Stem Cell Seeded Collagen Matrices

Tissue engineered bone constructs require sufficient mechanical strength to withstand physiological stresses and strains *in vivo* and maintain dimensional stability when implanted in the damaged or diseased area. Investigations described in the last two chapters indicated that tensile strain combined with osteogenic supplements could induce expression of osteogenic markers in hMSCs cultured in three-dimensional collagen matrices. The study described in this chapter focuses on determining the effects of strain, culture medium, and culture duration on tensile properties of the hMSC-seeded collagen matrices that were exposed to osteogenic differentiating conditions.

## 7.1 Introduction

Critical requirements for functional bone tissue engineering include successful osteogenesis of the cells, leading to matrix mineralization, and sufficient strength of the tissue engineered bone construct in order to withstand physiological stresses and strains after implantation [1, 105].

Collagen has been used as a scaffold material for many tissue engineering applications due to its ability to mimic the natural extracellular matrix.[2] Type I collagen is the most abundant extracellular matrix protein in bone and contains RGD (arginine-glycine-aspartic acid) sequences that promote cell adhesion and proliferation [2]. In addition, cell behavior in three dimensional collagen matrices has been well characterized [90, 108, 109, 151]. Therefore, Type I collagen holds great promise as a scaffold material for functional bone tissue engineering. Mesenchymal stem cells (MSCs), with their capacity to differentiate down the osteogenic pathway, have been investigated as a potential cell source for bone tissue engineering [3, 5, 8-10, 152]. Use of osteogenic supplements such as dexamethasone, ascorbic acid, and β-glycerophosphate in culture media promote osteogenesis in both two-dimensional (2D) [6, 8-10] and three-dimensional (3D) [18, 30, 138] culture conditions *in vitro*. Under these osteogenic conditions, human MSCs (hMSCs) up regulate expression levels of Type I collagen (COLI), alkaline phosphatase (ALPL), bone morphogenetic protein-2 (BMP-2), and osteocalcin (OCN) [9, 10, 64, 135]. Cyclic tensile strain, as a stimulus in combination with osteogenic supplements in culture medium, has been shown to promote osteogenesis in hMSCs cultured on monolayers [16, 17, 28, 78]. Recent studies by the authors have shown that

hMSCs maintain their viability up to two weeks in 3D Type I collagen matrices under 10 and 12% uniaxial cyclic tensile strain *in vitro*[106] and, further, that application of 10 and 12% uniaxial cyclic tensile strains to hMSCs cultured in 3D collagen matrices induced expression of BMP-2[106] COLI, and OCN mRNA in hMSCs indicative of osteogenic induction [unpublished data]. While mRNA expression of some of these bone markers depended solely on strain (COLI and BMP-2), others were depended upon combined effects of strain and osteogenic media conditions (OCN). These studies have shown that hMSCs remain viable and potentially differentiate down osteogenic pathways under the combined effects of cyclic tensile strain and osteogenic media conditions. It is equally important to understand the changes in material properties of these hMSC-seeded collagen matrices to determine the feasibility of using them as tissue engineered bone constructs. These hMSC-seeded collagen matrices need to possess sufficient strength to withstand physiological stresses and strains for them to maintain their stability [1, 105]. However, the effects of cyclic tensile strain and osteogenic media conditions on the material properties of hMSC-seeded 3D collagen matrices have not been reported.

The purpose of this study was to investigate the effects of cyclic tensile strain, culture medium and culture duration on osteogenesis of hMSCs; and, the resulting change in tensile properties of hMSC-seeded Type I collagen matrices. We hypothesized that cyclic tensile strain in the presence of osteogenic supplements would increase mRNA expression levels of ALPL in hMSCs as well as increase the tensile moduli and failure stresses of hMSC-seeded collagen matrices. To test our hypothesis, hMSCs were cultured in 3D Type I collagen

matrices and subjected to 10 and 12% cyclic tensile strain in either complete growth or osteogenic differentiation media for a period of 14 days.

## 7.2 Materials and Methods

### 7.2.1 Cell culture

Human bone marrow derived MSCs (24 year old Caucasian male donor; Tulane University, New Orleans, LA) were expanded to passage 3 in complete growth medium consisting of fetal bovine serum (FBS), 4 mM L-glutamine, 0.05 units/ml penicillin, and 0.05 μg/ml streptomycin (Cambrex).

### 7.2.2 Fabrication of hMSC- seeded 3D collagen matrices

The TissueTrain$^{TM}$ culture system (Flexcell International, Hillsborough, NC) was used to create hMSC-seeded linear 3D collagen matrices as previously reported.[106, 107] Briefly, hMSCs cultured to 80-85% confluence were suspended in a premixed collagen solution (30,000 cells per 200 μl) consisting of 70% v/v Type I collagen (Vitrogen; Angiotech BioMaterials Corp, Palo Alto, CA; neutralized to pH 7.0 with 1 N sodium hydroxide), 20% v/v 5x minimum essential medium (Sigma), and 10% v/v FBS (Cambrex). The 3D hMSC-seeded collagen matrices were created using six-well TissueTrain$^{TM}$ culture plates by dispensing the cell-seeded gel suspension into linear groves at the center of each well. The plate assembly was then incubated at 5% $CO_2$ and 37 $^0$C for 2 hours to allow the collagen to polymerize, after which MSCGM was added to each well. The matrices were further incubated for 24 hours prior to medium change and application of strain. Separate

groups of hMSC-seeded collagen matrices were maintained in MSCGM (n=3) and osteogenic differentiating medium (ODM) (n=3) consisting of MSCGM supplemented with 0.5% dexamethasone, 1% β-glycerophosphate and 0.5% ascorbic acid (Cambrex).

### 7.2.3 Application of uniaxial cyclic tensile strain

The Flexercell FX-4000 strain unit (Flexcell International) was used to apply uniaxial cyclic strain to the hMSC seeded collagen matrices. The matrices were subjected to uniaxial cyclic tensile strains of 0, 10 or 12% at 1 Hz for 4 hours/day, for up to 14 days. The hMSC-seeded collagen matrices maintained in static (applied strain = 0%) culture served as unloaded controls.

### 7.2.4 Real-time polymerase chain reaction

After 7 and 14 days, the unstrained and strained hMSC-seeded collagen matrices were removed from the culture wells and frozen at -80 $^{0}$C. Total RNA from the hMSCs was isolated using Perfect RNA Eukaryotic Mini kit (Eppendorf, Westbury, NY) and concentration of total RNA was determined using a Ribogreen RNA quantitation kit (Molecular Probes Inc., OR). The isolated total RNA (60-180 ng) was used to synthesize first strand cDNA in a 25 μl reverse transcriptase (RT) reaction using Superscript III RT with oligo(dT) primers (Invitrogen, Carlsbad, CA). An ABI Prism 7000 system (Applied Biosystems) with primer probe oligonucleotide sets (Assays-on-Demand, Applied Biosystems, CA) for glyceraldehyde-3-phosphate dehydrogenase (GAPDH)

(Assay HS99999905_M1) and alkaline phosphatase (ALPL, Assay HS00758162_M1) was used to amplify the synthesized cDNA. Expression levels of ALPL mRNA were normalized to GAPDH expression and the fold change in expression was calculated using the relative quantification method relative to the same day unstrained control cells (0% strained) [136]. All reactions were performed in triplicate. An unpaired Student's t-test was used to analyze all mRNA expression data with statistical significance defined as $p < 0.05$. The p values of $p < 0.06$ and $p < 0.09$ were also indicated. Data were presented as mean ± standard deviation.

### 7.2.5 Endogenous alkaline phosphatase activity

After 7 and 14 days, unstrained and strained hMSC-seeded collagen matrices were washed twice with phosphate buffered saline (PBS) and fixed using 10% formalin for 15 minutes. The cell membranes were then permeabilized by incubating the matrices in 0.2% Triton X-100/ 0.5% bovine serum albumin (TBSA) in PBS for 10 minutes. Subsequently, the matrices were rinsed again in PBS and endogenous alkaline phosphatase activity (EALP) was detected by incubating matrices in 40 μL of 20-fold diluted alkaline phosphatase substrate (ELF 97; Molecular Probes) for 15 minutes [153, 154]. The phosphatase reaction was subsequently stopped by adding 5 mM Levamisol and 25mM EDTA (Sigma) in PBS (wash buffer). The matrices were further rinsed three times with wash buffer to remove excess ELF 97 and to prevent formation of background crystals. The center and both ends of each matrix were imaged using a fluorescence microscope (Leica Microsystems Inc., Bannockburn, IL) with an excitation at 350 nm and emission at 535 nm using a 10X objective. At least three

different images were obtained from each matrix location. The area of EALP activity in each image was measured and expressed as a percentage of total area. These percentage areas were normalized to those of same day unstrained controls.

### 7.2.6 Modulus and Failure Stress

***Specimen preparation*:** The matrices were detached from the anchors and placed on the edge of a glass slide (Fig. 7.1A). The glass slide was alternatively rotated $90^0$ to image both width (Fig 7.1B and 7.1D) and thickness (Fig. 7.1C and 7.1E) of each matrix using a Leica S6 StereoZoom® microscope (Leica Microsystems Inc., Bannockburn, IL) fitted with a Canon Powershot A95 digital camera (Canon USA Inc. Lake Success, NY). The thickness and width at 10 different points along the length of the hMSC-seeded collagen matrix were then measured from the images using Kodak ID image analysis software v3.6 (Eastman Kodak Co., NY). At least three different matrices for each condition were used for thickness and width measurements. The cross sectional area of the matrices was calculated by approximating the shape of the cross section to an ellipse where measured thickness was considered as the length of the minor axis and measured width was considered as the length of the major axis. Unstrained and strained hMSC–seeded collagen matrices were placed on a rectangular piece of paper through which an 11 mm diameter circular hole was cut at the center (Fig. 7.2A). Drops of an instant adhesive (Black max gel; Loctite Corporation, Newington, CT) were applied to both ends of the matrix. The ends of the paper were folded back onto the ends of the collagen matrix to create a sandwiched end (Fig.7.2B). The matrix-

paper assembly was clamped at both ends to obtain a gauge length of 10 mm. The sides of the rectangular piece of paper were then cut apart to allow the matrix to be gripped by each end (Fig. 7.2C).

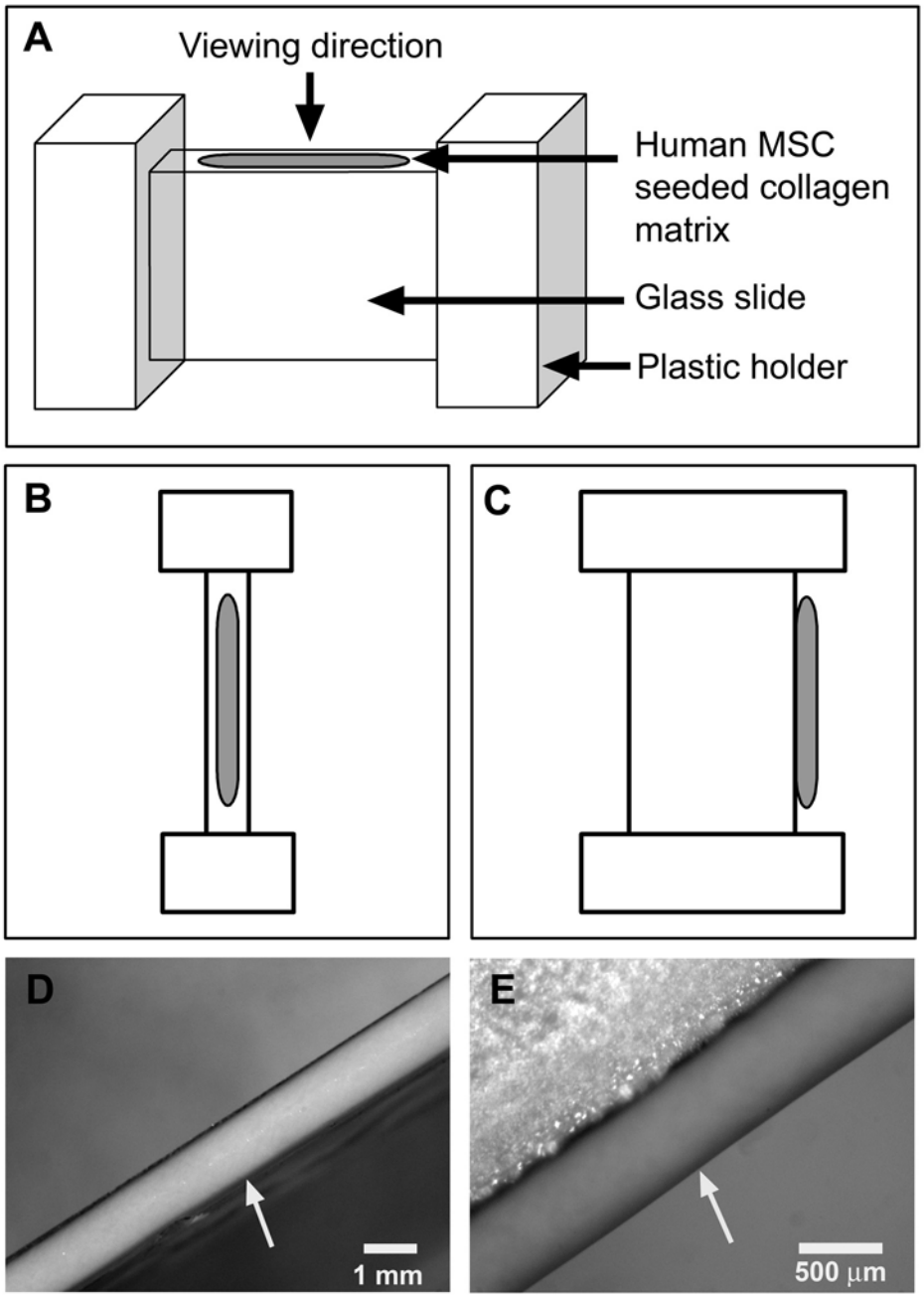


**Figure 7.1.** Width and thickness measurement of hMSC-seeded Type I collagen matrices. A) Human MSC-seeded collagen matrix placed on edge of a glass slide afixed to two plastic holders, B) Collagen matrix placed on the slide was viewed from top to measure the width, C) The holder-matrix set-up was rotated $90^0$ in the clockwise direction and viewed from top to measure the thickness of the matrix, D) Microscopic view of collagen matrix showing the width, E) Microscopic view of collagen matrix showing the thickness. Arrows indicate collagen matrix.

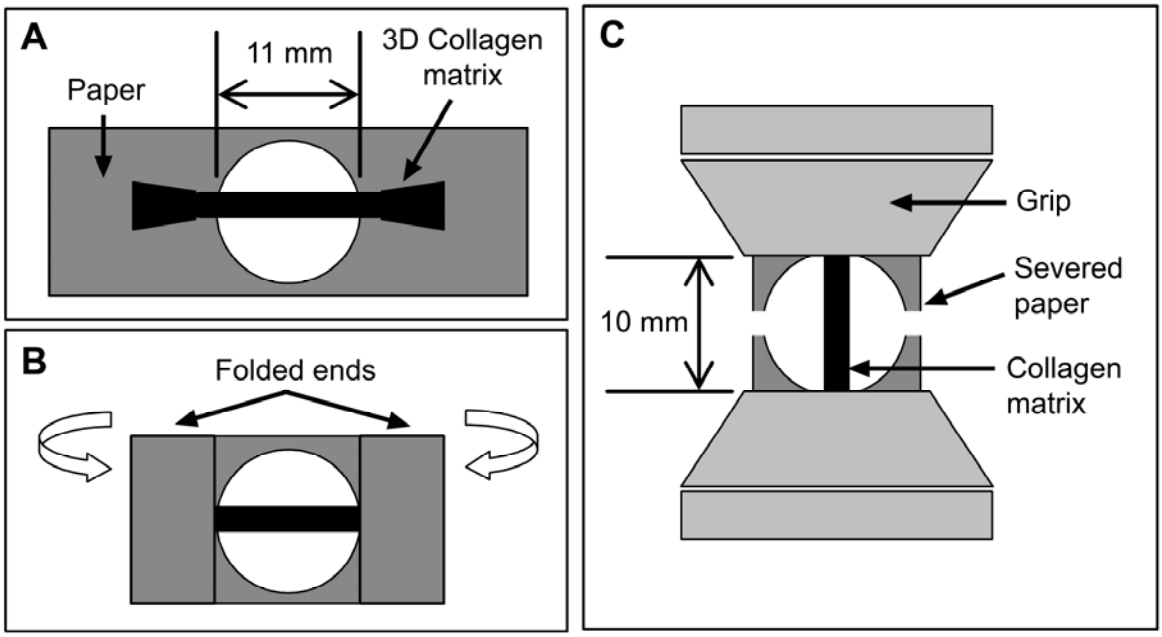


**Figure 7.2.** Specimen preparation for tensile testing. A) Human MSC-seeded collagen matrix placed on a rectangular paper with a circular hole cut in the center, B) The ends of the paper were folded onto the matrix after applying instant adhesive to the ends of the ends of the collagen matrix and, C) The remaining paper was cut out at both sides to allow collagen matrix to be held with the grips.

***Tensile testing*:** The Young's moduli and failure stresses of unstrained and strained hMSC-seeded collagen matrices after 1, 7 and 14 days were measured using an ElectroForce® 3200 load frame (Enduratec; Bose Corporation, Eden Prairie, MN). The matrices were stretched by applying a constant strain rate of 0.5% per second until matrix failure using a 500 g load cell with a force resolution of 0.03 g. The collagen matrices were kept moist with PBS

throughout testing. Force and displacement data were recorded at a sampling frequency of 7 Hz. The cross sectional areas of the matrices were used to calculate and plot stress-strain curves for each collagen matrix. At least three different matrices for each condition were used to determine the average Young's modulus and failure stress. Factorial effects of culture medium, culture duration, and strain on Young's modulus and failure stress were investigated using F-tests from an analysis of variance (ANOVA) appropriate to the complete, crossed, 2 × 2 × 3 experimental design. For modulus and failure stress, responses were contrasted with reference to those of same day unstrained matrices having similar experimental conditions.

## 7.3 Results

### 7.3.1 Alkaline phosphatase mRNA expression

Human MSCs cyclically strained at 12% and cultured in both MSCGM and ODM for one week had significantly lower ALPL mRNA expression levels compared to unstrained controls (Fig. 7.3A). Expression levels of ALPL increased after two weeks in both 10 and 12% strained hMSCs cultured in ODM (Fig. 7.3B). However, compared to unstrained controls, this increase was significant only in 10% strained hMSCs. Both 10 and 12% strained hMSCs cultured in ODM had significantly higher ALPL mRNA expression after two weeks compared to those cultured in MSCGM (Fig. 7.3B). Compared to unstrained controls, ALPL expression was significantly down regulated after two weeks in hMSCs subjected to 12% strain in MSCGM (Fig. 7.3B).

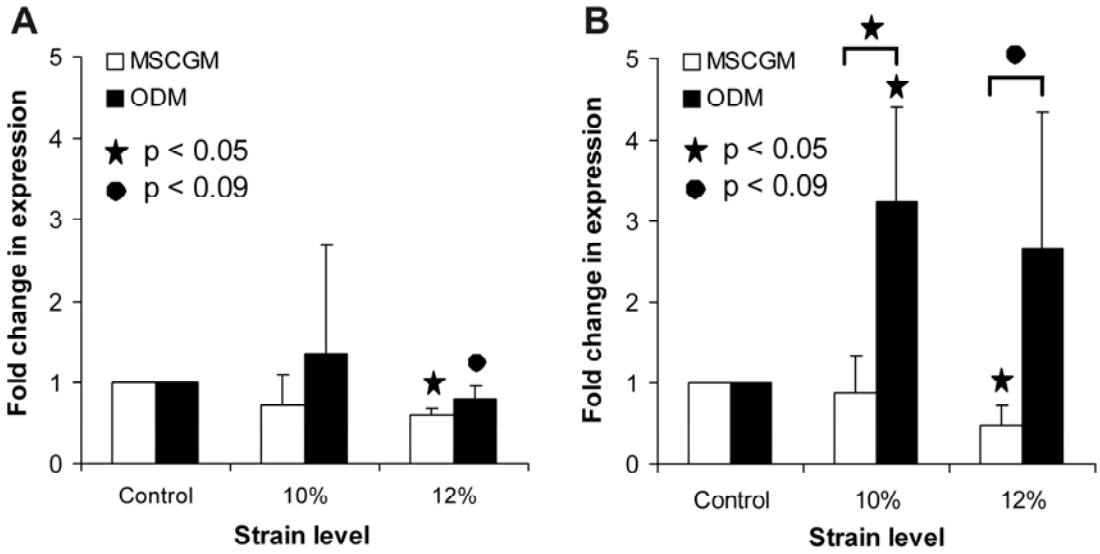


**Figure 7.3.** Fold change in expression levels of alkaline phosphatase mRNA in hMSCs cultured in 3D collagen matrices and subjected to 0% (control), 10%, and 12% cyclic tensile strains. A) Cultured for 1 week, B) Cultured for 2 weeks. Control denotes same day unstrained hMSCs maintained in identical media conditions. Unless indicated otherwise with a horizontal bracket, statistical significance symbols represent significance with reference to same day unstrained control. MSCGM = complete growth medium; ODM = osteogenic differentiating medium.

### 7.3.2 Endogenous alkaline phosphatase activity

ODM: Compared to the unstrained controls, both 10 and 12% strained hMSCs cultured in ODM had lower endogenous alkaline phosphatase activity (EALP) activity after one week (Fig 7.4A, B and C). However, at the end of the second week, EALP activity in 10% strained hMSCs increased to 13 ± 2 fold compared to the unstrained controls while 12% strained hMSCs had a 16 ± 2 fold increase compared to unstrained controls (Fig. 7.4D, E and F).

MSCGM: EALP activity in MSCGM followed a similar trend as that in ODM. The EALP activity in 12% strained hMSCs cultured in MSCGM after one week was slightly higher (2 ± 1 fold) than that of the unstrained controls. No EALP activity was observed in 10% strained hMSCs after one week in MSCGM. Similar to 10% and 12% strained hMSCs cultured in ODM, those cultured in MSCGM had increased EALP activity relative to their unstrained controls at the end of the second week (data not shown).

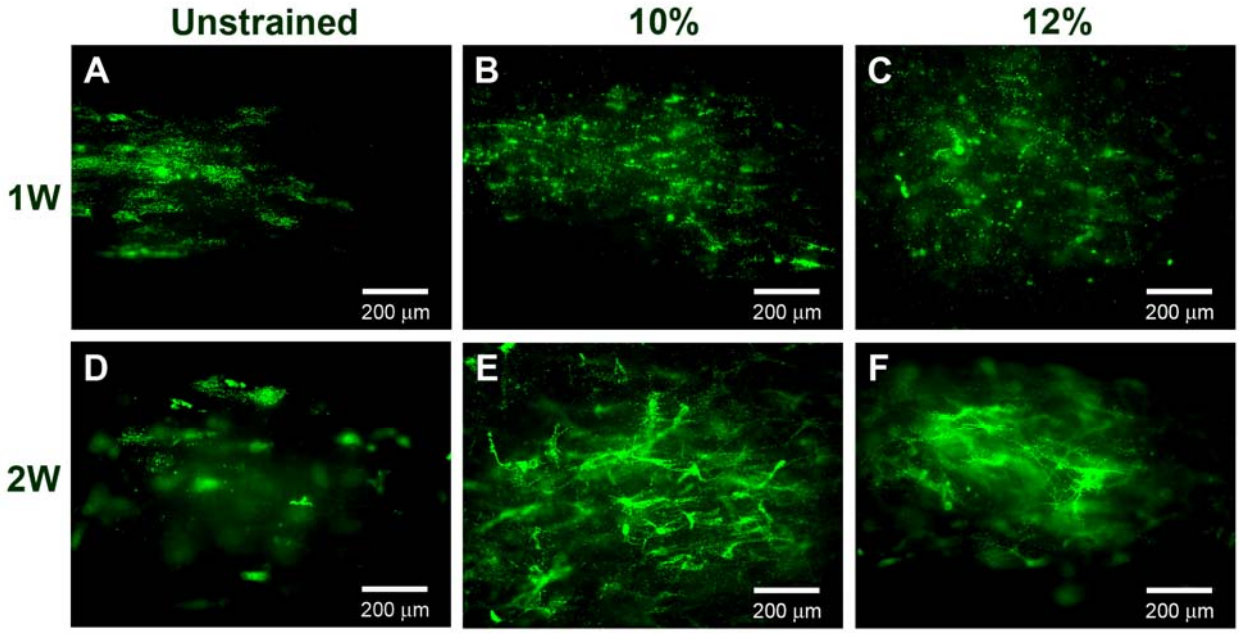


**Figure 7.4.** Localization of endogenous alkaline phosphatase activity in unstrained and strained hMSC-seeded Type I collagen matrices cultured in osteogenic differentiation medium for 1 and 2 weeks using ELF 97 alkaline phosphatase substrate. A, D) Unstrained for A) 1 week and D) 2 weeks, B, E) Strained at 10% for B) 1 week and E) 2 weeks, C, F) Strained at 12% for C) 1 week and F) 2 weeks. 1W = 1 week and 2W = 2 weeks.

### 7.3.3 Young's Modulus and failure stress

The stress-strain curves of unstrained and strained hMSC-seeded collagen matrices exhibited typical linear and failure regions. The differences in stress-strain curves due to the effects of culture media (MSCGM vs. ODM) (Fig. 7.5A and B) and culture duration (1 week vs. 2 weeks) (Fig. 7.5C and D) were clearly distinguishable.

The Young's moduli of both unstrained and strained hMSC-seeded collagen matrices were significantly affected by two-way interactions between culture medium and time ($p$ = 0.0036). Strain, medium or culture duration did not significantly influence Young's moduli of collagen matrices during the first week (Fig 7.6A). However, by the end of the second week, hMSC-seeded collagen matrices strained at 10% in MSCGM had higher moduli compared to both unstrained and 12% strained matrices (Fig. 7.6B). After two weeks, all matrices cultured in MSCGM had significantly higher moduli than those cultured in ODM (Fig. 7.6B). Culture duration significantly affected the moduli of matrices cultured in MSCGM such that the moduli of all matrices cultured in MSCGM significantly increased with time. However, among matrices cultured in ODM, only 10% strained matrices had a significant increase in moduli with time.

The ultimate failure stress of unstrained and strained hMSC-seeded matrices was significantly affected by strain ($p$ = 0.0077), culture duration ($p$ = 0.0017) and culture medium ($p$ < 0.0001). After the first week, both unstrained and 12% strained matrices cultured in ODM had significantly higher failure stresses than those cultured in MSCGM (Fig. 7.7A). At the end of the second week, both unstrained and 10% strained matrices cultured in ODM had significantly higher failure stresses compared to those cultured in

MSCGM (Fig. 7.7B). Matrices strained at 10 and 12% and cultured in ODM had significantly lower failure stresses than those that were unstrained (Fig. 7.7B). Culture duration only significantly affected unstrained matrices cultured in ODM.

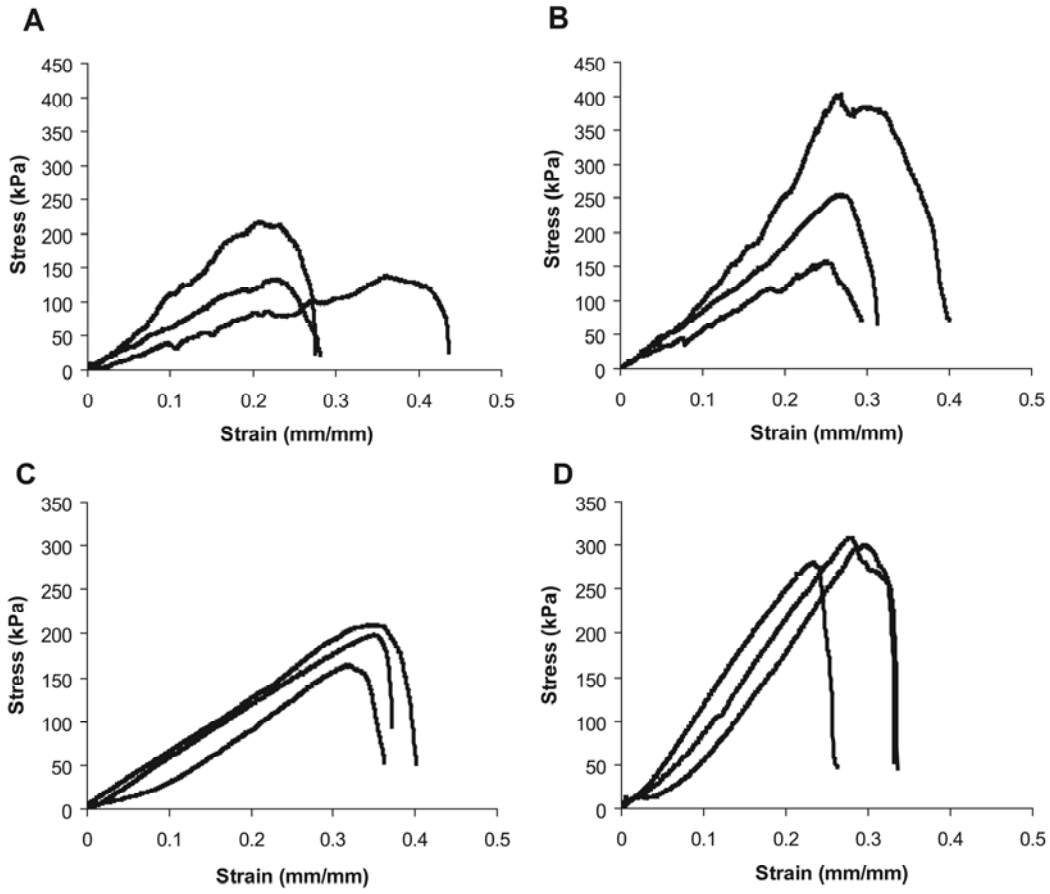


**Figure 7.5.** Representative stress-strain curves of unstrained and strained hMSC-seeded Type I collagen matrices showing the effects of media and culture duration on stress-strain profiles. A, B) Unstrained matrices cultured for 1 week in A) Complete growth medium and B) Osteogenic differentiation medium, C, D) 10% strained matrices cultured in osteogenic medium for C) 1 week and D) 2 weeks.

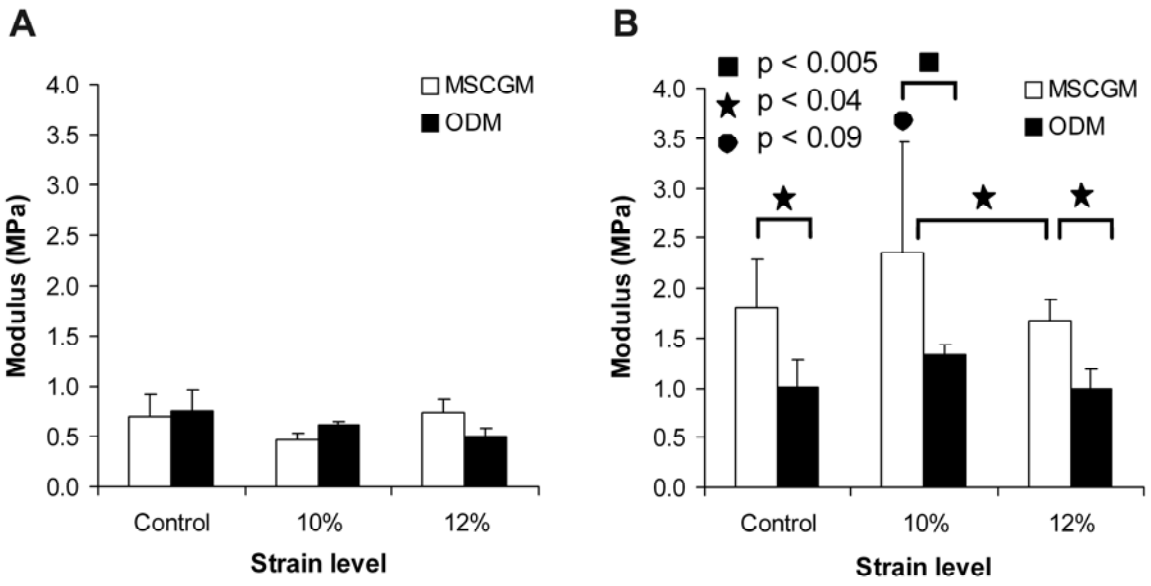


**Figure 7.6.** Average Young's moduli of hMSC seeded Type I collagen matrices subjected to 0%, 10%, and 12% cyclic tensile strains. A) Cultured for 1 week, B) Cultured for 2 weeks. Unless otherwise indicated with a horizontal bracket, statistical significance symbols represent significance with reference to same day unstrained control (0% strained). MSCGM = complete growth medium; ODM = osteogenic differentiating medium.

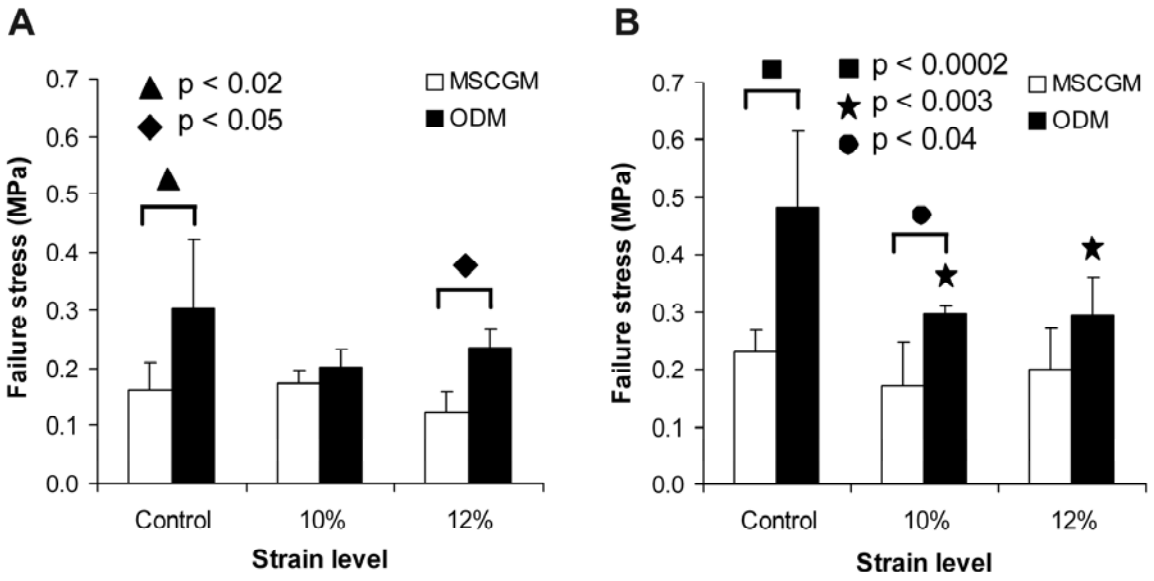


**Figure 7.7.** Failure stress of hMSC seeded Type I collagen matrices subjected to 0%, 10%, and 12% cyclic tensile strains. A) Cultured for 1 week, B) Cultured for 2 weeks. Unless otherwise indicated with a horizontal bracket, statistical significance symbols represent significance with reference to same day unstrained control (0% strained). MSCGM = complete growth medium; ODM = osteogenic differentiating medium.

## 7.4 Discussion

Tissue engineered bone constructs for functional bone tissue engineering should possess cells with an osteogenic phenotype and have sufficient strength to withstand the *in vivo* physiological environment. Many investigators have focused on the osteogenic differentiation capability of cells used in tissue engineered bone constructs by analyzing combinations of osteogenic medium and mechanical stimulation with 2D and 3D cultures. In this study, we investigated the individual and combined effects of uniaxial cyclic tensile strain, culture medium, and culture duration on tensile properties of hMSC-seeded 3D collagen matrices; and, osteogenesis of mesenchymal stem cells cultured in 3D Type I collagen matrices. Human MSC-seeded collagen matrices were cyclically strained at 0 (control), 10, and 12% in either MSCGM or ODM for 7 or 14 days and analyzed for ALPL mRNA expression, EALP activity of hMSCs, Young's moduli, and failure stresses of hMSC-seeded collagen matrices.

We have previously shown that hMSCs remain viable in 3D collagen matrices up to 2 weeks under 10 and 12% cyclic tensile strain.[106] In this study, in addition to providing a 3D biomimetic scaffold material for hMSC growth and proliferation, the collagen matrices had sufficient tensile properties to withstand cyclic loading at strain levels of 10 and 12% for up to 14 days.

Alkaline phosphatase is a primary cellular marker for osteogenesis [4]. Increased activity of ALPL has been found during formation of cartilage and first osteoid (between 5 and 6 days) in chick tibia development [4]. Yoneno et al. [11] reported that expression of ALPL mRNA by bone marrow derived hMSCs cultured in Type I collagen matrices in ODM for 5

days increased 3-fold as compared to those cultured in MSCGM. The effect of a strain stimulus on ALPL expression was not investigated in their study. In contrast, studies by Frank et al. [135] showed that expression of ALPL mRNA by human bone marrow derived stromal cells remained unchanged after 20 days of culture in ODM under static, monolayer conditions. They observed similar results with mRNA expressions of Type I collagen, osteocalcin, and osteonectin.

This study investigated the effects of strain, culture medium, and culture duration on ALPL mRNA expression. We found that ALPL mRNA expression in all strained hMSCs cultured in ODM increased between 2-3 fold at the end of the second week. The highest expression of ALPL mRNA was observed in 10% strained hMSCs cultured in ODM for two weeks. This suggests that ALPL mRNA expression by hMSCs was dependent on combined effects of osteogenic medium and cyclic tensile strain. Interestingly, ALPL mRNA expression in hMSCs peaked during the second week, i.e. after 7 days, later than that observed by Yoneno et al.[11]. This might be due to the difference in osteogenic medium and the type of culture between the two studies (2D vs. 3D culture).

Expression of ALPL further downstream during osteogenesis can be investigated using various ALPL assays. Increase of ALPL activity by human bone marrow stromal cells cultured under static monolayer conditions in ODM has been reported from day 6 [64]. Similarly, Frank et al. [135] reported that ALPL activity reached its maximum in human bone marrow stromal cells cultured in ODM under static conditions during the first week of culture, after which expression remained constant through day 20. In 3D collagen matrices under static culture conditions, bone marrow derived hMSCs cultured in ODM have been

reported to have ALPL activity 1.5-fold higher than those cultured in MSCGM after 14 days [138]. Cyclic strain at 8% combined with dexamethasone in the culture medium increased activity of ALPL in hMSCs cultured in monolayers after 4 and 7 days [16]. Although our method of ALPL activity measurement was different from assay-based methods, our results also showed a 2-fold increase in endogenous ALP activity after 7 days in 12% strained hMSCs cultured in MSCGM. In the present study, the large increase of EALP activity after 14 days in all strained hMSCs, cultured in either MSCGM or ODM media, suggests that cyclic strain might induce expression of ALPL, potentially indicative of hMSC osteogenic differentiation. Our results correlate with studies by Jagodzinski et al.[16] in which ALPL activity in hMSCs was increased with 8% strain alone (without dexamethasone in the culture medium) after 7 days. In our findings, we showed that EALP activity continued to increase up to 14 days in the presence of cyclic strain, with and without osteogenic supplements in the culture medium.

Tensile properties of the hMSC-seeded 3D Type I collagen matrices are governed by a multitude of factors, which could also affect physical properties of the collagen fibrils and their microstructure. These factors include polymerization conditions such as collagen concentration and pH, cell-seeding density, proliferation and differentiation of cells, and degree of collagen matrix contraction by cells. Roeder et al. [155] reported that changes in collagen concentration affected the density of collagen fibrils while maintaining a constant fibril diameter. They also showed that pH of the polymerization solution affected both collagen fibril length and diameter [155]. The amount of extracellular matrix protein and calcium nodules produced by hMSCs during proliferation and osteogenic differentiation could strongly influence the tensile properties of hMSC-seeded collagen matrices. In the

current study, both collagen concentration and pH of the collagen polymerizing solution were maintained constant to allow investigation of other factors on tensile properties of the collagen matrices. Since cell seeding density was constant in all matrices, tensile properties of the hMSC-seeded collagen matrices would be predominantly affected by the degree of cell proliferation and capacity of hMSCs to differentiate down an osteogenic pathway.

In the current study, stress-strain curves of all unstrained and strained collagen matrices exhibited a linear region followed by an ultimate failure point. In contrast to previous studies [114, 155, 156], stress strain profiles of most hMSC-seeded collagen matrices in our study did not exhibit a toe region (exponential behavior at low stresses), corresponding to the removal of crimp in collagen fibrils. This might indicate that fibrils in the collagen matrices were straight. The cyclic strain applied to the collagen matrices as well as the strain presence due to anchoring of the matrices at both ends may have straightened the fibrils in our collagen matrices. In general, moduli of hMSC-seeded collagen matrices cultured in both MSCGM and ODM for two weeks were higher than that after the first week. This could be due to increased hMSC proliferation leading to an increased matrix protein synthesis.

Increased ALPL mRNA expression and EALP activity in hMSCs cultured in ODM suggests that the increase in moduli in those matrices could be due to increased synthesis of matrix proteins by hMSCs differentiating down an osteogenic pathway. The fact that matrix mineralization could also contribute to an increase in moduli of matrices cultured in ODM cannot be disregarded [157]. However, further studies need to be carried out to determine the extent of matrix mineralization in order to confirm these results. At the end of two weeks, collagen matrices cultured in MSCGM had higher moduli than those cultured in ODM. Since

hMSCs do not terminally differentiate in MSCGM, the proliferative capacity of hMSCs is maintained throughout the culture duration [9]. Therefore, significantly higher moduli of collagen matrices cultured in MSCGM could have resulted from increased matrix protein synthesis by a higher number of hMSCs in those matrices.

A significant increase in failure stress of matrices cultured in ODM compared to those cultured in MSCGM could be due to increased synthesis of matrix proteins by hMSCs in ODM. Our results showed a significant decrease in failure stress of all strained matrices at the end of the second week compared to that of the unstrained. Girton et al. [158] reported that crosslinks between collagen fibrils directly influence the mechanical properties of the collagen matrix. Wagenseil et al. [159] showed that peak force of fibroblast populated collagen matrices was higher at the first strain cycle than at subsequent strain cycles for a given strain amplitude during cyclic loading. They suggested that this could be due to reorientation of collagen fibers caused by breakage of interfiber and intrafiber crosslinks during repeated stretch cycles. Similarly, in the present study, the low ultimate failure stress of strained matrices could have resulted from the breakage of interfiber and intrafiber crosslinks during cyclic strain. If the unstrained matrices had all crosslinks intact until the end of culture duration, they might exhibit comparatively higher failure stresses than strained matrices.

Interestingly, hMSC-seeded collagen matrices strained at 10% in MSCGM had the highest moduli. Our results also showed higher EALP activity in 10% strained hMSCs cultured in MSCGM. In addition, we have shown previously that expression of BMP-2 mRNA was markedly increased in 10% strained hMSCs cultured in MSCGM.[106] These data suggest that cyclic tensile strains of 10% have been more influential in inducing hMSCs to

differentiate down an osteogenic pathway, which could cause an increase in moduli of those matrices.

In summary, we have investigated the effects of cyclic tensile strain, culture medium and culture duration on osteogenesis of hMSCs and tensile properties of hMSC-seeded Type I collagen matrices. Culture duration and combined effects of osteogenic medium and strain caused an increase in ALPL mRNA in hMSCs. While EALP activity was increased by both cyclic strain and culture duration, culture medium did not cause a change in EALP activity in hMSCs. The moduli of hMSC-seeded collagen matrices increased under cyclic tensile strain in the presence of MSCGM. Although culture medium and duration affected the failure stress of unstrained matrices, cyclic tensile strain did not cause an increase in failure stress of collagen matrices. Results of this study suggest that osteogenesis of hMSCs seeded in 3D collagen matrices can be induced by combined effects of cyclic tensile strain and osteogenic medium while Young's moduli but not ultimate failure stresses of such matrices increase due to cyclic strain.

## 7.5 Summary

We have recently shown that application of cyclic tensile strain to hMSCs cultured in three-dimensional (3D) collagen matrices in the absence of chemical stimuli induces mRNA expression of Type I collagen and bone morphogenetic protein-2, indicative of osteogenic differentiation. However, the effects of cyclic tensile strain, osteogenic medium, and culture duration on tensile properties of these hMSC-seeded 3D Type I collagen matrices has not been investigated. Synthesis of extracellular matrix protein and matrix mineralization during osteogenesis of human mesenchymal stem cells (hMSCs) cultured in collagen matrices *in vitro* should directly influence mechanical properties of the final tissue engineered construct. We hypothesized that cyclic tensile strain, osteogenic medium and culture duration would induce osteogenesis of hMSCs and increase tensile properties of hMSC-seeded collagen matrices. Bone marrow-derived hMSCs seeded in 3D Type I collagen matrices were subjected to uniaxial cyclic tensile strains of 0, 10 and 12% at 1 Hz for 4 hours/ day for 7 and 14 days in either complete growth medium or osteogenic medium. RT-PCR studies on alkaline phosphatase mRNA expression revealed that cyclic strain and osteogenic medium collectively increased alkaline phosphatase mRNA expression in hMSCs. An increase in endogenous alkaline phosphatase activity in hMSCs was observed with cyclic tensile strain and with increase in culture duration. The stress-strain curves of both unstrained and strained hMSC-seeded collagen matrices exhibited a linear elastic region and a failure region. All strained matrices cultured in growth medium for two weeks had higher Young's moduli than those cultured in osteogenic medium. The Young's moduli increased with time in all matrices cultured in growth medium and in 10% strained matrices cultured in osteogenic

medium. In general, failure stresses of all matrices cultured in osteogenic medium increased independent of strain and culture duration. However, all strained matrices in osteogenic medium had lower failure stresses than unstrained matrices at the end of 14 days. This is the first study to show that stimulation of hMSCs in 3D collagen matrices by cyclic tensile strain induces expression of mRNA indicative of osteogenesis, increases tensile modulus, but decreases ultimate strength.

# 8 Human Mesenchymal Stem Cells Cultured at High Density Upregulate Bone Markers under Cyclic Tensile Strain

The work described in the previous chapters used an intial hMSC seeding density of $1.5 \times 10^5$ cells/mL in collagen matrices. The possibility of using $3 \times 10^5$ cells/mL as the hMSC seeding density with three-dimensional collagen matrices without matrix failure was revealed by the matrix contraction study described previously. It is necessary to determine the optimum hMSC seeding density to establish protocols for osteogenesis of hMSCs *in vitro*. The next study describes findings on the effects of cyclic tensile strain, culture medium, and culture duration on the expression of bone markers by hMSCs seeded at high density ($3 \times 10^5$ cells/mL) in three-dimensional collagen matrices.

## 8.1 Introduction

Culture conditions for osteogenesis of human mesenchymal stem cells (hMSCs) in three dimensional collagen matrices need to be optimized for successful creation of bone constructs *in vitro.* These culture conditions include hMSC seeding density, culture medium, culture duration and type of external stimuli.

Mesenchymal stem cells exhibit differentiation capacity down a multitude of pathways including osteogenesis [5]. Their intramembranous bone formation capacity *in vivo* has been well investigated by Caplan and Pechak using chick embryos [4]. In the presence of osteogenic differentiation supplements such as dexamethasone, ascorbic acid, and β-glycerophosphate, hMSCs have been shown to readily differentiate down an osteogenic pathway in monolayer cultures *in vitro* [6, 9, 10]. Under these static, monolayer culture conditions, hMSCs have expressed bone markers such as Type I collagen (COLI) [64, 135], alkaline phosphatase (ALPL) [9, 10, 135], bone morphogenetic protein-2 (BMP-2) [64, 135] and osteocalcin (OCN) [9, 10, 64]. Mechanobiological models [13, 26, 41] have suggested that low to moderate tensile strains and low hydrostatic stresses induce intramembranous bone formation. Recent finite element analyses [14] and experimental studies [15] of distraction osteogenesis using a rat model have shown that tensile strains of 10-12% promote intramembranous bone formation *in vivo*. In order to mimic 3D *in vivo* conditions and successfully create tissue engineered bone constructs *in vitro*, hMSC proliferation and osteogenesis need to be investigated using 3D culture conditions. A recent study by the authors has shown that hMSCs cultured in 3D Type I collagen matrices *in vitro* maintain

their viability when subjected to uniaxial cyclic tensile strains of 10 and 12% over a period of 14 days.[106] In addition, the authors showed that cyclic tensile strains of 10 and 12% induced mRNA expression of bone morphogenetic protein -2 (BMP-2) in hMSCs without any osteogenic supplements in the culture medium.[106] These initial studies used hMSCs seeded at a low density ($1.5 \times 10^5$ cells/mL) in 3D collagen matrices to investigate the effects of cyclic tensile strain, culture medium and duration on hMSC osteogenesis. Previous studies have suggested that self-renewal, recruitment, and differentiation of mesenchymal stem cells in response to dexamethasone in culture medium were dependent on initial cell seeding density [160, 161]. However, the effects of these factors on osteogenesis of hMSCs seeded at a high density ($3 \times 10^5$ cells/mL) in 3D Type I collagen matrices have not been investigated.

The objective of this study was to investigate the effects of cyclic tensile strain, culture medium and culture duration on the expression of osteogenic markers by hMSCs seeded at a high density in 3D collagen matrices. We hypothesized that application of cyclic tensile strain would increase mRNA expression levels of COLI, ALPL, BMP-2 and OCN. To test our hypothesis, hMSCs were cultured in 3D collagen matrices at a seeding density of $3 \times 10^5$ cells/mL and subjected to cyclic tensile strain at 10 or 12% in either complete growth medium or osteogenic differentiating medium for up to 14 days.

## 8.2 Materials and Methods

### 8.2.1 Cell culture

Bone marrow derived hMSCs (26 year old African American male donor; Cambrex Bio Science, Walkersville, MD) were expanded to passage 3 or 4 in complete growth medium (MSCGM) consisting of fetal bovine serum (FBS), 4 mM L-glutamine, 0.05 units/ml penicillin, and 0.05 μg/ml streptomycin (Cambrex).

### 8.2.2 Fabrication of hMSC- seeded 3D collagen matrices

The TissueTrain$^{TM}$ culture system (Flexcell International, Hillsborough, NC) was used to create hMSC-seeded linear 3D collagen matrices as previously reported.[106, 107] Briefly, hMSCs were cultured to 80-85% confluency in MSCGM and detached using 0.05% trypsin/0.53 mM EDTA (Cambrex) to suspend in a premixed collagen solution at 60,000 cells per 200 μl ($3 \times 10^5$ cells/mL), twice the cell seeding density of our previous study. The premixed collagen solution consisted of 70% v/v Type I collagen (Vitrogen; Angiotech BioMaterials Corp, Palo Alto, CA; neutralized to pH 7.0 with 1 N sodium hydroxide), 20% v/v 5x minimum essential medium (Sigma), and 10% v/v FBS (Cambrex). Six-well TissueTrain$^{TM}$ culture plates comprised of flexible well bottoms (membrane) and nylon non-woven anchors on two opposing sides were fitted with cylindrical posts. The cylindrical posts consisted of a linear groove across their central axes. A vacuum was applied to the plate assembly to deform the membrane downward into the grooves of the cylindrical posts

creating linear troughs into which the hMSC seeded-collagen suspension was dispensed. Once the hMSC seeded Type I collagen solution was dispensed into the troughs, the assembly was incubated at 5% $CO_2$ and 37 $^0$C for 2 hours to allow the collagen to polymerize and attach to the nonwoven anchors. The vacuum was released after 2 hours and MSCGM was added to each well. The plate assembly with hMSC seeded collagen matrices was further incubated 24 hours before changing the medium. While one group of hMSC seeded collagen matrices was maintained in MSCGM, another group was maintained in osteogenic differentiating medium (ODM) consisting of MSCGM supplemented with 0.5% dexamethasone, 1% β-glycerophosphate and 0.5% ascorbic acid (Cambrex). Media changes were carried out every 3 days through 7 and 14 days of culture.

### 8.2.3 Application of uniaxial cyclic tensile strain

Application of uniaxial cyclic tensile strain to hMSC seeded collagen constructs using the Flexercell FX-4000 strain unit (Flexcell International) was initiated 24 hours after creating the collagen matrices (after first change of culture media). The collagen matrices were subjected to uniaxial cyclic tensile strains of 10 or 12% at 1 Hz for 4 hours/day, for up to 7 and 14 days. Human MSC seeded collagen matrices maintained in static (strain = 0%) culture with all other conditions equal were used as same day unstrained controls. Three separate matrices were analyzed for each combination of strain, culture medium and culture duration.

### 8.2.4 Cell viability

After 7 and 14 days, viability of hMSCs in unstrained and strained collagen matrices was determined using a live/dead viability/cytotoxicity kit (Molecular Probes, Eugene, OR). The hMSC seeded collagen matrices were washed twice in phosphate buffered saline (PBS) prior to incubating in a staining solution containing 4 μM calcein AM and 4 μM EthD-1 for 45 minutes in the dark. Live cells were stained green by Calcein AM while dead cells were stained red by ethidium homodimer-1. Stained matrices were then mounted on glass slides and observed through a fluorescence microscope (Leica Microsystems Inc., Bannockburn, IL) with a 10 × objective. SimplePCI image analysis software (Compix Inc. Imaging systems, Cranberry Township, PA) was used to capture at least three different images each from the center and both ends of the constructs. The area occupied by live and dead cells at each location of the collagen matrix was measured using Adobe Photoshop (Adobe Systems Inc., San Jose, CA) and expressed as a percentage of the total area imaged.

### 8.2.5 Real-time polymerase chain reaction

After 7 and 14 days, all hMSC-seeded collagen matrices were removed from the culture plates and immediately frozen at -80 $^{0}$C. Total RNA was isolated from the hMSCs using Perfect RNA Eukaryotic Mini kit (Eppendorf, Westbury, NY) and Total RNA concentration of each isolation was determined subsequently using a Ribogreen RNA quantitation kit (Molecular Probes Inc., OR). First strand cDNA was synthesized from 60-180 ng of isolated total RNA using Superscript III RT with oligo(dT) primers (Invitrogen,

Carlsbad, CA) in a 25 µl reverse transcriptase (RT) reaction. The ABI Prism 7000 system (Applied Biosystems) was used to amplify the cDNA in the presence of primer probe oligonucleotide sets (Assays-on-Demand, Applied Biosystems, CA) for glyceraldehyde-3-phosphate dehydrogenase (GAPDH) (Assay HS99999905_M1), collagen Type 1 alpha 2 (COL1A2, Assay HS00164099_M1), alkaline phosphatase (ALPL, Assay HS00758162_M1), BMP-2 (Assay HS00154192_M1) and osteocalcin (OCN, Assay HS01587813_g1). Expression levels of all mRNA were normalized to GAPDH expression and the fold change in expression was calculated according to the relative quantification method [136] in relation to the mRNA expression levels of same day unstrained control hMSCs. All PCR reactions were performed in triplicate and the data were analyzed using the unpaired Student's t-test. Statistical significance was defined as $p < 0.05$, and significance at $p < 0.06$ and $p < 0.09$ were also indicated. Data are presented as mean ± standard deviation.

### 8.2.6 Endogenous alkaline phosphatase activity

Endogenous alkaline phosphatase activity of hMSCs after 1 week was determined using enzyme labeled fluorescence (ELF) -97 phosphate, which creates an intensely fluorescent yellow green precipitate at the site of alkaline phosphatase activity. The unstrained and strained hMSC-seeded collagen matrices were first washed twice with phosphate buffered saline (PBS) and then fixed using 10% formalin for 15 minutes. Permeabilization of the cell membranes was carried out by incubating the matrices in 0.2% Triton X-100/ 0.5% bovine serum albumin (TBSA) in PBS for 10 minutes. After rinsing the

matrices again in PBS, endogenous alkaline phosphatase activity (EALP) of the hMSCs was detected by incubating matrices in 40 μL of 20-fold diluted alkaline phosphatase substrate (ELF 97; Molecular Probes) for 15 minutes [153, 154]. A wash buffer containing 5 mM Levamisol and 25mM EDTA (Sigma) in PBS was subsequently added to stop the phosphatase reaction. In order to remove excess ELF 97 and prevent formation of background crystals, the matrices were further rinsed three times with wash buffer. A fluorescence microscope (Leica Microsystems Inc., Bannockburn, IL) with an excitation at 350 nm and emission at 535 nm with a 10× objective was then used to detect EALP activity and image the center and both ends of each matrix. At least three different images were obtained from each matrix location. The area of EALP activity in each image was measured and calculated as a percentage of total area. These percentage areas were normalized to those of same day unstrained controls and an increase or decrease in EALP activity was expressed as a fold change relative to unstrained control hMSCs.

## 8.3 Results

### 8.3.1 Cell viability

The area occupied by live hMSCs in the 3D collagen matrices comprised over 99% of the total area imaged, irrespective of the strain level and culture medium (Fig. 8.1). There was no significant effect of culture duration on hMSC viability.

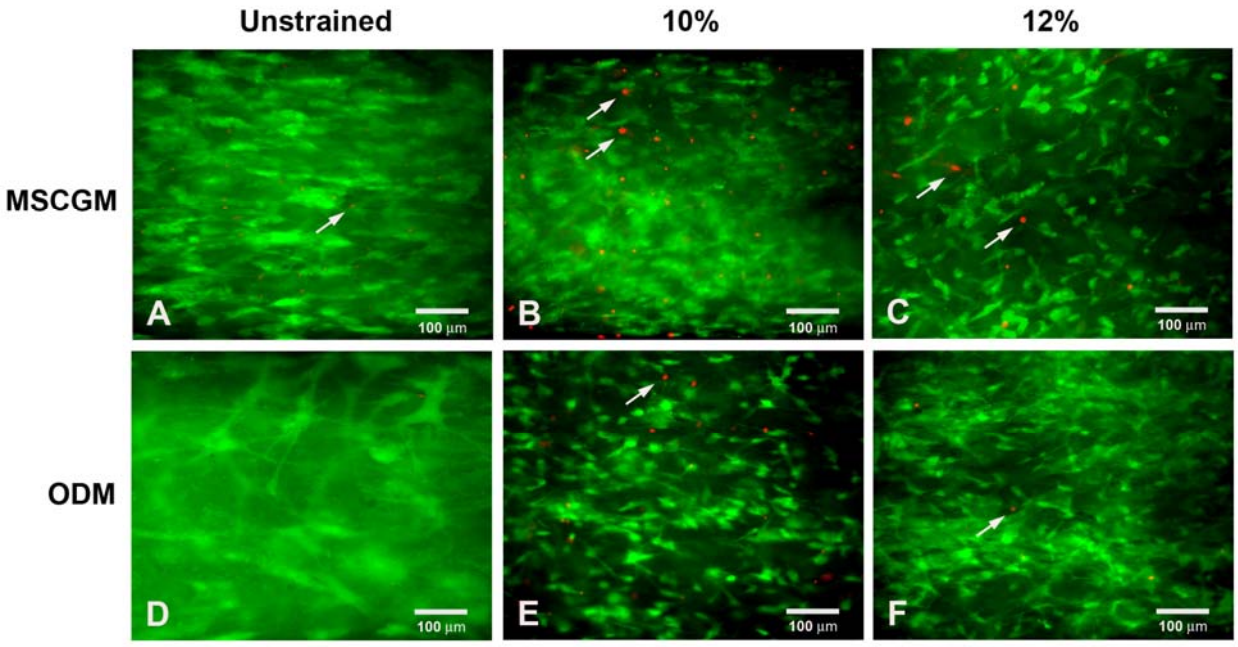


**Figure 8.1.** Unstrained and strained hMSCs in Type 1 collagen matrices cultured in complete growth medium (MSCGM) (A, B and C) and osteogenic differentiating medium (ODM) (D, E and F) for 2 weeks and stained with calcein AM and EthD-1 for live (green) and dead (red) cells, respectively. Arrows indicate dead cells. A, D) Unstrained (0% strain), B, E) 10% strained and C, F) 12% strained hMSCs.

### 8.3.2 COLI mRNA expression

All unstrained and strained hMSCs expressed COL1 mRNA at detectable levels. Cyclic strain or culture duration did not significantly affect expression levels of COL1 mRNA in hMSCs cultured in MSCGM (Fig. 8.2). The effect of ODM on COL1 mRNA expression was different between 10 and 12% strained hMSCs after 1 week (Fig. 8.2A). Compared to unstrained control and 12% strained hMSCs, 10% strained hMSCs cultured in ODM expressed significantly lower levels of COL1 mRNA after 1 week (Fig. 8.2A). In contrast, 12% strained hMSCs cultured in ODM expressed significantly higher levels of COL1 mRNA compared to both unstrained and 10% strained hMSCs after 1 week (Fig. 8.2A). Both these expression levels were significantly different compared to those in MSCGM (Fig. 8.2A). Neither strain nor culture media significantly affected COL1 mRNA expression levels in hMSCs after 2 weeks (Fig. 8.2B).

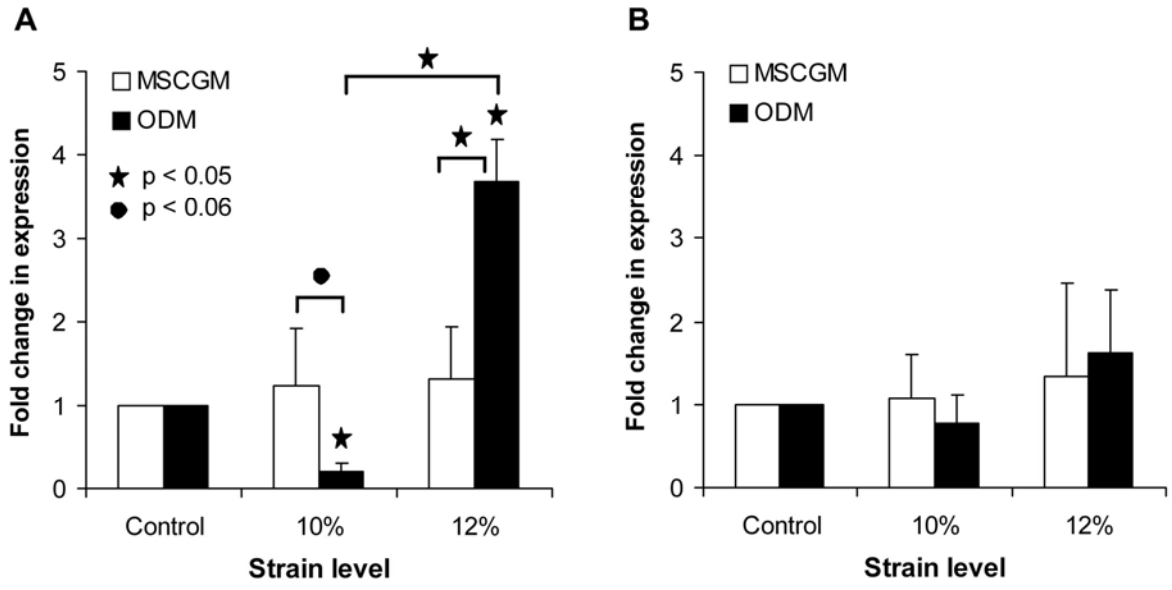


**Figure 8.2.** Fold change in COLI mRNA expression levels in hMSCs cultured in 3D collagen matrices and subjected to cyclic tensile strains of 0% (control), 10%, and 12%. A) Cultured for 1 week, B) Cultured for 2 weeks. Control denotes same day unstrained hMSCs maintained in identical media conditions. Unless indicated otherwise with a horizontal bracket, statistical significance symbols represent significance with reference to same day unstrained control. MSCGM = complete growth medium; ODM = osteogenic differentiating medium.

### 8.3.3 ALPL mRNA expression

The effect of strain on the expression of ALPL mRNA in hMSCs after 1 week was dependent on culture media (Fig. 8.3A). While there was a down regulation of ALPL mRNA in 10% strained hMSCs cultured in both MSCGM and ODM after 1 week, an upregulation was observed in 12% strained hMSCs cultured in ODM (Fig. 8.3A). A combined effect of strain and culture media on ALPL expression in hMSCs existed after 2 weeks (Fig. 8.3B).

All cyclically strained hMSCs cultured in ODM expressed significantly higher levels of ALPL mRNA after 2 weeks (Fig. 8.3B). Cyclic strain at 12% decreased ALPL mRNA expression in hMSCs cultured in MSCGM after 2 weeks (Fig. 8.3B). Culture duration increased ALPL mRNA expression in 10% strained hMSCs cultured in MSCGM and both 10% and 12% strained hMSCs cultured in ODM.

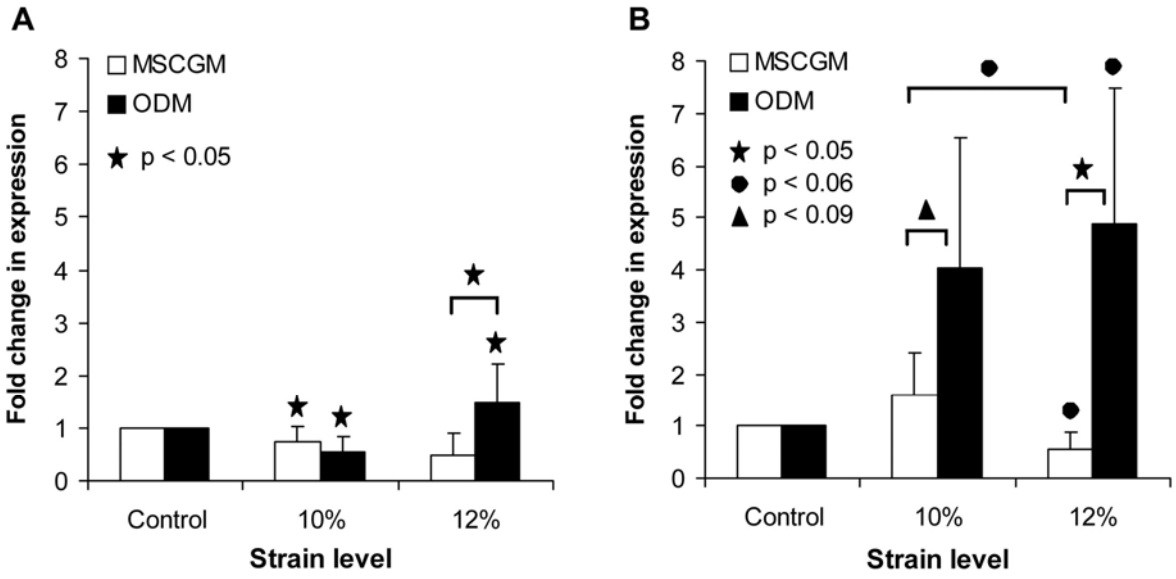


**Figure 8.3**. Fold change in ALPL mRNA expression levels in hMSCs cultured in 3D collagen matrices and subjected to cyclic tensile strains of 0% (control), 10%, and 12%. A) Cultured for 1 week, B) Cultured for 2 weeks. Control denotes same day unstrained hMSCs maintained in identical media conditions. Unless indicated otherwise with a horizontal bracket, statistical significance symbols represent significance with reference to same day unstrained control. MSCGM = complete growth medium; ODM = osteogenic differentiating medium.

### 8.3.4 BMP-2 mRNA expression

On average, cyclic tensile strain caused an increase in BMP-2 mRNA expression levels in all strained hMSCs irrespective of culture duration and medium. Higher BMP-2 mRNA expression levels observed in strained hMSCs cultured in MSCGM after 1 week were maintained until the end of the second week (Fig. 8.4A and 8.4B). Combined effects of cyclic strain and ODM were evident by an increased expression of BMP-2 mRNA in all strained hMSCs cultured in ODM after both 1 and 2 weeks (Fig. 8.4A and 8.4B). Expression levels of BMP-2 mRNA in hMSCs cyclically strained at 10% and cultured in ODM exceeded 14-fold compared to those of unstrained after 2 weeks (Fig. 8.4B). While there was no significant change in BMP-2 mRNA expression in hMSCs cultured in MSCGM between 1 and 2 weeks, those hMSCs strained and cultured in ODM had significantly higher expression levels at 2 weeks compared to 1 week.

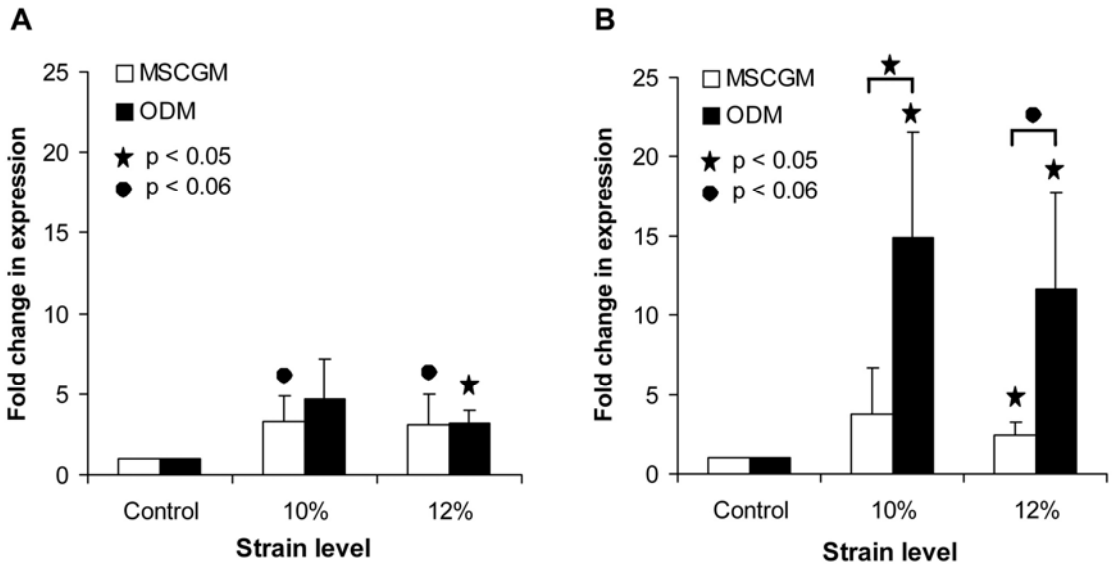


**Figure 8.4.** Fold change in BMP-2 mRNA expression levels in hMSCs cultured in 3D collagen matrices and subjected to cyclic tensile strains of 0% (control), 10%, and 12%. A) Cultured for 1 week, B) Cultured for 2 weeks. Control denotes same day unstrained hMSCs main tained in identical media conditions. Unless indicated otherwise with a horizontal bracket, statistical significance symbols represent significance with reference to same day unstrained control. MSCGM = complete growth medium; ODM = osteogenic differentiating medium.

### 8.3.5 OCN mRNA expression

Cyclic strain alone did not cause any significant change in OCN mRNA expression in strained hMSCs after 1 week. However, the combination of strain and ODM increased OCN mRNA expression (Fig. 8.5A). The expression levels of OCN mRNA in strained hMSCs cultured in ODM for 2 weeks were lower than those cultured for 1 week (Fig. 8.5B). However, unlike others, the expression levels in 10% strained hMSCs cultured in ODM was

higher than that of the unstrained control (Fig. 8.5B). There was no significant effect of culture duration on OCN expression in hMSCs.

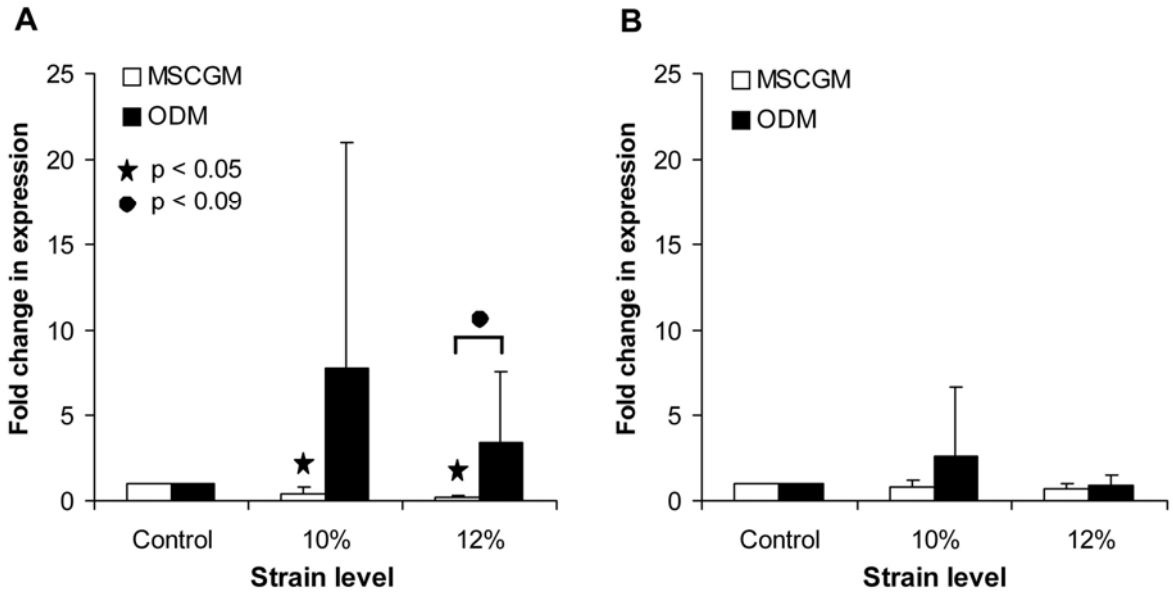


**Figure 8.5.** Fold change in OCN mRNA expression levels in hMSCs cultured in 3D collagen matrices and subjected to cyclic tensile strains of 0% (control), 10%, and 12%. A) Cultured for 1 week, B) Cultured for 2 weeks. Control denotes same day unstrained hMSCs maintained in identical media conditions. Unless indicated otherwise with a horizontal bracket, statistical significance symbols represent significance with reference to same day unstrained control. MSCGM = complete growth medium; ODM = osteogenic differentiating medium.

### 8.3.6 Endogenous alkaline phosphatase activity

Areas of endogenous alkaline phosphatase activity were observed in both unstrained and strained hMSC seeded collagen matrices (Fig. 8.6). At the end of the first week, the mean area of EALP activity was 10-fold higher in 10% strained matrices cultured in MSCGM compared to that of unstrained matrices (Fig. 8.6A, B). In contrast, the mean area of EALP activity in 12% strained matrices cultured in MSCGM was single fold higher than that of unstrained hMSCs (Fig. 8.6A, C). In ODM, the area of EALP activity in 10% strained matrices was 8-fold higher than that of unstrained matrices (Fig. 8.6D, E) while the area of EALP activity in 12% strained matrices was 17-fold higher than that of unstrained matrices (Fig. 8.6D, F).

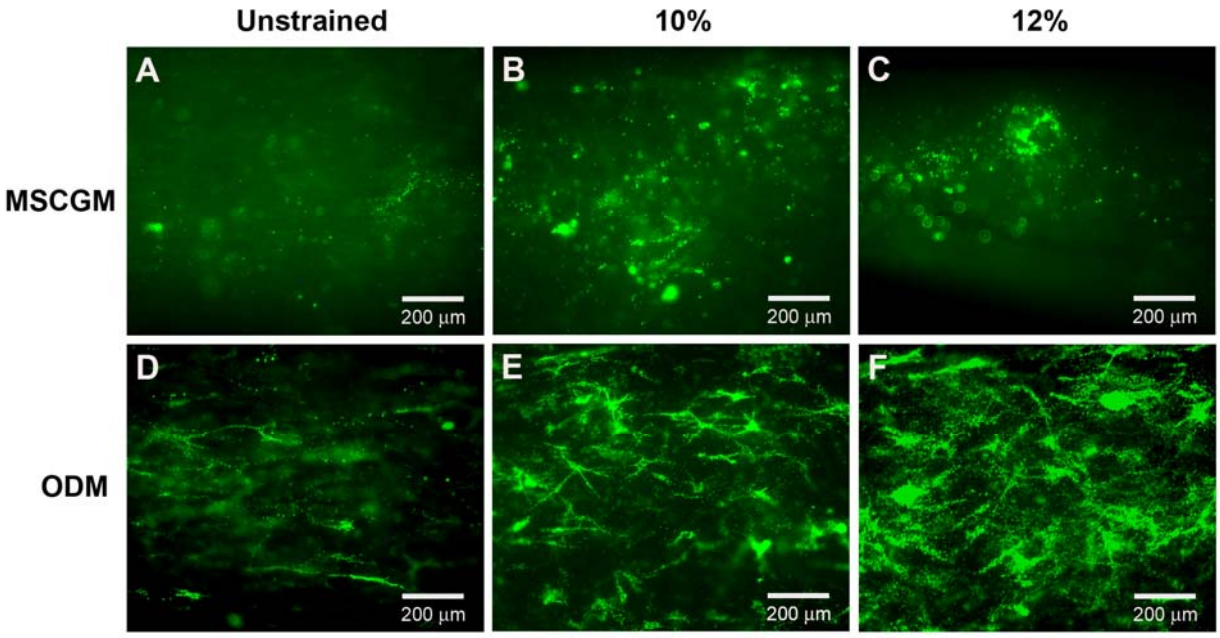


**Figure 8.6.** Localization of endogenous alkaline phosphatase (EALP) activity in unstrained and strained hMSCs in Type I collagen matrices cultured in complete growth medium (MSCGM) (A, B and C) and osteogenic differentiation medium (ODM) (D, E and F) for 1 week using enzyme labeled fluorescence (ELF)- 97 alkaline phosphatase substrate. A, D) Unstrained, B, E) 10% strained and C, F) 12% strained.

## 8.4 Discussion

Previous investigations of *in vitro* osteogenesis of hMSCs have predominantly used monolayer cultures under static conditions. In order to mimic physiological conditions and understand hMSC behavior in a 3D culture environment, it is vital to examine hMSC proliferation and osteogenesis in 3D culture conditions combined with mechanical loading. Investigations of critical factors involved in bone tissue engineering such as cell seeding density, culture duration, media conditions, and mechanical stimuli provide valuable information to establish protocols for generation of tissue engineered bone constructs *in vitro*.

In the present study, we investigated the effects of cyclic tensile strain, culture medium and culture duration on osteogenesis of adult bone marrow derived hMSCs seeded at high density ($3 \times 10^5$ cells/mL) in 3D Type I collagen matrices. Viability of hMSCs was maintained throughout the 14-day culture period irrespective of the level of cyclic tensile strain and media conditions to which the hMSCs were exposed. Cyclic tensile strain at 12% combined with osteogenic media conditions caused an upregulation of COLI mRNA expression after the first week. The increase in expression of ALPL mRNA after the second week in both 10 and 12% strained hMSCs was also dependent on osteogenic supplements in the culture media. An upregulation of BMP-2 mRNA was observed in all strained hMSCs cultured in both MSCGM and ODM from the first week. These observations verified our findings on BMP-2 mRNA expression previously where tensile strain alone caused an increase in BMP-2 mRNA expression. While this upregulation of BMP-2 mRNA at the end of the first week was independent of the media conditions, a noticeable increase was

observed at the end of the second week, affected by both osteogenic media conditions and cyclic tensile strain.

Increase in expression of OCN mRNA after the first week was dependent on combined effects of cyclic tensile strain and ODM. Synthesis of alkaline phosphatase by hMSCs during the first week increased with 10% cyclic strain without any osteogenic supplements in the culture media. With osteogenic supplements in the media, both 10 and 12% strains caused an increase in alkaline phosphatase production by hMSCs.

Our previous studies [106] and recent studies by others [11] have shown that hMSCs can be cultured in 3D collagen matrices without significant loss of cell viability. While confirming these results, the current study showed that hMSCs could be successfully seeded at 60,000 cells/ 200μL collagen gel solution ($3 \times 10^5$ cells/ mL) and cultured up to 14 days in the presence of cyclic tensile strains at 10% and 12%. Use of a higher initial cell seeding density could prove beneficial since previous studies have shown that self-renewal and differentiation of MSCs in the presence of dexamethasone were dependent on initial cell seeding density [160, 161].

Type I collagen is one of the major matrix proteins in bone [162] and is expressed during the initial stages of bone development [4]. In the present study, upregulation of COLI mRNA after the first week was observed in 12% strained hMSCs cultured in ODM. These results correlate well with results of static 3D culture [11] and dynamic monolayer culture [16] studies, which showed an increase in COLI expression by hMSCs in the presence of osteogenic supplements alone, or osteogenic supplements combined with cyclic strain, respectively. Under static 3D culture conditions, the expression of COLI mRNA in hMSCs cultured in

ODM increased after 5 days [11]. Similarly, with 8% cyclic tensile strain in the presence of ODM in monolayer cultures, hMSCs expressed peak levels of COLI mRNA after 4 days and continued to express higher levels up to 7 days [16]. Our data also showed that COLI mRNA expression in hMSCs in the presence of cyclic strain and ODM was triggered at an early stage during culture, which subsequently decreased after 14 days. This down regulation could be due to the saturation of COLI synthesized by hMSCs in collagen matrices after 7 days which was not investigated in this study.

Alkaline phosphatase is one of the major markers of osteogenesis and is expressed during the formation of first osteoid (between 5 and 6 days) in chick tibia development [4]. Studies by Yoneno et al. showed that hMSCs under static 3D culture conditions in the presence of ODM increased expression of ALPL mRNA after 5 days [11]. Similar studies by Frank et al. using bone marrow derived stromal cells in monolayer culture conditions showed an increase in ALPL expression at 7 days, which was maintained above normalized levels up to 20 days. We observed high levels of ALPL mRNA expression (4-5 fold) at 14 days in strained hMSCs in the presence of ODM in this study. This shows that ALPL mRNA expression was induced by the combined effects of cyclic strain and ODM.

Bone morphogenetic proteins, which are low molecular weight glycoproteins and belong to the transforming growth factor-β (TGF-β) super family [60], have been reported to be involved in the expression of cytokines and growth factors that affect osteogenic differentiation of MSCs [139]. Previous studies have reported that bone marrow derived hMSCs under static monolayer culture conditions, and in the presence of dexamethasone express maximum levels of BMP-2 after 20 days [64, 135]. We have previously shown that cyclic tensile

strain alone increased BMP-2 mRNA expression in hMSCs [106]. In contrast, in the present study, BMP-2 mRNA expression in strained hMSCs increased within 7 days as a function of both strain alone (without ODM) and strain in the presence of ODM. Although after two weeks BMP-2 mRNA expression levels in strained hMSCs cultured in MSCGM remained approximately unchanged from expression levels at one week, there was a significant increase of BMP-2 mRNA levels (above 14 fold) in those cultured in ODM when cyclically strained. This clearly shows that BMP-2 mRNA expression in hMSCs was accelerated by the combined effects of cyclic tensile strain and ODM.

Osteocalcin is a strong calcium binding protein [44, 45] found to be responsible for the maturation of mineral crystals [148]. It also elicits inhibitory effects on bone formation through osteoclast recruitment and activity [149, 150]. It has been reported that pre-osteoblasts undergoing osteogenic differentiation express OCN during the initial mineralization stages of bone formation [45, 66, 147]. Although there was high variability in levels of OCN mRNA expression by strained hMSCs in the present study, average expression levels indicated that OCN mRNA was expressed more in 10% strained hMSCs in the presence of ODM. However, there is not enough data from the present study to suggest a link between OCN mRNA expression by hMSCs and maturation of minerals or inhibitory effects on bone formation. Our results correlate with the observations by Jagodzinski et al. [16] who showed that neither cyclic strain nor dexamethasone influenced the expression of OCN mRNA in human bone marrow stromal cells cultured on monolayers after 7 days.

Observations on EALP activity in hMSCs in the present study correlate with previous observations made with human bone marrow stromal cells cultured under static monolayer

conditions in the presence of osteogenic supplements [64, 135]. Both those studies reported maximum ALPL activity in bone marrow stromal cells after 6 or 7 days. Jagodzinski et al. [16] reported that monolayer cultured hMSCs exposed to cyclic strain at 8% exhibited maximum ALPL activity after 4 and 7 days in the presence of dexamethasone, and after 7 days without dexamethasone in the culture media. In the present study, we observed similar results in 10% strained cells cultured in MSCGM where there was a high EALP activity after 7 days. However, in ODM, both 10% and 12% strained hMSCs showed higher EALP activities after 7 days with 12% strained hMSCs showing a 2-fold higher EALP activity than that in 10% strained hMSCs. It appears from the current results that cyclic tensile strain at 10% triggers hMSCs to synthesize ALPL earlier without any chemical stimulation. However, in the presence of osteogenic supplements, the effect on EALP activity was much higher with 12% cyclic strain.

In summary, we have shown that viability of hMSCs seeded at high density ($3 \times 10^5$ cells/mL) in 3D Type I collagen matrices and cultured in either MSCGM or ODM can be maintained for up to 14 days while undergoing cyclic tensile strains of 10 and 12% for 4 hours per day at 1 Hz. Both COLI and ALPL mRNA expressions in strained hMSCs were dependent on combined effects of uniaxial cyclic tensile strain and osteogenic supplements in the culture media. Although cyclic tensile strain alone caused an increase in BMP-2 mRNA in hMSCs from the first week, the combined effects of strain and osteogenic supplements on BMP-2 mRNA expression after 2 weeks was much more significant. High EALP activity after 7 days further suggested that hMSCs could be induced to differentiate down an osteogenic pathway with both strain and ODM. Except with COLI mRNA expression and

EALP activity, the current study did not show a significant difference between the 10 and 12% cyclic strain levels with respect to their stimulatory effect on ALPL, BMP-2 and OCN mRNA expression. This differs from our previous low density ($1.5 \times 10^5$ cells/mL) study where we observed higher expression of COLI, ALPL, BMP-2 and OCN in 10% strained hMSCs than in those strained at 12%. Results of this study suggest that hMSCs seeded at high density in 3D collagen matrices can be successfully induced by cyclic tensile strain and ODM to express mRNAs indicative of ostoegenic differentiation.

## 8.5 Summary

We have previously investigated the effects of cyclic tensile strain, culture duration and culture medium on osteogenesis of human mesenchymal stem cells (hMSCs) seeded at low density ($1.5 \times 10^6$ cells/mL) in collagen matrices. In this study, we increased hMSC seeding density to $3 \times 10^6$ cells/mL and investigated the influence of cyclic tensile strain, culture duration, and medium on osteogenesis of hMSCs. hMSCs seeded in three-dimensional collagen matrices were subjected to 0, 10 and 12% uniaxial cyclic tensile strain at 1 Hz for 4 hours/day for 7 and 14 days in complete growth and osteogenic media. Viability of hMSCs was maintained over 99% irrespective of cyclic strain and media conditions. Cyclic strain at 12% in osteogenic medium caused an increase in Type I collagen mRNA expression by hMSCs after 7 days. Increased expression of alkaline phosphatase mRNA was observed after 2 weeks in hMSCs exposed to both cyclic tensile strain and osteogenic medium. Higher expressions of bone morphogenetic protein-2 (BMP-2) mRNA were observed within 7 days in strained hMSCs both in the presence and absence of osteogenic supplements. Combined effects of osteogenic medium and cyclic strain caused an over 10-fold increase in BMP-2 expression after 2 weeks. Strain and osteogenic medium increased osteocalcin mRNA expression in hMSCs after 7 days. Endogenous alkaline phosphatase activity (EALP) in hMSCs increased with cyclic strain and osteogenic medium. This study shows that hMSCs cultured at high density in collagen matrices could be induced for osteogenesis by cyclic tensile strain combined with osteogenic medium.

# 9 Expression of Proinflammatory Cytokines by Bone derived Human Mesenchymal Stem Cells under Cyclic Tensile Strain

Osteogenesis of hMSCs is evaluated in most studies by analyzing the expression of osteogenic marker genes or deposition of calcium in the matrix. Recent studies have revealed that proinflammatory cytokines also play a direct or indirect role in modulating osteogenic differentiation and bone resorption. The expression of these proinflammatory cytokines in hMSCs need to be determined in order to understand their function during osteogenic differentiation. This chapter describes a study analyzing the effects of cyclic tensile strain, culture medium, and culture duration on expression of proinflammatory cutokines by hMSCs cultured in three-dimensional collagen matrices.

## 9.1 Introduction

Stimulation of human mesenchymal stem cells (hMSCs) by tensile strains and osteogenic media conditions to induce osteogenic differentiation has been widely investigated. [16, 17, 28] These investigations have primarily focused on determining appropriate strain levels[13-17, 28] and media supplements[6, 9, 10] required to achieve osteogenesis of hMSCs. A typical investigation of hMSC osteogenesis includes analysis of bone markers and their corresponding proteins or calcium deposition in the extracellular matrix.[9, 10, 64, 106, 135]

Recent studies have indicated production of proinflammatory cytokines such as tumor necrosis factor-α (TNF-α), interleukin-1β (IL-1β), interleukin-6 (IL-6) and interleukin-8 (IL-8) by hMSCs[12, 163-165] and their involvement in either osteogenic differentiation[166, 167] or bone resorption.[168-170] Interleukin-1β is a major mediator of host inflammatory response and generates systemic responses including fever and the release of acute phase protein from liver.[171] TNF-α is also an inflammatory cytokine secreted by macrophages/monocytes during acute inflammation [172] and after toxicity.[173] Its numerous signaling events within cells can cause necrosis and apoptosis.[172] Both TNF-α and IL-1β are involved in bone metabolism and in regulating the function of osteoblasts and osteoclasts.[170, 174, 175] Interleukin-6 is a multifunctional cytokine with a major role in inflammatory responses, cell proliferation, and inducing acute phase proteins.[176] Increased concentration of IL-6 in the bone microenvironment causes enhanced bone resorption via indirect modulation of osteoclast differentiation.[177] IL-8, formerly known as neutrophil attractant/activating protein 1 (NAP-1), is a chemotactic cytokine[178, 179] and functions as a pro-inflammatory substance involved in recruitment and trafficking of neutrophils during immunologic or inflammatory responses.[179]

Interleukin-8 is produced and released by many cells, including osteoblasts derived from mesenchymal progenitors.[180, 181]

Findings from previous investigations indicated that cytokine involvement during osteogenic differentiation and bone resorption exhibit the presence of an autocrine or paracrine mechanism in hMSCs to modulate bone regeneration and resorption. Analysis of cytokines involved in such a system would provide valuable information on signaling mechanisms or pathways involved during osteogenic differentiation of hMSCs. However, the effects of various osteogenic differentiation conditions on the expression of these cytokines have not been investigated.

We hypothesized that application of tensile strain in the presence of osteogenic supplements would increase expression levels of TNF-α, IL-1β, IL-6 and IL-8. To test our hypothesis, hMSCs were cultured in 3D collagen matrices and subjected to cyclic tensile strain at 10% or 12% (f = 1 Hz, 4 hours/day) in either complete growth medium or osteogenic differentiating medium for up to 14 days. The purpose of this study was to investigate the effects of cyclic tensile strain, culture medium, and culture duration on the expression of TNF-α, IL-1β, IL-6 and IL-8 cytokines by hMSCs cultured in three-dimensional (3D) collagen matrices.

## 9.2 Materials and Methods

### 9.2.1 Cell culture

Bone marrow derived hMSCs (24 year old Caucasian male donor; Tulane University, New Orleans, LA) were expanded to passage 3 in complete growth medium (MSCGM) consisting of fetal bovine serum (FBS), 4 mM L-glutamine, 0.05 units/ml penicillin, and 0.05 μg/ml streptomycin (Cambrex).

### 9.2.2 Fabrication of hMSC- seeded 3D collagen matrices

Linear 3D collagen matrices seeded with hMSCs were created using the TissueTrain™ culture system (Flexcell International, Hillsborough, NC) as previously reported.[106, 107] Briefly, hMSCs were cultured to 80-85% confluence and detached using 0.05% trypsin/0.53 mM EDTA (Cambrex) and suspended in a collagen solution at 30,000 cells per 200 μl. The collagen solution consisted of 70% v/v Type I collagen (Vitrogen; Angiotech BioMaterials Corp, Palo Alto, CA; neutralized to pH 7.0 with 1 N sodium hydroxide), 20% v/v 5x minimum essential medium (Sigma), and 10% v/v FBS (Cambrex). Six-well TissueTrain™ culture plates consisting of flexible well bottoms (membrane) and nylon non-woven anchors on two opposing sides were fitted with flat cylindrical posts that have a linear groove across their central axes. A vacuum was applied to the plate assembly to deform the membrane downward into the grooves of the cylindrical posts creating linear troughs. The hMSC seeded Type I collagen solution was then dispensed into the troughs to create hMSC-seeded 3D collagen constructs. The assembly was then incubated at 5% $CO_2$

and 37 $^{0}$C for 2 hours for collagen to polymerize and attach to the nonwoven anchors after which the vacuum was released and MSCGM was added to each well. The hMSC-seeded collagen matrices were further incubated 24 hours, after which the medium was changed. Separate groups of hMSC seeded collagen matrices were maintained in MSCGM and in osteogenic differentiating medium (ODM) consisting of MSCGM supplemented with 0.5% dexamethasone, 1% β-glycerophosphate and 0.5% ascorbic acid (Cambrex) throughout the culture period. The medium was changed every 3 days through 14 days of culture.

### 9.2.3 Application of uniaxial cyclic tensile strain

The hMSC-seeded collagen matrices were subjected to 10 or 12% uniaxial cyclic tensile strains at 1 Hz for 4 hours/day, for up to 14 days using the Flexercell FX-4000 strain unit (Flexcell International). Human MSCs seeded into Type I collagen gels as described above and maintained in static (strain = 0%) culture served as unloaded controls. Three separate constructs were analyzed for each combination of strain, culture medium, and time point.

### 9.2.4 Cell viability

Viability of hMSCs in unstrained and strained collagen matrices after 14 days was determined using a live/dead viability/cytotoxicity kit (Molecular Probes, Eugene, OR). Briefly, the collagen matrices were washed twice in phosphate buffered saline (PBS) followed by 45 minutes incubation in a staining solution containing 4 μM calcein AM and 4

μM ethidium homodimer-1 (EthD-1) in the dark. Calcein AM stained live cells green while EthD-1 stained dead cells red. Stained matrices were then mounted on glass slides and the center and two ends of the constructs were imaged using a fluorescence microscope (Leica Microsystems Inc., Bannockburn, IL) with a 10× objective to obtain at least 2 different images each from the center and both ends of each construct. The images were captured using SimplePCI image analysis software (Compix Inc. Imaging systems, Cranberry Township, PA). Live and dead cells at each location of the collagen matrix were quantified by separately measuring the area they occupied using Adobe Photoshop (Adobe Systems Inc., San Jose, CA) and presented as percentage area of live and dead cells.

### 9.2.5 Measurement of cytokines in culture media

The expressions of TNF-α, IL-1β, IL-6 and IL-8 were measured using the Bio-Plex suspension array system (Bio-Rad Laboratories, Hercules, CA). Samples of culture media were removed from the culture wells of unstrained and strained hMSC-seeded collagen constructs at $1^{st}$, $2^{nd}$, $4^{th}$ and $6^{th}$ media changes allowing the determination of cytokine expression by hMSCs between 0-1, 1-3, 6-9, and 12-14 days of culture. A multiplexing assay consisting of beads conjugated with antibodies that specifically bind to cytokines was incubated with 50μL culture medium from each treatment in a 96-well filter plate. The beads were then incubated with a fluorescent-labeled reporter molecule that specifically binds the analyte and produces fluorescence relative to the magnitude of the reaction. The contents of each well were analyzed in the Bio-Plex array reader, allowing for the quantitation of

specific cytokines relative to a standard curve. The expression of cytokines by strained (strain = 10% or 12%) hMSCs was normalized against that of same day unstrained (strain = 0%) hMSCs. Three hMSC-seeded matrices were used for each treatment combination and the assay was carried out in triplicate.

### 9.2.6 Statistical analysis

Factorial effects of culture medium, strain, and culture duration on normalized cytokine expressions were investigated using F-tests from an analysis of variance (ANOVA) appropriate to the complete, crossed, $2 \times 3 \times 4$ experimental design. The significance level was defined as $p < 0.05$.

## 9.3 Results

### 9.3.1 Cell viability

The fluorescence microscopy images of hMSC-seeded collagen matrices cultured in both MSCGM and ODM showed greater than 98% area occupied by live cells after 14 days, irrespective of the strain level applied (Fig. 9.1).

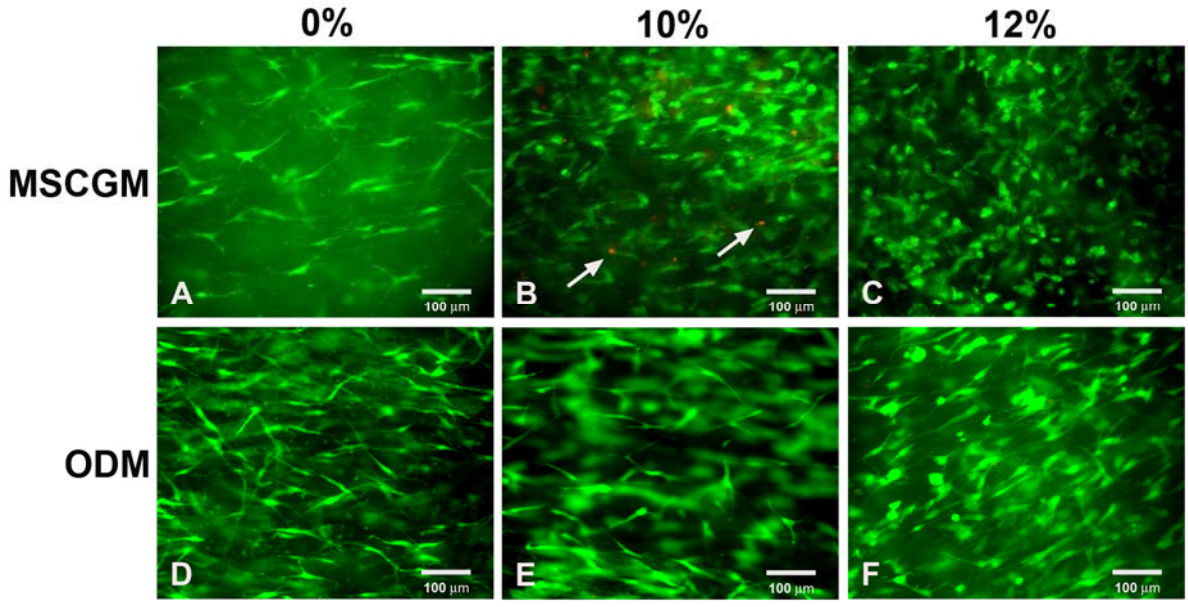


**Figure 9.1.** Strained and unstrained hMSC-seeded type 1 collagen matrices cultured in complete growth (MSCGM) (A, B and C) and osteogenic differentiating medium (ODM) (D, E and F) for 2 weeks and stained with calcein AM and EthD-1 for live (green) and dead (red) cells, respectively. Arrows indicate dead cells. A, D) Unstrained, B, E) Strained at 10%, C, F) Strained at 12%.

### 9.3.2 Expression of IL-6

The concentration levels of IL-6 in hMSCs cultured in MSCGM significantly increased during 6-9 days and continued to increase until 14 days (Fig 9.2A). The concentrations of IL-6 in hMSCs significantly reduced in the presence of dexamethasone in culture media after 1-3 days (Fig 9.2B). On average, all cyclically strained hMSCs cultured in MSCGM showed statistically significant lower levels of IL-6 expression compared to their unstrained controls (0% strained hMSCs) during 0-1, 6-9 and 12-14 days with the exception of 1-3 days (Fig. 9.3). Compared to unstrained controls and 12% strained hMSCs, there was a significant increase in IL-6 expression in 10% strained hMSCs cultured in MSCGM between 1 and 3 days (Fig. 9.3). However, the expression level in both strained hMSCs (10 and 12%) significantly reduced during 6-9 days culture and remained unchanged until 14 days. After day 1, IL-6 expression levels in 10% strained hMSCs cultured in MSCGM were significantly higher than those of 12% strained hMSCs (Fig. 9.3). In contrast to hMSCs cultured in MSCGM, those cultured in ODM and strained at both 10 and 12% showed significantly higher IL-6 expression levels between 1-3 and 6-9 days compared to their unstrained controls and 12-14 days (Fig. 9.4). The 12% strained hMSCs cultured in ODM had a significantly higher IL-6 expression after day 1 than those cultured in MSCGM (Fig. 9.3 and 9.4).

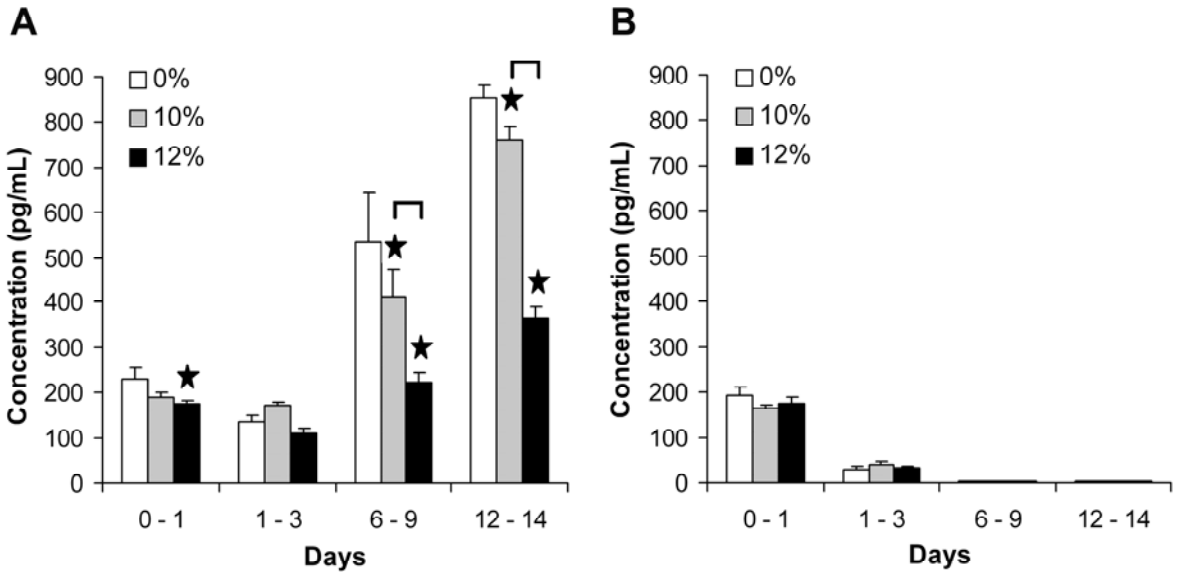


**Figure 9.2.** Expression of IL-6 by hMSCs seeded in 3D collagen matrices and subjected to 0% (control), 10%, and 12% cyclic tensile strains in; A) Complete growth medium (MSCGM), and B) Osteogenic differentiation medium (ODM). Unless indicated otherwise with a horizontal bracket, statistical significance symbols represent significance with reference to same day unstrained control (0% strained). Statistical significance; $p < 0.05$.

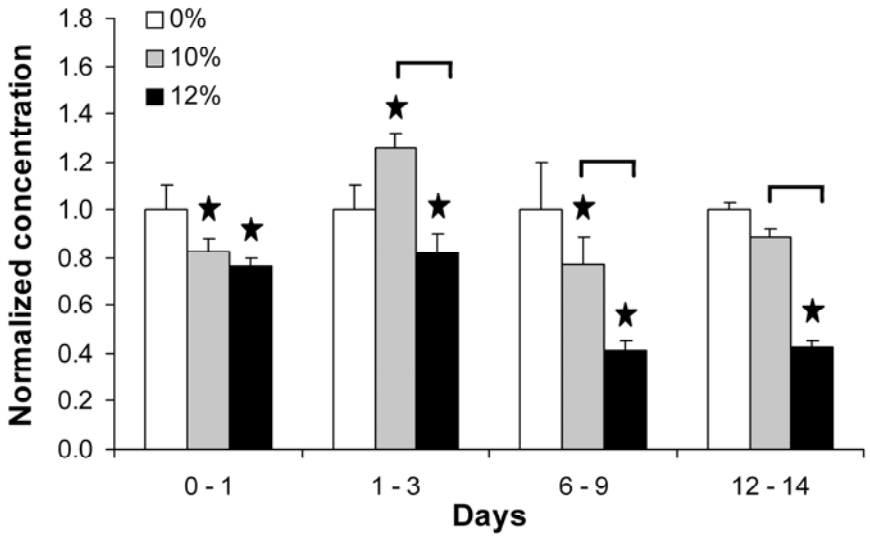


**Figure 9.3.** Fold change in expression of IL-6 by hMSCs seeded in 3D collagen matrices and cultured in complete growth medium (MSCGM) under 0% (control), 10%, and 12% cyclic tensile strains. Fold change in expression calculated by normalizing expression against same day unstrained control (0% strained). Unless indicated otherwise with a horizontal bracket, statistical significance symbols represent significance with reference to same day unstrained control (0% strained). Statistical significance; $p < 0.05$.

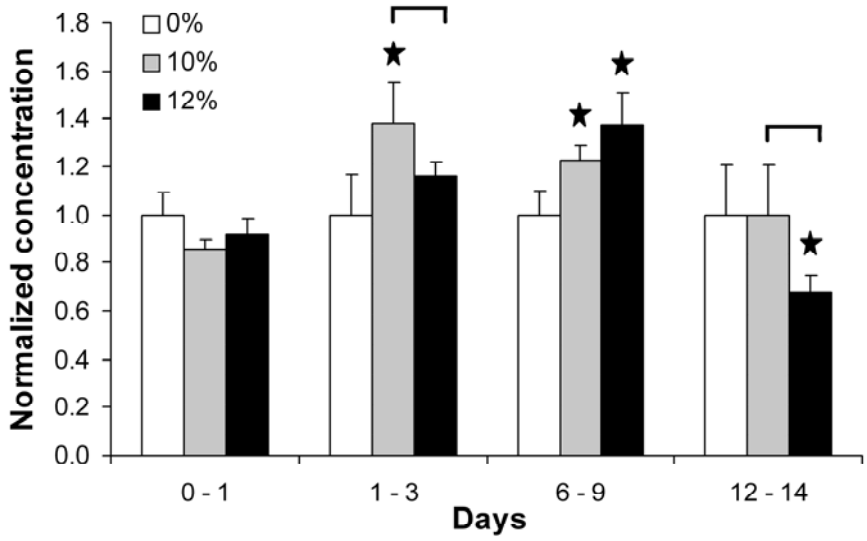


**Figure 9.4.** Fold change in expression of IL-6 by hMSCs seeded in 3D collagen matrices and cultured in osteogenic differentiation medium (ODM) under 0% (control), 10%, and 12% cyclic tensile strains. Fold change in expression calculated by normalizing the expression against same day unstrained control (0% strained). Unless indicated otherwise with a horizontal bracket, statistical significance symbols represent significance with reference to same day unstrained control (0% strained). Statistical significance; $p < 0.05$.

### 9.3.3 Expression of IL-8

The highest expression of IL-8 in strained hMSCs cultured in MSCGM was observed during 1-3 days (Fig. 9.5A) while the highest IL-8 expression was observed in ODM cultures during 12-14 days (Fig. 9.5B). On average, the concentration of IL-8 in media of hMSCs cultured in the presence of dexamethasone (component of ODM) continuously increased from day 1 to day 14 with the exception of 10% strained hMSCs between 6-9 days. These expression levels were significantly higher than samples cultured without dexamethasone (cultured in MSCGM) in culture media after 6-9 days, and 12-14 days (Fig. 9.5). Both 10 and

12% strained hMSCs cultured in MSCGM expressed significantly higher levels of IL-8 during 1-3 and 6-9 days compared to 0-1 and 12-14 days (Fig. 9.6). In ODM, the hMSCs strained at 10% showed the greatest IL-8 expression levels from day 1-3 (Fig. 9.7). This increased IL-8 expression significantly continued to decrease through 14 days (Fig. 9.7).

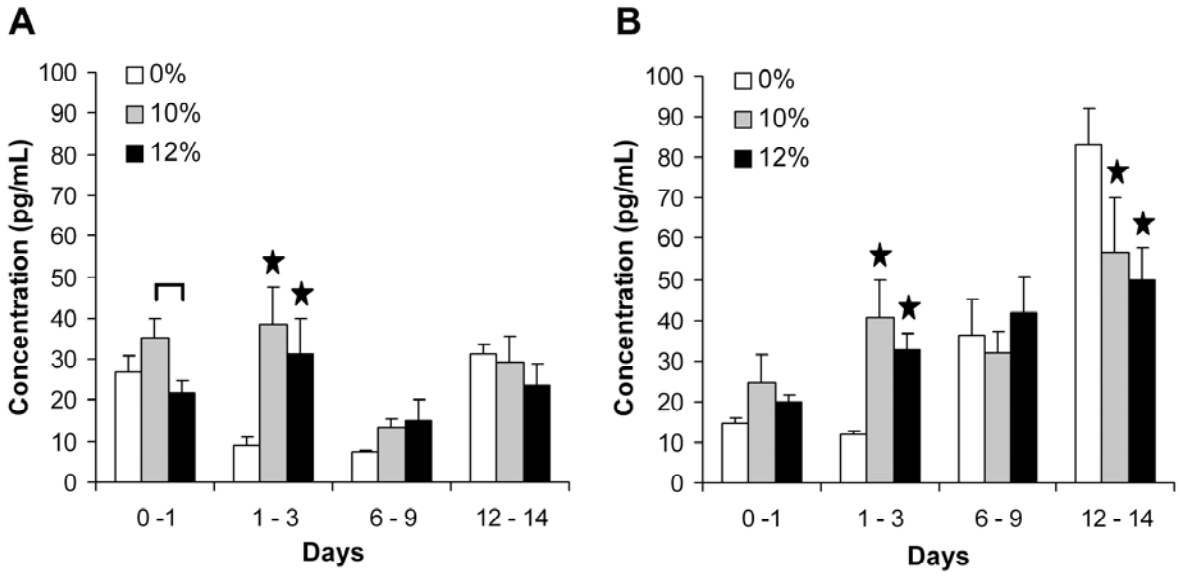


**Figure 9.5.** Expression of IL-8 by hMSCs seeded in 3D collagen matrices and subjected to 0% (control), 10%, and 12% cyclic tensile strains in; A) Complete growth medium (MSCGM) and B) Osteogenic differentiation medium (ODM). Unless indicated otherwise with a horizontal bracket, statistical significance symbols represent significance with reference to same day unstrained control (0% strained). Statistical significance; $p < 0.05$.

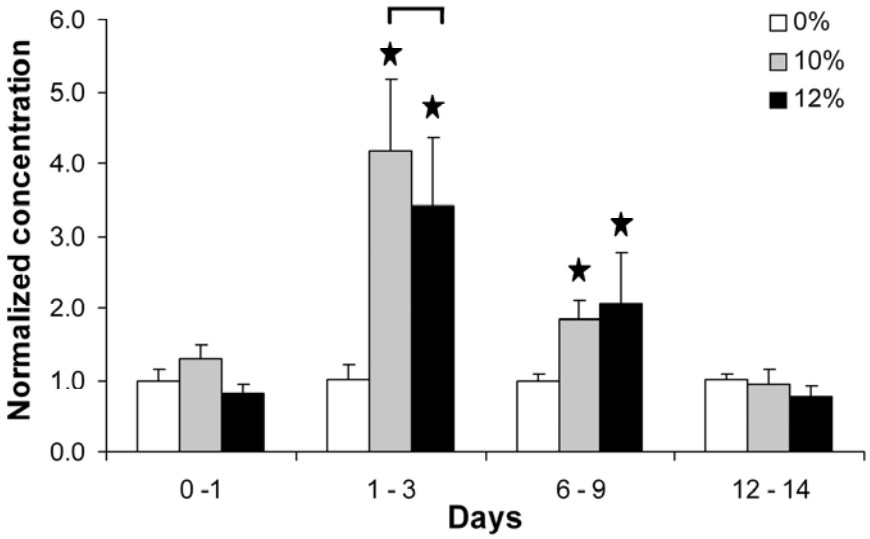


**Figure 9.6.** Fold change in expression of IL-8 by hMSCs seeded in 3D collagen matrices and cultured in complete growth medium (MSCGM) under 0% (control), 10%, and 12% cyclic tensile strains. Fold change in expression calculated by normalizing the expression against same day unstrained control (0% strained). Unless indicated otherwise with a horizontal bracket, statistical significance symbols represent significance with reference to same day unstrained control (0% strained). Statistical significance; $p < 0.05$.

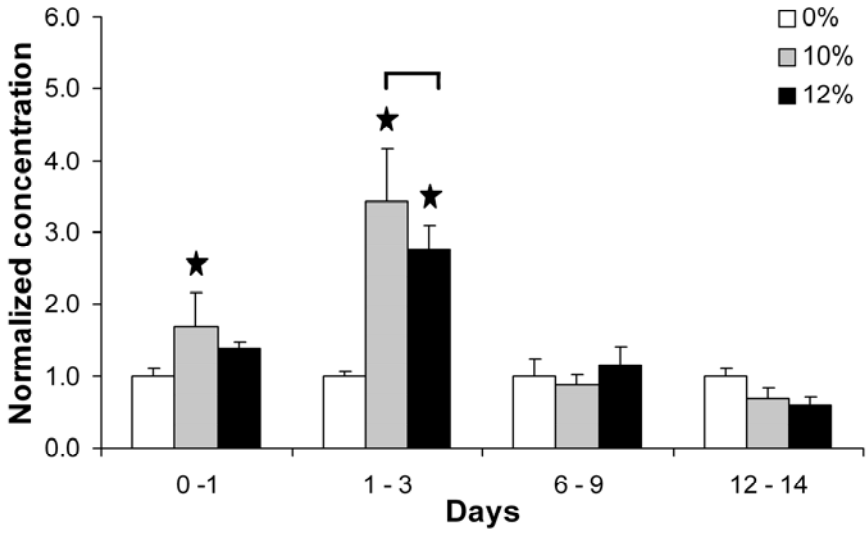


**Figure 9.7.** Fold change in expression of IL-8 by hMSCs seeded in 3D collagen matrices and cultured in osteogenic differentiation medium (ODM) under 0% (control), 10%, and 12% cyclic tensile strains. Fold change in expression calculated by normalizing the expression against same day unstrained control (0% strained). Unless indicated otherwise with a horizontal bracket, statistical significance symbols represent significance with reference to same day unstrained control (0% strained). Statistical significance; $p < 0.05$.

### 9.3.4 Expression of TNF-α and IL-1β

Unstrained and strained hMSCs cultured in both MSCGM and ODM had very low expression of TNF-α between 0-1, 1-3, 6-9, and 12-14 days of culture (data not shown). The mean concentration of TNF-α in the hMSCs ranged from 0 to 0.1 pg/mL. Similarly, mean expression of IL-1β in both strained and unstrained hMSCs ranged from 0 to 0.04 pg/mL. There was no significant effect from strain, culture medium or culture duration on either TNF-α or IL-1β expressions.

## 9.4 Discussion

The mitotic, metabolic and developmental activities of mesenchymal stem cells are regulated by components in the extracellular environment including autocrine and paracrine factors synthesized by the hMSCs themselves. Signals that modulate the growth and differentiation capacity of mesenchymal stem cells provide valuable information on signal cascades involved in their terminal differentiation. The existence of, and changes in, these signals during *in vitro* osteogenic differentiation need to be investigated in order to identify key factors and to understand the mechanisms of osteogenesis of hMSCs. The proinflammatory cytokines TNF-α, IL-1β, IL-6 and IL-8 have been reported to be expressed in hMSCs under normal growth conditions and have also been found to be indirectly or directly connected with modulating bone resorption. However, the effects of different *in vitro* osteogenic differentiating conditions on the expression of these cytokines in hMSCs have not been investigated.

Cell viability studies indicated that the hMSCs remained viable throughout the experimental period irrespective of the strain levels and media conditions. Previous studies indicate that both TNF-α and IL-1β play a role in bone metabolism and regulate the function of osteoblasts and osteoclasts.[170, 174, 175] Investigations by Thomson et al.[170] showed that TNF-α stimulated bone resorption by osteoclasts in the presence of osteoblasts or when supernatants of osteoblasts were added to the culture media. This indicated that activation of bone resorption by TNF-α requires signal molecules from the osteoblasts. Filipak et al.[163] reported that terminal differentiation of 3T3 T MSCs down the adipogenic pathways was inhibited by TNF-α. However, his study did not investigate the effect of TNF on osteogenic

differentiation of MSCs. The maximum release of TNF-α by human epidermal keratinocytes (HEK) exposed to toxic conditions has been observed at 4 hours, after which it decreased in a time dependent manner.[173] Release of TNF-α by HEKs has also been shown to induce IL-8 release from HEKs.[173, 182, 183] In the present study, the expression levels of TNF-α and IL-1β observed in both unstrained and strained hMSCs were very low. In contrast to observations with HEKs [173, 182, 183], hMSCs did not release significant amounts of TNF-α and were not observed to foster IL-8 release from hMSCs. According to observations made by Thomson et al.,[170] this may be due to the absence of signal molecules from already differentiated osteoblasts.

Bone marrow derived hMSCs have been reported to continually express IL-6 under normal growth conditions. [12, 164, 165, 184] Haynesworth et al.[12] and Majumdar et al.[165] reported that the expression of IL-6 by human bone marrow derived MSCs was significantly inhibited by the presence of dexamethasone in the culture medium. Kim et al.[164] also reported that the initial expression of IL-6 in bone marrow derived MSCs was decreased when MSCs were subjected to osteogenic differentiation conditions (in the presence of dexamethasone) for two weeks. IL-6 has been found to mediate signals through receptors that use gp130 in its signaling pathway and shown to regulate bone marrow stromal cell differentiation.[166] Interleukin-6 has also been reported to increase cell proliferation, expression of alkaline phosphatase and decrease mRNA expression of osteocalcin.[12] However, bone marrow derived hMSCs do not express membrane bound or soluble IL-6 receptors, but when receptors are added in the presence of dexamethasone, hMSCs have been reported to express alkaline phosphatase.[167] In the present study, observations on initial IL-6 concentration data

indicated a significant down regulation of IL-6 expression in all hMSCs after day 1 in the presence of dexamethasone, irrespective of strain. This could be due to the decrease in cell proliferation of hMSCs in the presence of osteogenic differentiating media.[9] These results correlate well with previous investigations where an inhibition of IL-6 expression was observed in the presence of dexamethasone.[12, 164, 165] The initial concentration data in the present study was normalized against same day unstrained controls (0% strained hMSCs) to determine the effect of strain on IL-6 expression. The effect of strain on IL-6 expression was dependent on culture medium and time. The IL-6 expression in hMSCs was upregulated briefly (during 1-3 days of culture) by 10% strain stimuli regardless of the media conditions, while the temporary (1-3 and 6-9 days of culture) IL-6 upregulation by 12% strain stimuli occurred only in the presence of dexamethasone in culture media. However, increased IL-6 expression levels due to both 10% and 12% strain stimuli in the presence of dexamethasone remained elevated longer than those without dexamethasone. These results indicated that strain stimuli might decrease the inhibition of IL-6 expression by dexamethasone. Since IL-6 is released during irritation[185, 186], it is also possible that irritation of hMSCs caused by cyclic strain could trigger release of IL-6 even in the presence of dexamethasone.

Previous studies have reported that IL-8 can function as an inhibitor to osteoclast bone resorptive activity.[168, 169] Investigations by Sunyer et al.[187] showed that bone resorption was modulated in avian marrow derived osteoclast like cells through nitric oxide (NO) production that was upregulated by IL-8 action. Fuller et al.[168] reported that IL-8, while inhibiting the proportion of osteoclasts that were resorbing bone, also stimulated osteoclast motility. Similar to IL-6, the expression of IL-8 has been reported to be down regulated in the

presence of dexamethasone.[188, 189] In addition, recent investigations have shown that IL-8 expression in human bone marrow osteoprogenitor cells was increased by treatment with IL-1β.[188] Kim et al.[164] reported that expression of IL-8 was slightly upregulated when bone marrow derived MSCs were subjected to osteogenic differentiation conditions for 14 days. In the present study, we observed a continuous upregulation of IL-8 in both unstrained and strained hMSCs in the presence of dexamethasone. Our results with hMSCs that were unstrained and cultured in MSCGM correlate with observations made by Kim et al.[164] but contradict the conclusions made by Chaudhary et al. that dexamethasone inhibits IL-8 expression in hMSCs under normal growth conditions.[14, 188, 189] In the present study, analysis of strain, medium, and culture duration on IL-8 expression revealed that strain briefly increased IL-8 expression in hMSCs. The significant effects of strain stimuli were observed to remain longer (during 1-3 and 6-9 days) in hMSCs cultured without dexamethasone, while in the presence of dexamethasone IL-8 expression was increased during the first three days. Since IL-8 has been shown to be released during irritation[185, 186], the initial increase in IL-8 even in the presence of dexamethasone could be due to similar conditions caused by cyclic strain. The elevation of IL-8 by hMSCs due to cyclic strain irrespective of the presence of dexamethasone suggests that stimulation of hMSCs by strain not only induces expression of genes indicative of osteogenic differentiation[106] but also produces factors such as IL-8 to inhibit bone resorption.

In summary, we have investigated the effects of cyclic tensile strain, culture duration, and culture medium on the expression of TNF-α, IL-1β, IL-6 and IL-8 cytokines by bone marrow derived hMSCs cultured in 3D collagen matrices. Results of this study indicated that

expression of TNF-α and IL-1β were not detected in hMSCs under the culture conditions investigated in this study. The presence of dexamethasone caused a decrease in IL-6 expression in all hMSCs irrespective of the level of strain but strain decreased the inhibition of IL-6 expression by dexamethasone. The expression of IL-8 in strained hMSCs suggested that cyclic strain induced hMSCs to produce IL-8, which could lead to inhibition of bone resorption during osteogenesis. This study provides useful information on the activity of cytokines involved in regulating bone resorption and remodeling during osteogenic induction of hMSCs cultured in a 3D environment under cyclic tensile strain and in the presence of dexamethasone.

## 9.5 Summary

Mesenchymal stem cells produce proinflammatory cytokines at a steady level during their normal growth. Direct or indirect regulation of bone resorption by these cytokines has been reported. However, the effects of osteogenic conditions utilized during *in vitro* bone tissue engineering on expression of cytokines have not been investigated. In this study, we investigated the effects of uniaxial cyclic tensile strain, culture medium and culture duration on the expression of tumor necrosis factor-α (TNF-α), interleukin-1β (IL-1β), interleukin-6 (IL-6) and interleukin-8 (IL-8) by bone marrow derived human mesenchymal stem cells seeded in three-dimensional Type I collagen matrices and subjected to 0%, 10% and 12% uniaxial cyclic tensile strains at 1 Hz for 4 hours/day for 7 and 14 days in complete growth or osteogenic medium. Viability of hMSCs was maintained irrespective of strain level and media conditions. Expression of both TNF-α and IL-1β was not observed in hMSCs under the conditions investigated in this study. Interleukin-6 expression in hMSCs was reduced in the presence of dexamethasone in culture media. Expression of IL-6 was dependent on culture medium and cyclic tensile strain where a brief increase in IL-6 expression was caused by both 10% and 12% strain levels. Presence of dexamethasone in culture media increased the IL-8 expression by hMSCs. Both 10% and 12% strain levels caused an increase in IL-8 production by hMSCs that was dependent on the presence of dexamethasone in culture media. Both TNF- α and IL-1β was not detected during the observed time points while IL-6 and IL-8 were expressed in a strain, time, and dexamethasone dependent manner. Interleukin-6 and interleukin-8 expressions by hMSCs were induced by cyclic tensile strain

and osteogenic differentiating media, indicating that IL-6 and IL-8 may be functioning as autocrine signals during osteogenic differentiation of hMSCs.

# 10 Melt Spun Microporous Fibers Using Poly (Lactic acid) and Sulfopolyester Blends for Tissue Engineering Applications

In studies described in the preceding chapters, hMSCs were cultured in three-diemnsional collagen matrices to determine their osteogenesis under chemical and mechanical stimuli. While Type I collagen enhances adhesion and proliferation of hMSCs, its structural instability due to high contraction by hMSCs continuously poses a challenge for creating large tissue constructs that may be needed to treat crtitical bone defects. Therefore, scaffolds fabricated using other polymeric materials and techniques need to be investigated to find an alternative to collagen. Most techniques used for scaffold fabrication result in porous three-dimensional scaffolds; however, they still lack the diffusional properties to allow sufficient and uniform media flow throughout the scaffold leading to loss of cell viability in some regions. Therefore, scaffolds with higher diffusional properties are needed to maintain uniform cell viability and also to enhance angiogenesis. This chapter described the study on the use of binary polymer blends to create microporous fibers that can be used to fabricate three-dimensional nonwoven scaffolds with increased diffusional properties.

## 10.1 Introduction

Apart from biocompatibility, bioresorption, and mechanical stability, three-dimensional scaffolds for tissue engineering applications require increased diffusional properties to allow flow of culture media throughout the scaffold leading to uniform cell growth.[190, 191] Scaffolds fabricated using polymeric fibers provide controllability of strength, pore size, and porosity as well as controllability of bioresorption rate.[2] However, increased thickness of three-dimensional scaffolds is limited by decreased media diffusion to the center of the scaffolds. Successful development of three dimensional tissue constructs will be governed by the availability of scaffolds with greater diffusional properties.

Nonwoven structures with their inherent porosity and random fiber arrangement can be tailored to mimic the extracellular matrix of a tissue and thus are regarded as a suitable source for tissue-engineering scaffolds. Although nonwoven structures possess fiber interstices and pores that could create channels for media flow, increases in thickness of these structures could create barriers to media flow in the transverse direction. Replacement of solid fibers with microporous hollow fibers or fibers consisting of microchannels to fabricate nonwoven scaffolds would greatly enhance their diffusional properties. Hollow fibers can be spun using existing bicomponent fiber technology. However, creation of micropores on fiber surfaces or microchannels in fibers poses a challenge, hence this should be addressed first.

Previous studies have shown that polyester can be physically modified to create pores by adding 0.2- 2% of dry process silica with an average primary particle size of 0.1 μm[192] or 0.4 - 5% of colloidal $CaCO_3$ with a size of 0.02 - 0.3 μm[192] or 0.5 - 5% of kaolinite.[192] In

addition, chemical substances such as 3% Na alkanesulfonate, 1% Na magnesium dicarboxybenzene-sulfonate and a 1.2% mixture of polyethylene glycol and C12 - 13 alkanesulfonic acid sodium salt added to polyester result in better pore formation during treatment with alkali after spinning. In the case of polyolefins, the crystallization characteristics of the polymer alone can be utilized to form micropores. Micropores that extend from the surface to the interior of the fiber can be created using a combination of heat and draw steps during spinning of polyolefins.[192] Fatty acid systems such as oleic acid, linoleic acid or soybean mixtures have been added as diluents to polypropylene (PP). By controlling the temperature of the coagulation bath, a thermally induced phase separation takes place and the mobility of the diluent determines the size of the micropores within the PP spherulite.[193] The use of liquid paraffin and polybutene as diluent agents in PP has been explored.[192] Similar to PP, it is possible to process polyethylene (PE) with diluents as plasticized melt. Mixtures of high density polyethylene (HDPE) with 2-butoxyethyl oleate, BU stearate or bis(2-ethylehexyl) phthalate can be spun into hollow fibers and made microporous by cooling with iso-propanol and leaching in ethanol.[192] However to date the use of a hydrolysable polymer blended with a more stable polymer to create micropores in the fibers have not been fully investigated.

The purpose of this study was to investigate the use of a hydrodispersible polymer, sulfopolyester as a minor phase dispersed in a poly(lactic acid) matrix, to create micropores in PLA/sulfopolyester composite fibers. A compounder was used to blend PLA with sulfopolyester at different proportions in the molten state and melt extrude fibers. The resultant fibers were analyzed for their thermal properties and localization of sulfopolyester

in composite fibers. The sulfopolyester was removed from the composite fibers by hydrodispersion and the resultant fibers were microscopically analyzed for the presence of pores.

## 10.2 Materials and Methods

### 10.2.1 Preparation of polymers

Poly(lactic acid) (PLA) (Nonwovens Corporative Research Center, North Carolina State University, Raleigh, NC) in granule form and water dispersible sulfopolyester (AQ; batch number: E011-053, Eastman Chemical Company, Kingsport, Tennessee,) in flake form were stored in desiccators and vacuum dried prior to use. The weight average molecular weight of AQ was 20000.

### 10.2.2 Characterization of polymers

#### 10.2.2.1 Differential scanning calorimetry

Thermal properties of the PLA and AQ polymers were measured by differential scanning calorimetry (DSC) using a PerkinElmer Diamond DSC (PerkinElmer Life and Analytical Sciences, Shelton, CT) equipped with Pyris software (V5.0). Approximately 3-5mg of polymer flakes were placed in an aluminum pan (volatile) that was subsequently sealed using a press. The PLA polymer samples were heated from room temperature to 200 $^0$C at 20 $^0$C/min, held for 4 minutes at 200 $^0$C and then cooled from 200 $^0$C to 25 $^0$C at 20 $^0$C/min to obtain glass transition temperature, premelt, and melt points for each specimen. The AQ polymer samples were heated from 25 $^0$C to 350 $^0$C at 20 $^0$C/min and 25 $^0$C to 100 $^0$C at 20 $^0$C/min to determine thermal transition points. The glass transition temperature, premelt onset temperature, melt peak temperature and heat of fusion were measured using

Perkin Elmer Pyris software V5.0. The degree of crystallinity was calculated using Equation 10.1.[194] Three DSC scans were run for each sample to calculate average and standard deviation of each parameter.

$$\text{Degree of Crystallinity} = \frac{\Delta H_m - \Delta H_C}{\Delta H_{m\,(100\%)}} \qquad (10.1)$$

Where, $\Delta H_{m\,(100\%)}$ = 93.6 J/g for 100% crystalline PLA [19, 195]

$\Delta H_m$ = Measured enthalpy of melting

$\Delta H_c$ = Measured enthalpy of crystallization

### 10.2.2.2 Thermogravimetric analysis

The decomposition temperature and thermal stability of AQ at extrusion temperature was measured using a Pyris 1 thermogravimetric analyzer (TGA) (PerkinElmer Life and Analytical Sciences, Shelton, CT) equipped with Pyris V5.0 software. Approximately 10 mg of AQ polymer samples were used to measure the decomposition temperature and thermal stability. For determining decomposition temperature, AQ samples were heated from 25 $^0$C to 950 $^0$C at 30 $^0$C/min. The thermal stability of AQ was measured by heating polymer samples from 25 $^0$C to 200 $^0$C at 50 $^0$C/min and holding at 200 $^0$C for 30 minutes.

### 10.2.2.3 Fourier Transform Infrared Spectroscopy (FTIR)

In order to build reference spectra of PLA and AQ, both 100% PLA and 100% AQ polymers were scanned using a Fourier Transform Infrared Spectrophotometer (Nicolet Model 510P) fitted with an attenuated total reflectance (ATR) attachment and a deuterated triglycine sulfate (DTGS) detector. A total of 64 scans were aggregated between 600 and 3000 $cm^{-1}$ with each spectrum at 2 $cm^{-1}$ resolution. The bands in the spectra were analyzed using OMNIC v7.2 software.

### 10.2.2.4 Viscosity average molecular weight

The viscosity average molecular weight of PLA was measured using intrinsic viscosity of PLA in chloroform. Reduced specific viscosity of PLA solutions (Equation 10.2)[196] having concentrations of 0.02, 0.04, 0.06, 0.08 and 0.10 g/dL were measured using an Ubbelohde viscometer at 25 $^0$C and plotted against concentration of PLA solutions (Huggins plot)[196] to obtain intrinsic viscosity of PLA in chloroform (Equation 10.3).[196] The viscosity average molecular weight of PLA was calculated using the Mark-Houwink equation (Equation 10.4).[196-198]

$$\text{Reduced specific viscosity} = \left(\eta/\eta_0 - 1\right)/C \qquad (10.2)$$

Where, $\eta$ = Solution viscosity

$\eta_0$ = Solvent viscosity

C = Concentration of solution (dL/g)

$$\text{Intrinsic viscosity} = [\eta] = \lim_{C \longrightarrow 0} \ln\left(\eta/\eta_0\right)/C \qquad (10.3)$$

$$\text{Intrinsic viscosity} = [\eta] = KM^{\alpha} \qquad (10.4)$$

Where K and α are Mark-Houwink constants and M is the viscosity average molecular weight. For PLA in chloroform at $25^0$C, K= $5.45 \times 10^{-4}$ and α = 0.73.[197]

### 10.2.3 Filament extrusion

Blending of PLA and AQ was carried out at their molten state. Briefly, PLA was ground to particle form and physically mixed with varying proportions of sulfopolyester to obtain 99%PLA/1%AQ, 97%PLA/3%AQ, 95%PLA/5%AQ and 90%PLA/10%AQ polymer mixtures. The filaments from each polymer mix were extruded using a HAAKE MiniLab micro compounder (Thermo Electron, Newington, NH) (Fig. 10.1) fixed with counter rotating conical twin screws with nitrogen as inert gas. The polymer mix was heated at 175°C with a 10-15 minutes recirculation (residence) time in the micro compounder before extruding through a 0.5 mm orifice fitted externally to the body of the compounder. In addition to the above polymer blends, filaments were extruded using 100% PLA and 100% AQ and used as controls. The spinning was followed by hot drawing at a constant draw ratio.

**Figure 10.1.** HAAKE MiniLab micro compounder

### 10.2.4 Hydrodispersion of sulfopolyester from composite fibers

The resultant fibers of 99%PLA/1%AQ, 97%PLA/3%AQ, 95%PLA/5%AQ and 90%PLA/10%AQ were then hydrodispersed for two hours in 50 mL of deionized water using an orbital reciprocating water bath (Boekel Scientific, Feasterville, PA) at 70 $^{0}$C and 140 rpm and subsequently in an ultrasonicator (Cole-Parmer Instrument Company, Chicago, IL) at 70°C. Fibers were then dried in a vacuum oven for 24 hrs at 55 °C.

### 10.2.5 Analysis of composite fibers

#### 10.2.5.1 Minor phase morphology

Morphology of the AQ minor phase in PLA/AQ fiber blend was studied by analyzing the melt viscosity data acquired from the mini compounder. The viscosities of both 100%

PLA and 100% AQ were used to calculate the viscosity ratio, i.e. the viscosity of the dispersed phase (AQ)/ the viscosity of the matrix (PLA). These ratios were plotted against time to determine the behavior of minor phase (AQ) in the PLA matrix during resident (blending) time in the micro compounder.

### 10.2.5.2 Differential scanning calorimetry

The thermal properties of the composite fibers were measured by differential scanning calorimetry (DSC) using a PerkinElmer Diamond DSC (PerkinElmer Life and Analytical Sciences, Shelton, CT) equipped with Pyris software (V5.0) as described previously. Approximately 3-5mg of composite fiber was placed in an aluminum pan (volatile) that was subsequently sealed using a press. The composite fiber samples were heated from 25 $^0$C to 200 $^0$C at 20 $^0$C/min, held for 3 minutes at 200 $^0$C and then cooled from 200 $^0$C to 25 $^0$C at 40 $^0$C/min to obtain glass transition temperature, premelt and melt points for each specimen. The glass transition temperature, premelt onset temperature, melt peak temperature and heat of fusion were measured using Perkin Elmer Pyris software V5.0. The degree of crystallinity was calculated using Equation 6.1.[194] Three DSC scans were run for each sample to calculate average and standard deviation of each parameter.

### 10.2.5.3 Preparation of composite fiber cross sections

Three fiber samples having an approximate length of 2 inches were cut randomly along the length of each extruded composite filament. The fibers from each composite

filament were placed in a polyethylene capsule and embedded in a resin using PELCO® Eponate 12T embedding kit (Ted Pella Inc. Redding, CA). The embedding media formulation for soft block preparation was used to create these fiber-embedded blocks. The sample assembly in embedding media was subsequently cured at 60 $^0$C for 24 hours in an air-circulated oven. After 24 hours, the blocks were removed from the capsules and used for preparing fiber cross sections. The resin embedded fiber cross sections with thicknesses of 20 μm and 40 μm were cut using a microtome (Reichert Microscope Services, Depew, NY).

### 10.2.5.4 Fourier Transform Infrared Spectroscopy (FTIR)

In an attempt to detect localization of AQ in the composite fiber cross sections, the 20 μm thick composite fiber cross sections were mapped using a Fourier Transform Infrared Spectrophotometer (Thermo Nicolet Nexus 470) fitted with a Continuμm microscope and a Mercury Cadmium Telluride (MCT) detector. The fiber cross sections were mounted on a mirror and viewed at 150 ×. The microscope was fitted to a motorized stage, which allowed specific areas of the fiber cross sections to be mapped. A point on the mirror was designated as the background point while a map of the area to be scanned on each fiber cross section was created using Atlμs v7.7 mapping software. Three fiber cross sections of unhydrolysed 1% AQ/ 99% PLA and 10% AQ/ 90% PLA fibers were mapped using two different mapping configurations (Fig.2). One cross section from each type of fiber was mapped at center, right, left, top and bottom using an area map having a total area of 169 μm$^2$ (step size 10 μm, number of points in X – axis = 13 and number of points in Y – axis = 13). Two more cross

sections from the same type of fiber were mapped across the fiber diameter using an area map having 60 µm width and length based on the diameter of the fiber (step size 10 µm, number of points in X – axis = 6 and number of points in Y – axis = decided by diameter of fiber). A total of 64 scans in reflectance mode were aggregated between 600 and 3000 $cm^{-1}$ with each spectrum at 2 $cm^{-1}$ resolution. The spectra of both 100% AQ and 100% PLA were analyzed to identify and define a band unique to 100% AQ using OMNIC v7.2 software. This identified band was selected in the acquired spectra of unhydrolysed composite fiber samples to identify the localization of AQ in composite fiber cross sections. The specific localization of AQ was presented in the form of contour (2D) and 3D area maps showing location and intensity of the bands.

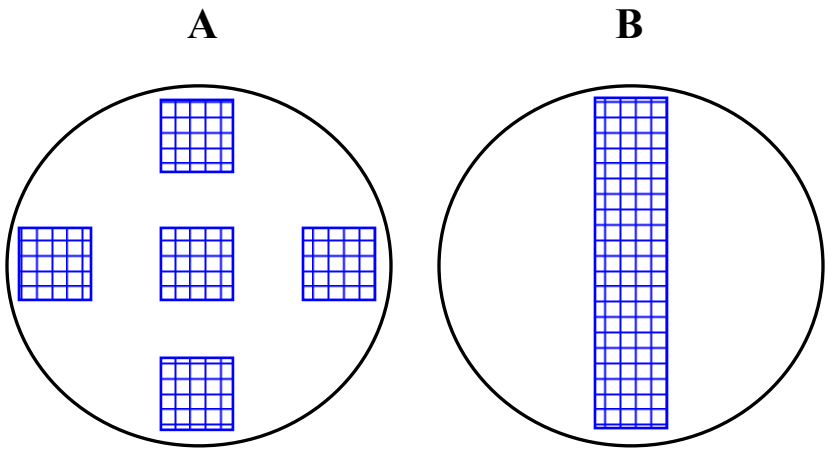


**Figure 10.2.** Arrangement of area maps on 20 µm thick unhydrolized composite fiber cross sections for analysis using mapping function of Fourier Transform Infrared Spectrophotometer. A) Arrangement of maps for the first fiber cross section and B) Arrangement of the map for second and third fiber cross sections of the same fiber.

### 10.2.5.5 Microscopic analysis and pore size measurement

In order to ascertain the extent of hydrolysis and micropores on the fiber surface and throughout fiber cross sections, the surfaces of the hydrolysed and unhydrolysed composite fibers and their 40 μm cross sections were viewed under a scanning electron microscope (SEM). The composite fibers and fiber cross sections were mounted on aluminum stubs using conductive self-adhesive tape (Ted Pella Inc. Redding, CA). Subsequent to mounting, the samples were coated with gold/palladium using a HUMMER 6.2 sputter coating instrument (ANATECH Ltd, Springfield VA) to obtain an average uniform coating thickness of 20 nm. In order to obtain a uniform coating, the samples were coated four times where, after each cycle, they were rotated $90^0$ clockwise. During the fifth coating cycle they were placed flat directly facing the plasma. Images of the coated samples were acquired from a JEOL JSM 5900 Scanning Electron Microscope (JEOL USA, Inc., Peabody, MA) using an accelerating voltage of 15 kV and a spot size of 15 nm. Multiple random micrographs of fiber cross sections were obtained at 1000× and 2500× while fiber surfaces were micrographed at 200×, 2500× and 5000×. The scanning electron micrographs of the fiber surfaces taken at 2500× were used to measure the size of pores on hydrolysed fiber surfaces. Each area analyzed under 2500× amounted to 0.02 $mm^2$ area of the fiber surface. SimplePCI image analysis software (Compix, Inc. Image Systems, Cranberry Township, PA) was used to analyze the images and measure the pore sizes by intensity threshold. The number of pores per $mm^2$ area of the fiber surface was presented as a frequency distribution.

## 10.3 Results

### 10.3.1 Characterization of polymers

#### 10.3.1.1 Differential scanning calorimetry

Results of the DSC measurements of PLA and AQ polymers are presented in Tables 10.1 and 10.2. Corresponding thermograms are shown in Figures 10.3 and 10.4. The thermograms of PLA exhibited a glass transition at 61.93 $^0$C, a pre-crystallization peak near 75 $^0$C, and a melt peak in the range of 163 - 168 $^0$C (Fig. 10.3). Results showed that PLA is a crystalline polymer with a crystallinity 36.04 ± 1.28 %. In contrast, all AQ polymer samples examined had glass transitions at 55.77 $^0$C without a melt peak (Fig.10.4) indicating that AQ was an amorphous polymer.

**Table 10.1.** Crystallinity of PLA using Differential Scanning Calorimetry

| Polymer | | Pre-crystall. temp ($^0$C) | Heat of fusion at crystal., $\Delta H_c$ (J/g) | Melting temp. ($^0$C) | Heat of fusion at melt , $\Delta H_m$ (J/g) | Degree of crystallinity (%) | |
|---|---|---|---|---|---|---|---|
| | | | | | | Average | Stdev |
| PLA | A | None | None | 168.59 | 35.047 | | |
| | B | 75.00 | -2.719 | 163.15 | 35.411 | 36.04 | 1.28 |
| | C | 76.27 | -2.708 | 163.40 | 36.182 | | |

**Table 10.2.** Glass transition temperature of PLA and AQ polymers.

| Polymer | | Onset temperature ($^0$C) | Glass transition temperature ($^0$C) | | |
|---|---|---|---|---|---|
| | | | Expt. value | Average | Stdev |
| PLA | A | 66.37 | 67.06 | 61.93 | 4.58 |
| | B | 58.16 | 58.24 | | |
| | C | 59.61 | 60.49 | | |
| AQ | A | 55.09 | 56.30 | 55.77 | 0.50 |
| | B | 54.22 | 55.70 | | |
| | C | 54.43 | 55.30 | | |

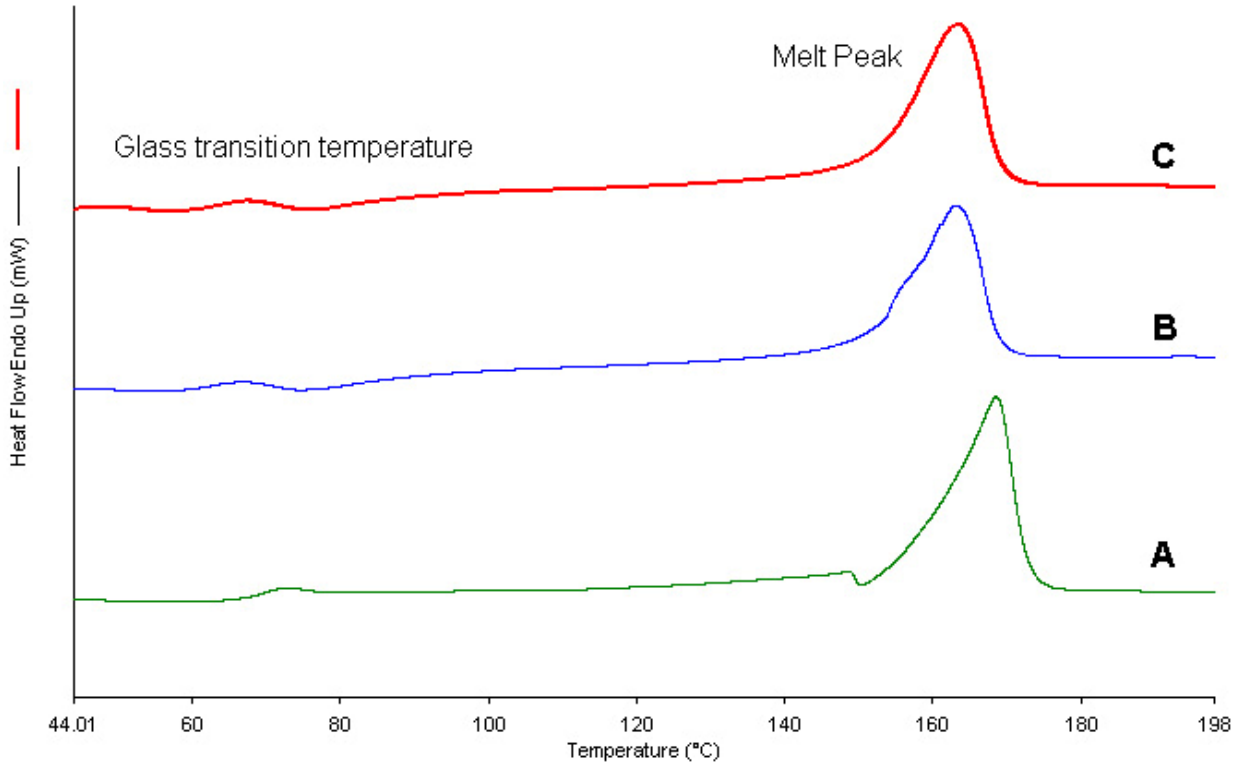


**Figure 10.3.** Differential scanning calorimetry (DSC) thermograms of poly(lactic acid) polymer.

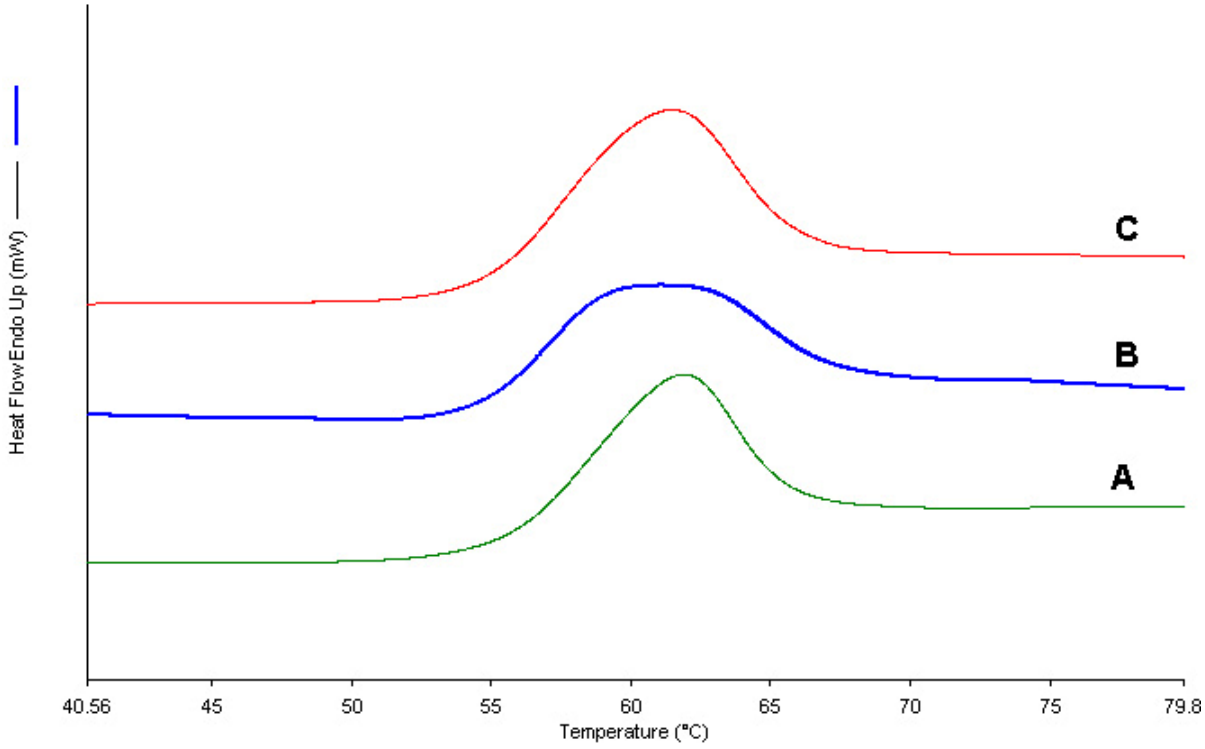


**Figure 10.4.** Differential scanning calorimetry (DSC) thermograms of sulfopolyester (AQ) polymer.

### 10.3.1.2 Thermogravimetric analysis

The TGA thermograms of AQ are presented in Figure 10.5. The major decomposition which accounted for 80% of AQ decomposition occurred between approximately 369 ± 15 $^{0}$C and 539 ± 18 $^{0}$C. Exposure of AQ to 200 $^{0}$C for 30 minutes did not change its composition indicating that AQ could be subjected to melting at 175 $^{0}$C during filament extrusion without any decomposition.

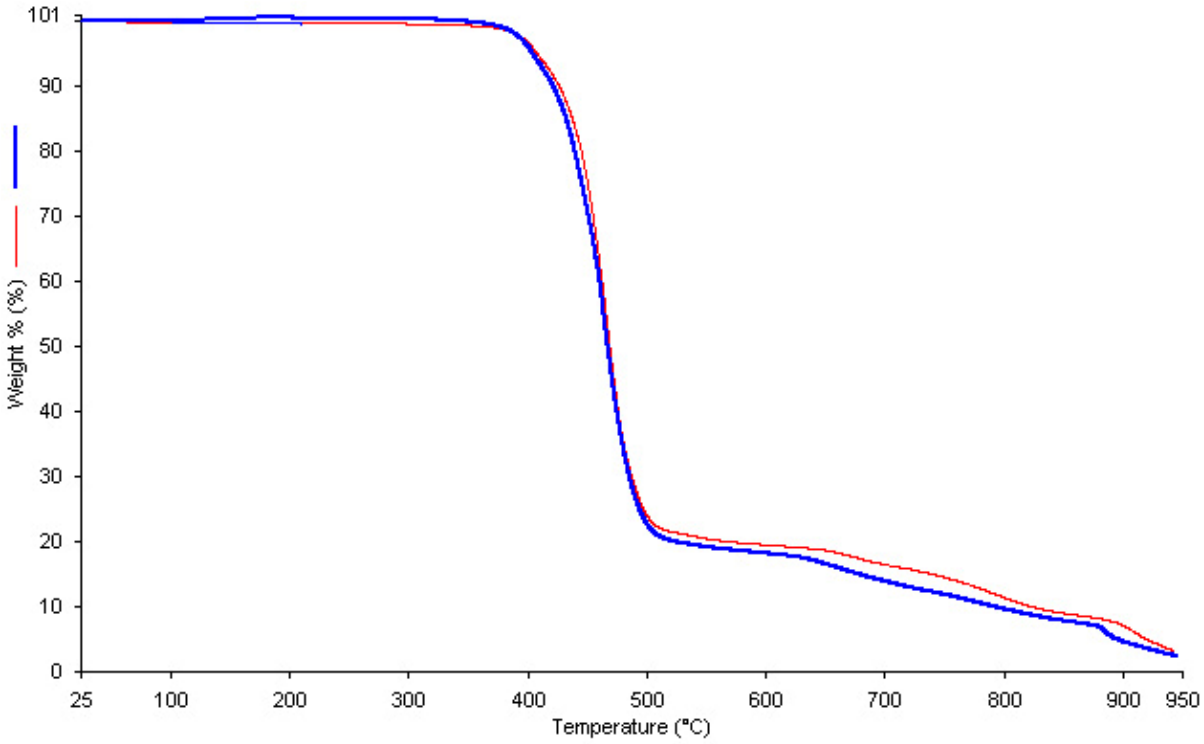


**Figure 10.5.** Thermogravimetric Analysis (TGA) thermograms of sulfopolyester (AQ).

### 10.3.1.3 Fourier Transform Infrared Spectroscopy (FTIR)

Fourier Transform Infrared Spectra of 100% PLA and 100% AQ polymers are presented in Figure 6. The FTIR spectra of 100% PLA polymer had bands typically observed in PLA. The spectra consisted of an aliphatic C-H stretching region between 3000 and 2850 $cm^{-1}$ (not, shown), C=O stretching band at 1752 $cm^{-1}$ and asymmetric stretching vibrations of

$$\begin{matrix} & & O & & \\ & & \| & & \\ C & - & C & - & O \end{matrix} \quad \text{and} \quad O - C - C$$

between 1300 $cm^{-1}$ and 1100 $cm^{-1}$ (Fig.10.6B).[199] In addition, bands characteristic to PLA where also observed at 1268, 1183, 1129, 1086 and 1046 $cm^{-1}$.[199] Similar to PLA, FTIR spectra of 100% AQ polymer consisted of a C=O stretching band at 1717 $cm^{-1}$ (Fig.10.6A). The high intensity band at 1246 $cm^{-1}$ could be assigned to - C– O stretching vibration in complex in-plane ring ester modes[200, 201] while the band at 1098 $cm^{-1}$ could be assigned to symmetric C-C stretching vibrations of glycol groups (Fig.10.6A).[200] The strong band at 726 $cm^{-1}$ of 100% AQ could be assigned to ring CH out of plane deformation. The bands existed in the 1430 – 1330 $cm^{-1}$ range could be due to asymmetric $SO_2$ stretching from sulfonates in AQ polymer (Fig.10.6A).

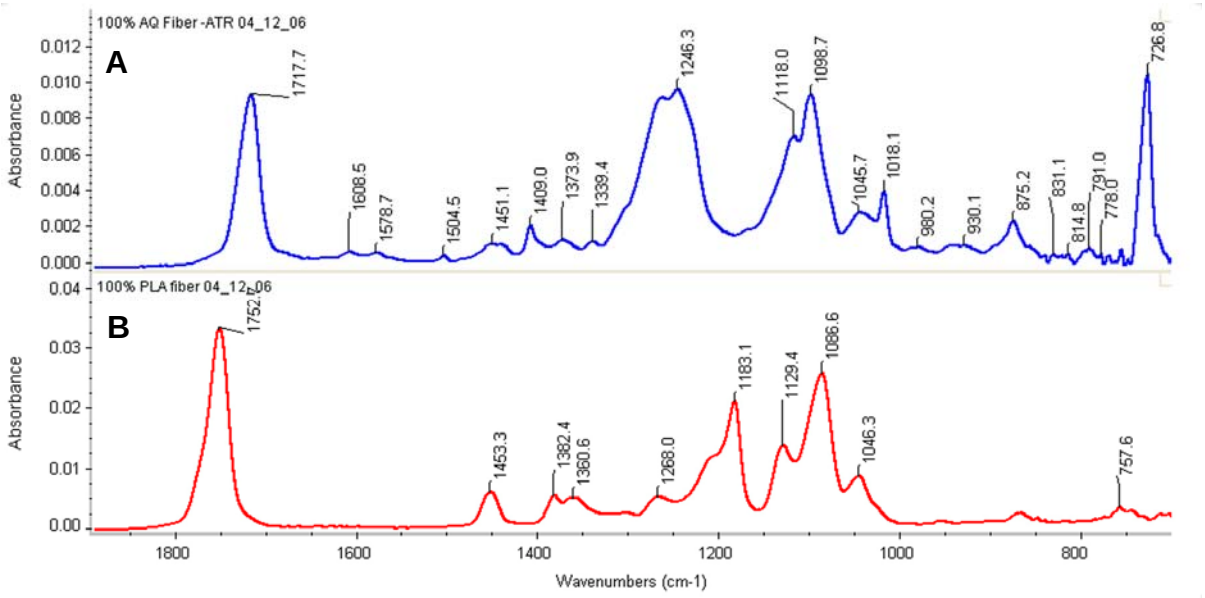


**Figure 10.6.** Fourier Transform Infrared Spectra of 100% sulfopolyester (AQ) (top) and 100% poly (lactic acid) (bottom) polymers.

### 10.3.1.4 Viscosity average molecular weight

The Huggins plot (reduced specific viscosity vs. concentration of polymer solution) is presented in Figure 10.7. According to this plot, the intrinsic viscosity of PLA was 1.88 dL/g and the viscosity average molecular weight of PLA calculated using Mark-Houwink equation was approximately 70000.

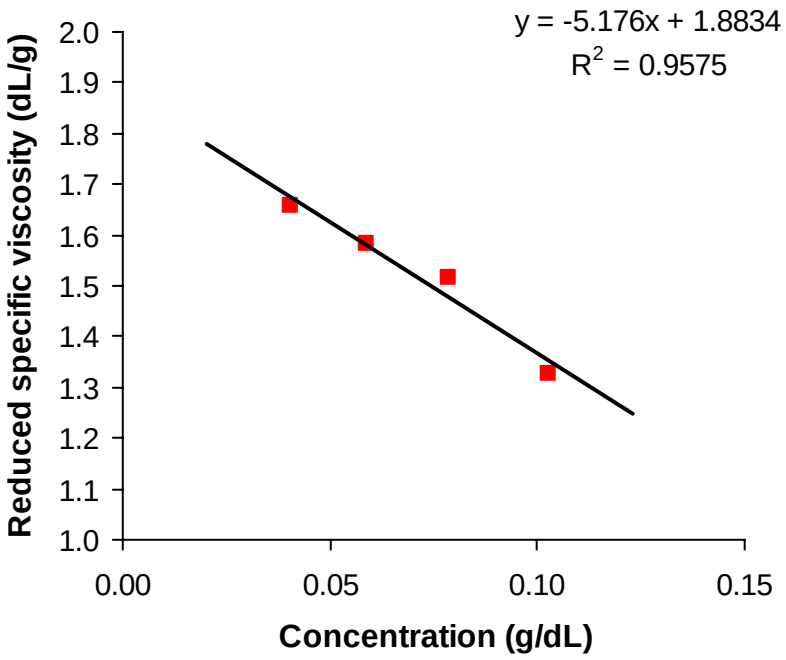


**Figure 10.7.** Huggins plot of PLA in chloroform at 25 $^{0}$C.

### 10.3.2 Analysis of composite fibers

#### 10.3.2.1 Minor phase morphology in AQ/PLA blend

The initial melt viscosity of both pure polymers and PLA/AQ polymer blends (Fig. 10.8) decreased during mixing. The melt viscosity of both polymers observed after 2 minutes of resident time in the mini compounder showed that 100% PLA had a higher melt viscosity than that of 100% AQ. The calculated torque ratio (torque of the dispersed phase/torque of the matrix) using torques of 100% PLA and 100% AQ remained below 1 during the mixing period (Fig. 10.9).

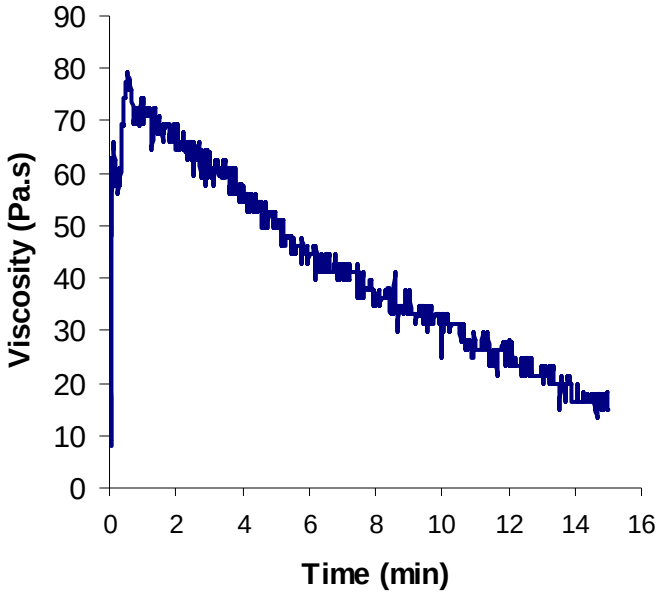


**Figure 10.8.** Change in melt viscosity of 1% AQ/99% PLA during mixing

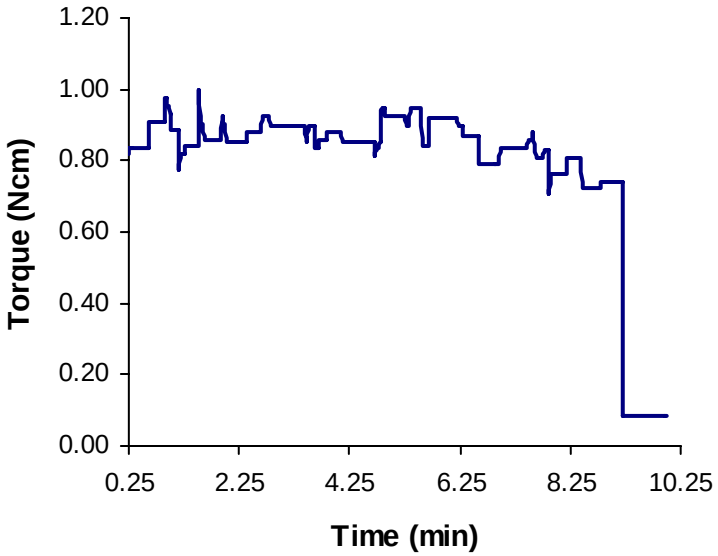


**Figure 10.9.** Change in torque ratio of 100% PLA and 100% AQ

### 10.3.2.2 Differential scanning calorimetry

The glass transition temperatures of all unhydrolysed fibers are presented in Table 10.3. Corresponding thermograms are presented in Figure 10.10. The pre-crystallization and melt results of unhydrolysed 100% PLA and composite fibers are presented in Table 4 with their corresponding thermograms in Figure 10.11. All unhydrolysed composite fibers and 100% PLA showed a glass transition temperature around 55 $^{0}$C while glass transition temperatures of unhydrolysed 100% AQ fibers were lower (Table 10.3). A secondary glass transition in addition to the main glass transition was observed in 10% AQ/90% PLA composite fibers. Except for 100% AQ fibers, all other unhydrolysed fibers showed a pre-crystallization exotherm and a melt endotherm (Table 10.4). The melt endotherm of all fibers

consisted of a split peak (Fig. 10.11). The percent crystallinity calculations revealed that the extruded 100% PLA and composite fibers were amorphous (Table 10.4).

**Table 10.3.** Glass transition temperatures of unhydrolysed pure and composite fibers

| Fiber | Glass transition temperature ($^0$C) | |
|---|---|---|
| | Average | Stdev |
| 100% AQ | 43.88 | 0.94 |
| 100% PLA | 55.55 | 0.25 |
| 1% AQ/ 99% PLA | 56.23 | 0.52 |
| 3% AQ/ 97% PLA | 55.43 | 0.53 |
| 5% AQ/ 95% PLA | 55.50 | 0.09 |
| 10% AQ/90% PLA | 54.92 | 0.30 |

**Table 10.4.** Differential scanning calorimetric data of unhydrolysed 100% PLA and composite fibers

| Fiber | Mean Pre-crystall. temp ($^0$C) | Heat of fusion at crystal., $\Delta H_c$ (J/g) | Mean Melting temp. ($^0$C) | Heat of fusion at melt , $\Delta H_m$ (J/g) | Crystallinity (%) | |
|---|---|---|---|---|---|---|
| | | | | | Average | Stdev |
| 100% PLA | 115.62 | -37.32 ± 1.54 | 163.61 | 37.05 ± 0.58 | Amorphous | |
| 1% AQ/ 99% PLA | 116.41 | -38.07 ± 1.84 | 163.82 | 38.32 ± 1.81 | 0.30 | 0.23 |
| 3% AQ/ 97% PLA | 116.77 | -38.99 ± 0.88 | 161.16 | 36.75 ± 0.44 | Amorphous | |
| 5% AQ/ 95% PLA | 113.25 | -39.11 ± 0.52 | 162.42 | 39.20 ± 0.63 | Amorphous | |
| 10% AQ/90% PLA | 115.62 | -37.32 ± 1.54 | 163.61 | 37.06 ± 0.58 | 0.91 | 0.97 |

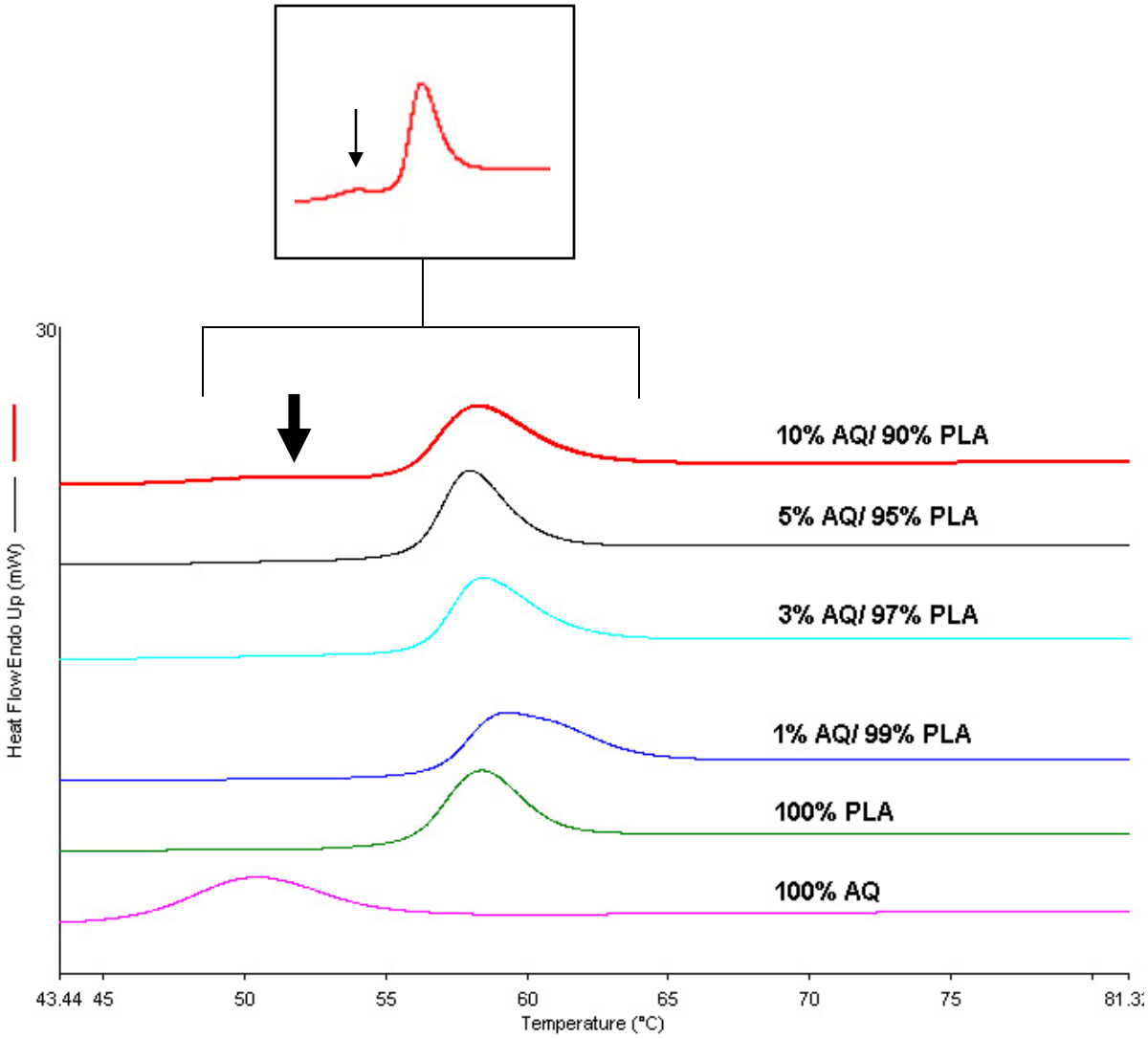


**Figure 10.10.** Glass transitions of unhydrolysed pure and composite fibers. The arrow indicates a secondary glass transition in 10% AQ/90% PLA composite fibers.

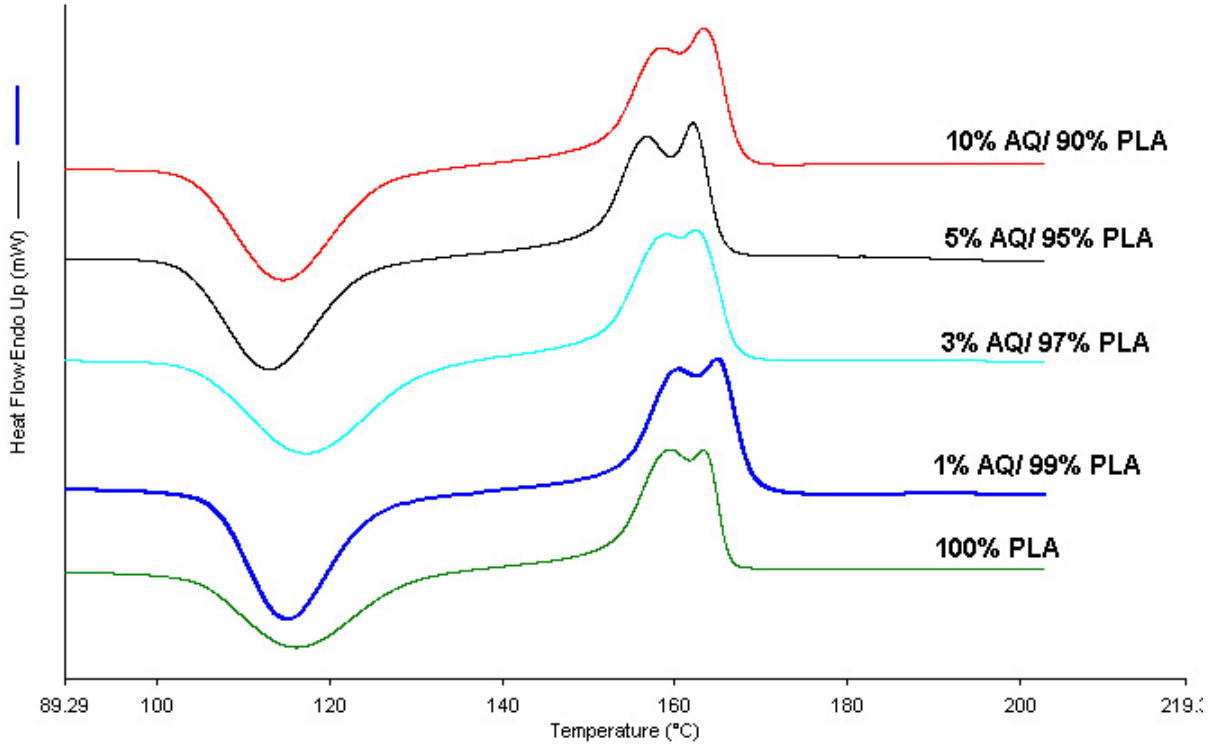


**Figure 10.11.** Representative pre-crystallization exotherms and melt endotherms of unhydrolysed 100% PLA and composite fibers.

### 10.3.2.3 Fourier Transform Infrared Spectroscopy (FTIR)

The FTIR band at 1717.7 $cm^{-1}$ which corresponds to C=O stretching[199] in 100% AQ polymer was used to detect the localization of AQ polymer in composite fiber cross sections (Fig. 10.12). Analysis of peak heights of 1717.7 $cm^{-1}$ band using 2D contour maps and 3D maps showed that AQ polymer was more randomly distributed throughout the composite

fiber cross section in fibers with 10% AQ than those with 1% AQ content. The contour maps (Figs. 10.13 and 10.14) and 3D spectral images (Figs. 10.15 and 10.16) of 10% AQ/ 90% PLA fiber cross sections at random locations (Figs. 10.14 and 10.15) and across the fiber diameter (Fig. 10.16) revealed that the peak height of 1717.7 $cm^{-1}$ band was over 1.0 at most locations. In contrast, contour maps (Fig. 10.17) and 3D spectral images (Figs. 10.18 and 10.19) at random locations (Figs. 10.17 and 10.18) and across the fiber diameter (Fig. 10.19) of 1% AQ/ 99% PLA fiber cross sections showed that peak height of 1717.7 $cm^{-1}$ band was lower than 0.75 at most locations. Compared to 10% AQ/ 90% PLA fibers, 1% AQ/ 99% PLA fibers had AQ localized either at the center or at the edges of the fiber (Fig. 10.17). The maximum peak height of 1717.7 $cm^{-1}$ band at these locations was 1.1 (Figs. 10.18 & 10.19). Additional 3D maps are presented in Appendix I.

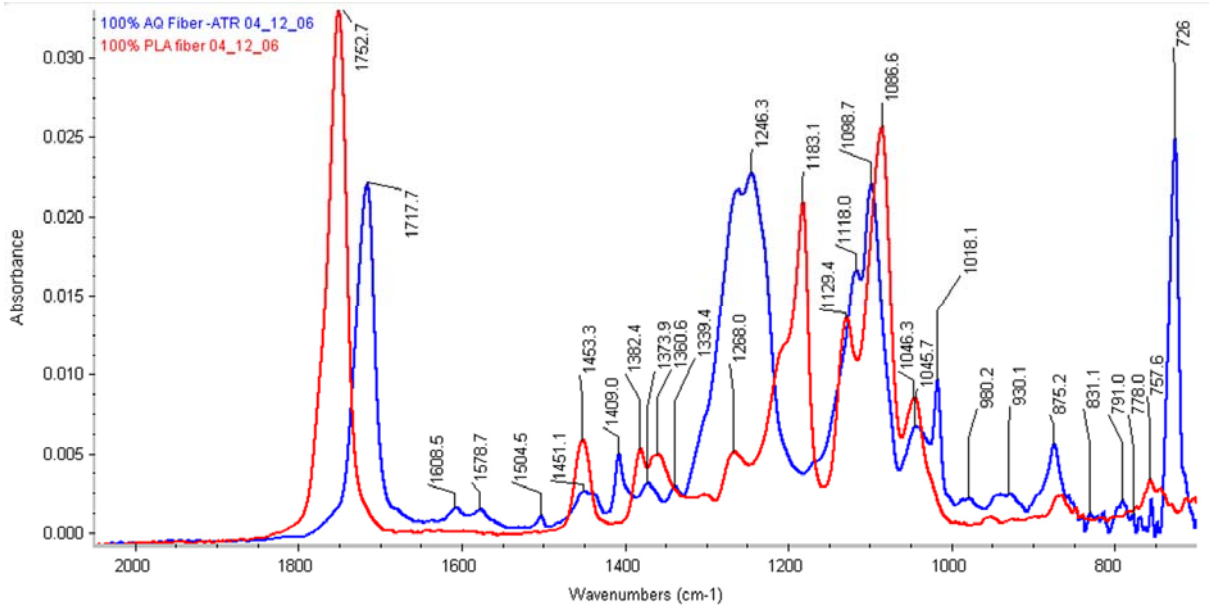


**Figure 10.12.** Overlapped Fourier Transform Infrared Spectra of 100% PLA and AQ polymers.

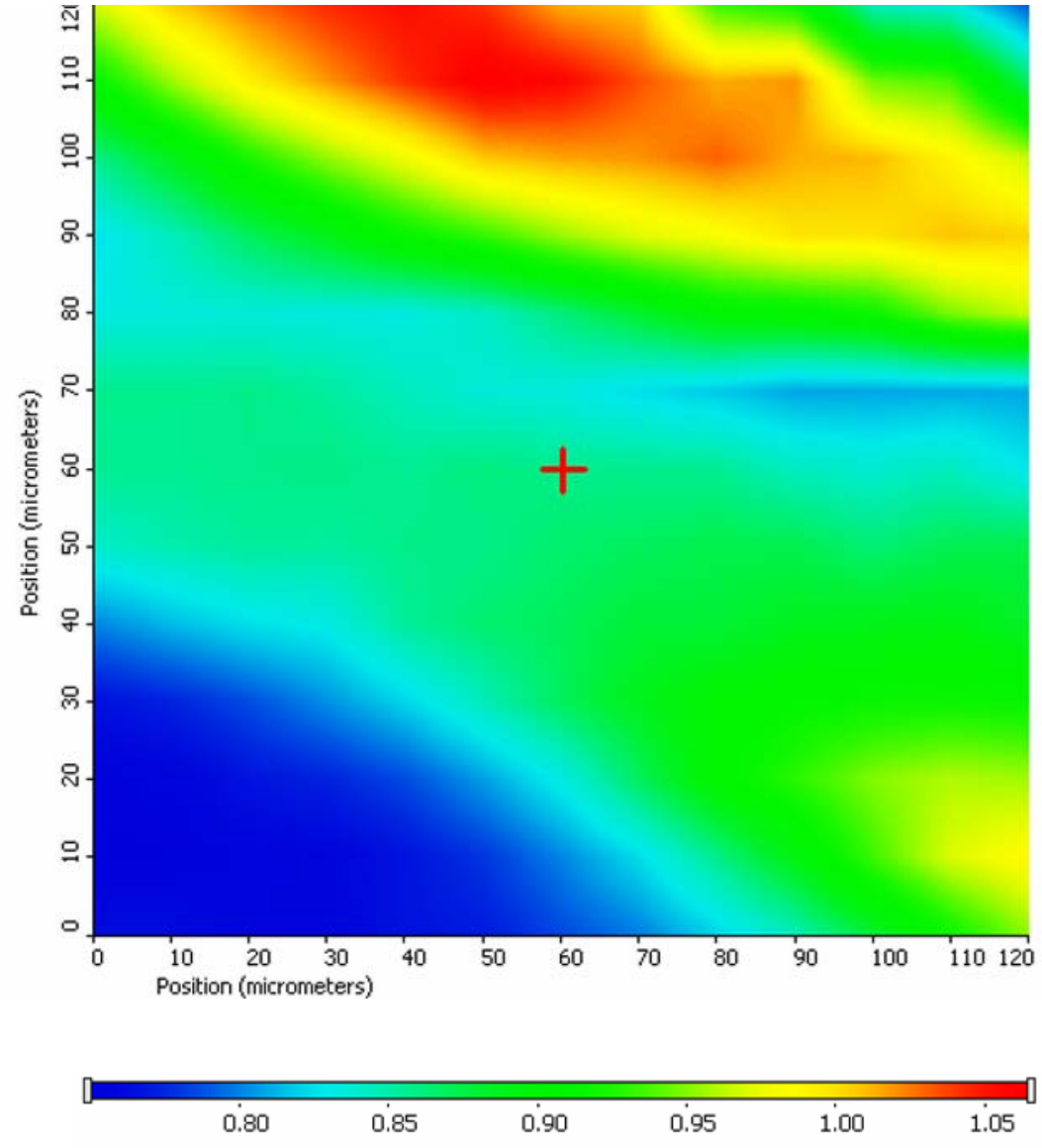


**Figure 10.13.** Contour map showing variation in peak height of 1717.7 cm-1 band indicative of sulfopolyester localization at the center region of an unhydrolysed 10% AQ/ 90% PLA composite fiber cross section. The rainbow bar shows the corresponding colors for the variation of peak intensity.

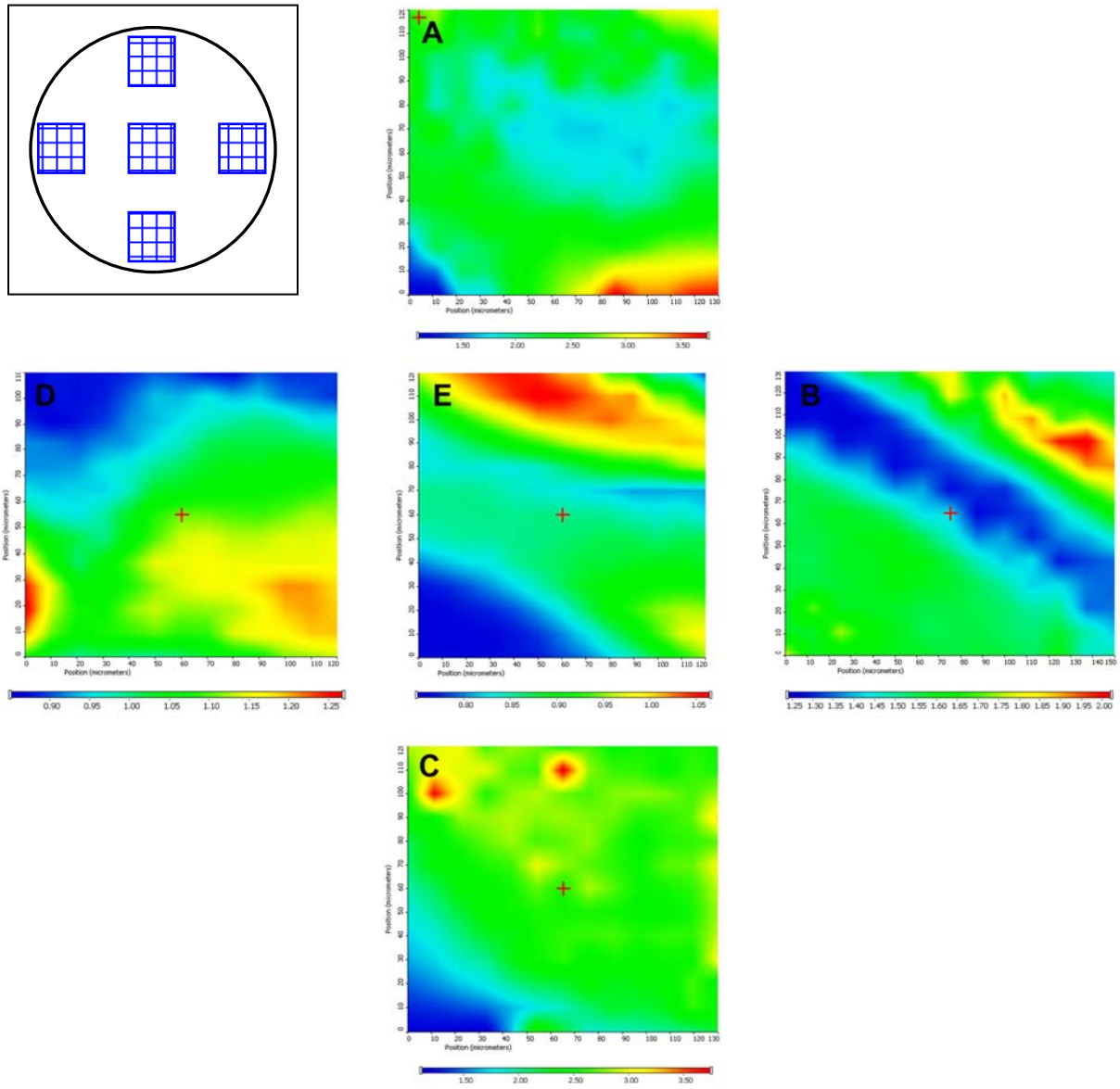


**Figure 10.14.** Contour maps showing the variation in peak height of 1717.7 cm-1 band indicative of localization of sulfopolyester in regions of an unhydrolysed 10% AQ/ 90% PLA composite fiber cross section. A) Top edge, B) Right edge, C) Bottom edge, D) Right edge and E) Center of the fiber. Inset: Corresponding areas mapped on the fiber cross section. The rainbow bar shows the corresponding colors for the variation of peak height.

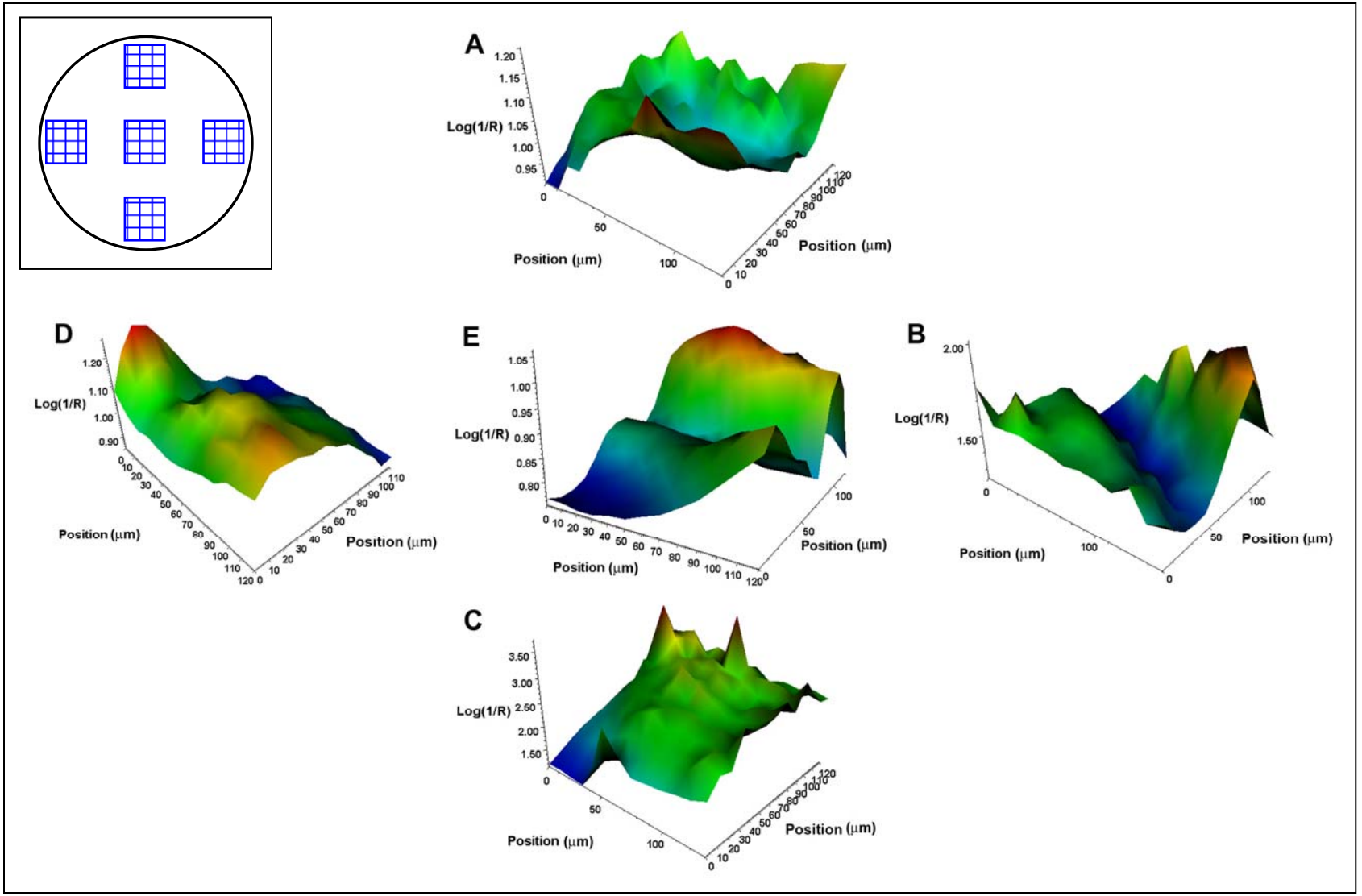


**Figure 10.15.** Three-dimensional (3D) Fourier Transform Infrared maps showing the variation in peak height of 1717.7 cm-1 band (localization of sulfopolyester; AQ) at different areas of unhydrolised 10% AQ/ 90% PLA composite fiber cross section. A) Top edge, B) Right edge, C) Bottom edge, D) Left edge and E) Center of the fiber. Inset: Corresponding areas mapped on the fiber cross section.

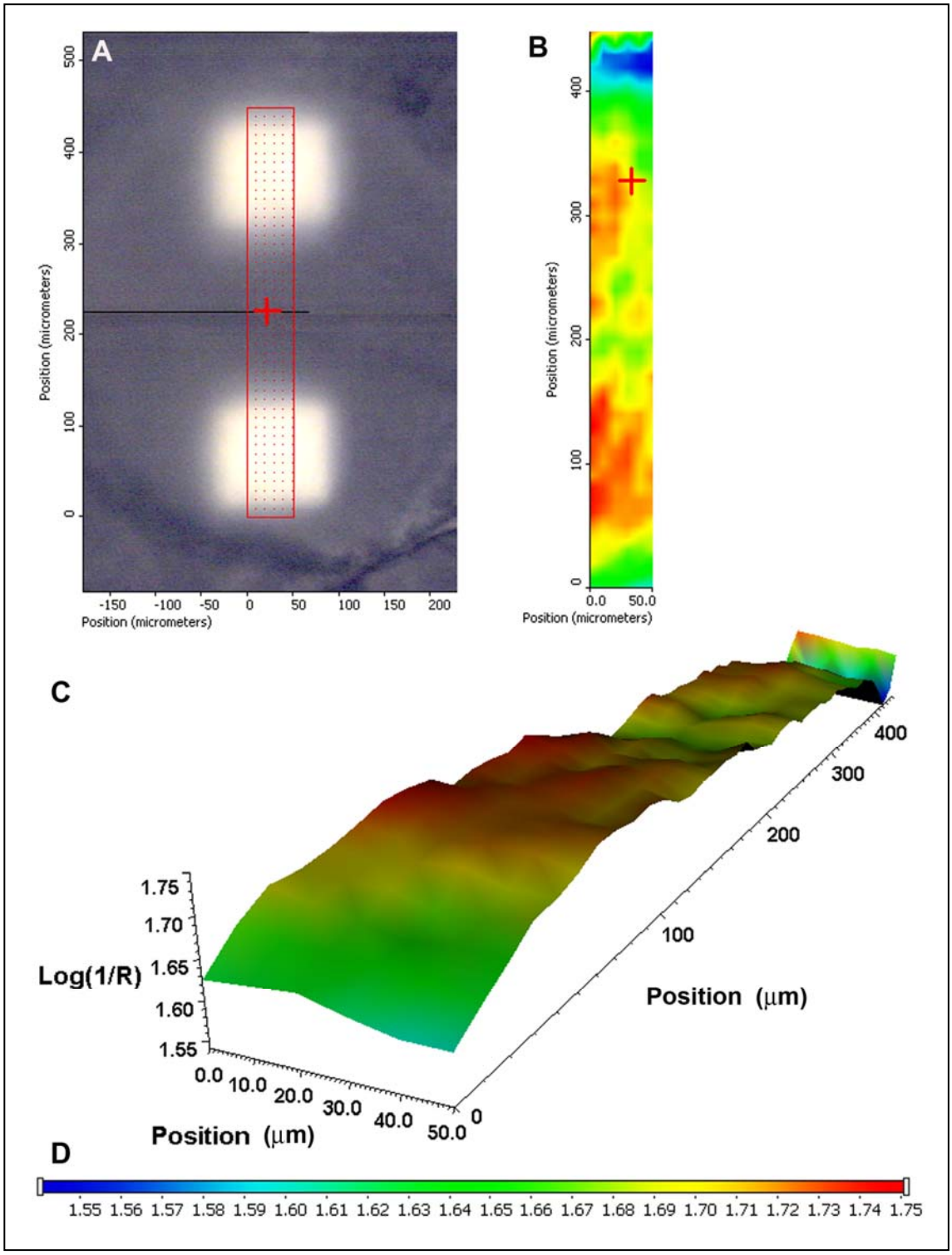


**Figure 10.16.** Variation in peak height of 1717.7 cm-1 band (localization of sulfopolyetser; AQ) across the diameter of an unhydrolysed 10% AQ/ 90% PLA composite fiber. A) Video image of the mapped area; red grid shows the scanned points, B) Contour map with intensity gradients, C) 3D image and D) Rainbow bar showing color assignment for peak heights.

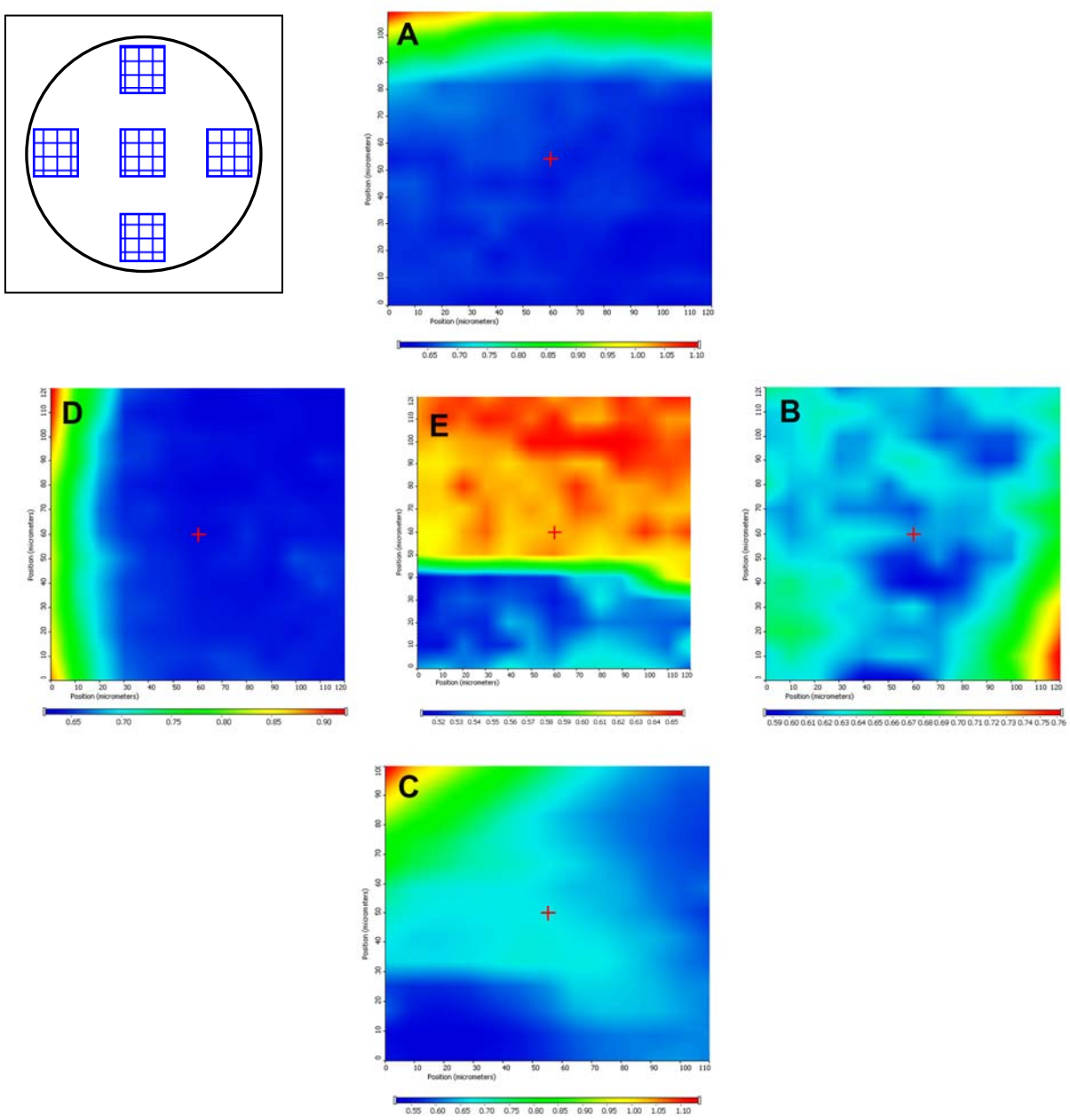


**Figure 10.17.** Contour maps of peak intensity at 1717.7 cm-1 indicative of localization of sulfopolyester in regions of an unhydrolysed 1% AQ/ 90% PLA composite fiber cross section. A) Top edge, B) Right edge, C) Bottom edge, D) Left edge and E) Center of the fiber. Inset: Corresponding areas mapped on the fiber cross section. The rainbow bar shows the corresponding colors for the variation of peak intensity.

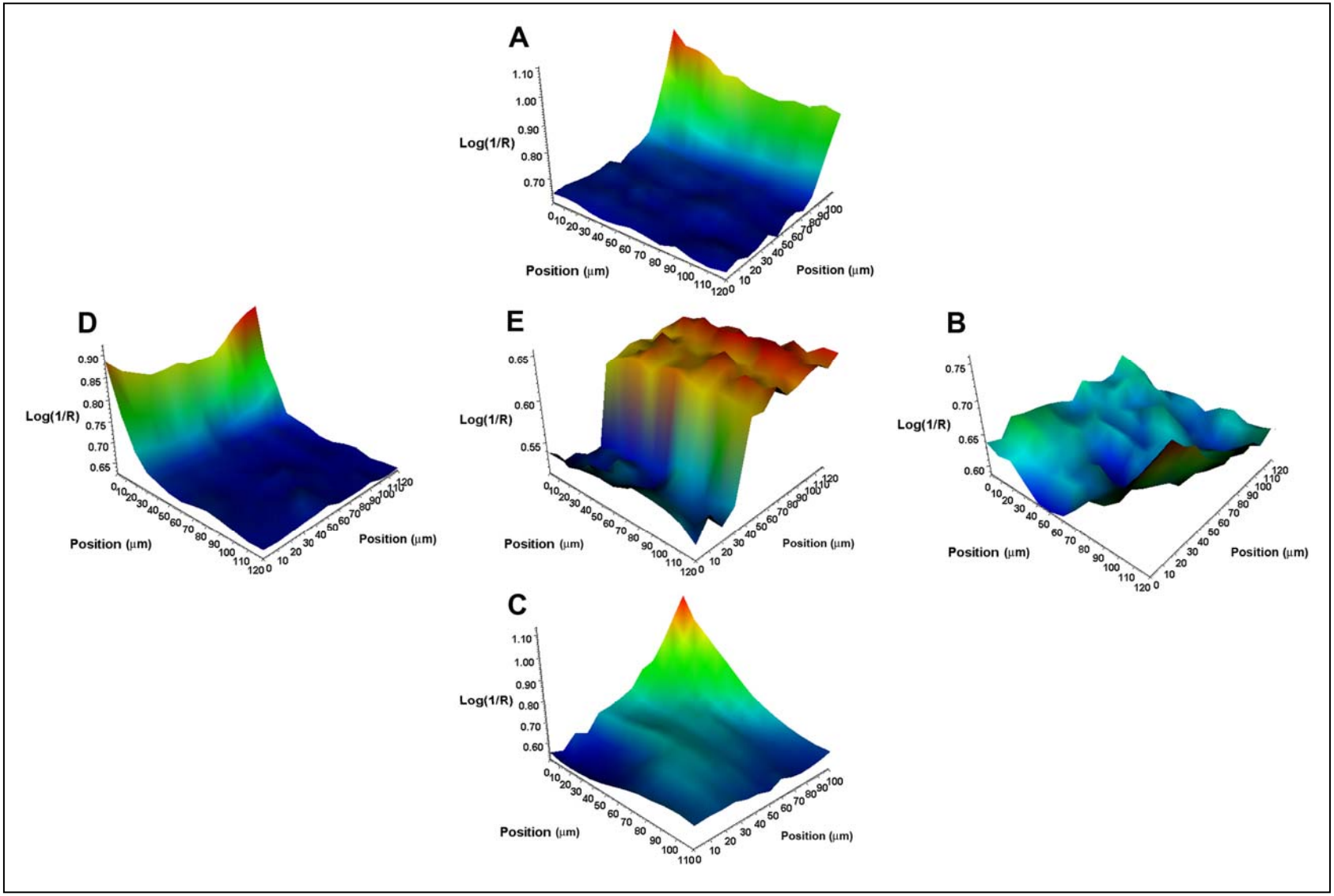


**Figure 10.18.** Three dimensional (3D) Fourier Transform Infrared maps showing peak height of 1717.7 cm-1 (localization of sulfopolyester; AQ) in different areas of unhydrolised 1% AQ/ 90% PLA composite fiber cross section. A) Top edge, B) Right edge, C) Bottom edge, D) Left edge and E) center of the fiber. Inset: Corresponding areas mapped on the fiber cross section.

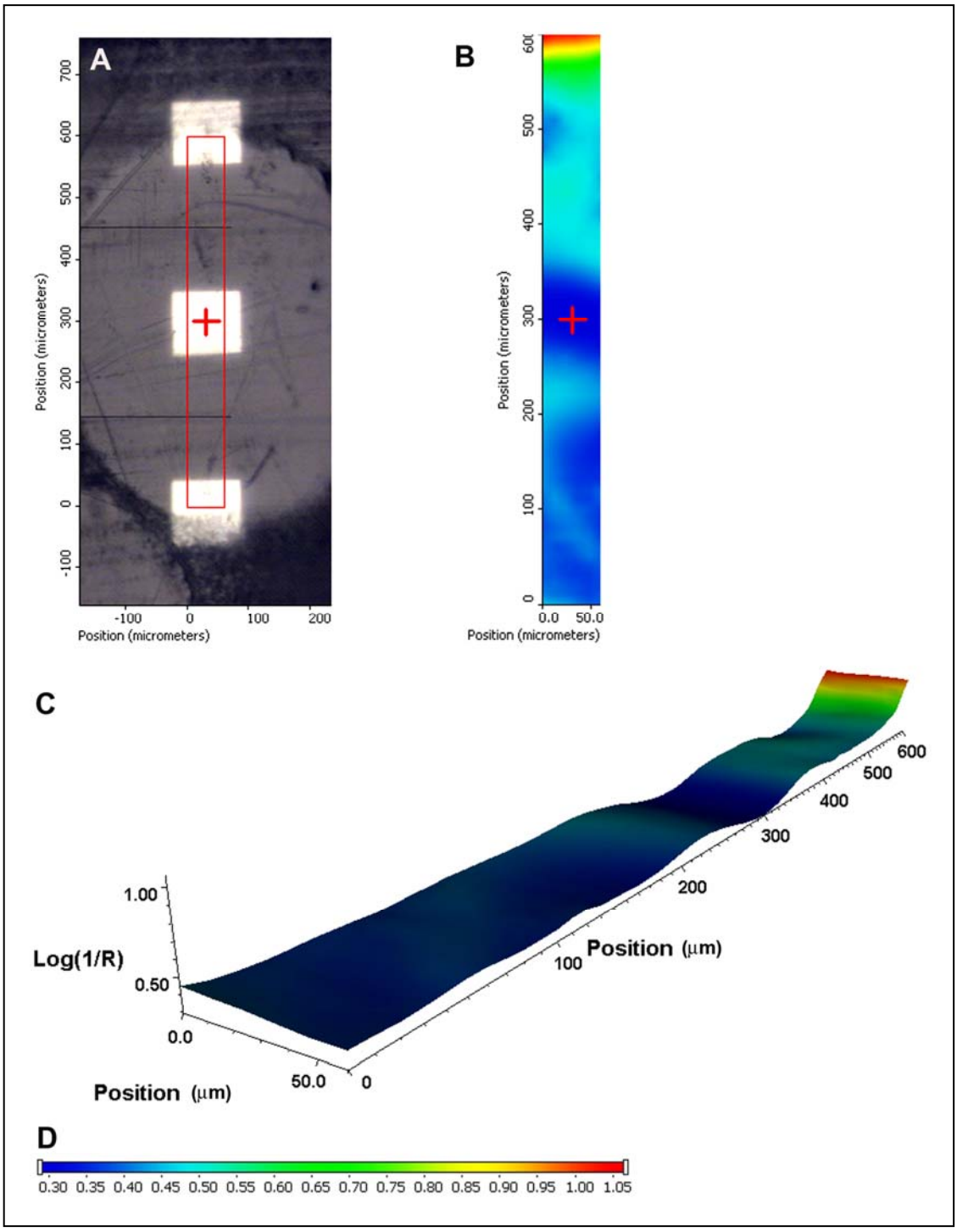


**Figure 10.19.** Variation in peak height of 1717.7 cm-1 band indicating sulfopolyester (AQ ) localization across the diameter of an unhydrolysed 1% AQ/ 90% PLA composite fiber. A) Video image of the mapped area; red grid shows the scanned points, B) Contour map with intensity gradients, C) 3D image and D) Rainbow bar showing color assignment for peak heights.

### 10.3.2.4 Microscopic analysis and pore size measurement

Scanning electron micrographs of unhydrolysed/hydrolysed 100% PLA and composite fiber surfaces and their 40 μm cross sections are presented in Figures 10.20 to 10.22. The micropores on composite fiber surfaces caused by hydrolysis of AQ were visible in all composite fibers at all compositions (Fig. 10.20). Analysis of micrographs revealed that the pores were randomly distributed over the fiber surface irrespective of the percentage of AQ used in composite fibers. Scanning electron micrographs of these pores obtained at higher magnification showed the depth of the pores and their continuation into the fiber (Fig. 10.21) Although micropores were not observed in 1% AQ/ 99% PLA fiber cross sections (Fig. 10.22), fibers with 3%, 5% and 10% AQ/ 90% PLA (Fig. 10.22) showed randomly distributed pores in their cross sections. The majority of the pores in composite fibers with less than 10% AQ content had areas below 1 $\mu m^2$ while composite fibers with 10% AQ content had a significant number of pores with areas greater than 1 $\mu m^2$ (Fig. 10.23).

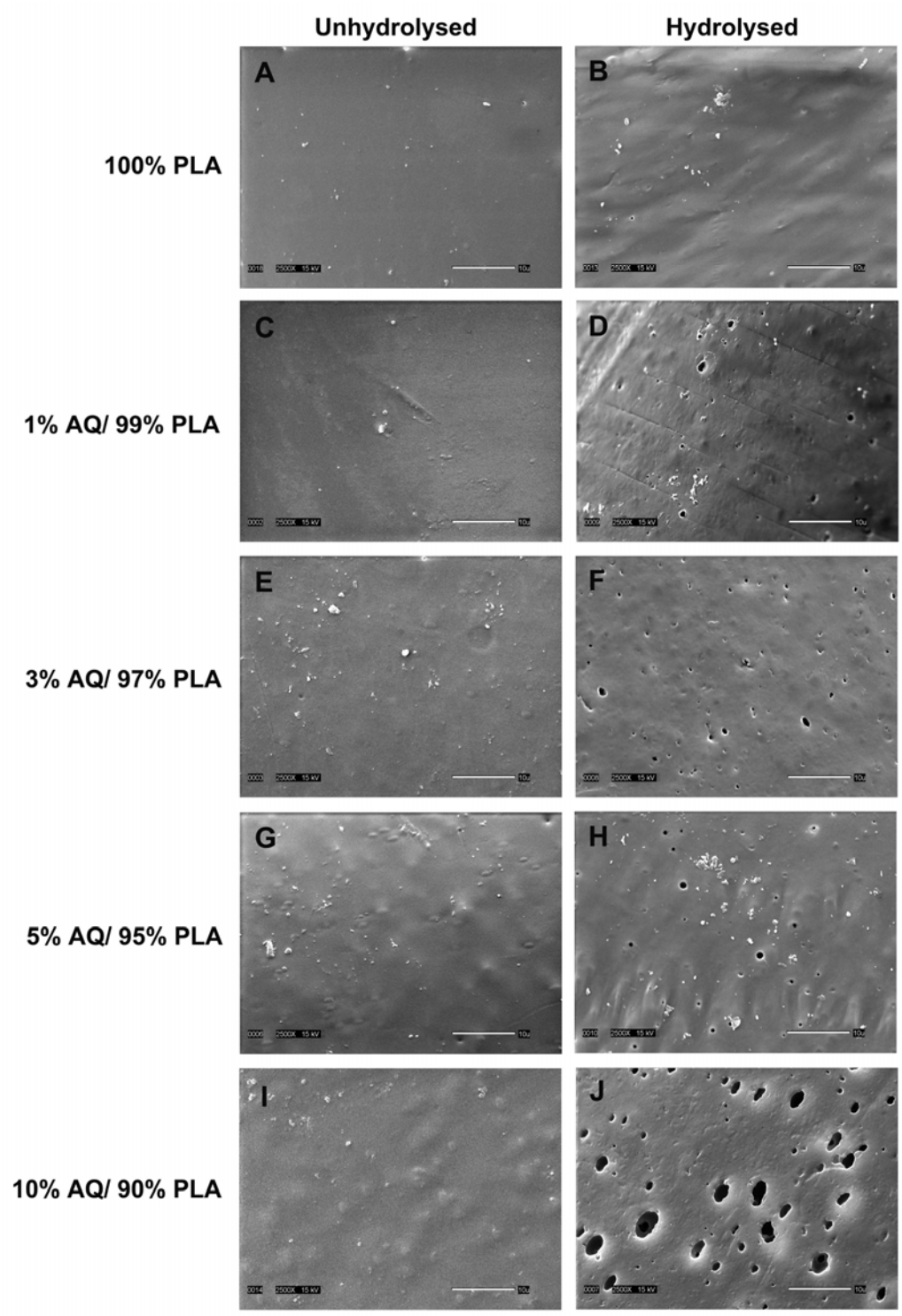


**Figure 10.20.** Scanning electron micrographs of unhydrolysed (A, C, E, G and I) and hydrolysed (B, D, F, H and J) 100% PLA and composite fibers. Mag.: 2500×

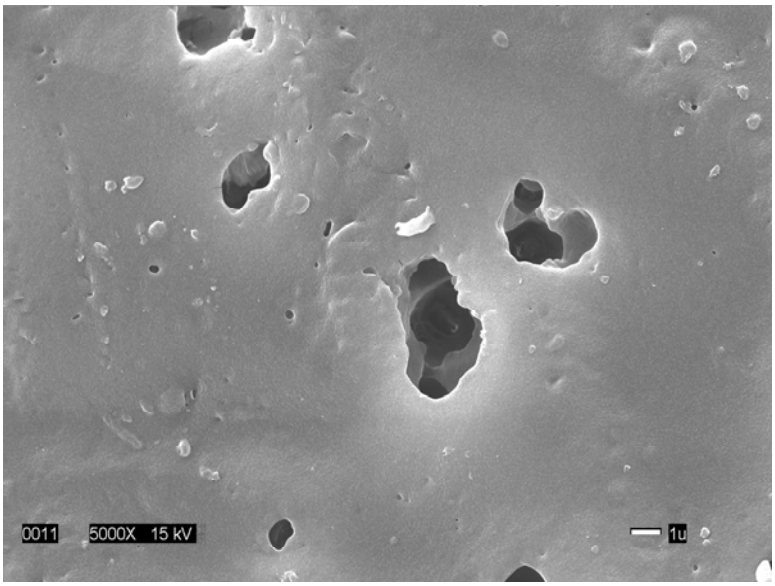


**Figure 10.21.** Scanning electron micrograph of hydrolysed 10% AQ/ 90% PLA fiber aquired at a magnification of 5000 × showing micro pores that continue deep into the fiber.

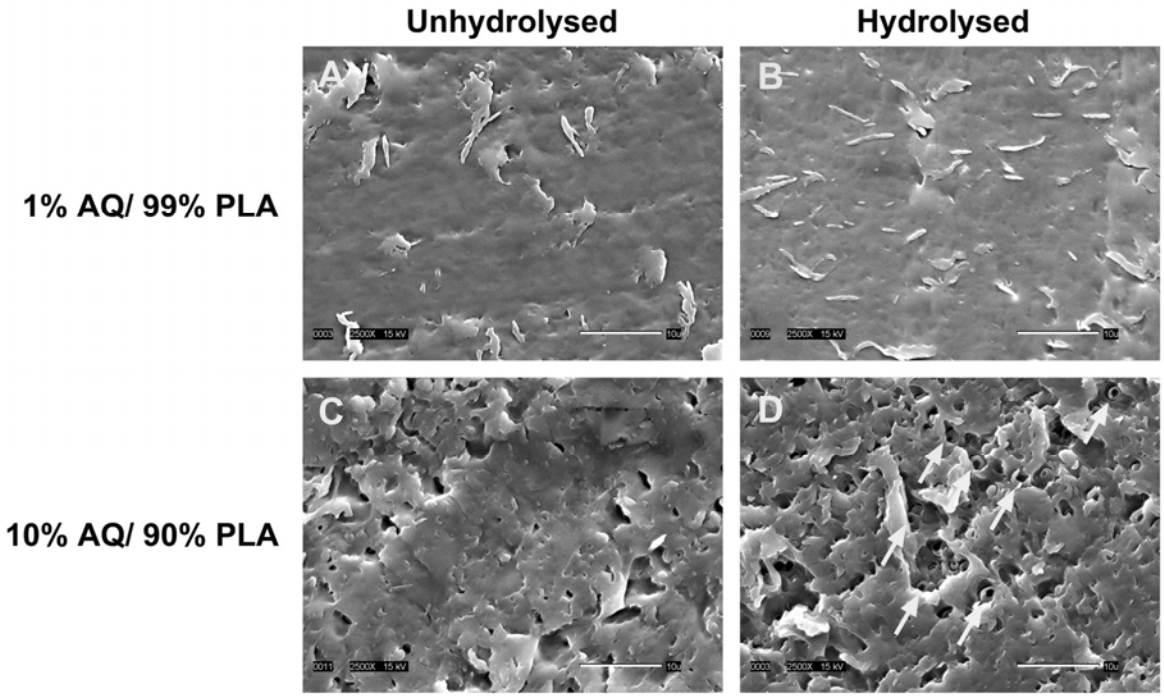


**Figure 10.22.** Scanning electron micrographs of 40 μm thin sections of unhydrolysed (A and C) and hydrolysed (B and D) composite fibers. A, B) 1% AQ/ 99% PLA and C, D) 10% AQ/ 90% PLA composite fibers. Micropores on hydrolysed fiber cross sections are indicated by arrows. Magnification: 2500×

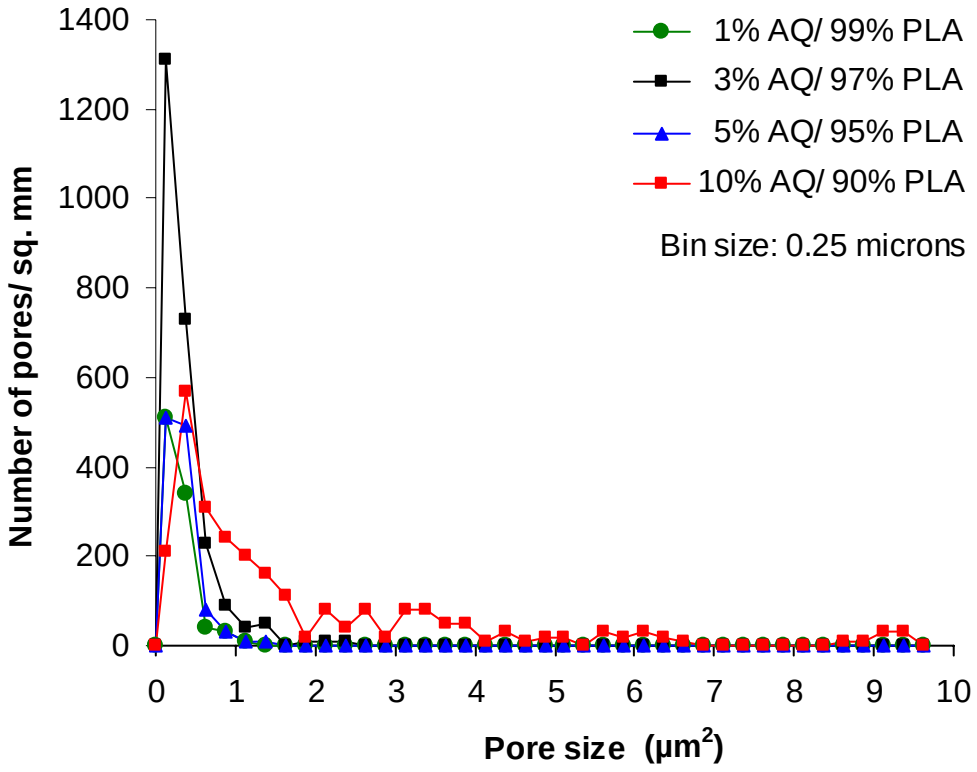


**Figure 10.23.** Pore size distribution of hydrolysed composite fibers.

## 10.4 Discussion

Three-dimensional scaffolds designed for tissue engineering applications require sufficient porosity to maintain continuous diffusion of culture media for uniform cell growth and proliferation throughout the scaffold.[190] Although scaffolds fabricated using nonwoven structures provide a high degree of porosity in both the lateral and longitudinal direction of the structure, increased thickness of the scaffold would still reduce the degree of porosity and detrimentally affect diffusion of culture media to the center of the scaffold. Therefore, it is important to investigate means of improving diffusional properties of polymeric scaffolds for tissue engineering applications.

Increase of liquid transfer properties along the longitudinal and lateral directions of a nonwoven structure can be accomplished using two methods. The first is the use of microporous hollow fibers[202] to fabricate nonwoven structures. The hollow fibers would improve media diffusion in the longitudinal direction of the structure while micropores on the hollow fiber walls would allow media diffusion in the transverse direction of the structure. This configuration would significantly increase the final diffusional properties of the structure in both directions. The second method consists of generating micropores that run as channels inside the fibers with their pore openings on the surface of the fiber. These continuous micropores and channels in fibers would also increase media diffusional properties in the longitudinal and transverse directions of the structure. The first stage of developing either microporous hollow fibers or fibers containing micro channels is to determine an appropriate method of creating random and well-distributed micropores on fiber surfaces.

In this study, we have investigated the use of a hydrodispersible polymer combined with a more stable polymer to develop micro porous fibers via a melt extrusion process. A hydrodispersible polymer, sulfopolyester (AQ) was blended at molten state with PLA and melt-extruded to produce filaments having 1% AQ/99% PLA, 3% AQ/97% PLA, 5% AQ/ 95% PLA and 10% AQ/90% PLA composite fibers. The AQ components of these composite fibers were removed by a short hydrodispersing stage followed by ultrasonication at 70 $^0$C. Characterization experiments revealed that unprocessed PLA polymer with a viscosity average molecular weight of 70333 consists of a glass transition temperature at 61.9 ± 4.6 $^0$C and a crystallinity of 36.0 ± 1.3%. In contrast, sulfopolyester (AQ) was observed to be amorphous with a glass transition temperature at 55.8 ± 0.5 $^0$C. The stability of AQ at prolonged exposure to 175 $^0$C during filament extrusion was confirmed using thermogravimetric analysis. The DSC analysis showed that the melt extrusion process resulted in completely amorphous 100% PLA and composite fibers. The hydrodispersion of AQ created random pores with varying size on the composite fibers. There was a clear increase in size of micropores in 10% AQ/90% PLA fibers compared to other composite fibers. The FTIR mapping of composite fiber cross sections revealed a random dispersion of AQ in the PLA matrix. This random dispersion of AQ in the PLA matrix was more prominent in fibers with 10% AQ than those with 1% AQ fibers.

Previous studies have reported the use of dissolvable additives to form micropores in fibers. Dry silica or colloidal $CaCO_3$ has been added to create pores in polyesters.[192] Chemical additives such as Na alkanesulfonate, Na magnesium dicarboxybenzene-sulfonate, and a mixture of polyethylene glycol and C12 - 13 alkanesulfonic acid sodium salt has also been reported to create pores when added to polyester.[192] Use of a secondary polymer to

create micropores in a fiber has not been fully investigated. A secondary polymer having comparable thermal properties to the matrix polymer could be used to create micropores in the resultant fibers via melt spinning. In such a binary polymer blend, the morphology of the minor phase achieved during melt mixing would delineate the size and the arrangement of pores in the fiber. Previous studies have shown that the final morphology of the minor phase depends on; 1) Viscosity or torque ratio, 2) Composition, 3) Shear stress and 4) Interfacial characteristics between the two polymers.[203]

Previous investigations have shown that the minor component would be finely and uniformly distributed if it has a lower viscosity than the major component.[203] Avgeropolous et al.[204] and Karger-Kocsis et al.[205] reported that the particle size of the minor phase increased with viscosity ratio (calculated as torque ratio). Favis et al.[206] showed that the size of the minor phase was reduced below a torque ratio of 1 with a minimum particle size appearing at a torque ratio of 0.15. In the present study, the torque ratio between 100% AQ and 100% PLA remained below 1 during which mixing took place. This indicated that AQ (minor component) was uniformly distributed in the PLA matrix during mixing and a fine particle size could be achieved using the present processing protocol. The sulfopolyester used in this study was highly hydrodispersible allowing easy removal from the composite fiber.[207] The compatible thermal properties of AQ and PLA created an intimate but phase separated mixture to create a hybrid composite fiber. This random dispersion of AQ in the PLA matrix resulted in well-distributed, discrete micropores in the fibers. As shown by the FTIR studies, AQ was localized more randomly throughout the fiber cross sections in composite fibers with 10% AQ than those with 1% AQ. The glass transition temperature of both AQ and PLA polymers decreased after melt extruding them into fibers. This indicated a microstructural

change in both polymers during the extrusion process, which could have created more micro voids leading to increased chain mobility and thus a decrease in glass transition temperature. The glass transition temperature ($T_g$) of composite fibers was higher than that of 100% AQ fibers but similar to that of 100% PLA polymer. The $T_g$ of composite fibers behaved according to the $T_g$ of a typical polymer blend with the measured values similar to calculated values by the Fox equation ($1/T_g = w_1/T_1 + w_2/T_2$; $w_1$, $w_2$, $T_1$ and $T_2$ are weight fractions and pure component glass transitions of PLA and AQ fibers).[208] The DSC thermograms of composite fibers showed a single glass transition temperature, especially at low AQ contents, indicating a miscible blend between PLA and AQ.[208, 209] However, it is also possible that at low content of AQ (≤ 10%) in composite fibers, the glass transition of the composite fibers was not affected by AQ. It has been shown that the $T_g$ of pure components should differ by at least 20 $^0$C in order to resolve and distinguish them in thermograms.[208] This accounts for a minimum of 10% to 20 wt% of the minor component (AQ) in the composite fiber. In the present study, presence of a very weak transition at temperatures closer to $T_g$ of AQ fiber was observed in the DSC endotherms of 10% AQ/ 90% PLA fibers indicating a partial miscibility of PLA and AQ at 10% AQ content in the composite fibers.[208] Depression of the melting point during blending of crystalline with amorphous polymers has been reported by other authors.[210] However, in the present study, a depression of the melting point was not observed, indicating that the AQ content used in composite fibers was not sufficient to create a significant effect on melting. Unlike previous studies[209] in the present study, there was no considerable change in the crystallization temperature of composite fibers compared to that of the extruded 100% PLA fibers. The melt endotherm of composite fibers consisted of a split peak, which indicated the presence of two types or sizes of crystals [211, 212] However,

with the high crystallization exotherm that existed in DSC thermograms, these extruded composite fibers were observed to be amorphous. The extrusion process and minimum drawing of fibers after extrusion may have caused the extruded fibers to be amorphous. In addition, it has also been shown that crystalline lamellae have a tendency to thicken via partial melting and reorganize at the heating rates provided in the DSC experiment.[213] This phenomenon could be another reason to observe multiple melt endotherms in composite fibers in the present study.

Localization of AQ in the PLA matrix was determined using FTIR mapping technique. Compared to unhydrolysed 1% AQ/99% PLA fibers, the locations where AQ was highly concentrated were randomly distributed in 10% AQ/90% PLA fibers. This was clearly indicated by the randomly distributed high intensity areas of 1717.7 $cm^{-1}$ band in unhydrolised 10% AQ/90% PLA fiber cross sections. The highly concentrated areas of AQ in unhydrolysed 1% AQ/99% PLA fibers were located at either the core or perimeter of the composite fibers. This indicated that 1% AQ content was not sufficient to obtain a randomly distributed minor phase in PLA and AQ polymer blends with the spinning conditions used in this study.

Scanning electron microscopy studies showed that it was possible to create micropores by hydrodispersing the AQ component in the composite fibers using the protocol presented in this study. Both fiber surface and cross sections consisted of randomly distributed pores with varying sizes. The pore size distribution was dependent on the AQ content in the composite fibers where larger pores were observed with 10% AQ content than with others fibers. It has been reported that in an immiscible polymer blend, a wide range of sizes and shapes could be obtained for the dispersed phase (minor phase) during

processing.[203] These shapes that range from submicron to a hundred microns could be spherical, ellipsoidal, cylindrical, ribbonlike, co-continuous and subinclusion types.[203] A spherical dispersed phase of AQ would result in a random distribution of pores on the fiber surface after hydrodispersion while a co-continuous phase of AQ would create continuous microchannels in the hydrodispersed fiber. In the present study, SEM analysis showed the presence of micropores on both the fiber surface and fiber cross sections of hydrodispersed composite fibers. This indicated that the AQ was dispersed in PLA matrix either in a spherical (droplet) or co-continuous morphology. However, recent investigations on PE-PS blends have shown that a ratio of 50/50 blend is required to maintain a stable co-continuous structure[214], which instigate doubts on our observations of a co-continuous morphology in PLA/AQ blend.

In summary, we have investigated the use of sulfopolyester as a minor phase and PLA as a major phase in a multiphase polymer blend to create micropores in melt extruded AQ/PLA composite fibers. Thermal analysis using DSC showed that a partial miscibility could be obtained between PLA and AQ polymers using the extrusion protocol used in this study. Random dispersion of AQ throughout AQ/PLA fiber cross sections was evident by FTIR studies. This random distribution of AQ was more prominent in fibers with 3%, 5% and 10% AQ than fibers with 1% AQ. The micropores observed on both fibers and fiber cross sections indicated that AQ was dispersed in PLA either in a droplet or co-continuous phase morphology. The size of micropores was affected by the AQ content in composite fibers.

These results show that micropores can be successfully created in fibers using a blend of sulfopolyester and PLA and hydrodispersing sulfopolyester from the resultant fibers. This

technology can be used to create microporous hollow fibers or fibers with microchannels. Nonwoven scaffolds fabricated using these fibers for tissue engineering applications may have increased media diffusional properties allowing uniform cell growth throughout the scaffold.

## 10.5 Summary

Functional tissue engineering requires three-dimensional scaffolds with increased porosity to create three-dimensional tissues. Microporous fibers can be used to increase diffusional properties of three-dimensional nonwoven scaffolds. We have investigated the use of a hydrodispersible polyester; sulfopolyester (AQ) to create micropores in composite fibers containing a blend of AQ and poly(lactic acid) (PLA) at 1%, 3%, 5% and 10% AQ content. Poly (lactic acid) and AQ were blended at 175 $^{0}$C with a resident time of 10-15 minutes in a micro compounder followed by extrusion of composite fibers. Sulfopolyester was removed from the composite fiber using a short hydrolysis step to form micropores in the fibers. Differential scanning calorimetric studies on unhydrolysed composite fibers showed that AQ was partially miscible in PLA. Fourier transform infrared mapping of composite fiber cross sections revealed that AQ was randomly dispersed throughout the cross section where random dispersion depended on the AQ content in composite fibers. Scanning electron micrographs of hydrolysed fibers showed randomly distributed micropores on fiber surfaces. The size of the micropores was dependent on the AQ content in composite fibers. The micropores on the hydrolysed fiber cross sections were observed in fibers with 3%, 5% and 10% AQ indicating that at least 3% AQ content is needed to produce droplet morphology of AQ in these fibers. These results show that AQ can be successfully used in a blend with PLA to produce melt spun microporous fibers to be used in fabricating nonwoven structures with higher diffusional properties that can be used as three-dimensional scaffolds for tissue engineering applications.

# 11 Conclussions and Recommendations for Future Research

## 11.1 Conclusions

Several major factors of functional bone tissue engineering were investigated in this dissertation. This body of work was designed using human MSCs derived from bone marrow as the cell source and 3D Type I collagen matrices as the scaffold material. Both chemical stimuli by means of osteogenic supplements in the culture media and mechanical stimuli by means of cyclic tensile strain were used to induce hMSCs to differentiate down osteogenic pathways. Initial experiments were conducted to determine the effects of uniaxial cyclic tensile strain, hMSC seeding density, culture medium, and culture duration on collagen matrix contraction, hMSC morphology, and orientation in collagen matrices. Separate analyses were performed to determine the effect of strain on bone morphegenetic protein-2 expression by hMSCs and the combined effects of strain and culture medium on the expression of COLI, ALPL, BMP-2 and OCN. While one series of experiments investigated these gene expressions using a low hMSC seeding density of $1.5 \times 10^5$ cells/mL, the other used a higher hMSC seeding density ($3 \times 10^5$ cells/mL). Changes in Young's moduli and ultimate tensile strength of hMSC-seeded collagen matrices exposed to strain and osteogenic culture conditions were also examined. Expression of proinflammatory cytokines by hMSCs was investigated using similar culture conditions. In order to overcome the drawbacks of 3D collagen scaffolds (i.e. limited size and failure due to matrix contraction), an alternative way of fabricating 3D scaffolds with enhanced diffusional properties was also investigated. Binary blends of PLA and sulfopolyester were used to melt spin PLA/sulfopolyester composite fibers and create micropores by hydrodispersing the sulfopolyester from the

composite fibers. The type of resultant blend and the micropores created were analyzed using DSC, FTIR and SEM techniques.

As described in Chapter 3, the results of these investigations revealed that hMSCs when seeded at either $1.5 \times 10^5$ cells/mL or $3 \times 10^5$ cells/mL could be cultured with over 98% viability in 3D Type I collagen matrices under both 10% and 12% cyclic tensile strain either in MSCGM or ODM for up to 14 days.

Contraction of the collagen matrix by hMSCs was discussed in Chapter 3. Contraction profiles of collagen matrices exhibited a rapid and then slower contraction phase. The rate of matrix contraction was higher with higher initial cell seeding density. Matrices treated with MSCGM contracted in the order of 10%> 0%> 12% strain levels while those treated with ODM had maximum contraction on the order of 12%> 0%> 10% strain levels. Increase of intial cell seeding density from $1.5 \times 10^5$ cells/mL to $3 \times 10^5$ cells/mL increased the matrix contraction only in unstrained and 10% strained matrices. The difference in contraction between 10% and 12% strain levels suggests an existence of a threshold level of strain that influences cellular response to combined effects of strain and culture medium.

Chapter 4 descibed investigations on the change in hMSC nuclei shape and orientation due to cyclic strain, culture medium, culture duration and hMSC seeding density. Nuclei in strained matrices were more spherical and oriented away from the direction of strain. A high initial seeding density in strained matrices caused nuclei to remain spherical but orient in the direction of strain. High density may have provided less freedom for the cells to orient themselves, causing most cells to align in the direction of strain. Nuclei that are more spherical were observed in ODM than in MSCGM. It is possible that osteogenic differentiation of hMSCs is associated with change in nuclei shape. Changes in morphology

and orientation of hMSC nuclei appear to be caused by morphological and orientation changes of hMSCs in response to strain.

Chapters 4 and 5 descibed investigations on osteogenic differentiation of hMSCs cultured at low seeding density in 3D collagen matrices under tensile strain. Initial investigations to determine the effect of strain alone on the expression of BMP-2 mRNA in hMSCs indicated that 10% strain significantly increased BMP-2 mRNA expression in hMSCs. Significant increase in BMP-2 expression was observed with 12% strained hMSCs only after 14 days.

Investigations using both strain and chemical stimuli (culturing in ODM) indicated that COLI mRNA expression after 7 days was dependent on cyclic tensile strain. Expression of BMP-2 mRNA in hMSCs was induced by the combined effects of strain and osteogenic media conditions while highest expression of OCN was observed in 10% strained hMSCs cultured in ODM. Cyclic tensile strain and osteogenic medium collectively affected the expression of ALPL mRNA in hMSCs. Endogenous alkaline phosphatase activity in hMSCs was induced by cyclic tensile strain and increased culture duration.

The change in mechanical properties of final tissue constructs after subjecting to strain and osteogenic media conditions was discussed in Chapter 7. Stress-strain curves of both unstrained and strained hMSC-seeded collagen matrices exhibited a linear elastic region and a failure region. A higher Young's modulus was observed in strained matrices cultured in MSCGM. The Young's moduli increased with time in all matrices cultured in MSCGM, but only in 10% strained matrices cultured in ODM. Failure stress of all matrices cultured in ODM was higher than those cultured in MSCGM and this difference was independent of

strain and culture duration. However, all strained matrices in ODM had lower failure stresses than unstrained matrices at the end of 14 days.

Chapters 8 described investigations on osteogenic differentiation of hMSCs cultured at high seeding density in 3D collagen matrices under tensile strain. Investigations with higher initial hMSC seeding density ($3 \times 10^5$ cells/mL) revealed that cyclic tensile strain at 12% in ODM increased COLI mRNA expression in hMSCs after 7 days. Combined effects of strain and osteogenic medium increased expression of ALPL mRNA in hMSCs after 14 days. Higher expression of BMP-2 mRNA observed in the first week was dependent on strain. The effect of osteogenic medium on BMP-2 expression in strained hMSCs was also significant with a greater than 10-fold increase in BMP-2 expression after 2 weeks in hMSCs exposed to both strain and ODM. Expression of OCN mRNA was dependent on the combined effects of strain and osteogenic medium. Endogenous ALP activity in hMSCs increased with cyclic tensile strain and osteogenic medium. Human MSCs strained at 12% in ODM showed the highest endogenous ALP activity after 7 days.

Investigations into cytokine expression by hMSCs under cyclic tensile strain and osteogenic media conditions in Chapter 9 revealed that hMSCs do not express TNF-α and IL-1β under the culture conditions and time points investigated. Expression of IL-6 in hMSCs was reduced in ODM culture. Interleukin-6 expression was dependent on culture medium and cyclic tensile strain where a brief increase in IL-6 expression was caused by both 10% and 12% strain levels. Presence of dexamethasone in culture media increased IL-8 expression by hMSCs. Both 10% and 12% strain levels caused an increase in IL-8 production by hMSCs when cultured in ODM. These results indicated that cyclic tensile strain temporarily caused an increase in the expression of both IL-6 and IL-8 in hMSCs when cultured in ODM.

Chapter 10 described the investigations on fabricating a microporous fiber to be used to develop a 3D nonwoven scaffold with improved media transfer properties. Poly(lactic acid) (PLA) and sulfopolyester (AQ) were successfully blended and extruded using a microcompounder to produce PLA/AQ composite fibers. Sulfopolyester was removed from the composite fibers by a short hydrodispersing step to create micrpores on the fibers. Differential scanning calorimetric studies on unhydrolysed composite fibers showed that AQ was partially miscible in PLA. Fourier transform infrared mapping of composite fiber cross sections revealed that AQ was randomly dispersed throughout the cross section, which was dependent on AQ content in the composite fibers. As indicated by scanning electron micrographs of the fiber surfaces, the size of the micropores was dependent on the AQ content in composite fibers. The micropores on hydrolysed fiber cross sections were observed in fibers with 3%, 5%, and 10% AQ indicating that at least 3% AQ content is needed to produce droplet morphology of AQ, in these fibers. Sulfopolyester can be successfully blended with PLA to produce melt spun microporous fibers that can be used to fabricate nonwoven scaffolds with increased diffusional properties.

As expounded in this dissertation, the combined effects of mechanical and chemical stimulation induced osteogenic differentiation of hMSCs cultured in 3D collagen matrices. This adds to the existing knowledge on hMSCs cultured on 2D substrates that hMSCs can be cultured in 3D matrices and induced toward osteogenesis by mechanical and chemical stimulation. Engineering of bone constructs *in vitro* depends on the ability to maintain viability of hMSCs in 3D culture condtions and be able to achieve necessary differentiation of the cells leading to matrix mineralization. The findings of this dissertation will assist in planning future investigations related to engineering large bone tissue constructs *in vitro*.

## 11.2 Recommendations for future research

One of the drawbacks of the studis using collagen was the contraction of the collagen matrices that limited culture duration to 14 days. In order to induce hMSCs to produce calcium nodules and fully differentiate into osteoblasts, culture duration should be increased to 28 days. Further investigations should be carried out to determine means of maintaining the dimensions of 3D collagen matrices longer without impairing their elasticity.

As a result of high contraction observed in the collagen matrices, it would be difficult to create large bone constructs. This would hinder the use of this technology to treat critical bone defects, which are usually over 3 mm. Therefore, the size of the collagen matrix should be increased and this size needs to be maintained during the culture period. Alternative materials that are more stable and elastic can also be used to fabricate 3D scaffolds. Use of other scaffold material such as nonwoven structures fabricated from bioresorbable polymers should be investigated. Types of polymers that will render elasticity to the final structure should be selected to fabricate these structures.

Absence of a feedback system in the Flexercell FX-4000 strain unit prevented the identification of exact strain levels applied to hMSC-seeded collagen matrices, and the changes in strain over the full culture period. Since the matrices can become stiffer over time

during hMSC osteogenesis, it is important to maintain the same strain level by having a feedback system, which can monitor this change in modulus and alter the force applied to the matrices to have a constant strain level throughout the culture duration. Therefore, a strain system with feedback control needs to be developed to overcome this drawback.

Although strain values at the macro level are known, there is a possibility that the levels of micro strains experienced by hMSCs will differ depending on the location of the cells in the 3D collagen matrix. Change in microstrains throughout the 3D collagen matrix needs to be investigated to determine the distribution of strain in the collagen matrix and actual microstrain levels to which the cells are exposed.

The cyclic tensile strain in this study was applied continuously for 4 hours per day (4 hours cyclic strain + 20 hours rest period) using a sinusoidal waveform. In order to determine the optimal strain regimen for hMSC osteogenesis, more analysis needs to be carried out with different strain regimens.

# 12 References


1. Langer, R., Tissue engineering, Mol Ther, 1, 12, 2000.

2. Godbey, W. T. and Atala, A., In vitro systems for tissue engineering, Ann N Y Acad Sci, 961, 10, 2002.

3. Bruder, S. P., Fink, D. J. and Caplan, A. I., Mesenchymal stem cells in bone development, bone repair, and skeletal regeneration therapy, J Cell Biochem, 56, 283, 1994.

4. Caplan, A. I. and Pechak, D. G., The cellular and molecular embryology of bone formation, Bone and Mineral Res/5, 5, 117, 1987.

5. Caplan, A. I. and Bruder, S. P., Mesenchymal stem cells: Building blocks for molecular medicine in the 21st century, Trends Mol Med, 7, 259, 2001.

6. Bruder, S. P., Jaiswal, N. and Haynesworth, S. E., Growth kinetics, self-renewal, and the osteogenic potential of purified human mesenchymal stem cells during extensive subcultivation and following cryopreservation, J Cell Biochem, 64, 278, 1997.

7. Bruder, S. P., Kurth, A. A., Shea, M., Hayes, W. C., Jaiswal, N. and Kadiyala, S., Bone regeneration by implantation of purified, culture-expanded human mesenchymal stem cells, J Orthop Res, 16, 155, 1998.

8. Jaiswal, R. K., Jaiswal, N., Bruder, S. P., Mbalaviele, G., Marshak, D. R. and Pittenger, M. F., Adult human mesenchymal stem cell differentiation to the osteogenic or adipogenic lineage is regulated by mitogen-activated protein kinase, J Biol Chem, 275, 9645, 2000.

9. Jaiswal, N., Haynesworth, S. E., Caplan, A. I. and Bruder, S. P., Osteogenic differentiation of purified, culture-expanded human mesenchymal stem cells in vitro, J Cell Biochem, 64, 295, 1997.

10. Halvorsen, Y. D., Franklin, D., Bond, A. L., Hitt, D. C., Auchter, C., Boskey, A. L., Paschalis, E. P., Wilkison, W. O. and Gimble, J. M., Extracellular matrix mineralization and osteoblast gene expression by human adipose tissue-derived stromal cells, Tissue Eng, 7, 729, 2001.

11. Yoneno, K., Ohno, S., Tanimoto, K., Honda, K., Tanaka, N., Doi, T., Kawata, T., Tanaka, E., Kapila, S. and Tanne, K., Multidifferentiation potential of mesenchymal stem cells in three-dimensional collagen gel cultures, J Biomed Mater Res A, 75, 733, 2005.

12. Haynesworth, S. E., Baber, M. A. and Caplan, A. I., Cytokine expression by human marrow-derived mesenchymal progenitor cells in vitro: Effects of dexamethasone and il-1 alpha, J Cell Physiol, 166, 585, 1996.

13. Carter, D. R., Beaupre, G. S., Giori, N. J. and Helms, J. A., Mechanobiology of skeletal regeneration, Clin Orthop Relat Res, S41, 1998.

14. Loboa, E. G., Fang, T. D., Parker, D. W., Warren, S. M., Fong, K. D., Longaker, M. T. and Carter, D. R., Mechanobiology of mandibular distraction osteogenesis: Finite element analyses with a rat model, J Orthop Res, 23, 663, 2005.

15. Loboa, E. G., Fang, T. D., Warren, S. M., Lindsey, D. P., Fong, K. D., Longaker, M. T. and Carter, D. R., Mechanobiology of mandibular distraction osteogenesis: Experimental analyses with a rat model, Bone, 34, 336, 2004.

16. Jagodzinski, M., Drescher, M., Zeichen, J., Hankemeier, S., Krettek, C., Bosch, U. and van Griensven, M., Effects of cyclic longitudinal mechanical strain and dexamethasone on osteogenic differentiation of human bone marrow stromal cells, Eur Cell Mater, 7, 35, 2004.

17. Simmons, C. A., Matlis, S., Thornton, A. J., Chen, S., Wang, C. Y. and Mooney, D. J., Cyclic strain enhances matrix mineralization by adult human mesenchymal stem cells via the extracellular signal-regulated kinase (erk1/2) signaling pathway, J Biomech, 36, 1087, 2003.

18. Grayson, W. L., Ma, T. and Bunnell, B., Human mesenchymal stem cells tissue development in 3d pet matrices, Biotechnol Prog, 20, 905, 2004.

19. Barbanti, S. H., Santos, A. R., Jr., Zavaglia, C. A. and Duek, E. A., Porous and dense poly(l-lactic acid) and poly(d,l-lactic acid-co-glycolic acid) scaffolds: In vitro degradation in culture medium and osteoblasts culture, J Mater Sci Mater Med, 15, 1315, 2004.

20. Meinel, L., Karageorgiou, V., Hofmann, S., Fajardo, R., Snyder, B., Li, C., Zichner, L., Langer, R., Vunjak-Novakovic, G. and Kaplan, D. L., Engineering bone-like tissue in vitro using human bone marrow stem cells and silk scaffolds, J Biomed Mater Res A, 71, 25, 2004.

21. Li, W. J., Tuli, R., Huang, X., Laquerriere, P. and Tuan, R. S., Multilineage differentiation of human mesenchymal stem cells in a three-dimensional nanofibrous scaffold, Biomaterials, 26, 5158, 2005.

22. Chen G, Ushida T and Tateishi T, Scaffold design for tissue engineering, Macromol Biosci, 2, 67, 2004.

23. Saad, B., Matter, S., Ciardelli, G., Uhlschmid, G. K., Welti, M., Neuenschwander, P. and Suter, U. W., Interactions of osteoblasts and macrophages with biodegradable and highly porous polyesterurethane foam and its degradation products, J Biomed Mater Res, 32, 355, 1996.

24. Seal BL, Otero TC and A, P., Polymeric biomaterials for tissue and organ regeneration, Mater Sci Eng R, 34, 147, 2001.

25. Banes, A. J., Tsuzaki, M., Yamamoto, J., Fischer, T., Brigman, B., Brown, T. and Miller, L., Mechanoreception at the cellular level: The detection, interpretation, and diversity of responses to mechanical signals, Biochem Cell Biol, 73, 349, 1995.

26. Claes, L. E. and Heigele, C. A., Magnitudes of local stress and strain along bony surfaces predict the course and type of fracture healing, J Biomech, 32, 255, 1999.

27. Stanford, C. M., Morcuende, J. A. and Brand, R. A., Proliferative and phenotypic responses of bone-like cells to mechanical deformation, J Orthop Res, 13, 664, 1995.

28. Koike, M., Shimokawa, H., Kanno, Z., Ohya, K. and Soma, K., Effects of mechanical strain on proliferation and differentiation of bone marrow stromal cell line st2, J Bone Miner Metab, 23, 219, 2005.

29. Ignatius, A., Blessing, H., Liedert, A., Schmidt, C., Neidlinger-Wilke, C., Kaspar, D., Friemert, B. and Claes, L., Tissue engineering of bone: Effects of mechanical strain on osteoblastic cells in type i collagen matrices, Biomaterials, 26, 311, 2005.

30. Takahashi, Y. and Tabata, Y., Effect of the fiber diameter and porosity of non-woven pet fabrics on the osteogenic differentiation of mesenchymal stem cells, J Biomater Sci Polym Ed, 15, 41, 2004.

31. Gomes, M. E., Sikavitsas, V. I., Behravesh, E., Reis, R. L. and Mikos, A. G., Effect of flow perfusion on the osteogenic differentiation of bone marrow stromal cells cultured on starch-based three-dimensional scaffolds, J Biomed Mater Res A, 67, 87, 2003.

32. Sikavitsas, V. I., Bancroft, G. N., Holtorf, H. L., Jansen, J. A. and Mikos, A. G., Mineralized matrix deposition by marrow stromal osteoblasts in 3d perfusion culture increases with increasing fluid shear forces, Proc Natl Acad Sci U S A, 100, 14683, 2003.

33. Fell, H. B., The histogenesis of cartilage and bone in the long bones of the embryonic fowl., J Morphol Physiol, 40, 417, 1925.

34. Fell, H. B., The osteogenic capacity *in vitro* of perisoteum and endosteum isolated from the limb skeleton of fowl embryos and young chicks., Anat, 66, 157, 1932.

35. Fell, H. B. and Robinson, R., The growth, development and phosphatase activity of embryonic avian femora and limb buds cultivated *in vitro*, Biochem J, 23, 767, 1929.

36. Pechak, D. G., Kujawa, M. J. and Caplan, A. I., Morphological and histochemical events during first bone formation in embryonic chick limbs, Bone, 7, 441, 1986.

37. Bruder, S. P. and Caplan, A. I., Cellular and molecular events during embryonic bone development, Connect Tissue Res, 20, 65, 1989.

38. Carter, D. R., Blenman, P. R. and Beaupre, G. S., Correlations between mechanical stress history and tissue differentiation in initial fracture healing, J Orthop Res, 6, 736, 1988.

39. Blenman, P. R., Carter, D. R. and Beaupre, G. S., Role of mechanical loading in the progressive ossification of a fracture callus, J Orthop Res, 7, 398, 1989.

40. Giori, N. J., Ryd, L. and Carter, D. R., Mechanical influences on tissue differentiation at bone-cement interfaces, J Arthroplasty, 10, 514, 1995.

41. Lacroix, D. and Prendergast, P. J., A mechano-regulation model for tissue differentiation during fracture healing: Analysis of gap size and loading, J Biomech, 35, 1163, 2002.

42. Long, M. W., Osteogenesis and bone-marrow-derived cells, Blood Cells Mol Dis, 27, 677, 2001.

43. von der Mark, K., von der Mark, H. and Gay, S., Study of differential collagen synthesis during development of the chick embryo by immunofluroescence. Ii. Localization of type i and type ii collagen during long bone development, Dev Biol, 53, 153, 1976.

44. Ducy, P., Desbois, C., Boyce, B., Pinero, G., Story, B., Dunstan, C., Smith, E., Bonadio, J., Goldstein, S., Gundberg, C., Bradley, A. and Karsenty, G., Increased bone formation in osteocalcin-deficient mice, Nature, 382, 448, 1996.

45. Price, P. A., Otsuka, A. A., Poser, J. W., Kristaponis, J. and Raman, N., Characterization of a gamma-carboxyglutamic acid-containing protein from bone, Proc Natl Acad Sci U S A, 73, 1447, 1976.

46. Termine, J. D., Kleinman, H. K., Whitson, S. W., Conn, K. M., McGarvey, M. L. and Martin, G. R., Osteonectin, a bone-specific protein linking mineral to collagen, Cell, 26, 99, 1981.

47. Kelm, R. J., Jr., Swords, N. A., Orfeo, T. and Mann, K. G., Osteonectin in matrix remodeling. A plasminogen-osteonectin-collagen complex, J Biol Chem, 269, 30147, 1994.

48. Chang, P. and Prince, C., 1 alpha,25-dihydroxyvitamin d3 stimulates synthesis and secretion of nonphosphorylated osteopontin (secreted phosphoprotein1) in mouse jb6 epidermal cells, Cancer Res, 51, 2144, 1994.

49. Noda, M. and Rodan, G. A., Transcriptional regulation of osteopontin production in rat osteoblast-like cells by parathyroid hormone, J Cell Biol, 108, 713, 1989.

50. Beck, G. R., Jr., Zerler, B. and Moran, E., Phosphate is a specific signal for induction of osteopontin gene expression, Proc Natl Acad Sci U S A, 97, 8352, 2000.

51. Ishijima, M., Rittling, S. R., Yamashita, T., Tsuji, K., Kurosawa, H., Nifuji, A., Denhardt, D. T. and Noda, M., Enhancement of osteoclastic bone resorption and suppression of osteoblastic bone formation in response to reduced mechanical stress do not occur in the absence of osteopontin, J Exp Med, 193, 399, 2001.

52. Boskey, A. L., Spevak, L., Paschalis, E., Doty, S. B. and McKee, M. D., Osteopontin deficiency increases mineral content and mineral crystallinity in mouse bone, Calcif Tissue Int, 71, 145, 2002.

53. Massague, J., The tgf-beta family of growth and differentiation factors, Cell, 49, 437, 1987.

54. Sporn, M. B. and Roberts, A. B., Autocrine growth factors and cancer, Nature, 313, 745, 1985.

55. Bernard, A. and Peter, T., Controlling mesenchymal stem cell differentiation by tgf-beta family members, J Orthop Sci, 8, 740, 2003.

56. Bonewald, L. F. and Mundy, G. R., Role of transforming growth factor-beta in bone remodeling, Clin Orthop Relat Res, 261, 1990.

57. Thomas, T., Gori, F., Spelsberg, T. C., Khosla, S., Riggs, B. L. and Conover, C. A., Response of bipotential human marrow stromal cells to insulin-like growth factors: Effect on binding protein production, proliferation, and commitment to osteoblasts and adipocytes, Endocrinology, 140, 5036, 1999.

58. Feyen, J. H., Evans, D. B., Binkert, C., Heinrich, G. F., Geisse, S. and Kocher, H. P., Recombinant human [cys281]insulin-like growth factor-binding protein 2 inhibits both basal and insulin-like growth factor i-stimulated proliferation and collagen synthesis in fetal rat calvariae, J Biol Chem, 266, 19469, 1991.

59. Richman, C., Baylink, D. J., Lang, K., Dony, C. and Mohan, S., Recombinant human insulin-like growth factor-binding protein-5 stimulates bone formation parameters in vitro and in vivo, Endocrinology, 140, 4699, 1999.

60. Khan, S. N. and Lane, J. M., Bone tissue engineering: Basic science and clinical concepts. In: Goldberg, V. M. and Caplan, A. I.,eds. Orthopedic tissue engineering. New York, Marcel Dekker, Inc, 2004, pp. 161.

61. Sakou, T., Bone morphogenetic proteins: From basic studies to clinical approaches, Bone, 22, 591, 1998.

62. Wang, E. A., Israel, D. I., Kelly, S. and Luxenberg, D. P., Bone morphogenetic protein-2 causes commitment and differentiation in c3h10t1/2 and 3t3 cells, Growth Factors, 9, 57, 1993.

63. Akino, K., Mineta, T., Fukui, M., Fujii, T. and Akita, S., Bone morphogenetic protein-2 regulates proliferation of human mesenchymal stem cells, Wound Repair Regen, 11, 354, 2003.

64. Oreffo, R. O., Kusec, V., Romberg, S. and Triffitt, J. T., Human bone marrow osteoprogenitors express estrogen receptor-alpha and bone morphogenetic proteins 2 and 4 mrna during osteoblastic differentiation, J Cell Biochem, 75, 382, 1999.

65. Chaudhary, L. R., Hofmeister, A. M. and Hruska, K. A., Differential growth factor control of bone formation through osteoprogenitor differentiation, Bone, 34, 402, 2004.

66. Lian, J. B., Stein, G. S., Stein, J. L. and van Wijnen, A. J., Osteocalcin gene promoter: Unlocking the secrets for regulation of osteoblast growth and differentiation, J Cell Biochem Suppl, 30-31, 62, 1998.

67. Ducy, P., Zhang, R., Geoffroy, V., Ridall, A. L. and Karsenty, G., Osf2/cbfa1: A transcriptional activator of osteoblast differentiation, Cell, 89, 747, 1997.

68. Ziros, P. G., Gil, A. P., Georgakopoulos, T., Habeos, I., Kletsas, D., Basdra, E. K. and Papavassiliou, A. G., The bone-specific transcriptional regulator cbfa1 is a target of mechanical signals in osteoblastic cells, J Biol Chem, 277, 23934, 2002.

69. Lee, M. S., Lowe, G. N., Strong, D. D., Wergedal, J. E. and Glackin, C. A., Twist, a basic helix-loop-helix transcription factor, can regulate the human osteogenic lineage, J Cell Biochem, 75, 566, 1999.

70. Wershil, B. K., Furuta, G. T., Lavigne, J. A., Choudhury, A. R., Wang, Z. S. and Galli, S. J., Dexamethasone or cyclosporin a suppress mast cell-leukocyte cytokine cascades. Multiple mechanisms of inhibition of ige- and mast cell-dependent cutaneous inflammation in the mouse, J Immunol, 154, 1391, 1995.

71. Lavista Llanos, S. and Roldan, A., Effect of dexamethasone on nitric oxide (no.) production by cultured astrocytes, Biocell, 23, 29, 1999.

72. Tenenbaum, H. C. and Heersche, J. N., Dexamethasone stimulates osteogenesis in chick periosteum in vitro, Endocrinology, 117, 2211, 1985.

73. Gafni, R. I., McCarthy, E. F., Hatcher, T., Meyers, J. L., Inoue, N., Reddy, C., Weise, M., Barnes, K. M., Abad, V. and Baron, J., Recovery from osteoporosis through skeletal growth: Early bone mass acquisition has little effect on adult bone density, Faseb J, 16, 736, 2002.

74. Libby, P. and Aikawa, M., Vitamin c, collagen, and cracks in the plaque, Circulation, 105, 1396, 2002.

75. Boskey, A. L., Guidon, P., Doty, S. B., Stiner, D., Leboy, P. and Binderman, I., The mechanism of beta-glycerophosphate action in mineralizing chick limb-bud mesenchymal cell cultures, J Bone Miner Res, 11, 1694, 1996.

76. Chung, C. H., Golub, E. E., Forbes, E., Tokuoka, T. and Shapiro, I. M., Mechanism of action of beta-glycerophosphate on bone cell mineralization, Calcif Tissue Int, 51, 305, 1992.

77. Lennon, D. P., Development of a serum screen for mesenchymal progenitor cells from bone marrow., In Vitro Cell Dev Biol, 32, 602, 1996.

78. Frost, H. M., Perspectives: Bone's mechanical usage windows, Bone Miner, 19, 257, 1992.

79. Brighton, C. T., Strafford, B., Gross, S. B., Leatherwood, D. F., Williams, J. L. and Pollack, S. R., The proliferative and synthetic response of isolated calvarial bone cells of rats to cyclic biaxial mechanical strain, J Bone Joint Surg Am, 73, 320, 1991.

80. Jones, D. B., Nolte, H., Scholubbers, J. G., Turner, E. and Veltel, D., Biochemical signal transduction of mechanical strain in osteoblast-like cells, Biomaterials, 12, 101, 1991.

81. Buckley, M. J., Banes, A. J., Levin, L. G., Sumpio, B. E., Sato, M., Jordan, R., Gilbert, J., Link, G. W. and Tran Son Tay, R., Osteoblasts increase their rate of division and align in response to cyclic, mechanical tension in vitro, Bone Miner, 4, 225, 1988.

82. Kaspar, D., Seidl, W., Neidlinger-Wilke, C., Beck, A., Claes, L. and Ignatius, A., Proliferation of human-derived osteoblast-like cells depends on the cycle number and frequency of uniaxial strain, J Biomech, 35, 873, 2002.

83. Kaspar, D., Seidl, W., Neidlinger-Wilke, C. and Claes, L., In vitro effects of dynamic strain on the proliferative and metabolic activity of human osteoblasts, J Musculoskelet Neuronal Interact, 1, 161, 2000.

84. Winter, L. C., Walboomers, X. F., Bumgardner, J. D. and Jansen, J. A., Intermittent versus continuous stretching effects on osteoblast-like cells in vitro, J Biomed Mater Res A, 67, 1269, 2003.

85. Weyts, F. A., Bosmans, B., Niesing, R., van Leeuwen, J. P. and Weinans, H., Mechanical control of human osteoblast apoptosis and proliferation in relation to differentiation, Calcif Tissue Int, 72, 505, 2003.

86. Di Palma, F., Douet, M., Boachon, C., Guignandon, A., Peyroche, S., Forest, B., Alexandre, C., Chamson, A. and Rattner, A., Physiological strains induce differentiation in human osteoblasts cultured on orthopaedic biomaterial, Biomaterials, 24, 3139, 2003.

87. Li, Y., Ma, T., Yang, S. T. and Kniss, D. A., Thermal compression and characterization of three-dimensional nonwoven pet matrices as tissue engineering scaffolds, Biomaterials, 22, 609, 2001.

88. Akhouayri, O., Lafage-Proust, M. H., Rattner, A., Laroche, N., Caillot-Augusseau, A., Alexandre, C. and Vico, L., Effects of static or dynamic mechanical stresses on osteoblast phenotype expression in three-dimensional contractile collagen gels, J Cell Biochem, 76, 217, 1999.

89. Lan, C. W., Wang, F. F. and Wang, Y. J., Osteogenic enrichment of bone-marrow stromal cells with the use of flow chamber and type i collagen-coated surface, J Biomed Mater Res A, 66, 38, 2003.

90. Lee, C. H., Singla, A. and Lee, Y., Biomedical applications of collagen, Int J Pharm, 221, 1, 2001.

91. Tanaka, S. M., Li, J., Duncan, R. L., Yokota, H., Burr, D. B. and Turner, C. H., Effects of broad frequency vibration on cultured osteoblasts, J Biomech, 36, 73, 2003.

92. Niemeyer, P., Krause, U., Fellenberg, J., Kasten, P., Seckinger, A., Ho, A. D. and Simank, H. G., Evaluation of mineralized collagen and alpha-tricalcium phosphate as scaffolds for tissue engineering of bone using human mesenchymal stem cells, Cells Tissues Organs, 177, 68, 2004.

93. Ren, T., Ren, J., Jia, X. and Pan, K., The bone formation in vitro and mandibular defect repair using plga porous scaffolds, J Biomed Mater Res A, 74, 562, 2005.

94. Yoshimoto, H., Shin, Y. M., Terai, H. and Vacanti, J. P., A biodegradable nanofiber scaffold by electrospinning and its potential for bone tissue engineering, Biomaterials, 24, 2077, 2003.

95. Mooney, D. J., Mazzoni, C. L., Breuer, C., McNamara, K., Hern, D., Vacanti, J. P. and Langer, R., Stabilized polyglycolic acid fibre-based tubes for tissue engineering, Biomaterials, 17, 115, 1996.

96. Hutmacher, D. W., Scaffolds in tissue engineering bone and cartilage, Biomaterials, 21, 2529, 2000.

97. Schugens, C., Maquet, V., Grandfils, C., Jerome, R. and Teyssie, P., Polylactide macroporous biodegradable implants for cell transplantation. Ii. Preparation of polylactide foams by liquid-liquid phase separation, J Biomed Mater Res, 30, 449, 1996.

98. Whang, K., Thomas, C. and Healy, K., A novel method to fabricate bioabsorbable scaffolds, Polymer, 36, 837, 1995.

99. Whang, K., Healy, K. E., Elenz, D. R., Nam, E. K., Tsai, D. C., Thomas, C. H., Nuber, G. W., Glorieux, F. H., Travers, R. and Sprague, S. M., Engineering bone regeneration with bioabsorbable scaffolds with novel microarchitecture, Tissue Eng, 5, 35, 1999.

100. Meinel, L., Karageorgiou, V., Fajardo, R., Snyder, B., Shinde-Patil, V., Zichner, L., Kaplan, D., Langer, R. and Vunjak-Novakovic, G., Bone tissue engineering using human mesenchymal stem cells: Effects of scaffold material and medium flow, Ann Biomed Eng, 32, 112, 2004.

101. Chen, G., Ushida, T. and Tateishi, T., Development of biodegradable porous scaffolds for tissue engineering, Mat Sci Eng C, 17, 63, 2001.

102. Chen, G., Ushida, T. and Tateishi, T., Poly(dl-lactic-co-glycolic acid) sponge hybridized with collagen microsponges and deposited apatite particulates, J Biomed Mater Res, 57, 8, 2001.

103. Li, W. J., Laurencin, C. T., Caterson, E. J., Tuan, R. S. and Ko, F. K., Electrospun nanofibrous structure: A novel scaffold for tissue engineering, J Biomed Mater Res, 60, 613, 2002.

104. Awad, H. A., Butler, D. L., Harris, M. T., Ibrahim, R. E., Wu, Y., Young, R. G., Kadiyala, S. and Boivin, G. P., In vitro characterization of mesenchymal stem cell-seeded collagen scaffolds for tendon repair: Effects of initial seeding density on contraction kinetics, J Biomed Mater Res, 51, 233, 2000.

105. Bonassar, L. J. and Vacanti, C. A., Tissue engineering: The first decade and beyond, J Cell Biochem Suppl, 30-31, 297, 1998.

106. Sumanasinghe, R. D., Bernacki, S. H. and Loboa, E. G., Osteogenic differentiation of human mesenchymal stem cells in collagen matrices: Effect of uniaxial cyclic tensile strain on bone morphogenetic protein (bmp-2) mRNA expression, Tissue Eng, 2006 epub ahead of print.

107. Garvin, J., Qi, J., Maloney, M. and Banes, A. J., Novel system for engineering bioartificial tendons and application of mechanical load, Tissue Eng, 9, 967, 2003.

108. Bell, E., Ivarsson, B. and Merrill, C., Production of a tissue-like structure by contraction of collagen lattices by human fibroblasts of different proliferative potential in vitro, Proc Natl Acad Sci U S A, 76, 1274, 1979.

109. Bellows, C. G., Melcher, A. H. and Aubin, J. E., Contraction and organization of collagen gels by cells cultured from periodontal ligament, gingiva and bone suggest functional differences between cell types, J Cell Sci, 50, 299, 1981.

110. Guidry, C. and Grinnell, F., Studies on the mechanism of hydrated collagen gel reorganization by human skin fibroblasts, J Cell Sci, 79, 67, 1985.

111. Nishiyama, T., Tominaga, N., Nakajima, K. and Hayashi, T., Quantitative evaluation of the factors affecting the process of fibroblast-mediated collagen gel contraction by separating the process into three phases, Coll Relat Res, 8, 259, 1988.

112. Frey, J., Chamson, A., Raby, N. and Rattner, A., Collagen bioassay by the contraction of fibroblast-populated collagen lattices, Biomaterials, 16, 139, 1995.

113. Macieira-Coelho, A. and Azzarone, B., Correlation between contractility and proliferation in human fibroblasts, J Cell Physiol, 142, 610, 1990.

114. Feng, Z., Yamato, M., Akutsu, T., Nakamura, T., Okano, T. and Umezu, M., Investigation on the mechanical properties of contracted collagen gels as a scaffold for tissue engineering, Artif Organs, 27, 84, 2003.

115. Liu, X. D., Skold, M., Umino, T., Zhu, Y. K., Romberger, D. J., Spurzem, J. R. and Rennard, S. I., Endothelial cell-mediated type i collagen gel contraction is regulated by hemin, J Lab Clin Med, 136, 100, 2000.

116. Galois, L., Hutasse, S., Cortial, D., Rousseau, C. F., Grossin, L., Ronziere, M. C., Herbage, D. and Freyria, A. M., Bovine chondrocyte behaviour in three-dimensional type i collagen gel in terms of gel contraction, proliferation and gene expression, Biomaterials, 27, 79, 2006.

117. Bowman, N. N., Donahue, H. J. and Ehrlich, H. P., Gap junctional intercellular communication contributes to the contraction of rat osteoblast populated collagen lattices, J Bone Miner Res, 13, 1700, 1998.

118. Harris, A. K., Wild, P. and Stopak, D., Silicone rubber substrata: A new wrinkle in the study of cell locomotion, Science, 208, 177, 1980.

119. Wang, H., Ip, W., Boissy, R. and Grood, E. S., Cell orientation response to cyclically deformed substrates: Experimental validation of a cell model, J Biomech, 28, 1543, 1995.

120. Shirinsky, V. P., Antonov, A. S., Birukov, K. G., Sobolevsky, A. V., Romanov, Y. A., Kabaeva, N. V., Antonova, G. N. and Smirnov, V. N., Mechano-chemical control of human endothelium orientation and size, J Cell Biol, 109, 331, 1989.

121. Buck, R. C., Reorientation response of cells to repeated stretch and recoil of the substratum, Exp Cell Res, 127, 470, 1980.

122. Haynesworth, S. E., Goshima, J., Goldberg, V. M. and Caplan, A. I., Characterization of cells with osteogenic potential from human marrow, Bone, 13, 81, 1992.

123. Haynesworth, S. E., Baber, M. A. and Caplan, A. I., Cell surface antigens on human marrow-derived mesenchymal cells are detected by monoclonal antibodies, Bone, 13, 69, 1992.

124. Neidlinger-Wilke, C., Grood, E. S., Wang, J.-C., Brand, R. A. and Claes, L., Cell alignment is induced by cyclic changes in cell length: Studies of cells grown in cyclically stretched substrates, J Orthop Res, 19, 286, 2001.

125. Dartsch, P. C. and Betz, E., Cellular and cytoskelatal response of vascular cells to mechanical stretch, Medical Textiles for imlantation., p 193, 1992.

126. Huang, D., Chang, T. R., Aggarwal, A., Lee, R. C. and Ehrlich, H. P., Mechanisms and dynamics of mechanical strengthening in ligament-equivalent fibroblast-populated collagen matrices, Ann Biomed Eng, 21, 289, 1993.

127. Eastwood, M., Mudera, V. C., McGrouther, D. A. and Brown, R. A., Effect of precise mechanical loading on fibroblast populated collagen lattices: Morphological changes, Cell Motil Cytoskeleton, 40, 13, 1998.

128. Cha, J. M., Park, S. N., Noh, S. H. and Suh, H., Time-dependent modulation of alignment and differentiation of smooth muscle cells seeded on a porous substrate undergoing cyclic mechanical strain, Artif Organs, 30, 250, 2006.

129. Girton, T. S., Barocas, V. H. and Tranquillo, R. T., Confined compression of a tissue-equivalent: Collagen fibril and cell alignment in response to anisotropic strain, J Biomech Eng, 124, 568, 2002.

130. Bischofs, I. B. and Schwarz, U. S., Cell organization in soft media due to active mechanosensing, Proc Natl Acad Sci U S A, 100, 9274, 2003.

131. Wang, N., Butler, J. P. and Ingber, D. E., Mechanotransduction across the cell surface and through the cytoskeleton, Science, 260, 1124, 1993.

132. Ingber, D. E., Cellular tensegrity: Defining new rules of biological design that govern the cytoskeleton, J Cell Sci, 104 ( Pt 3), 613, 1993.

133. Thomas, C. H., Collier, J. H., Sfeir, C. S. and Healy, K. E., Engineering gene expression and protein synthesis by modulation of nuclear shape, Proc Natl Acad Sci U S A, 99, 1972, 2002.

134. Bruder, S. P., Ricalton, N. S., Boynton, R. E., Connolly, T. J., Jaiswal, N., Zaia, J. and Barry, F. P., Mesenchymal stem cell surface antigen sb-10 corresponds to activated leukocyte cell adhesion molecule and is involved in osteogenic differentiation, J Bone Miner Res, 13, 655, 1998.

135. Frank, O., Heim, M., Jakob, M., Barbero, A., Schafer, D., Bendik, I., Dick, W., Heberer, M. and Martin, I., Real-time quantitative rt-pcr analysis of human bone marrow stromal cells during osteogenic differentiation in vitro, J Cell Biochem, 85, 737, 2002.

136. Livak, K. J. and Schmittgen, T. D., Analysis of relative gene expression data using real-time quantitative pcr and the 2(-delta delta c(t)) method, Methods, 25, 402, 2001.

137. Kinoshita, S., Finnegan, M., Bucholz, R. W. and Mizuno, K., Three-dimensional collagen gel culture promotes osteoblastic phenotype in bone marrow derived cells, Kobe J Med Sci, 45, 201, 1999.

138. Yoneno, K., Ohno, S., Tanimoto, K., Honda, K., Tanaka, N., Doi, T., Kawata, T., Tanaka, E., Kapila, S. and Tanne, K., Multidifferentiation potential of mesenchymal stem cells in three-dimensional collagen gel cultures, J Biomed Mater Res A, 2005.

139. Sykaras, N. and Opperman, L. A., Bone morphogenetic proteins (bmps): How do they function and what can they offer the clinician?, J Oral Sci, 45, 57, 2003.

140. Onishi, T., Ishidou, Y., Nagamine, T., Yone, K., Imamura, T., Kato, M., Sampath, T. K., ten Dijke, P. and Sakou, T., Distinct and overlapping patterns of localization of bone morphogenetic protein (bmp) family members and a bmp type ii receptor during fracture healing in rats, Bone, 22, 605, 1998.

141. Rockwood, C. A. and Green, D. P., Fractures in adults. In: Philadelphia, Lippincott, 1984.

142. Rasubala, L., Yoshikawa, H., Islam, A. A., Nagata, K., Iijima, T. and Ohishi, M., Comparison of the healing process in plated and non-plated fractures of the mandible in rats, Br J Oral Maxillofac Surg, 42, 315, 2004.

143. Riser, B. L., Cortes, P., Zhao, X., Bernstein, J., Dumler, F. and Narins, R. G., Intraglomerular pressure and mesangial stretching stimulate extracellular matrix formation in the rat, J Clin Invest, 90, 1932, 1992.

144. Sumpio, B. E., Banes, A. J., Link, W. G. and Johnson, G., Jr., Enhanced collagen production by smooth muscle cells during repetitive mechanical stretching, Arch Surg, 123, 1233, 1988.

145. Harris, S. E., Harris, M. A., Mahy, P., Wozney, J., Feng, J. Q. and Mundy, G. R., Expression of bone morphogenetic protein messenger rnas by normal rat and human prostate and prostate cancer cells, Prostate, 24, 204, 1994.

146. Price, P. A., Role of vitamin-k-dependent proteins in bone metabolism, Annu Rev Nutr, 8, 565, 1988.

147. Hauschka, P. V., Lian, J. B., Cole, D. E. and Gundberg, C. M., Osteocalcin and matrix gla protein: Vitamin k-dependent proteins in bone, Physiol Rev, 69, 990, 1989.

148. Boskey, A. L., Gadaleta, S., Gundberg, C., Doty, S. B., Ducy, P. and Karsenty, G., Fourier transform infrared microspectroscopic analysis of bones of osteocalcin-deficient mice provides insight into the function of osteocalcin, Bone, 23, 187, 1998.

149. Glowacki, J., Rey, C., Glimcher, M. J., Cox, K. A. and Lian, J., A role for osteocalcin in osteoclast differentiation, J Cell Biochem, 45, 292, 1991.

150. Owen, T. A., Aronow, M., Shalhoub, V., Barone, L. M., Wilming, L., Tassinari, M. S., Kennedy, M. B., Pockwinse, S., Lian, J. B. and Stein, G. S., Progressive development of the rat osteoblast phenotype in vitro: Reciprocal relationships in expression of genes associated with osteoblast proliferation and differentiation during formation of the bone extracellular matrix, J Cell Physiol, 143, 420, 1990.

151. Strom, S. C. and Michalopoulos, G., Collagen as a substrate for cell growth and differentiation, Methods Enzymol, 82 Pt A, 544, 1982.

152. Bruder, S. P., Jaiswal, N., Ricalton, N. S., Mosca, J. D., Kraus, K. H. and Kadiyala, S., Mesenchymal stem cells in osteobiology and applied bone regeneration, Clin Orthop Relat Res, S247, 1998.

153. Cox, W. G. and Singer, V. L., A high-resolution, fluorescence-based method for localization of endogenous alkaline phosphatase activity, J Histochem Cytochem, 47, 1443, 1999.

154. Telford, W. G., Cox, W. G., Stiner, D., Singer, V. L. and Doty, S. B., Detection of endogenous alkaline phosphatase activity in intact cells by flow cytometry using the fluorogenic elf-97 phosphatase substrate, Cytometry, 37, 314, 1999.

155. Roeder, B. A., Kokini, K., Sturgis, J. E., Robinson, J. P. and Voytik-Harbin, S. L., Tensile mechanical properties of three-dimensional type i collagen extracellular matrices with varied microstructure, J Biomech Eng, 124, 214, 2002.

156. Feng, Z., Matsumoto, T. and Nakamura, T., Measurements of the mechanical properties of contracted collagen gels populated with rat fibroblasts or cardiomyocytes, J Artif Organs, 6, 192, 2003.

157. Landis, W. J., The strength of a calcified tissue depends in part on the molecular structure and organization of its constituent mineral crystals in their organic matrix, Bone, 16, 533, 1995.

158. Girton, T. S., Oegema, T. R. and Tranquillo, R. T., Exploiting glycation to stiffen and strengthen tissue equivalents for tissue engineering, J Biomed Mater Res, 46, 87, 1999.

159. Wagenseil, J. E., Wakatsuki, T., Okamoto, R. J., Zahalak, G. I. and Elson, E. L., One-dimensional viscoelastic behavior of fibroblast populated collagen matrices, J Biomech Eng, 125, 719, 2003.

160. Purpura, K. A., Aubin, J. E. and Zandstra, P. W., Sustained in vitro expansion of bone progenitors is cell density dependent, Stem Cells, 22, 39, 2004.

161. Aubin, J. E., Osteoprogenitor cell frequency in rat bone marrow stromal populations: Role for heterotypic cell-cell interactions in osteoblast differentiation, J Cell Biochem, 72, 396, 1999.

162. Faibish, D., Ott, S. M. and Boskey, A. L., Mineral changes in osteoporosis: A review, Clin Orthop Relat Res, 443, 28, 2006.

163. Filipak, M., Sparks, R. L., Tzen, C. Y. and Scott, R. E., Tumor necrosis factor inhibits the terminal event in mesenchymal stem cell differentiation, J Cell Physiol, 137, 367, 1988.

164. Kim, D. H., Yoo, K. H., Choi, K. S., Choi, J., Choi, S. Y., Yang, S. E., Yang, Y. S., Im, H. J., Kim, K. H., Jung, H. L., Sung, K. W. and Koo, H. H., Gene expression profile of cytokine and growth factor during differentiation of bone marrow-derived mesenchymal stem cell, Cytokine, 31, 119, 2005.

165. Majumdar, M. K., Thiede, M. A., Haynesworth, S. E., Bruder, S. P. and Gerson, S. L., Human marrow-derived mesenchymal stem cells (mscs) express hematopoietic cytokines and support long-term hematopoiesis when differentiated toward stromal and osteogenic lineages, J Hematother Stem Cell Res, 9, 841, 2000.

166. Gimble, J. M., Wanker, F., Wang, C. S., Bass, H., Wu, X., Kelly, K., Yancopoulos, G. D. and Hill, M. R., Regulation of bone marrow stromal cell differentiation by cytokines whose receptors share the gp130 protein, J Cell Biochem, 54, 122, 1994.

167. Erices, A., Conget, P., Rojas, C. and Minguell, J. J., Gp130 activation by soluble interleukin-6 receptor/interleukin-6 enhances osteoblastic differentiation of human bone marrow-derived mesenchymal stem cells, Exp Cell Res, 280, 24, 2002.

168. Fuller, K., Owens, J. M. and Chambers, T. J., Macrophage inflammatory protein-1 alpha and il-8 stimulate the motility but suppress the resorption of isolated rat osteoclasts, J Immunol, 154, 6065, 1995.

169. Collin, O. P., Kirsch, D., Anderson, F., Joost, O., Dean, A. and Osdoby, P., The chemokine il-8 as an autocrine inhibitor of osteoclast bone resorptive activity via il-8 receptors expressed by avain osteoclasts and human osteoclasts like cells., J Bone Miner Res, 11, S357, 1996.

170. Thomson, B. M., Mundy, G. R. and Chambers, T. J., Tumor necrosis factors alpha and beta induce osteoblastic cells to stimulate osteoclastic bone resorption, J Immunol, 138, 775, 1987.

171. Carty, T. J. and Laliberte, R. E., Meeting report. The biochemistry and pharmacology of interleukins-1 and -6, Agents Actions, 26, 391, 1989.

172. Idriss, H. T. and Naismith, J. H., Tnf alpha and the tnf receptor superfamily: Structure-function relationship(s), Microsc Res Tech, 50, 184, 2000.

173. Allen, D. G., Riviere, J. E. and Monteiro-Riviere, N. A., Identification of early biomarkers of inflammation produced by keratinocytes exposed to jet fuels jet a, jp-8, and jp-8(100), J Biochem Mol Toxicol, 14, 231, 2000.

174. Pacifici, R., Rifas, L., Teitelbaum, S., Slatopolsky, E., McCracken, R., Bergfeld, M., Lee, W., Avioli, L. V. and Peck, W. A., Spontaneous release of interleukin 1 from human blood monocytes reflects bone formation in idiopathic osteoporosis, Proc Natl Acad Sci U S A, 84, 4616, 1987.

175. Gowen, M., Wood, D. D., Ihrie, E. J., McGuire, M. K. and Russell, R. G., An interleukin 1 like factor stimulates bone resorption in vitro, Nature, 306, 378, 1983.

176. Kishimoto, T., The biology of interleukin-6, Blood, 74, 1, 1989.

177. Suda, T., Takahashi, N., Udagawa, N., Jimi, E., Gillespie, M. T. and Martin, T. J., Modulation of osteoclast differentiation and function by the new members of the tumor necrosis factor receptor and ligand families, Endocr Rev, 20, 345, 1999.

178. Dovio, A., Sartori, M. L., Masera, R. G., Peretti, L., Perotti, L. and Angeli, A., Effects of physiological concentrations of steroid hormones and interleukin-11 on basal and stimulated production of interleukin-8 by human osteoblast-like cells with different functional profiles, Clin Exp Rheumatol, 22, 79, 2004.

179. Wuyts, A., Proost, P. and Van Damme, J., Interleukin-8 and other cxc chemokines. In: Thompson, A.,eds. The cytokine handbook. London, Academic Press, 1998, pp. 271.

180. Bilbe, G., Roberts, E., Birch, M. and Evans, D. B., Pcr phenotyping of cytokines, growth factors and their receptors and bone matrix proteins in human osteoblast-like cell lines, Bone, 19, 437, 1996.

181. Lisignoli, G., Toneguzzi, S., Grassi, F., Piacentini, A., Tschon, M., Cristino, S., Gualtieri, G. and Facchini, A., Different chemokines are expressed in human arthritic bone biopsies: Ifn-gamma and IL-6 differently modulate IL-8, mcp-1 and rantes production by arthritic osteoblasts, Cytokine, 20, 231, 2002.

182. Monteiro-Riviere, N. A., Baynes, R. E. and Riviere, J. E., Pyridostigmine bromide modulates topical irritant-induced cytokine release from human epidermal keratinocytes and isolated perfused porcine skin, Toxicology, 183, 15, 2003.

183. Luger, T. A. and Schwarz, T., Evidence for an epidermal cytokine network, J Invest Dermatol, 95, 100S, 1990.

184. Majumdar, M. K., Thiede, M. A., Mosca, J. D., Moorman, M. and Gerson, S. L., Phenotypic and functional comparison of cultures of marrow-derived mesenchymal stem cells (mscs) and stromal cells, J Cell Physiol, 176, 57, 1998.

185. Grone, A., Keratinocytes and cytokines, Veterinary Immunology and Immunopathology, 88, 1, 2002.

186. Barker, J., Mitra, R., Griffiths, C., Dixit, V. and Nickoloff, B., Keratinocytes as initiators of inflammation, The Lancet, 337, 211, 1991.

187. Sunyer, T., Rothe, L., Jiang, X., Osdoby, P. and Collin-Osdoby, P., Proinflammatory agents, il-8 and il-10, upregulate inducible nitric oxide synthase expression and nitric oxide production in avian osteoclast-like cells, J Cell Biochem, 60, 469, 1996.

188. Chaudhary, L. R. and Avioli, L. V., Regulation of interleukin-8 gene expression by interleukin-1beta, osteotropic hormones, and protein kinase inhibitors in normal human bone marrow stromal cells, J Biol Chem, 271, 16591, 1996.

189. Chaudhary, L. R. and Avioli, L. V., Dexamethasone regulates il-1 beta and tnf-alpha-induced interleukin-8 production in human bone marrow stromal and osteoblast-like cells, Calcif Tissue Int, 55, 16, 1994.

190. Chen G, Ushida T and Tateishi T, Scaffold design for tissue engineering, Macromol Biosci, 2, 67, 2002.

191. Chapekar, M. S., Tissue engineering: Challenges and opportunities, J Biomed Mater Res, 53, 617, 2000.

192. Beyreuther R and Schauer G, Melt spinning of hollow fibers, progress in textiles., Science and Technology, 299, 2000.

193. Kim, J. J., Operation parameters for melt spinning of polypropylene hollow fiber membranes, Journal of Membrane Science, 108, 25, 1995.

194. Elenga, R., Seguela, R. and Rietsch, F., Thermal and mechanical behavior of crystalline poly (ethylene terephthalate) : Effects of higher temperature annealing and tensile behavior., Polymer, 32, 1975, 1991.

195. Zhang, J. F. and Sun, X., Mechanical properties and crystallization behavior of poly(lactic acid) blended with dendritic hyperbranched polymer., Polym Int, 53, 716, 2004.

196. Rudin, A., The elements of polymer science and engineering. In: San Diego, CA, Academic Press, 1998, pp. 95.

197. Schindler, A. and Harper, D., Polylactide. Ii. Viscosity molecular weight relationship and unperturbed chain dimensions., J of Polym Sci: Polym Chem Ed, 17, 2593, 1979.

198. Nakamura, T., Hitomi, S., Watanabe, S., Shimizu, Y., Jamshidi, K., Hyon, S. H. and Ikada, Y., Bioabsorption of polylactides with different molecular properties, J Biomed Mater Res, 23, 1115, 1989.

199. Catiker, E., Gumusderelioglu, M. and Guner, A., Degradation of pla, plga homo- and copolymers in the presence of serum albumin: A spectroscopic investigation, Poly Int, 49, 728, 2000.

200. Miyake, A., The infra-red spectrum of poly (ethylene terephthalate) i. The effect of crystallization., J Polym Sci, XXXVIII, 479, 1959.

201. Cole, K. C., Ajji, A. and Pellerin, E., New insights into the development of ordered structure in poly (ethylene terephthalate) 1. Results from external reflection infrared spectroscopy., Macromolecules, 35, 770, 2002.

202. Rovere, A. and Shambaugh, R. L., Melt-spun hollow fibers for use in nonwoven structures, Ind. Eng. Chem. Res., 40, 176, 2001.

203. Favis, B. D., Factors influencing the morphology of immiscible polymer blends in melt processing. In: Paul, D. R. and Bucknall, C. B.,eds. Polymer blends. New York, John Wiley and Sons, Inc., 2000, pp. 501.

204. Avgerpoulos, G. N., Weissert, F. C., Biddison, P. H. and Bohm, G. C. A., Rubber Chem Technol, 49, 93, 1976.

205. Karger-Kocsis, J., Kallo, A. and Kuleznev, V. N., Phase structure of impact-modified polypropylene blends, Polymer, 25, 279, 1984.

206. Favis, B. D. and Chalifoux, J. P., The effect of viscosity ratio on the morphology of polypropylene/polycarbonate blends during processing, Poly Eng Sci, 27, 1591, 1987.

207. Collyer, S. D., Bradbury, S. E., Hatfield, J. V. and Higson, S. P. J., A study of factors affecting the enhanced voltammetric stripping analysis of n-nitrosamines at sulfopolyester modified electrodes, Electroanalysis, 13, 332, 2000.

208. Kalika, D. S., Viscoelastic characterization of polymer blends. In: Paul, D. R. and Bucknall, C. B.,eds. Polymer blends. New York, John Wiley & Sons, 2000, pp. 291.

209. Shonaike, G. O., Miscibility of nylon 66/santoprene blends. In: Shonaike, G. O. and Simon, G. P.,eds. Polymer blends and alloys. New York, Mercel Dekker, Inc., 1999, pp. 235.

210. Greco, R., Mancarella, M., Martuscelli, E., Ragosta, G. and Jinghua, Y., Polyolefin blends, 2: Effect of epr composition on structure, morphology and mechanical properties of ipp/epr alloys., Polymer, 28, 1987, 1929.

211. Collins, M. J., Zeronian, S. H. and Semmelmeyer, M., The use of aqueous alkaline hydrolysis to reveal the fine structure of poly(ethylene terephthalate) fibers., J App. Poly. Sci., 42, 2149, 1991.

212. Skoog, D. A., Holler, F. J. and Nieman, T. A., Principles of instrumental analysis. In: Orlando, FL, Hartcourt Brace College Pub, 1998, pp. 300.

213. Runt, J. P., Crystalline polymer blends. In: Paul, D. R. and Bucknall, C. B.,eds. Polymer blends. New York, John Wiley and Sons, Inc., 2000, pp. 167.

214. Mekhilef, N., Favis, B. D. and Carreau, P. J., Morphological stability, interfacial tension, and dual-phase continuity in polystyrene-polyethylene blends, J polym Sci, Polym Phys, 35, 293, 1997.

# APPENDIX

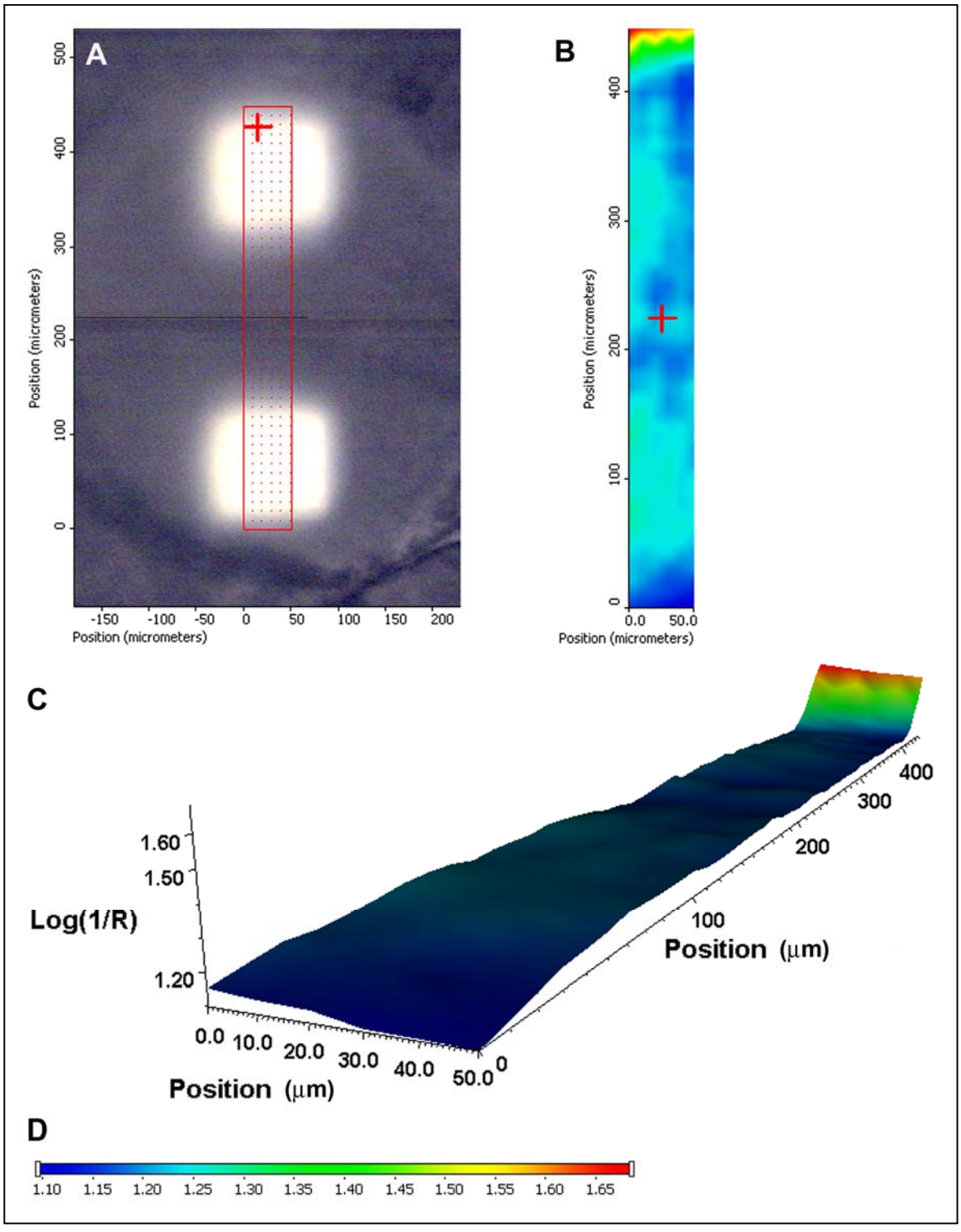


**Figure 13.1.** Variation in peak height of 1717.7 cm-1 band indicating sulfopolyetser (AQ) localization across the diameter of an unhydrolysed 10% AQ/ 90% PLA composite fiber. A) Video image of the mapped area; red grid shows the scanned points, B) Contour map with intensity gradients, C) 3D image and D) Rainbow bar showing color assignment for peak heights.

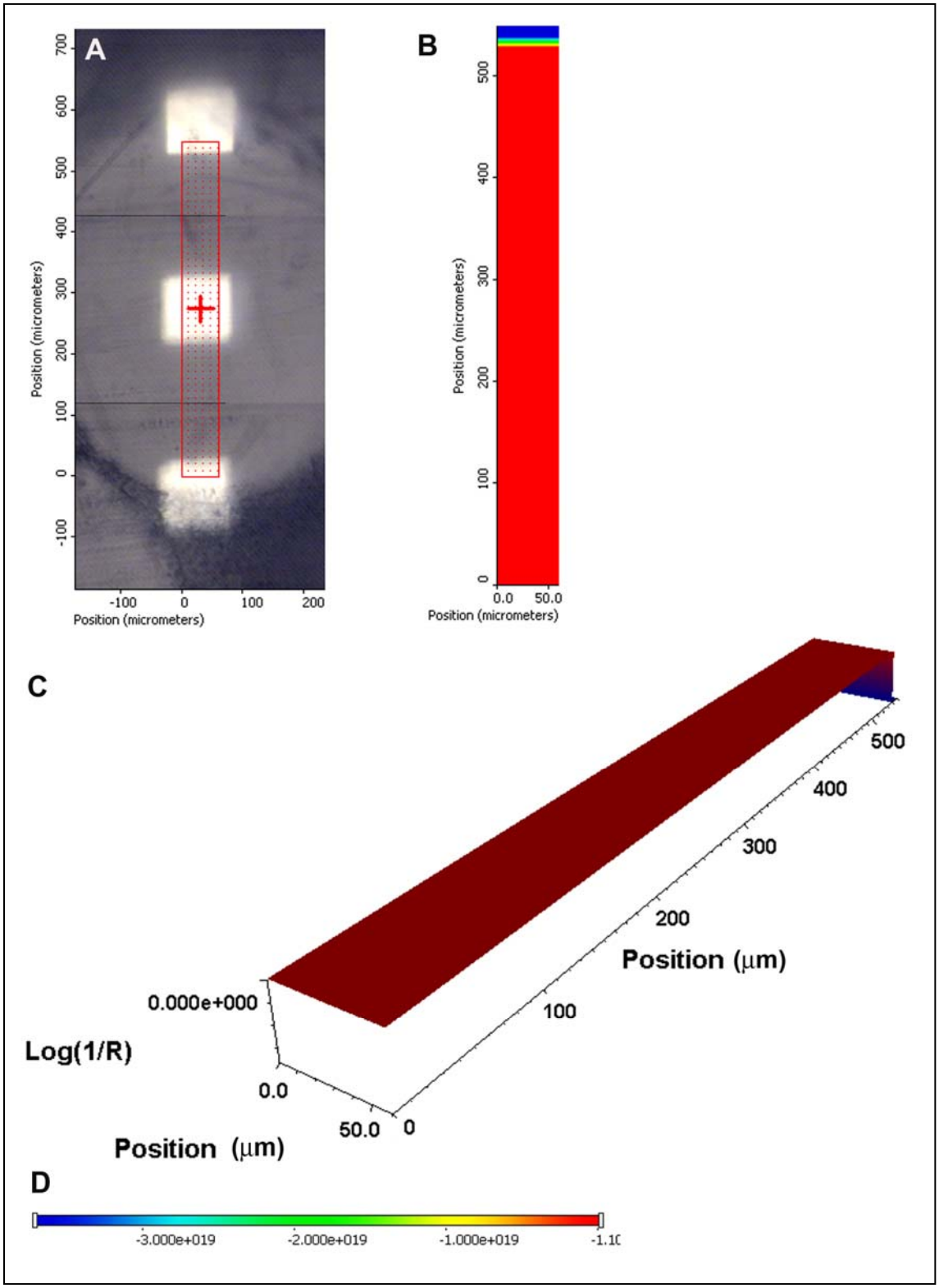


**Figure 13.2.** Variation in peak height of 1717.7 cm-1 band indicating localization of sulfopolyetser (AQ) across the diameter of an unhydrolysed 1% AQ/ 90% PLA composite fiber. A) Video image of the mapped area; red grid shows the scanned points, B) Contour map with intensity gradients, C) 3D image and D) Rainbow bar showing color assignment for peak heights.